THE INFLUENCE OF AGITATION ON MORPHOLOGY, RHEOLOGY AND ERYTHROMYCIN PRODUCTION IN *Saccharopolyspora erythraea* CULTURE

A thesis submitted to the University of London

for the degree of

DOCTOR OF PHILOSOPHY

by

Seyed Mohammad Heydarian M.Sc.

The Advanced Centre for Biochemical Engineering,

Department of Biochemical Engineering,

University College London.

Torrington Place,

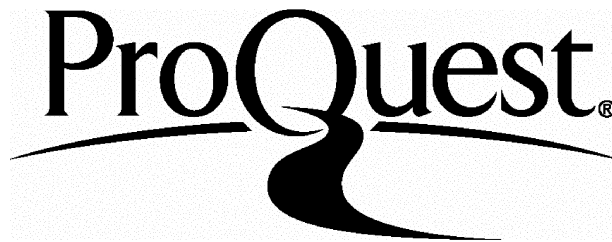London,   1998

ProQuest Number: U643631

All rights reserved

INFORMATION TO ALL USERS
The quality of this reproduction is dependent upon the quality of the copy submitted.

In the unlikely event that the author did not send a complete manuscript
and there are missing pages, these will be noted. Also, if material had to be removed,
a note will indicate the deletion.

ProQuest U643631

Published by ProQuest LLC(2016). Copyright of the Dissertation is held by the Author.

ProQuest LLC
789 East Eisenhower Parkway
P.O. Box 1346
Ann Arbor, MI 48106-1346

ABSTRACT

In spite of the importance of filamentous actinomycetes, the number of published reports for engineering aspects of fermentation (e.g. effect of agitation) are rare compared with filamentous fungi. Intensive mechanical agitation is necessary for adequate oxygen transfer rate and bulk mixing. However, excessive physical damage due to high agitation on the filamentous mycelia during the fermentation is usually undesirable. This report investigates the effect of agitation, and in particular, shear on *S. erythraea* fermentation.

Initially a relatively poor defined medium was used for *S. erythraea* fermentation at 7-L scale. It was shown that growth was inhibited at a low constant dissolved oxygen tension of 10% air saturation. However, the specific erythromycin production was virtually identical to that of a culture where DOT did not fall below 65%. In addition, at constant DOT (10%) a stirrer speed of 750 rpm caused serious mechanical damage to the mycelia compared with at 500 rpm. A bioassay was used for erythromycin measurements in this part of the study. A solid phase extraction method was developed for the purification and concentration of erythromycin for analysis by HPLC for future work.

A complex medium was used to investigate the effects of shear on the *S. erythraea* fermentation at laboratory scale (7-L) and pilot scale (450-L) fermenters. Morphological measurements using image analysis showed that the major axis of the mycelia (both freely dispersed and clumps) decreased after the end of the rapid growth phase to a relatively constant value (equilibrium size) dependent on the stirrer speed. Variation of other morphological parameters are also discussed. A model of hyphal breakage was set up based on stress cycling (fatigue) resulting from continuous recirculation through the high shear zone of the impeller. The critical strain energy of failure was used, the mycelium was assumed to have fractal properties and the individual hypha was assumed to behave elastically with a thickness that increases

2

linearly with the distance away from the growing tip. The comparison of the experimental data and the model showed reasonable agreement.

The effect of shear on growth is discussed in terms of dry cell weight. Maximum dry cell weight was slightly lower at higher speeds. Maximum biomass was 11.1 ± 0.5 gL^{-1} at 1250 rpm (tip speed = 4.45 ms^{-1}), whereas it was 12.7 ± 0.2 gL^{-1} at 350 rpm (tip speed =1.07 ms^{-1}). Specific erythromycin production was not stirrer speed dependent in the range of 350 to 1000 rpm (tip speed = 3.56 ms^{-1}) at 7-L scale, and it decreased by 10%, when the stirrer speed increased to 1250 rpm.

The rheology of the culture changed dramatically during the fermentation. Power law model had a good agreement with the experimental data and the consistency index was generally lower at higher stirrer speeds. A correlation was recommended between the consistency index and biomass ($K \propto (DCW)^{2.1}$) and the relation between morphology and rheology is discussed.

The mechanical properties of the cell wall of the *S. erythraea* were examined by disruption of fermentation broth in a homogeniser and it was shown that mechanical strength of the cell wall increased in a large extent during deceleration phase. These results were used to explain some aspect of mycelia breakage in the fermenter.

This research has shown that shear affects morphology of the *S. erythraea* culture. These effects are generally less compared with filamentous fungi culture and are not detrimental to growth and erythromycin production, if enough nutrients are provided in the medium. A consequence of this is the ability to rise the agitation rate to increase oxygen transfer and bulk mixing without significant mechanical damage or loss of productivity.

ACKNOWLEDGEMENT

CONTENT

1.0 INTRODUCTION

2.0   MATERIAL AND METHODS

3.0 RESULTS

4.0 TURBULENT BREAKAGE OF MYCELIA IN STIRRED TANK

5.0 DISCUSSION

6.0 CONCLUSION AND RECOMMENDATIONS

7.0   NOMENCLATURE

8.0   REFERENCES

LIST OF FIGURES

LIST OF TABLES

1.0 INTRODUCTION

1.1 Morphology of filamentous actinomycetes

Actinomycetes range from true mycelial organisms, e. g. the streptomycetes to groups such as the nocardia, which form mycelia that fragment readily and, under certain conditions, grow only as unicells. Filamentous actinomycetes and filamentous fungi exhibit major differences at the cellular level. Fungi possess membrane-bound organelles and cytoskeleton, providing subcellular structure and organisation which is important in cellular growth. These are absent in filamentous actinomycetes, which must therefore possess different growth mechanisms (Prosser and Tough, 1991). Another major difference is the size of the hyphae. Mycelial hyphae of fungi usually have a diameter of about 3-10 μm. Hyphae of actinomycetes are much narrower than those of fungi and usually have a diameter of only 0.5-1.5 μm. Despite this, the two groups show remarkable similarities, providing an example of convergent evolution (Prosser and Tough, 1991).

1.1.1 Growth and morphology of filamentous actinomycetes

Filamentous actinomycetes grow like filamentous fungi in multicellular structures called hyphal elements, which make up the mycelium. In submerged culture the hyphal elements may be present as pelleted and dispersed forms (Figure 3.18 & 3.19). There is no clear boundary between the two types. The filamentous form is widely referred to as freely dispersed mycelia which can entangle to form mycelial clumps. The entanglement of freely dispersed mycelia to form clumps may be permanent or temporary as a result of interaction between two or more mycelia in the liquid culture (Yang *et al.*, 1996).

Because of the fungus-like growth and differentiation, it is generally assumed that filamentous actinomycetes hyphae elongate by apical extension, that is, by deposition of wall polymers only at the very tip of the hyphae (Kretschmer, 1982). However, autoradiographic studies seem to indicate that wall synthesis was not restricted to the hyphal tip. Although there was a preferential incorporation of the N-acetyl-D-[1-^{3}H] glucosamine label, a precurser of peptidoglycan label at the tip, a relatively broad

segment of the hyphae also appeared labelled. The length of the labelled segment varied from 4 to 20 μm, depending on the strain and labelling conditions (Brana *et al.*, 1982; Gray *et al.*, 1990). Gray *et al.* (1990) believed labelling in distal regions was because of wall synthesis, turnover and thickening. However, further experiments by Miguelez *et al.* (1993) demonstrate that in *S. antibioticus*, wall growth takes place without the turnover of the peptidoglycan. The cell wall thickening could be one of the consequences of the addition of cell wall components in the region away from the tip (Miguelez *et al.*, 1993). It should be noted that increasing the thickness of the cell wall as a consequence of secondary wall formation in the regions away from tips for the filamentous fungi also have been previously reported by Trinci and Collinge (1975).

For fungal hyphae, there is strong evidence (Wessels, 1993) that new cell wall material is incorporated at the hyphal apex in plastic form which becomes more rigid in a time dependent process through covalent cross-linking of wall components. Wessels (1993) proposed that the cell wall initially is a semi-liquid matrix, and is rigidified as extension continues. A similar process may occur in prokaryotes (Davis, 1980). There appears to be four phases of peptidoglycan incorporation: 1) the rapid synthesis of water-soluble complex precursors 2) attachment to a membrane lipid, followed by further addition; 3) formation of linear polymer outside the membrane; and 4) crosslinking of these polymers, which may occur simultaneously with step 3.

Because the cytoplasm of walled cells typically contains more solute than the environment, these cells develop an hydrostatic pressure called turgor and the process of tip growth results from the balance between the extensive force of turgor pressure and the controlled extension of the apical cell wall (Kaminskyj and Heath, 1996). Turgor level and wall strength must be correlated, since turgor is balanced by tension in the cell wall (Koch, 1994). If a cell is growing when turgor is known to be low, then the apical wall must be soft in order to be deformed by low internal pressure. Conversely, if the wall is known to be soft, then turgor pressure must be low to maintain cellular integrity (Heath, 1995). Heath (1995) suggested that F-actin-rich elements of the cytoskeleton are important in tip morphogenesis of filamentous fungi.

There is no cytoskeleton to perform mechanical work in actinomycetes filamentous organisms, but instead has a covalently cross-linked fabric covering the entire cell that resists the cell's turgor pressure (Koch, 1994). Therefore, the growth appears to be driven by internal hydrostatic pressure which acts on an extension zone.

Studies on the early growth of *S. tendae* show that the total length of hyphae and the number of branches increase exponentially at the same specific rate (Reichl *et. al.*, 1990). The relationship between septation and branching in actinomycete hyphae is less well defined than in fungi. Branch formation have been associated with formation of septa in the case of the filamentous fungi and it usually forms behind the septum (Nielsen., 1992). However, in the case of the filamentous actinomycetes branches frequently formed in front of, rather than behind the septum (Gray *et al.*, 1987). This suggested that branch formation in filamentous actinomycetes does not result from accumulation of material behind septa and may be more closely related to the sites nucleoid aggregation (Prosser and Tough, 1991). The extent of branching also reflects the nutritional status of the medium, and on a nutritionally poorer medium, supporting lower specific growth rates, branching density can be reduced (Prosser and Tough, 1991; Martin *et al.*, 1996), where the mycelium will extend itself in the hope of reaching an environment where the growth condition are better, and it therefore forms long threads with very few branches. In the case of actinomycete filamentous organisms, lower branching frequency in a nutritionally poor media could be as a means of discovering fresh nutrients within the soil particle micro-habitat. An analogy of this would be long highways of hyphae radiating out into the soil (Martin *et al.*, 1996). On the other hand, Glazebrook and Vining (1991) have reported that slower grow rate was associated with increasing the percentage of clumps in the *S. akiyoshiensis* fermentation.

1.1.2 Fractal geometry for cellular morphology of filamentous actinomycetes

A fractal is an object in which similar structural pattern are repeated at different length scale, with the result that small sections of the object, upon magnification, appear very similar to the original object (Mihail et al., 1995). The morphology is quantified in fractal model by the value of fractal dimension (β), a parameter that represents the

distribution of mass in a fractal object. The mass m, contained in a volume element inside a three-dimensional fractal object is related to linear size, r, of the element according to the following power law equation which defines the fractal dimension:

$$m(r) \propto r^{\beta} \qquad\qquad (1.1)$$

The value of β can in principle vary between 1 for a rod to 3 for a perfect compact circular object.

The fractal model has been successfully applied and found very useful in various systems such as solution of branched polymer chains (Muthukumar, 1985), activated sludge flocs (Ganczarczk, 1990), microbial flocs (Longan, 1991), colloidal aggregates (Meakan, 1988) and protein aggregates (Ayazi Shamlou et al., 1995). In mycelia, the repeated branching of the hyphae in a tree-like form during organism growth gives rise to self-similarity and the fractal structure, and several studies have focused on the application of fractal geometry to understanding mycelia growth and biology (Jones et al., 1993; Obert, 1994; Mihail et al., 1994; Mihail et al., 1995). Patankar et al. (1993) using ultrasonic scattering procedure for measuring fractal dimension of three different mycelia organism reported a value of 2.0 to 2.7 for S. tendae and S. griseus and a value of 1.9 to 2.4 for P. chrysogenum. Even though fractal dimension is useful in quantifying structural properties of objects, it is not a unique, sufficient measure. For example, two objects may appear visually very different from one another in their structural characteristics and yet have the same fractal dimension (Smith et al. , 1996).

1.1.3 Factors affecting the morphology of filmentous actinomycetes

It has been reported for a number of filamentous actinomycetes that the number of viable spores in inoculum affects morphology. High concentration of spores tends to produce a mycelial form of growth, whereas a low concentration normally results in pellet formation (Hobbs et al., 1990). Vecht-Lifshitz et al. (1990) found that the average pellet size seemed to be inversely proportional to the order of magnitude of inoculum size.

Mycelial growth is more likely in rich, complex media, and pellets occur in chemically defined media. However, the effect of media can be extremely varied, and an individual component may only change the morphological state of a few strains (Whitaker, 1992). Kretschmer (1985) has reported that lower growth rate of *S. hygroscopicus* stimulates branching in casamino acids-limited chemostat culture, however in glucose limited chemostat culture the response was opposite. They concluded that an additional factor to growth rate determine the appearance of a branch. In *S. granticolor* culture, filamentous clumps were obtained in a complex medium but it was grown as fragmented mycelium in a defined medium (Whitaker, 1992). Shomura *et al.* (1979) found that *S. halstedii* fragmented in concentrated media and retained mycelium form in diluted medium. The presence of polyethylene-glycol in medium has been reported to favor the dispersed growth of *S. coelicolor* strain which normally form pellets (Hodgon, 1982). Addition of charged polymers to *S. lividans* cultures resulted in more dispersed growth and there exists an inverse relationship between pellet diameter and polymer concentration (Hobbs *et al.*, 1989). It may be that both electrostatic repulsion and increased medium viscosity contribute to dispersed growth (Hobbs *et al.*, 1989).

Physical fermentation condition (e.g. pH, stirrer speed and dissolved oxygen tension) can affect the morphology of filamentous actinomycetes. Glazebrook and Vining (1992) have reported that low pH of the media in the early stage of the growth phase minimize the percentage of clumps in *S. akiyoshiensis* fermentation. The effect of the environmental conditions (dissolved oxygen concentration and shear) is discussed comprehensively in section 1.3.

1.2 *Saccharopolyspora erythraea*

1.2.1 Taxonomy and growth conditions

The genus Saccharopolyspora are aerobic, gram positive, sporoactinomycetes. They were considered originally in genera of streptomyces and particularly *Saccharopolyspora erythraea* was known as *Streptomyces erythreus*. Thus, a lot of relevant literature is found under its old species name. The main differences between them and streptomyces are, that the cell wall of Streptomyces normally contain L-diaminopimelic acid (DAP) and mycolic acids while Saccharopolyspora species cell walls contain large amounts of mesodiaminopimelic acid, but no mycolic acid. This is the main reason that *S. erythraea* was renamed from the genus Streptomycetes in 1987 by Labeda. However, the two genera are not completely strange to each other. They share many macroscopic morphological characteristics, such as the form of colonies or creation of spores (Holt *et al.*, 1994).

S. erythraea grows through the formation of long multicellular hyphae with hyphal diameter of 0.4-0.8 μm, developed as branched septate. It grows between 20 to 42 °C, with an optimum of 28 to 30 °C. Like other filamentous actinomycetes the liquid cultures of *S. erythraea* require considerable aeration and agitation for the supply of oxygen and mixing necessary for maximum growth. For better supply of oxygen and mixing, flasks need to be incubated on a shaker at high speeds (e.g., 200-250 rpm). High number of growth sources (spores or hyphal fragments) must be introduced into a flask or fermenter to achieve heavy, dispersed growth and avoid pellet formation. *S. erythraea* is resistant to many antibiotics, but susceptible to lysozyme. Its cell wall envelope is rich in iso- and anteiso- branched fatty acids (Holt *et al.*, 1994).

The spores of *S. erythraea* are hydrophobic and their suspensions can be transferred more successfully if 1% Tween 80 (Polysorbitan mono-oleate) is added to the suspending medium to decrease the apparent high affinity of the spores for glass containers and pipettes (Stark and Smith, 1961). Stark and Smith (1961) have reported a decrease in erythromycin production as well as a change in morphological type when the wild strain was transferred repeatedly on agar media.

1.2.2 Biosynthesis of erythromycin

1.2.2.1 Erythromycin properties

Erythromycins which is produced by *S. erythraea* fermentation are known as one of the safest antibiotics used in human medicine. They act mainly bacteriostatically at low concentration 0.01-0.5 µg mL^{-1} by binding covalantly to prokaryotic ribosomes. Bactericidal action has been reported at high concentration above 2.5 µg mL^{-1} (against *S. aureus*). Erythromycin A is usually the main product with B, C, D, E and F as minor component. The structure of erythromycins is shown in Fig 1.1. All types of erythromycin have a desosamine ring but vary from four R groups. Erythromycin A and B have cladinose sugar, whereas erythromycin C has a mycarose sugar. They have very similar properties.
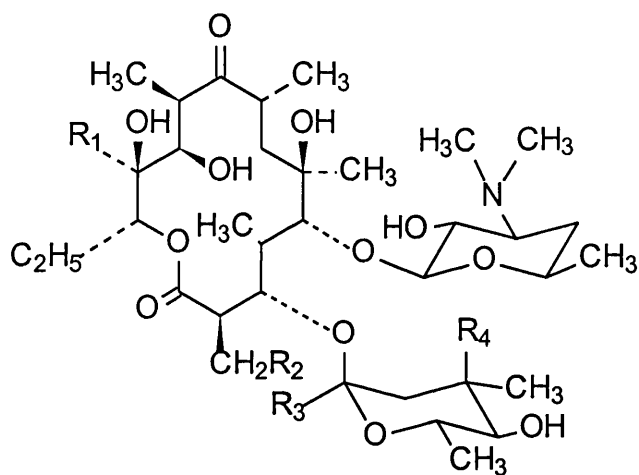
Erythromycin	R$_1$	R$_2$	R$_3$	R$_4$
A	OH	H	H	OCH$_3$
B	H	H	H	OCH$_3$
C	OH	H	H	OH
D	H	H	H	OH
E	OH	-O-		OCH$_3$

Fig 1.1: Chemical structure of erythromycin

1.2.2.2 Effect of fermentation environment on erythromycin production

Saccharopolyspora erythraea can grow over a wide pH range (pH 5-9), but the optimum for erythromycin production is between pH 7-7.2 (Osman *et al.*, 1968, Warren, 1994), and therefore a very strict pH control within ± 0.2 pH unit is required. In the literature there is very little information about the effect of temperature on erythromycin production in *S. erythraea* fermentation. Cheury and Durand (1979) recommended 35 °C for optimum erythromycin production, and Kuzentov (1985) recommended 30-35 °C.

Only a few studies have been published on the impact of the engineering environment on erythromycin production which is necessary for process optimisaton. The lack of published papers in this case is presumably due to the commercial sensitivity of the research. Brinburg (1959) reported that improving the aeration conditions increased erythromycin production (mgL^{-1}). The increase in volumetric erythromycin synthesis was due to a higher biomass production. Nikoli *et al.* (1993) reported an increased percentage of erythromycin D production, when using a mutant strain of *S. erythraea* at low dissolved oxygen tension (5% of air saturation). They have not reported any quantitative results for their experiments. Clark *et al.* (1995) reported that oxygen limitation can induce microbial secondary metabolite formation of erythromycin. Dry cell weight decreased from 6 gL^{-1} in oxygen-sufficient culture to 3 gL^{-1} in oxygen-limited-culture, while specific erythromycin production (mg (g cell)$^{-1}$) in oxygen-limited culture was 4.2 times more than oxygen-sufficient cultures. They concluded that oxygen limitation acts in an analogous manner like other substrate limitation (e.g. glucose limitation) and stimulates erythromycin production .

The effect of partial pressure of carbon dioxide was studied by Nash (1974). Carbon dioxide was added to the incoming air at 0.1 vvm or 11% (v/v) of the inlet air from 15 h to 138 h fermentation. The exposure of the cells to increased partial pressure of carbon dioxide inhibited erythromycin synthesis by 40% but had no effect on growth. The inhibition of erythromycin was not due to a reduction in pH as it remained between 6.8 and 7.0 in both carbon dioxide sparged and unsparged systems.

Martin and Bushell (1996) have shown that when *S. erythraea* biomass from submerged culture was filtered (100-120 μm sintered glass filter), the antibiotic yield of the retentate (mean hyphal particle diameter 103 μm) was significantly higher than that of the filtrate (mean hyphal particle diameter 88 μm). They hypothesise that there is a critical particle diameter, below which the particle is incapable of producing antibiotic. This would be a consequence of the site of the antibiotic production occurring at a fixed distance from the growing hyphal tip. They have proposed a protocol for calculation of the hypothetical critical hyphal diameter which led to 88 μm critical diameter for erythromycin production in their case. They have also shown, while mean hyphal diameter decreased from 124 μm at 750 rpm to 70 μm at 1500 rpm, the specific erythromycin production (mg (g cell)$^{-1}$) at 1500 rpm was only 5% less than 750 rpm experiments. Bushell *et al.* (1997) also studied the morphology and erythromycin production of *S. erythraea* fermentation in shake flasks without baffle, shake flasks with baffle and in stirred tank. The final morphology and erythromycin production was the same in all three experiments, while at the beginning, hyphal diameter and erythromycin production was higher in shake flasks without baffle compared with the two other experiments.

1.2.2.3 Composition of the medium for erythromycin production

The proposed pathway for the latter stages of macrolide antibiotics and in particular erythromycin biosynthesis have been reviewed by Higashide (1984). Erythromycin production has been observed to take place during the transition from logarithmic growth phase to stationary phase when a specific nutrient becomes growth rate limiting (Stark and Smith, 1961). Stark and Smith (1961) argued that once the nitrogen source is depleted, carbohydrate is then available for antibiotic production. Hence, the majority of erythromycin at a fast production rate occurs after the growth phase. Trilli *et al.* (1987) found evidence to suggest that erythromycin production was strongly growth-linked from the relationship between the specific growth rate and specific erythromycin production rate in a phosphate limited chemostate culture. Bushell *et al.* (1997b) have shown that in carbon limited batch culture, induction of erythromycin coincided with glucose limitation later in the culture. On the other hand, they have shown that in a nitrogen-limited culture, erythromycin production occurred

throughout the culture when nitrate was used as the only nitrogen source. They suggested that the substrate affinity for nitrate is significantly lower than that of glucose, resulting in nitrogen limitation effectively occurring throughout the culture. Wilson and Bushell (1995) have shown that in both carbon- and nitrogen-limited cultures, onset of antibiotic production coincided with the minimal protein synthesis rate.

Glucose, fructose or sucrose are all useful carbon sources for erythromycin production (Corum *et al.*, 1954) although D-glucose may have a repressive effect at high concentration (Wallace *et al.*, 1992, Escalante *et al.*, 1982). Erythromycin production enhanced when galactose was used rather than glucose (Badyopadhyay *et al.*, 1990). Glycine, glutamine, analine, valine, leucine, theonine and aspargine are appropriate nitrogen sources for growth and erythromycin production (Stark and Smith, 1961). Nitrogen limiting media have been found to produce greater yields of antibiotic than carbon limited due to the repressive effect of ammonium salts on erythromycin production (Flores and Sanchez, 1985; Potvin and Peringer, 1994). Inorganic ammonium salt was shown to severely suppress erythromycin A production (a 92% yield decrease at 50 mM ammonium initial content compared to 10 mM) (Flores and Sanches, 1985). Ammonium sulphate exerted the most suppressive effect compared with ammonium chloride and nitrate (Potvin and Peringer, 1994). There is some indirect evidence that high levels of phosphate may have a negative effect on erythromycin production. For example, high extracellular phosphate concentrations have been reported to repress the synthesis of antibiotic. Furthermore, the intracellular level of ATP (adenosine triphosphate) has often been shown to drop sharply prior to secretion of secondary metabolites (Bushell, 1988).

Typical complex industrial medium for erythromycin production includes corn starch, soybean meal, corn steep, and soybean oil as used by Abbott Laboratories (Martin and Rosenbrook, 1967). The fed batch control of erythromycin with carbon source feeding is the usual industrial procedure for optimising erythromycin production (Warren, 1994). The mineral requirements for the erythromycin fermentation have been determined (Stark and Smith, 1961). The requirement for magnesium and phosphate

appear to be the most critical, followed by a need for iron, zinc, cobalt and calcium. When either magnesium or potassium phosphate are excluded, both cell growth and erythromycin synthesis can become very poor. Mandal *et al.* (1988) found that, magnesium sulphate was essential for erythromycin biosynthesis and its optimum level was 0.05% (w/v).

The influence of n-propanol on growth and antibiotic production by an industrial strain of *S. erythraea* (p-1060) was examined by Potvin and Peringer (1993). When 1% propanol was supplemented before inoculation, the erythromycin final titre increased by 106% after 72 hr.

1.3 Effect of environment on micro-organism fermentation

1.3.1 Effect of dissolved oxygen concentration

1.3.1.1 Effect of dissolved oxygen concentration on growth and morphology

The effect of dissolved oxygen on cell growth is reported by many authors (Kubick *et al.*, 1980; Vardar and Lilly 1982; Yegneswaran and Gray 1991; Suphantharica *et al.*, 1994; Rollins *et al.*, 1991; Chen and Wilde 1990). Onken and Liefke (1989) reported a review for the effect of dissolved oxygen on growth of some organisms. Oxygen, like any other substrate, may be limiting factor for growth in aerobic cultures when its concentration in the medium falls below a critical value. Often it is considered that respiration rate becomes independent of dissolved oxygen concentration above its critical value. Critical oxygen concentration depends not only on the strain of micro-organism, but also on other variables such as the state of growth, concentration and nature of carbon, nitrogen, mineral and vitamins, accumulation of toxic compounds and products, temperature and pressure (Kargi and Moo-young, 1985). The critical oxygen concentration, below which the reaction rate is oxygen concentration controlled, is a variable that is determined by biological as well as by mixing parameters (Wang and Fewkes, 1977; Enfors and Mattiason ,1988). Wang and Fewkes (1977) showed that any change in morphology of mycelium organisms can affect response to the level of dissolved oxygen concentration. Wang and Fewkes (1977) reported lower critical dissolved oxygen for *Streptomyces niveus* fermentation at higher agitation speed.

The mass transfer of oxygen molecules from gaseous into the culture fluid is a physical process involving a number of resistances (see figure 1.2):

(i) gas film resistance between the bulk of the gas and the gas-liquid interface,

(ii) gas-liquid interfacial interface,

(iii) liquid film resistance between the bulk of the liquid and the liquid-gas interface,

(iv) liquid path resistance.
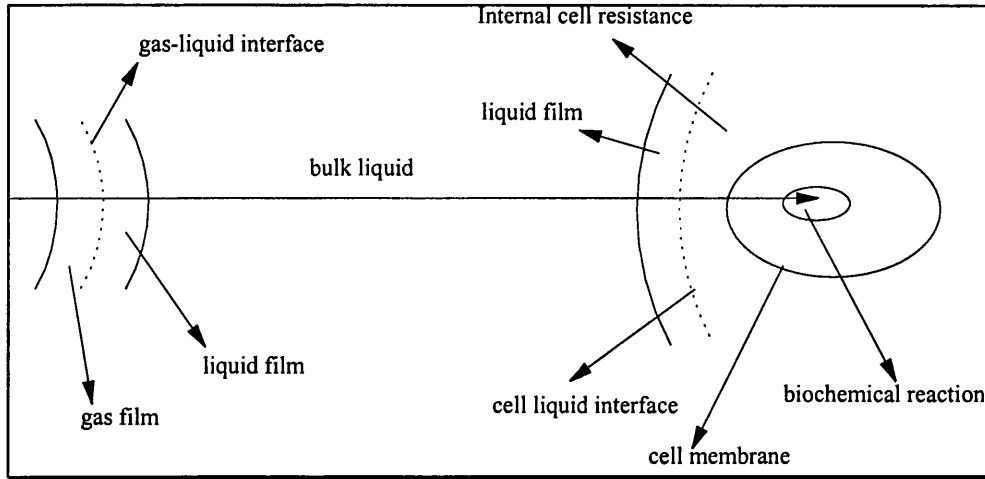
Figure 1.2: Mechanism of oxygen transfer from the air bubble to the microbial cell (produced from Bailey and Ollis , 1986).

The gas film resistance (i) is negligible compared to the liquid film resistance (iii). The gas-liquid interface has been proven as the major limiting step (Bartholomew *et al.*, 1950a). The liquid path resistance is negligible due to eddy diffusion.

Two oxygen transfers (OTR) are involved in dissolving oxygen in liquid as:

$$OTR = K_G a \ (P_{G1} - P_{G2}) \qquad (1.2)$$

and

$$OTR = K_L a \ (C^* - C_L) \qquad (1.3)$$

Where P_{G1} is oxygen partial pressure in gas phase, P_{G2} is oxygen partial pressure in gas-liquid interface, C^* is oxygen concentration at gas-liquid interface, C_L is oxygen concentration in liquid phase, K_L is oxygen transfer coefficient and 'a' is the gas-liquid interfacial area per unit volume dispersion.

For perfectly mixed vessels, these two equations are connected by Henry's constant, H, as follows:

$$H = C^*/P_{G2} \qquad\qquad (1.4)$$

The resistance of gas interface is very much less than liquid interface, so it can be assumed that

$$P_{G2} \approx P_{G1} \qquad\qquad (1.5)$$

therefore:

$$OTR = K_La \, (H \times P_{G1} - C_L) \qquad\qquad (1.6)$$

After oxygen has been dissolved, it must be distributed and delivered to individual microbial cells or their aggregates. Without adequate solid-liquid contacting, stagnant layer of liquid low in oxygen and high in carbon dioxide will surround the cells or the aggregates. While in unicellular culture, usually the limiting step is the solubility of oxygen, in filamentous cultures it is usually the transfer of oxygen to the cell surface (Bushell, 1988; Wang and Fewkes, 1977).

The effect of high dissolved oxygen concentration on morphology of filamentous organism has been investigated by various authors. Dion *et al.* (1954) have reported thicker, shorter and highly branched mycelium in penicillin fermentation when oxygen was used instead of air for aeration. Zetelati and Vas (1968) when using oxygen instead of air found a considerable decrease in the viscosity of *A. Niger* culture, even though the biomass concentration in the oxygenated culture was higher. They also found that the cell wall in the oxygenated culture were thinner and they suggested that higher flexibility of these walls could be the reason for the lower viscosity. They did not report any changes in hyphal morphology. Van Suijdam (1981a) examined the effect of dissolved oxygen concentration on filamentous fungi continuous cultures and found no significant influence of oxygen tension upon morphology for a wide range of dissolved oxygen tensions.

Vecht *et al.* (1990) studied pellet formation and cellular aggregation in *Streptomyces tendae* in submerged fermentation. They found, conditions leading to oxygen limitation tended to reduce the average pellet size and induced pulpy growth, whereas oxygen sufficiency induced pellet formation. They proposed that main forces inducing cellular aggregation in *S. tenadae* are hydrophobic interactions and are controlled by availability of dissolved oxygen.

1.3.1.2 Effect of dissolved oxygen concentration on secondary metabolite production

Dissolved oxygen concentration is known to be an important parameter in industrially antibiotic fermentation. The importance of maintaining dissolved oxygen concentration above certain minimum level for maximum specific productivity of Penicillin has been reported by various authors (Konig *et al.*, 1981; Vardar and Lilly, 1982). However, not all antibiotic fermentations are improved by maintaining DOT at relatively high levels. For example, increased production of gramcidin S has been observed under low DOT levels in *Bacillus brevis* fermentation (Vandamme *et al.*, 1981; Agathos *et al.*, 1986).

Chen and Wilde (1991) examined the effect of different dissolved oxygen concentrations and aeration rates imposed on a *S. fradiae* batch culture during the antibiotic producing phase. The rates of cellular growth, oil consumption, and tylosin production were severely reduced when the DOT fell below 25% saturation. In organisms that produce antibiotic after the end of the rapid growth phase, the yield of secondary metabolites can be influenced by the culture's previous growth history. Thus a high degree of oxygen transfer during the exponential growth phase may ultimately lead to improved antibiotic production. However, when antibiotic biosynthesis and rapid growth are taking place concurrently, and if both require oxygen as in *S. clavuligerus*, the much greater competition for oxygen could create severe dissolved oxygen deficiencies at a critical stage in antibiotic production (Rollins *et al.*, 1988). During growth of *S. clavuligerus*, control of DOT at 50% and 100% saturation increased the rate of specific cephamycin C production 2- and 3- fold respectively, compared to the experiments without DOT control (Rollins *et al.*, 1988). They suggested that the higher

antibiotic production was likely the result of increased biosynthetic enzyme activities (Rollins *et al.*, 1990).

Clark *et al.* (1995) suggested that oxygen limitation acts in an analogous manner to substrate limitation imposed by dissolved nutrients, stimulating secondary metabolite production in some cases (e.g. erythromycin production of *S. erythraea*) and inhibiting it in others (e.g. vancomycin production of *A. orientalis*). To summarise, while there are many reports for the effect of dissolved oxygen concentration on secondary metabolite production, there have been only few attempts to find the exact rule of dissolved oxygen on secondary metabolite production.

1.3.1.3 Effect of fluctuation of oxygen concentration

The region around the impeller represents a zone of high energy dissipation and therefore a region of high mass transfer rate. The remainder of the fermenter volume may suffer from inadequate supplies of nutrients and oxygen because of relatively poor mixing and stagnant zones. The viscosity of a mycelial culture with pseudoplastic properties decreases with increasing shear stress. Therefore, culture broth viscosity increases with increasing distance from the agitator in a stirred fermenter. Air bubbles sparged into the bottom of the fermenter rise through the vessel by the path of least resistance through the well-stirred, less viscous, central zones. Therefore there is an oxygen gradient in radial direction especially in large commercial fermenters.

As an effect of insufficient mixing, the oxygen transfer rate in the fermenter will vary. In combination with the slow solubility of oxygen in fermentation broths and high oxygen consumption rate this will give local variation in the oxygen concentration in a fermenter. Therefore, the culture may suffer from oxygen limitation or even oxygen starvation. Oosterhuis and Kossen (1984) have shown that this is true even for a low viscosity broth. The micro-organisms in a large fermenter are thus subjected to a continuously changing dissolved oxygen concentration in their environment. Exposure to low levels of dissolved oxygen could result in loss of productivity on scale-up. The influence of oscillating dissolved oxygen has been reported by many authors (Yegneswaren *et al.*, 1991; Bucs *et al.*, 1992; Trager *et al.*, 1992; Rollins *et al.*, 1988).

Vardar and Lilly (1982) showed that cycling oxygen concentration reduces the product formation rate and when the respiration rate is reduced to 90% of maximum value no product is formed at all. They also showed, when the conditions in a large fermenter were simulated by cycling the DOT (23-37%) in a small fermenter the specific production rate of penicillin was lower than for fermentation at constant 30% air saturation. Larsson and Enfors (1988) showed the oxygen starvation for a period of 1 minute corresponded to a 4.7% inhibition of the oxygen uptake capacity of *P. chrysogenum*. The mixing time in large fermentors is in the range of minutes (Charles *et al.*, 1978) and is sufficient to damage the metabolic capacity of cells due to oxygen starvation. To summerise, the variation of dissolved oxygen in a stirred tank usually is undesirable for growth and productivity of many organisms. This variation in dissolved oxygen will be increased with increasing the scale and pseudoplastic behavior of the cultures and it is a problem in scale up.

1.3.2 Effect of mixing and shear

For an aerated stirred tank fermenter the agitator has two main functions: the mixing of the vessel contents and the enhancement of heat and mass transfer. Many cells are delicate and can be adversely affected by agitation. Damage due to hydrodynamic forces in a bioreactor is generally referred to as shear damage. In the strict sense of the word, `shear' should only refer to the action of a force on, and parallel to, a cell surface. However, `shear' in common usage in biotechnology has become rather ambiguous, referring to all sorts of mechanical forces that might influence cells (Thomas, 1993).

In general, the size of a typical unicellular bacteria and yeast are less than the size of the microscale of turbulence (10-50 µm) in a stirred tank (Shamlou *et al.*, 1994). Furthermore, bacteria have strong cell wall and in case of yeast, its cell wall is thick and expected to be shear resistant. However, Wase and Patel (1985) have reported changes in bacterial cell volume due to agitation, Edwards *et al.* (1989) observed increases in *E. coli* cell length, and Vrana and Seichert (1988) have shown that budding yeast cells can be damaged by mechanical agitation. Despite these reports it is reasonable to assume that shear of unicellular bacteria and yeasts in fermentation is of no practical importance

(Thomas, 1993). On the other hand, filamentous fungi and actinomycetes can be several hundred microns long being comparable with microscale of turbulence in a stirred tank, and previous studies suggested that they can be damaged in shear environment (Van Suijdam and Metz, 1981; Smith *et al.*, 1990).

1.3.2.1 Effect of mixing and shear on release of intracellular material

The leakage of low molecular weight nucleotides from filamentous fungi and actinomycetes due to agitation was reported by Tanaka *et al.* (1975 a,b). They proved as the agitation speed in 5 L fermenter was increased in the range of 0-800 rpm, the release of nucleic-acid related substances also increased. This leakage was not caused by cell breakage. Eighteen strains of filamentous micro-organisms were studied, showing that the leakage phenomenon is common, and it was shown that the rate of leakage depended on strain, cultural condition, mycelia age and agitation.

In contrast, Musilkova *et al.* (1981) found that a high level of agitation led to a morphologically compact and strong mycelium and therefore the cell wall was able to provide a greater resistance to the action of hydrolysis. Ujcova *et al.* (1980) used different strains of *A.niger*. They found some of the tested strains exhibited a direct dependency of the mycelial ability to release of nucleic acid bases on increasing mixer speed. But it could not be generally presumed that the increasing mechanical forces in the fermenter bring about an increased release of nucleotides from filamentous micro-organisms into the medium. In some microbial strains this dependence could even be reciprocal. They also suggested, the release of nucleotides is probably accomplished by the cell membrane, not by the cell wall.

1.3.2.2 Effect of mixing and shear on morphology of filamentous organisms

Mechanical forces on filamentous micro-organisms might change the morphology of the filamentous organisms both by physical breakage of hyphae and by changing the development of morphology during growth. Camposano (1959) found for *A.niger*, increasing the stirrer speed from 250 to 750 in a 10 litre fermenter caused a shift toward shorter, thicker and more branched hyphae. Mitrad and Riba (1988) used an

annular reactor, and tested the effect of shear on morphology of *A.niger*. They found, at high shear rate, the filamentous organism became more branched and this resulted to higher mechanical resistance.

Studies on the effect of fermentation conditions including stirrer speed on fungal morphology were reviewed and extended by van Suijdam and Metz (1981 a). For studies on *P.chrysogenum*, morphology was characterised in terms of the main hyphal length, total length and the hyphal growth unit . For 5-L and 14-L continuous culture, it was found that morphology depended on growth rate and stirrer speed, but at a constant specific growth rate, agitation caused the hyphae to become shorter and more highly branched. By analysis of the results, they concluded that the influence of shear stress upon the hyphal length was limited. To get a substantial decrease in length an enormous increase in energy input is necessary. Therefore, this effect seems to be of little practical value as a method to decrease the viscosity of filamentous mycelium broth.

The effect of agitation on pellet forms of filamentous micro-organisms has been widely studied (Taguchi *et al.*, 1968; Elmayerg, 1975; van Suijdam and Metz 1981 b; Schugerl *et al.*, 1983 Masanory *et al.*, 1994). Taguchi *et al.* (1968) suggested two classes of fungi with respect to ease of pellet formation. Coagulating species have spores that often aggregate early in the germination process, giving pellets containing many spores. High impeller speeds in a stirred tank creates a great dispersion of spores which can be a suitable means of avoiding pellet formation of this type (Mitrad and Riba, 1988). Even after the formation of aggregates, Taguchi *et al.* (1968) noticed the damages caused by high shear stresses near the impeller. They observed two physical effects of agitation upon pellets of two fungal species. There was a decrease in pellet diameter by chipping off pellicles from the surface, and there was direct rupture of pellets.

While, there are many reports for the effect of shear environment on morphology of filamentous fungi in the stirred tank (e.g. Dion et al., 1954; Van Suijdam and Metz, 1981a.b; Mitrad and Riba ,1988; Smith *et al*, 1990; Makagiansar *et al.*,1993; Justen *et*

al., 1996; Cui *et al.*, 1997), there is very few quantitative studies in the case of the actinomycetes filamentous organisms. Belmar Campero and Thomas (1990) studied the effect of stirrer speed in 5-L batch fermentation for *S. clavuligerus* using semiautomatic image analysis method for morphological measurement. They found that increasing the stirrer speed accelerated the fragmentation and subsequent regrowth. Martin *et al.* (1996) reported in *S. erythraea* fermentation, mean mycelia diameter decreased from 124 µm to 70 µm when the stirred speed in a 3-L fermenter increased from 750 rpm to 1500 rpm. There is no suggesting model or even correlation for breakage of the actinomycetes filamentous organisms in stirred tank in the open literature, while the breakage model for the filamentous fungi has been studied by many authors which will be discussed in section (1.4.6).

1.3.2.3 Effect of mixing and shear on growth

Higher agitation improves culture homogeneity, preventing aggregation of solid particles and cells, assisting gas to liquid and liquid to cell mass transfer and may reduce the viscosity of the filamentous fermentation. These can improve the growth of the organism. Konig *et al.* (1981) studied the effect of stirrer speed for two strains of *Penicillium chrysogenum*. They reported, at lower stirrer speed, gas dispersion was inadequate and the insufficient oxygen transfer rate was a limiting factor. At higher stirrer speed, the oxygen supply was improved and more cell mass was formed. This result was the same for both strains.

On the other hand agitation can be detrimental for growth of the filamentous orgainsms. Tanaka *et al.* (1975) found an influence of agitation shock on *Mucor javanicus* and *Rhizopus javanicus* mycelia. According to these authors, intracellular nucleotides were released into the medium. Since these nucleotides had to be continually replaced by the organism its ability to grow was affected and the growth rate decreased.

Belmar Campero and Thomas (1990) reported the effect of stirrer speed on growth of *S. clavuligerus* in 5 litre batch fermentation. They found cell growth was not dependent on stirrer speed, although the final biomass concentration was less at lower

34

stirrer speed. Dissolved oxygen was above 60% in all the experiments, and they suggested it is above critical dissolved oxygen for growth. Choi *et al.* (1996) used oil as carbon source in *S. fradiae* 3-L batch fermentation at constant dissolved oxygen tension (40%). They reported oil consumption increased at higher stirrer speeds (650 and 900 rpm) compared with lower (250 and 400 rpm) stirrer speed. Dry cell weight and mophological parameters were not measured. The viscosity was less at higher stirrer speeds, but it was not clear if it is because of breakage of the mycelia or lower biomass concentration. Wang and Fewkes (1977) observed an increase in biomass production and specific oxygen uptake rate of *Streptomyces niveus* at constant DOT levels with increasing stirrer speed and related it to the liquid to cell mass transfer rate. To summarise, low cell growth at low stirrer speeds is generally related to oxygen transfer, while low cell growth at high stirrer speeds is usually related to cell damage.

1.3.2.4 Effect of mixing and shear on productivity

It is difficult to distinguish the effect of mechanical shear forces from other effects such as oxygen transfer. The filamentous form of the mycelial hyphae easily causes suspensions that can be very viscous and at lower stirrer speeds the culture may be oxygen limited. Although the organisms may suffer greater shear damage as the stirrer speed is increased, the increased oxygen transfer may result in an increased titre. There will be an optimum stirrer speed at which increased transfer no longer compensates for the increased cell damage and titre will begin to decrease.

Camposano *et al.* (1959) reported a severe reduction under high shear conditions, in kojic acid production by *Aspergillus flavus,* and concluded that mechanical agitation maintained the mycelium in a state which increased the branching of hyphae and thickening of the cell wall. This diverted the glucose metabolism from partial oxidation to kojic acid, towards the production of cell material. Ujocova *et al.* (1980) used various species of *A.niger* in laboratory scale fermenter. They reported optimal stirrer speed for citric acid production. They related low productivity in the range of low mixer speed to the shortage of dissolved oxygen. The optimal stirrer speed for various strains was different. Stirrer speed for maximum citric acid production was

not the same as for maximum biomass growth. For example for one of the strains the optimal stirrer speed for citric acid production was 600 rpm, although the maximum biomass growth was reached at 800 rpm. Makangiansar *et al.* (1993) studied the effect of agitation on the morphology and production of *Penicillium chrysogenum* in different scale. To separate the effect of dissolved oxygen tension from shear forces, they did their experiment above critical dissolved oxygen. They reported, the specific rate of penicillin production (q_{pen}) and the mean main hyphal length during the linear penicillin production were lower at high agitation speed.

There is little work published on the effect of stirrer speed on the cell growth and productivity of filamentous actinomycetes. Tarbuck *et al.* (1985) varied stirrer speed in 10 L batch fermentation of *Streptomyces clavuligerus* and found a dramatic decrease in clavulanic acid production when the stirrer speed was increased from 375 rpm to 500 rpm. These results were not discussed. At a lower stirrer speed (250 rpm), the productivity was less than at 375 rpm, which could be related to oxygen transfer. Belmar Campero and Thomas (1990) used *S. clavuligerus* in 5 litre fermentation at different speed 490, 990 and 1300 rpm. They used similar medium as Tarbuck *et al.* (1985), but their results on clavulanic acid production showed little dependence on stirrer speed. They compared their results with productivity of several fungi in other literature, which were stirrer speed dependent. They concluded, it was possible that streptomycetes are less sensitive to shear in comparison with fungi because of their smaller size in length and diameter. Wang and Fewkes (1977) examined the effect of operating and geometric parameters on antibiotic production of *S. niveus*. They reported significantly higher novobiocin production at higher stirrer speed, but specific novobiocin productivity (g (g cell)$^{-1}$) did not change significantly. They concluded that the direct consequence of the final antibiotic titre is a result of the amount of cell biomass. Tylosin production increased when stirred speed increased from 250 rpm to 400 rpm in 3-L batch fermentation of *S. fradiae* at constant dissolved oxygen tension (40%), and a further increase in stirrer speed led to lower tylosin production (Choi *et al.*, 1996). These authors used oil as carbon source and biomas data was not reported by them. Therefore it is impossible to find the effect of stirrer speed on specific tylosin production. Specific erythromycin production decreased only

by 5% when stirrer speed increased from 750 to 1500 rpm in a 2-L *S. erythraea* batch fermentation (Martin *et al.*, 1996). To summarise, the comparison of available reports in open literature suggests that in the majority of the cases the effect of stirrer speed on secondary metabolite production of filamenous actinomycetes is less pronounced in comparison with filamentous fungi. Changes in morphology, the chemical composition of cell wall, permeability of the cell membrane and metabolite path way could be some of the consequences of variation in shear rate which can affect the productivity, assuming that the dissolved oxygen is above the critical level.

1.4 Turbulent breakage of particles in stirred tank

1.4.1 Fluid motion in stirred tank aerated vessel

The Rushton turbine is the most common impeller type using in stirred tanks for dispersions. This impeller produces radial flow and high shear rates near the impeller, which are important for air dispersion in aerobic fermentations, whereas other axial flow impellers such as pitched-blade paddles are employed when high circulation rates are desired or if lower shear rates are necessary.

Flow visualization studies carried out by Van't Riet & Smith (1975) showed that flow around the impeller blade created a pair of trailing vortices behind each blade. These vortices were found to contain high velocity gradients and have been considered as a region of very high shear. However, when gas is added to a turbine-impeller stirred tank, it is drawn to the low pressure regions at the rear of the blades, forming ventilated gas cavities and the strong vortex is not present anymore. Therefore, it is likely that dispersion in aerated stirred tank will take place in the jet stream coming from the impeller. The dispersion area will probably not extend far behind this jet stream in the case of pseudoplastic fluids due to increased viscosity at some distance from the impeller. Investigations by van't Riet *et al.* (1975), Nienow *et al.* (1983) and Ismail *et al.* (1984) clearly indicate that gas filled cavities have a major influence on the hydrodynamics and power drawn of an impeller. Cavities cover the rear of the blades, reducing the impeller power consumption, the interfacial area and the rate of interface mass transfer.

1.4.2 Turbulence energy dissipation rate in a stirred tank

The flow regions of a stirred vessel may be classified into the circulation region and the region surrounding the impeller. The two main regions of the flow field differ substantially in terms of macroscopic and microscopic flow characteristics. The flow region with the highest turbulence intensity and high energy dissipation is the impeller region and the region of low turbulence intensity and low rates of energy dissipation is the circulation region. The importance of this high energy dissipation near the impeller is that material circulating around the vessel will be exposed to different

shear environments, and damage might depend on the rate of circulation in high shear zones, average shear rate or peak shear rate (Smith *et al.*, 1990; Makangiansar *et al.*, 1993; Justen *et al.*, 1996). Even in a sparged vessel, high shear occurs near the impeller blades.

Cutter (1960) has indicated, on the basis of indirect measurements, that the local rate of energy dissipation varies by several orders of magnitude throughout a stirred tank. Okamoto et al. (1981), Costes and Couderc (1988), Wu and Patterson (1989) also reported different values for maximum energy dissipation rate around the Rushton turbine impellers which are summarized in table 1.1. There is a substantial variation in the reported results, which is due to differences in the tank geometry and consideration of the different volume around the impeller for this maximum dissipation rate. The variation for unbaffled and baffled tanks indicates that the flow in a baffled tank is more homogeneous than the flow in unbaffled tank (Okamoto *et al.*, 1981).

Table 1.1 : Energy dissipation rate in the stirred tank with Rushton turbine impeller

References	$\varepsilon_i/\varepsilon_{ave}$	$\varepsilon_b/\varepsilon_{ave}$	$\varepsilon_i/\varepsilon_b$
Cutter (1960)	7.7	0.26	30
Okamoto *et al.* (1981), baffled tank	6.5	0.16	41
Okamato *et al.* (1981), unbaffled tank	11.3	0.21	53
Costes and Couderc (1988)	5 - 10	0.05 - 0.07	100 - 140
Wu and Patterson (1989)	22	-	-

Okamoto *et al.* (1981) considered different geometry for the Rushton turbine impeller and reported the following correlation for the local turbulence energy dissipation rates in the impeller stream ε_i, and in the circulation region ε_b (Equation 1.7 & 1.8). These equations give lower $\varepsilon_i/\varepsilon_{ave}$ for higher D/T . This indicates that flow in a tank with high D/T ratio is more homogeneous than the tank with low D/T ratio.

$$\varepsilon_i/\varepsilon_{ave} = 7.8(D/T)^{-1.38} \exp(-2.46D/T) \qquad (1.7)$$

$$\varepsilon_b/\varepsilon_{ave} = 0.9\ (D/T)^{1.1} \qquad (1.8)$$

The main reason for discrepancy between the reported energy dissipation rate around the impeller is the dissipation volume. Placek and Tavlarides (1985) considered simply the cube of impeller diameter for calculation of energy dissipation around the impeller, D^3. Wu and Patterson (1989) found that the energy dissipation is greatest between $1.08R < r < 2.26R$ where r is the radial distance from the impeller center and R' is the impeller radius (i.e. $= D/2$). This defines an annular region of high turbulence with volume equal to $1.24D^3$. Kresta and Wood (1991) considered the highly turbulent volume near the impeller as an annular cylinder, and found this cylinder to be bounded by $-0.5W_i < z < 0.5\ W_i$ and $R' < r < 1.45\ R'$ This defines a region of volume $0.17D^3$. Aloi and Cherry (1996) considered the space around the impeller occupied with vortices for calculating the maximum power dissipation. They used Van't Riet and Smith (1975) photographs, considering 2 vortices per blade with radius of $W_i/4$, a vortex length of $6W_i$ and considering vortices cylindrical in shape with a conical end, ,concluding that the total volume for all 12 vortices is equal to $0.075\ D^3$.

Zhou and Kresta (1996) examined the maximum turbulence energy dissipation rate for Rushton turbine, pitched blade turbine and fluid foil turbine. They showed that the maximum local dissipation is larger for impellers with a larger power number. The maximum dissipation was located on the traverse immediately below the impeller for the three axial impellers, and on the traverse at the tip of the impeller blades for the Rushton turbine, and the variation of dissipation energy was more for Rushton turbine comparing with axial flow impellers (e.g. pitched blade turbine).

It should be noted that pseudoplastic fluids can localise fluid motion around the impeller (Metzener and Taylor, 1960) and this leads to high values of ($\varepsilon_i/\varepsilon_{ave}$) compared with Newtonian fluids. However, little has been published on local

dissipation energy and shear rates in non-Newtonian fluids in stirred tanks, except as a means of predicting the total power consumption.

1.4.3 Shear rate in a stirred tank

Shear rate is defined as velocity gradient dv/dx, therefore has a unit of s^{-1}. The average shear rate has been related to impeller speed (Metzner & Taylor, 1960) as:

$$\gamma_{ave} = K_s \cdot N \qquad (1.9)$$

where γ_{ave} is the mean shear rate and K_s is the impeller shear rate constant dependent on the geometry of the impeller. This concept originated by Metzner and Otto (1957), strictly applies to the laminar and flow regime, but has been used for turbulent flow situations by some researchers. Equation 1.9 suggests the impeller diameter has no effect on average shear rate. However, Metzner and Taylor (1960) showed for two different impeller size, that shear rate at a given distance from the impeller is slightly greater for the larger impeller. They also showed that this difference in shear rate is larger for Newtonian fluid than pseudoplastic fluid. They concluded that the effect of diameter on shear rate decreases with increasing pseudoplasticity.

Metzner and Taylor (1960) for pseudoplastic fluids reported, local fluid shear rates were directly proportional to impeller speed, but that the shear rate decreased much faster with increasing radial position as compared to Newtonian fluids. The fluid velocities in the horizontal plane of the impeller varied almost linearly with rotational speed in Newtonian systems, on the other hand movement in pseudoplastic systems increased exponentially with impeller speed. They reported a value of K_s of 34.5 at the impeller tip which reduced to a value of 3 at a distance of 2.5 cm from the impeller (D = 10cm). They also reported that the fluid motion is localised around the impeller zone in pseudoplastic fluid and therefore increases the shear rates (e.g. K_s was 78 at impeller tip for the 1.2% CMC solution)

In dispersion processes, the effect of average shear rate and maximum shear rate will determine the ultimate particle size. However, if the material is in the mixing tank

long enough (e.g. batch fermentation in stirred tank), then the ultimate particle size will be determined by the maximum shear rate around the impeller zone, since the particle will eventually move into that zone. It is not as yet possible to describe mathematically the complex flow field around a rotating impeller in a tank (Boye et al., 1996). However, with some simplification, a few correlations for shear rate of turbine impeller in a fully baffled stirred tank have been compared with experimental data. For example Cutter (1966) has shown for water at high Reynolds number the maximum shear rate in a stirred tank with Rushton impeller can be obtained by equation 1.10:

$$\gamma_{max}/N = 4.8\ Re^{0.5} \qquad (1.10)$$

Wichterle et al. (1984) have shown the shear rate on turbine impeller for Newtonian and pseudoplastic fluids as:

$$\gamma_{max} \propto (1 + 5.3\ n)^{1/n}\ Re^{\ 1/n+1} \qquad (1.11)$$

Another quantity often used to characterize the shear field in a stirred tank is the local intensity of mechanical energy dissipation ($\varepsilon = \tau\gamma/\rho$), which leads to (Wichterle et al., 1984)

$$\gamma = (\varepsilon/v)^{0.5} \qquad (1.12)$$

Equation 1.12 has been applied to the calculation of shear rate in turbulent regime by many authors (Parker et al., 1972; Tomi and Bagster, 1978; Matsuo and Unno, 1981; Ayazi shamlou et al., 1994). It should be noted that substitution of $Re = \rho ND^2/\mu$, in equation 1.10 leads to $\gamma_{max} = 4.8\ N^{1.5}D/v^{0.5}$ and for impellers with the same geometry in turbulent flow regime $(N^{1.5}D/v) \propto (\varepsilon/v)^{0.5}$. Therefore, equation 1.10 also leads to $\gamma_{max} \propto (\varepsilon/v)^{0.5}$ which is similar to equation 1.12.

1.4.4 Isotopic turbulence theory

In a typical stirred tank fermenter, especially with high impeller tip speed, turbulent or at least locally turbulent fluid flow can be assumed in the impeller region. Primary eddies have a scale (λ) proportional to the diameter of impeller (D). These large scale eddies contain almost all of the energy and no energy is dissipated by them. The large scale eddies are usually unstable and disintegrate into smaller eddies of intermediate size. These eddies transfer kinetic energy from the large to small eddies, and because this transfer occurs in different directions, directional information of the large eddies is gradually lost and they are called isotropic, i.e. no preference for any direction exists. These last range of eddies has been termed the universal equilibrium range. Kolmogorov (1941) suggested that for fully turbulent flow conditions, the properties of the eddies in universal subrange are determined only by the energy input. This has been further divided into two subranges, inertial subrange and viscous dissipation subrange. Eddies in the so-called viscous dissipation subrange have sizes smaller than the Kolmogorov microscale of turbulence, while eddies with sizes greater than Kolmogorov microscale belong to the inertial convection subrange.

By dimensional analysis, Kolmogorov microscale of turbulence has been related to energy dissipation rate per unit mass, ε (m^2s^{-3}) and the kinematic viscosity, ν (m^2s^{-1}), with equation 1.13.

$$\lambda = (\nu^3/\varepsilon)^{1/4}$$ (1.13)

1.4.5 Prediction of Particle size in fully turbulent flow in a stirred tank

Turbulence has been associated with the presence of eddies and the interaction between eddies and particles has been considered as a mechanism for disruption of the particle by many authors (Thomas, 1963; Tombo and Hozumi, 1979; Ayazi Shamlou *et al.*, 1994; Cui *et al.*, 1997). Relative size of the eddies and particles are one of the parameters affecting the mechanism of the fluid-particle interactions in turbulent flow (Tomi and Bagster, 1978; Ayazi Shamlou *et al.*, 1994). Thomas (1963) has given the mechanism of rupture of solid aggregates in turbulent flow in inertial subrange for the particles which have the size (d) bigger than the size of the microscale of turbulence

43

(d >> λ). He postulated that the basic mechanism leading to aggregate deformation and rupture can be described to be instantaneous pressure difference on opposite side of the unit, p(d). These pressure differences will lead to rupture providing that:

$$\sigma_{crit} \leq p(d) \qquad (1.14)$$

The term, σ_{crit}, represents the limiting material strength of the unit. The instantaneous pressure difference on opposite side of the unit are induced by velocity fluctuations experienced over the surface of the aggregate. These velocity fluctuations are represented by the term $u'_r(d)$ which was defined as the root mean square value of the difference in relative velocity over a scale, d (equation 1.15)

$$[u'_r(d)]^2 = [u'_r(d + x) - u'_r(x)]^2 \qquad (1.15)$$

Thomas (1968) assumed that fluctuations of velocity in the fluid will produce the same fluctuations across the particle even if the particle is moving relative to the liquid. Thus:

$$u'_r(d) \sim u'_f(d) \qquad (1.16)$$

Where $u'_f(d)$ is the mean square velocity difference between two points in the fluid separated by a distance d. Therefore, the pressure fluctuation, p(d), was estimated by:

$$p(d) = C\, \rho u'_r(d)^2 \sim C\rho u'_f(d)^2 \qquad (1.17)$$

Where C lies between 0.7 and 2 (Thomas, 1963 and Hinze, 1959). Value of $u'_f(d)$ in the inertial subrange have been found by application of the theory of local isotropy (Thomas, 1968).

$$u'_f(d) = (\varepsilon d)^{1/3} \qquad (1.18)$$

Combining equations (1.14), (1.17) and (1.18) at the critical conditions leads to:

$$\sigma_{crit} \propto \rho(\varepsilon d_{max})^{2/3} \qquad\qquad (1.19)$$

For a particle with uniform structure for which strength is independent of size, it leads to:

$$d_{max} \propto \varepsilon^{-1} \qquad\qquad (1.20)$$

Particles which are smaller than the turbulent microscale, reside within an eddy and breakage occurs by viscous stresses in the eddy. The viscous stresses are given by the product of the shear rate and the suspension viscosity (Boye *et al.*, 1996). Tambo and Hozumi (1979) suggest that the condition of viscous dissipation subrange is likely to be $d \leq \lambda$. However, these researchers described successfully the breakage of clay aluminum flocs in a mechanically stirred batch flocculator using the condition of viscous dissipation subrange even though the criterion of $d \leq \lambda$ was not strictly fulfilled. It has been suggested that the viscous dissipation subrange can be extended to eddies in size range of up to about $10\ \lambda$ (Tambo and Hozumi, 1979; Muhle and Domasch, 1991; Ayazi Shamlou *et al.*, 1995). The relative velocity fluctuations over the surface of a particle are due to localized velocity gradients, which may be represented by $(\varepsilon_i/v)^{0.5}$ as it was discussed in section (1.4.3), and the shear stresses acting across the particle is $\tau = \mu(\varepsilon_i/v)^{0.5}$ (Tomi and Bagster, 1978; Ayazi Shamlou *et al.*, 1994; Matsuo and Unno, 1981; Packer *et al.*, 1972).

Another mechanism has been recommended for disruption of animal cells (Cherry and Papoutsakis, 1986), oil drops in suspensions (Leng and Quarderer, 1982; Kumar *et al.*, 1991; Boye *et al.*, 1996) is breakage in boundary layer. Relatively large shear rates and shear stresses are expected in the boundary layer around solid objects submerged in the stirred tank. The moving impeller would be expected to have the highest velocity relative to the fluid, and relatively high shear rate are expected in the boundary layer around the disk or the blades of a rotating Rushton turbine. A particle present in the boundary layer around the disk or blades of a rotating Rushton turbine can experience strong shearing action leading to its breakage provided the particle

size is smaller than the boundary layer thickness and the residence time of the particle is enough for the breakage (Boye *et al.*, 1996).

The gradients in a direction along the blade can be assumed to be small compared to those in a perpendicular direction to the blade (Kumar *et al.*, 1991). When particles are moving in a direction perpendicular to the blade they experience varying rates of shear. It is not as yet possible to describe mathematically the complex flow field around the rotating disk in a tank. However, with some degree of reasonable simplification the shear rate in the boundary layer of the impeller has been derived (Boye *et al.*, 1996).

Schlichting (1979) states that for a rotating disk, the transition from laminar to turbulent flow occurs at a disk Reynolds number ($Lu_\infty/2\nu$) of approximately 3×10^5. Boundary layer thickness (δ_t) defined as the distance from the impeller surface at which the fluid velocity reaches 99% of the free fluid velocity (u_∞), is given by

$$\delta_t = 5(L/2)Re_d^{0.5} = 5 \ (\nu L/2u_\infty)^{0.5} \text{ for laminar boundary layer} \qquad (1.23)$$

and

$$\delta_t = 0.37 \ (L/2)/Re^{0.2} \text{ for turbulent boundary layer.} \qquad (1.24)$$

The maximum shear rate in the boundary layer is in the order of u_∞ /δ_t (Boye *et al.* 1996), where u_∞ is the liquid velocity at the tip of the disk (α ND), which leads to

$$\gamma_{max} \ \alpha \ u_\infty/ \ \delta_t \ \alpha \ ND/\delta_t \qquad (1.25)$$

By substitution of the boundary layer thickness from equation (1.23) and (1.24), and assuming L is proportional to disk diameter (L α D) due to geometrical similarity, this gives:

$$\gamma_{max} \ \alpha \ N^{1.5} \ D \ \nu^{-0.5} \qquad \text{for laminar boundary layer} \qquad (1.26)$$

$$\gamma_{max} \; \alpha \; N^{1.2} \, D^{0.4} \, v^{-0.2} \qquad \text{for turbulent boundary layer} \qquad (1.27)$$

Maximum shear rate in boundary layer (equation 1.26 or 1.27) has been used to predict the maximum particle size in the stirred tank (Grace *et al.*, 1982; Boye *et al.*, 1996).

1.4.6 Application of turbulent breakage for filamentous organisms

While, there is many reports for breakage of the filamentous fungi in a stirred tank, only few researcher recommend a mathematical model for the effect of the shear environment (Bhavaraju and Blanch, 1976; van Suijdam and Metz, 1981 a & b; Smith *et al.*, 1990; Ayazi Shamlou *et al.*, 1994a; Cui *et al.*, 1997). As far as breakage of the filamentous actinomycetes is concern there is very few reports for the effect of shear environment in stirred tank (see section 1.3.2.2) and there is no correlation or model for this filamentous organisms in the open literature.

The collisions of particles either with each other or with impeller blades or baffles are unlikely to happen in the case of fungal or microorganisms in general (Ayazi Shamlou *et al.*, 1994a; Cui *et al.*, 1997). These particles have a density of the same order of magnitude as the suspending fluid and hence can be assumed to follow the streamlines of the fluid and consequently, the drag and body forces acting on such organisms will be negligible (Matsuo and Unno, 1981). Experimental evidence of this has been given by Tanaka (1976), who showed that fracture of hyphal particles caused by collisions with baffles and stirrer blades did not happen.

The model for fungal break up has been developed based upon the same fundamentals as already mentioned for particles in sections 1.4.5 (Bhavaraju and Blanch, 1976; van Suijdam and Metz, 1981 a & b). With the Kolmogorov scale of turbulence in stirred bioreactors typically in the range of 10-50 µm (Ayazi Shamlou and Titchener-Hooker, 1993) and hyphal length in the range of 100-300 µm or pellet diameter in the range of 0.1 -5 mm, it is likely that breakage will take place in the inertial subrange. Therefore,

the velocity fluctuations experienced over the surface of the organism can then be given by

$$u' = c(\varepsilon d_p)^{1/3} \qquad (1.28)$$

where d_p is the diameter of the pellet or dispersed mycelia. Diameter of the dispersed mycelia has been defined by Martin *et al.* (1996) and it is the same as major axis in this reports (see section 2.3.8). Therefore, the pressure difference between the points at opposite end of the organism can be written by equation (1.29):

$$P(d_p) = C \rho(\varepsilon d_p)^{2/3} \qquad (1.29)$$

This pressure difference leads to shear forces. A constant ratio was assumed between the breakup forces (F_b) and the coherence forces (F_c) among the hyphae (Van Suijdam and Metz, 1981 a & b; Metz *et al.*, 1981). The breakup forces assumed to be proportional to the product of turbulent shear forces and cross sectional area of the pellet or surface of the dispersed mycelial.

$$F_b \propto p(d).d_p^2 \qquad (1.30)$$

The coherence forces were written (Bhavaraju and Blanch, 1976; Van Suijdam and Metz, 1981 a & b; Metz *et al.*, 1981) as:

$$F_c \propto \pi.d_p.w.\sigma \qquad \text{for pellet} \qquad (1.31a)$$

$$F_c \propto d_h.w.\sigma \qquad \text{for dispersed mycelia} \qquad (1.31b)$$

Where σ is the tensile strength of a hyphal structure, d_h is the hyphal outer diameter and w is the thickness of the outer layer of the pellet or the cell wall thickness of the mycelia. Equation (1.31a) was based upon the assumption that only a constant outer layer of the pellet of thickness w, contributes to the tensile strength. The constant force ratio was expressed by the dimensionless Weber number:

$We = p(d_p).(d_p)^2/d_p.w.\sigma$ for the pellet   (1.32a)

$We = p(d).(d_p)^2/d_h.w.\sigma$ for the dispersed mycelia   (1.32b)

Combination of equation (1.29) and (1.32a) for the pellet or equation (1.29) and (1.32b) for the mycelia and assuming that σ, w and d_h are constant, leads to

$d_p = c\varepsilon^{-0.4}$ for the pellet   (1.33a)

$d_p = c\varepsilon^{-0.25}$ for the dispersed mycelia   (1.33b)

Earlier data from Taguchi *et al.* (1968) were examined by van Suijdam & Metz (1981b) and it was found that the mean equilibrium pellet diameter was proportional to $\varepsilon^{-0.15}$, which was not in good agreement with theoretical equation (1.33a). Variation of tensile strength of the hyphae has been suggested to be one of the reasons for this disagreement. They showed good agreement with the model and their own experiments.

Van Suijdam and Metz (1981a) proposed a model for kinetic of breakage, based on the dynamic equilibrium between growth and break up of the hyphae, assuming that break up of the mycelia occurs when the local shear forces in the vessel are higher than the forces necessary to break the hyphae. Their model was based on the concept of a break up frequency which is proportional to the frequency of passage of mycelia in the dispersion zone around the impeller (V_{dis}). Making some assumptions, they concluded that the break up frequency for mycelia with an effective hyphal length (L_h) and hyphal diameter (d_h) can be expressed by equation 1.34.

$$\text{Break up frequency } \alpha \ N^{1.75} D^{0.5} \qquad (1.34)$$

Finally with additional assumptions, they deduced that the breakage rate can be expressed as:

$$-dL_h/dt = (C_1 N^{1.75} D^{0.5}/d_h^{0.38})L_h^2 - C_2 N^{0.25} d_h^{0.38}/D^{0.5} \qquad (1.35)$$

The model only gave qualitative agreement with experimental data. It was suggested that variations of tensile strength of hyphae with age and culturing condition could have been one cause of disagreement.

Reuss (1988) used non-septa fungi, *Rhizopus nigricans*, for his experiment. It was assumed that for non-septa fungi, cell-wall breakage should result in complete loss of intracellular material and cell death. They showed that an increase in stirrer speed (in a 137 L culture) from 217 rpm to 373 rpm reduced the maximum specific growth rate from 0.339 h^{-1} to 0.245 h^{-1}. However a decrease was also obtained at constant speed when only the volume of the culture was changed (by increasing the liquid height). Reuss (1988) deduced from these experiments that tip speed alone is not a good scale-up parameter. It was suggested that the ratio of power input to flow rate around the vessel ($P_t t_c/V_L$) might be a better parameter, with t_c representing circulation time which was calculated by equation 1.36

$$Nt_c = 0.76 \, (H/T)^{0.6} \, (T/D)^{2.7} \qquad (1.36)$$

Smith *et al.* (1990) suggested that hyphal break up depends on the frequency of mycelial circulation through the zone of high energy dissipation around the impeller. Using *Penicillium chrysogenum* they showed reasonably good agreement for hyphal break up and penicillin production by equation 1.37.

$$L_h \propto P_t / D^3 t_c \qquad (1.37)$$

Shamlou *et al.* (1994a) proposed that hyphae break as a result of direct tensile stresses acting at its opposite ends. Other forms of stress, e.g. direct compression, bending and torsional, were considered less significant. Assuming that the hyphae behave elastically under the prevailing stress condition, and using the classical strain energy criterion of failure they deduced that the equilibrium hyphal lenght (L_h) can be:

$$L_h \alpha \frac{\left(S_F E\right)^{3/7}}{\rho^{6/7} A^{3/7} \varepsilon^{4/7}}$$

(1.38)

Assuming A, S_f, E. and ρ are constant, equation (1.40) led to

$$L_{hmax} \; \alpha \; \varepsilon^{-4/7}$$

(1.40)

They showed reasonable good agreement between model and their own data and also data in the literature for fungi mycelia. Pellets showed a weaker dependency on ε, in the region where ε was less than 0.5 w/kg. They suggested that this is due to stronger mechanical properties of the pellets compared with mycelia.

Shamlou *et al.* (1994) using first-order kinetics for hyphal breakage correlated breakage rate constant K_b, to $P_t / D^3 t_c$. They assumed $t_c \; \alpha \; 1/N$ and in the turbulent flow regime $P_t \; \alpha \; N^3 D^5$ and derived $P_t / D^3 t_c \; \alpha \; N^4 D^2$. They used experimental data for *Penicillium chrysogenum* in 7, 20 and 150 L fermenter finding $K_b \; \alpha \; (P_t / D^3 \, t_c)^{0.2}$ and finally expressed, K_b, for the mycelia as $K_b \alpha \; N^{0.8} \, D^{0.4}$.

Justen *et al.* (1996) used the correlation recommended by Smith and Lilly (1990) and developed it for breakage of the *Penicillium chrysogenum* in stirred tanks using different impeller types including Rushton turbine, paddle, pitched blade, propeller and Prochem maxflow T. They considered the trailing vortices formed in the impeller as the volume in which breakage occured and modified the $(P_t/D^3)(1/t_c)$ recommended by Smith *et al.* (1990) to $(P_t/K'D^3)(1/t_c)$, where K' is dependent on geometry of the impeller and also on the number of the vortices formed per blade. The relation worked successfully for the range of experiments carried out by these authors. It should be noted that they carried out their experiments outside the fermentation and without aeration. Samples were taken from the fermenters and diluted and agitated for 30 min by different impellers. As was discussed earlier (section 1.4.1) in the case of aerated stirred tank, it is likely that dispersion will take place in the jet stream coming from the impeller not the trailing vortices behind the impeller.

Cui *et al.* (1997) have reviewed the correlations available in the literature for the equilibrium size of the dispersed mycelial fungi and concluded that $L_h \propto \varepsilon^{-(0.25 \pm 0.08)}$. They compared the relation ($L_h \propto \varepsilon^{-0.25}$) with Kolomogorov microscale of turbulence ($\lambda = \varepsilon^{-0.25} \nu^{0.75}$) and concluded that the size of the particles in the turbulent flow are often proportional to Kolmogorov microscale of turbulence.

1.5 Rheology of filamentous cultures

Filamentous fungi and actinomycetes consist of long, thin, usually branched, in three dimensional network which may give very viscous non-Newtonian broth rheology. The pelleted type of growth consisting of compact discrete masses of hyphae, generally lead to Newtonian behavior of the broth. In addition, there are some reports indicating non-Newotonian behaviour of the pelleted cultures (Witter *et al.*, 1983).

1.5.1 Rheological models

A very general equation for the rheologial behaviour of a time independent liquid is as follows:

$$\tau = \tau_0 + K \gamma^n \tag{1.40}$$

where

τ = shear stress

γ = shear rate

τ_0 = yield stress

K = consistency index

n = flow behavior

Table 1.2 shows some special forms of this equation and they are shown graphically in Figure 1.3.

Table 1.2: Rheological models

Rheological model	τ_0	n
Newtonian	0	1
Bingham plastic	non zero	1
Paeudoplastic	0	<1
Dilatant	0	>1
Hershschel-Bulkley	non zero	non zero
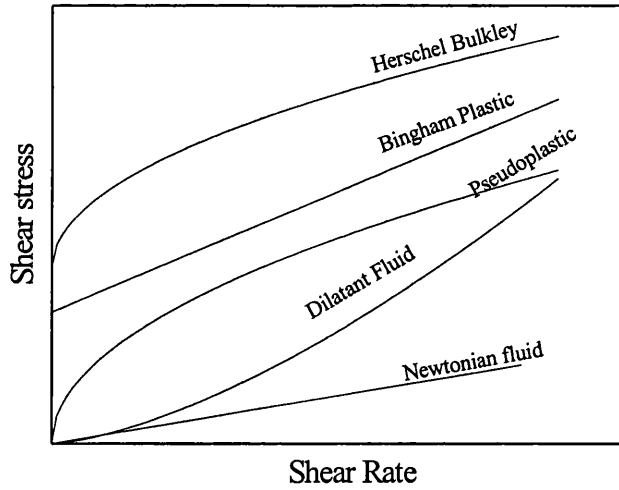
Figure 1.3: Rheological models

In Newtonian fluids there is a defined viscosity which is independent of shear rate. In all other cases there is no rigorously defined viscosity and the viscosity is shear rate dependent. Bingham plastic fluids behave as an elastic solid for stresses less than the yield stress and if the stress is exceeded they behave as a Newtonian fluid under a shear stress (τ - τ_0). In pseudoplastic fluids the ratio of shear stress to shear rate termed as apparent viscosity, μ_a, which falls progressively with shear rate and usually the flow curves become linear at very high shear rate. Apparent viscosity increases progressively with shear rate for dilatant fluids. The equation used for pseudoplastic and dilatant fluids is named as power law model as well. The Herschel-Bulkley is the power law model containing yield stress. All the rheological models shown in table 1.2 excluding dilatant have been used for fermentation cultures. The Casson model (equation 1.43) is another rheological model used for filamentous cultures.

$$\tau^{0.5} = \tau_0^{0.5} + K_c \gamma^{0.5} \tag{1.41}$$

where, K_c = Casson viscosity. While rheological models including Bingham plastic, Herschel-Bulkley, Casson and pseuodoplastic model have been used for morphological characterization of the filamentous fermentaion broths (see table 1.3). There is no theoretical justification in recommending any of these equations. The selection of an appropriate flow equation should be based on practical considerations,

e.g. the model equation should give an accurate fit of the experimental flow curve, it should have a minimum number of independent constants which are readily evaluated and preferably the constants should have some physical basis. By using a new generation of constant stress rheometers, Barnes and Holbrook (1993) demonstrated that yield stresses do not exist. On the other hand, Mohseni and Allen (1995) using the rotating vane has shown that yield stress does exist for *Aspergillus niger* and *Streptomyces levoris* fermentation broth. Mohseni *et al.* (1997) using the rotating vane technique have shown that there was a close agreement between the vane yield stress and those obtained by extrapolation of the shear rate against shear rate curve. However, in the case of the *A. niger* fermentation broths, the vane yield stress was much greater than those determined by conventional methods. Few researchers have reported time dependent behaviour for filamentous fermentation broths (Roles *et al.*, 1974; Blanch and Bhavaraju, 1976) and Mohseni *et al.* (1997) have reported viscoelastic behavior for *Aspergillus niger* and *S. levoris* fermentation broths.

1.5.2 Factors affecting rheology of filamentous cultures

An important feature of the batch fermentation process is the change in rheological behaviour during fermentation due to changes in mycelial concentration and the changing morphological characteristics of the broth. The extent of non-Newtonian behaviour of the broth is closely related to the growth of the biomass and the development of three dimensional network of highly branched mycelial microorgansims. Considerable work has been done to understand the relation between rheology and morphology and biomass concentration of the filamentous organisms which and summarized in Table 1.3. An examination of Table 1.3 shows that despite the importance, little progress has been made in obtaining useful correlations between the rheological properties of filamentous fermentation broths, the morphology and biomass concentration. This has been due to the wide range of parameters that are thought to influence the rheology of the cultures. These include the type of fermenter (e.g. a mechanically agitated vessel) the mode of the fermentation (e.g. batch, fed batch or continuous), the growth rate, the metabolite state of the organisms, the level of dissolved oxygen concentration, and pH levels of the culture, the level of mixing and the presence of solid debris, impurities, surfactants and additives. These

parameters critically affect the properties of the individual hyphae, e.g their length and length distribution, flexibility as well as the interaction between the hyphae (compactness and roughness) and between the hyphae and the continuous phase. The analysis of rheological data is further complicated by the degree of hyphae aggregation, i.e. formation of clumps. The superimposed effects of these parameters on broth rheology would be difficult to simulate. Measurement of the rheology with different rheometers and also different ranges of the shear and the problem of representative sampling (Solmon, 1980) are other reasons for this discrepancy between different reports (see Table 1.3).

Recent reports have shown that in many cases of filamentous fungi cultures, as much as 90% of the mycelium exist in clump form and not in freely dispersed form (Packer and Thomas, 1990; Tucker *et al.*, 1992) suggesting that the hyphal dimensions of free mycelia may influence broth rheology to a less extent in such fermentations. Thus the rheological properties of such fermentations should be correlated with morphological parameter describing the size and shape of these clumps (Tucker and Thomas, 1993; Olsvik *et al.*, 1993). It has been suggested that rheological properties of such fermentations are more likely to be related to roughness and compactness of clumps (Olsvik *et al.*, 1993). It has been also suggested that the compactness has less effect on rheology compared with the effect of roughness on rheology (Mohseni *et al.*, 1995). The roughness of the clumps may be expected to affect their interactions and possibly the flow between them. Increasing roughness should result in greater levels of interaction and more viscous broths (Tucker *et al.*, 1992).

Table 1.3: Rheology of the filamentous organisms

Microorganism	Rheological model	Variation of rheological parameters	Shear range(s^{-1})	Viscometer	Comments (REF)
A. niger (dispersed mycelia)	Power law	$K = 0.308 \, X^{3.15} \, d_p^{0.229}$ $n = 0.559 \, X^{-0.058} \, d_p^{-0.082}$	30-200	Pipe flow	2.3<X<11.2 (1)
A. niger (dispersed mycelia)	Power law Bingham Casson	$K = 4.3 \times 10^{-4} \, X^{3.3}$ $\tau_0 = 0.02 \, X^{2.3}$ $K_c = 0.048 \, X^{0.26}$ $\tau_0 = 2.5 \times 10^{-3} \, X^3$	50 - 650 for all three models	co-axial cylinder	Power law was preferred. Morphology changes not considered (2)
A. niger (dispersed mycelia)	Power law	$K = -0.56 + 1.8 \times 10^{-3} R X^{1.7}$ for continous culture and $K = 0.38 + 4.8 \times 10^{-5} \, R X^{2.9}$ for fed batch culture	10 - 50	Turbine impeller	-(3)
A. niger (dispersed mycelia)	power law for early stage (X<4 gL^{-1}), casson for later stage.	—	50-150	Turbine impeller & pipe flow	Results for two different viscometers were not consistent (4).
A. niger (dispersed mycelia)	Herschel-Bulkley	$\tau_0 = 4.2 \times 10^{-6} \times (X)^{2.6} (L_{hgu})^{0.65}$ $\tau_0 = 4.8 \times 10^{-7} \, X^{2.5} R^{3.2}$	-	Haake Rotovisco RV12	-(5)
A. awamori	Power law	$K = 6.9 \times 10^{-5} X^{3.96}$	-	Co-axial cylinder	Morphological changes not considered (2)
P. chrysogenum (dispersed mycelia)	Casson	$\tau_0 \, \alpha \, X^{2.5}$ $K_c = 1.4 \times 10^{-3} X^1 L_{hgu}^{0.6}$	-	Turbine impellre	Flexibility can affect rheology. (6)
P. chrysogenum (dispersed mycelia)	Power law Bingham Casson	$K = 3.6 \times 10^{-3} \, X^{2.5}$ $\tau_0 = 0.043 \, X^{2.1}$ $\mu_p = 2.2 \times 10^{-3} \, X^{0.78}$ $\tau_0 = 8.3 \times 10^{-3} X^{2.5}$ $K_c = 0.047 \, X^{0.19}$	50-650 for all three models	Co-axial cylinder	Morphology changes not considered. Power law was preferred. (2)
P. chrysogenum (dispersed mycelia)	Herschel-Bulkley Casson	$K = a \, X^{2.8} \, R^{0.7} \, Com^{1.2}$ $1-n = b \, X^{0.7} \, R^{0.6} \, Com^{0.9}$ $\tau_0 = c \, X^{3.2} \, R^{0.6} \, Com^{1.5}$ $\tau_0 = e \, X^{2.9} \, R^{0.6} \, Com^{1.0}$ $K_c = f \, X^{1.2} \, R^{0.1} \, Com^{1.0}$	3.5 - 75.8 for both models	Turbine impeller	Morphological measurements was for clump, which was more than 90% of total. (3)

continue

P. chrysogenum (dispersed mycelia)	Bingham	$\tau_0 = a\ X$	-	MacMichael viscometer	-(8)
P. chrysogenum (pellet)	Casson	$K_c = a\ E_x + b$ $\tau_0 = c\ (E_x/d)^3$	<20	-	$E_x =$ Pellet volume fraction (9)
S. levoris	Power law Bingham Casson	$K = 0.27\ X^{0.7}$ $\tau_0 = 1.1\ X^{0.75}$ $\mu_p = 5.9 \times 10^{-3}\ X^{0.32}$ $\tau_0 = 0.64\ X^{0.79}$ $K_c = 0.042\ X^{0.2}$	50 - 650 for all three models	Co- axial cylinder	Morphological changes not considered. Power law was preferred. (2)
S. levoris	Herschel-Bulkley	$\tau_0 = 4.2 \times 10^{-6} \times (X)^{2.6}(L_{hgu})^{0.65}$	-	Haake Rotovisco RV12	- (5)
S. fradiae	Herschel-Bulkley &Casson	Apparant viscosity, consistency index and yield stress changes with morphology.	< 1300	Co- axial cylinder	Mathematical relation was not shown. Casson was preferred. (10)
S. grisens	Bingham	τ_0 and plastic viscosity varied sinousidally with fermentation age.	-	-	- (11)
S. erythraea S. rimoscus A. roseourufa	Power law	Rheology was related to biomass, not morphology.	<250	Disk spindle impeller	Mean hyphal length was between 15 -25 μm. (12)

Notes:

a, b, c, d , e and f are constant parameters.

Refererences : (1) Fatile (1985); (2) Allen and Robinson (1990); (3) Olsvik et al. (1993); (4) Blakebrough et al. (1978); (5) Mohseni and Allen (1995); (6) Metz et al. (1979); (7) Roles et al. (1974); (8) Deindoerfer and Gaden (1970); (9) Witter et al. (1983); (10) Ghildyal et al. (1987); (11) Richards (1961); (12) Warren et al. (1995a & b)

A theoretical relationship between viscosity and fractal dimension in the case of polymer solutions has been previously recommended by Muthukumar (1985). Banes and Hobrook (1993) also have correlated the viscosity of the particle aggregate to fractal dimension. They argued that the more open aggregates lead to lower fractal dimensions which gives higher viscosity of the suspension. Several recent studies have been focused on the application of fractal geometry for morphological characterisation of filamentous organisms (see section 1.1.2), therefore it is likely possible to correlate rheological properties to the fractal dimension of the mycelial as it is was done previously for polymer solutions or particle aggregates.

Flexibility of the hyphae is another parameter affecting the rheology of the culture. Forgacs et al. (1957) has shown for cellulose fibres, that more flexible fibres give a lower suspension viscosity. In the case of the filamentous organisms changes in the flexibility of the hyphae may be due to changes in cell wall composition, changes in branching pattern or diameter of the hyphae, or variations in osmosic pressure (Metz et al., 1979). The cell wall composition is influenced by the culture conditions and changes during batch growth. Branching of hyphae makes them less flexible and higher osmotic pressures of the suspending medium makes the hyphae more flexible (Metz et al., 1979). Olsvik and Kristiansen (1992 and 1994) has shown that process variables such as specific growth rate, the level of dissolved oxygen concentration in the broth and the mixing time influence the relationship between rheology and biomass concentration. They have argued that the level of dissolved oxygen concentration has little effect on morphology, therefore its consequences should be changes in hyphal flexibility which leads to changes on rheology. The response of cells to oxygen partial pressure is a complex phenomenon (Mukhopadhyay and Ghose, 1976). Zetelaki and Vaz (1968) suggested that the dissolved oxygen tension in the broth would affect the cell wall composition and thus the flexibility of the hyphae. Another variable which is important in rheology of the culture is the charge on or close to the surface of the microorganism (Warren et al., 1995a). The variation of charge on or close to the surface of the organisms can affect their interaction and consequently the rheology of the culture.

59

To summarise, the rheology of the filamentous organisms is important in filamentous organism culture due to its interaction with transport processes and especially its effect on oxygen transfer and the heterogeneity of the dissolved oxygen due to the pseudoplastic behaviour of flow in stirred tank. Considerable work has been done in this field (Table 1.3). No view has yet emerged as how to correlate the rheology and morphology of the culture. Other physico-chemical properties of the hyphae such as flexibility and charges on or close to the surface of the mycelia are parameters which affect the interaction between the hyphae and consequently the rheology of the cultures. There is very little known about these parameters and they have not yet been measured.

1.6 Aims of the study

Over 60% of antibiotics of microbial origins are produced from actinomycetes and in particular from streptomyces (Wallace *et al.*, 1992). These includes: β-lactams, polyketides, aminoglycosides and peptide antibiotics. However, only a small number of literature reports exists concerning the production of antibiotics such as erythromycin and clavulanic acid. To maintain sufficient oxygen supply to a viscous filamentous mycelial culture a high degree of agitation and, hence, power input is required to produce adequate mixing. While, high agitation is beneficial for mass transfer, it has also been recognised that high agitation may cause rupture of the cell wall, changes in morphology of filamentous microorganisms, and variation in the rate of production of secondary metabolite. In addition, changes in morphology can affect the rheology of the culture, and its consequence is not only changes in mass transfer operation in the fermenter but also the downstream processing such as microfiltration.

The main objective of this research is to investigate the effect of shear environment in a stirred bioreactor on *S. erythraea* fermentation. This includes the effect on growth, morphology, rheology and erythromycin production. The interaction between these parameters also will be examined by mathematically. A mathematical model will be derived for the effect of shear on morphology of the filamentous actinomycetes and the experimental data from this study will be examined. Variation of mechanical properties of the cell wall during the fermentation will be investigated for better understanding of the effect of shear on *S. erythraea* fermentation.

2. MATERIALS AND METHODS

2.1 Chemicals

All chemicals were GPR grade and obtained from BDH chemicals (Merck Ltd., Lutterworht, U.K.), unless otherwise stated. The water used throughout this study was reversed osmosis (RO) water unless otherwise stated.

2.2 *Saccharopolyspora* fermentation

2.2.1 Organism

The culture used throughout this study was a mutant strain of *Saccharopolyspora erythraea* (CA 340) and kindly supplied by Abbott Laboratories (Chicago, U.S.A).

2.2.2 Fermentation media

Initialy defined medium was used and then complex medium was used due to the fact that higher biomass and erythromycin could be produced. Defined medium used belongs to Shell 'L' series media and is alleged to trigger erythromycin production by nitrogen limitation and its composition is listed in table 2.1. Composition of complex medium was adapted from Yamamoto (1986) and is listed in table 2.2. It is emphasised that this was a totally soluble media.

Yeast extract and bactopeptone were obtained from Oxoid Ltd, Basingstoke, U.K., and other chemicals were GPR grade from BDH Ltd. Berox FMT-30 (Water Management & Galmen Ltd., Droitwich, Woestershire, U.K.) was used as an antifoam.

Table 2.1: Composition of defined medium

Composition	mgL^{-1}
Glucose	35000
K_2HPO_4	7,000
KH_2PO_4	3,000
$NaNO_3$	2,300
$MgSO_4.7H_2O$	250
$FeSO_4.7H_2O$	25
$CuCl_2$	0.53
$CoCl_2.6H_2O$	1
$CaCl_2.2H_2O$	13.8
$ZnCl_2$	10.4
$MnCl_2.4H_2O$	9.75
$Na_2MoO_4.2H_2O$	0.35
Antifoam	500

Table 2.2: Composition of complex medium

Composition	gL^{-1}
Yeast extract	6
Bactopeptone	4
Glycine	2
$MgSO_4.7H_2O$	0.5
KH_2PO_4	0.68
Glucose	30
Antifoam	1

2.2.3 Fermentation scales and conditions:

Fermentations were carried out at laboratory scale (7-L) and pilot scale (450-L) at different stirrer speeds. Dissolved oxygen tension (DOT) was controlled in some of

the experiments by adding oxygen or nitrogen in the air inlet. The condition of the fermentations carried out in this study are summarised in table 2.3 and are explained in section 2.2.3.1 and 2.2.3.2.

Table 2.3: Characteristic of fermentation carried out in this study

Fermentation	Scale (L)	Media	Speed (rpm)	DOT
D500a	7	Defined	500	>65%, without control
D500b	7	Defined	500	10% with control
D750	7	Defined	750	10% with control
A350	7	Complex	350	>60% with control
B350	7	Complex	350	>60% with control
A500	7	Complex	500	>60% with control
B500	7	Complex	500	>60% with control
A750	7	Complex	750	>45% without control
B750	7	Complex	750	>45% without control
A1000	7	Complex	1000	>60% without control
A1250	7	Complex	1250	>70% without control
B1250	7	Complex	1250	>70% without control
P300	450	Complex	300	>50% with control
P450	450	Complex	450	> 60% without control

2.2.3.1 Fermentations using defined medium:

All the experiments were at 7-L scale. To find the effect of dissolved oxygen tension on growth and erythromycin production of *S. erythraea* two different fermentation were carried out at 500 rpm, one without dissolved oxygen tension control (D500a) another with dissolved oxygen tension controled at 10% (D500b), see Table 2.3. In addition a further fermentation was carried out at 750 rpm with dissolved oxygen tension controlled at 10% (D750), (Table 2.3).

2.2.3.2 Fermentations using complex medium

Five different stirrer speed were used at laboratory scale, 7-L, and two different speed were used at pilot scale, 450-L, (see table 2.3). To ensure the reproducibility of the fermentation, four experiments were carried out twice. In the 7-L scale the dissolved oxygen was always above 60% of air saturation at 1000 and 1250 rpm without any control. Dissolved oxygen was kept above 60% by adding oxygen to the air inlet automatically for fermentations at 350 and 500 rpm. Dissolved oxygen was above 60% without any control at 450 rpm for 450-L scale and was kept above 50% by overpressurising the vessel manually to 0.35 bar, in the rapid growth phase.

2.2.4 Fermenters and instrumentation

Laboratory scale fermenter was a 7-L LH fermenter 2000 series I (L.H. Fermentation Ltd., Reading, Berks, U.K.) with a working volume of 5 L. The pilot scale fermenter was a 450-L Chemap fermenter (Chemap AG Maennedorf, Switzerland) with a working volume of 300 L. Both fermenters had three equally spaced six bladed disk turbine and four equispaced tank baffles. Geometry of the vessel and impeller are shown in Figures 2.1, 2.2 and Table 2.4. Stirrer shaft entered the vessel from the top at 7-L scale and from bottom at 450-L scale.

Table 2.4: Fermenters dimensions (all dimension in mm)

Geometery	7-L fermenter	450-L fermenter
Vessel diameter, T	150	600
Liquid height, H_L	280	1200
Impeller diameter, D	68	200
Inter-impeller distance, H_i	90	300
Height of 1st impeller, H_b	30	200
Length of impeller, L_i	16.5	50
Impeller blade width, W_i	13	40
width of baffle, W_b	25	100
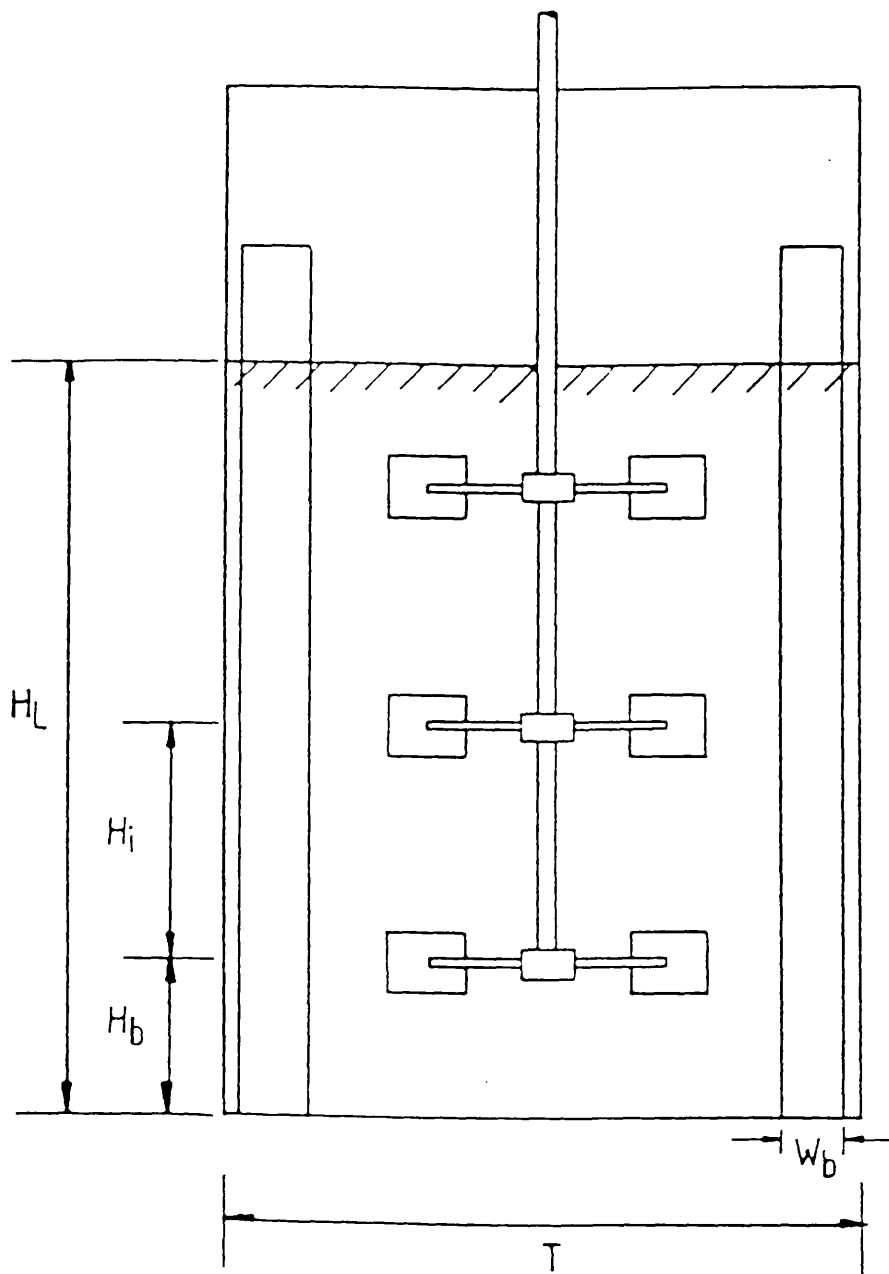
Figure 2.1 Vessel geometry
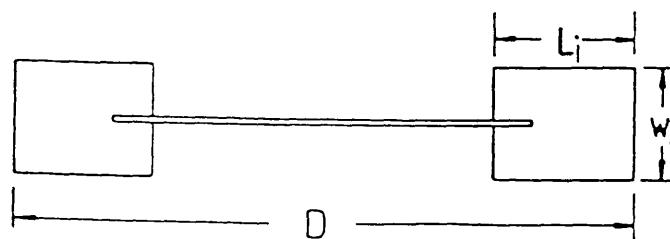
Figure 2.2 Impeller Geometry

The instrumentation in 7-L scale was a microprocessor based 8-loop controller model TCS 6358 (Turnbull control system Ltd., Worthing, Sussex, U.K.) which was capable of monitoring and controlling up to 8 parameters within the fermentation vessel. The instrumentation at 450-L scale was Scatt control 15 (Alfa-Laval, Switzerland).The controller had a PID (Proportional, Integral and Derivative) control action. The instrumentation was connected to a data logging system. Data logging was carried out using the RT-DAS program (Real Time Data Acquisition System) supplied by Acquisition Systems Ltd (Surrey, UK.). This system recorded the on-line variables consisting of stirrer speed, air flow rate, dissolve oxygen tension, pH and temperature.

The stirrer speed was monitored and controlled through a small belt - driven DC tachogenerator attached to the motor shaft. The dissolved oxygen tension (DOT) of medium was measured by a steam sterilizable polarographic dissolved oxygen electrode (Ingold Messtechnik AG, Industrie Nord, Urdorf, Switzerland). pH was measured by a steam sterilizable probe (Ingold Messtechnik AG,Industrie Nord, Urdorf, Switzerland) connected to the controller. pH was controlled by adding either 4 N NaOH or 5 N H_2SO_4 automatically. Peristaltic pumps which fed acid or base were activated if the pH changed from the set point. The pH was controlled within the range of 7.0 ± 0.1.

In 7-L scale a gas mixer was used to control DOT. There were two inputs for gases. The first gas (e.g. nitrogen) was passed through a HI-TEC series F-2000 thermal mass flow meter/controller (Bronkhorst High Tech B.V., Ruurlo, The Netherlands), then mixed with the second gas (e.g air) and passed through another thermal mass flow meter, which controlled the total gas flow rate. The DOT reading from the DOT probe was sent to a controller. The controller compared the DOT reading with the set point and sent an action to the first gas control valve. The control valve regulated the flow rate of first gas (e.g nitrogen) to control the dissolved oxygen tension.

The inlet and exit gases were filtered by passing through 0.2 μm Pall filter cartridges (Pall Europe Ltd., Portsmouth, U.K). There was a condenser in exit line before the

filter for separation of moisture from exit gas. The condenser was a shell and tube heat exchanger, through which cold water was passed to cool the exit gas and reduce evaporation.

Mass spectrometer was connected to all the fermenters to measure the composition of inlet and outlet gases every 15 minutes. Fermentaions were carried out in two different buildings, with different mass spectrometers. For fermentation using defined medium (D500a, D500b and D750), and also for A1000, a VG MMG-80 Mass spectrometer was used and VG Prima mass spectrometer (VG Gas Analysis Ltd, Cheshire, U.K) was used for the other experiments. Oxygen, carbon dioxide and nitrogen concentrations were measured and recorded by RT-DAS where calculations of carbon dioxide evolution rate (CER), Oxygen uptake rate (OUR) and respiratory quotient (RQ) were carried out by the comparison of the gas composition of air entering and existing the fermenter.

2.2.5 Spore preparation

Spores were produced from the mycelial grown on tap water agar medium and incubated at 28 °C for 20 days. The composition of medium was as follows:

Table 2.5: Composition of the medium for spore preparation

Composition	gL^{-1}
Glucose	2.0
Sucrose	1.0
Soy peptone	5.0
Yeast Extract	2.5
Calcium carbonate	1.0

Medium was sterilised for 20 minutes at 121 °C. pH of the medium was adjusted to 7 with sodium hydroxide before adding calcium carbonate and agar. Yeast extract and soy peptone were from Oxoid Ltd, Basingstoke, U.K., and other chemicals were GPR grade from BDH Ltd. Spore suspensions were prepared using 20% glycerol solution and 0.1%

Tween 80 and glass beads, to scour the surface of agar. Spore harvests were pooled, checked for sterility and stored at -70 °C.

2.2.6 Shake flask experiments

Difco Nutrient Broth (60 mL) in a 500 mL Erlenmeyer baffled flasks was incubated with spore suspension to give a concentration of 2×10^6 spore/mL. The flasks were incubated for 48 hours at 28 °C at 200 rpm on an ISF-I-V orbital shaker (Adolf Kuhner, Schmeiz, Switzerland). After 48 h of germination 20 mL of broth was transferred to a 2 L baffled flask with 250 mL complex medium (see Table 2.2 for the composition).

The glucose and potassium dihydrogen orthophosphate were sterilised separately and aseptically added to the medium. The pH of the medium was adjusted to 7.0 with sodium hydroxide solution before sterilisation. In some experiments, 21 gL^{-1} MOPS (3-[N-Morpholino]propane-sulfonic acid from Sigma) was added as a buffer to medium before adjusting the pH.

The cultures were incubated at 28 °C at 200 rpm in an orbital shaker for 7 days. 15 mL samples were taken once a day for measuring DCW, glucose and erythromycin.

2.2.7 Inoculum development
2.2.7.1 Inoculum development for 7-L scale fermenter

50 mL Difco Nutrient Broth in 500 mL Erlenmeyer baffled flasks was inoculated with spore suspension to give a concentration of 2×10^6 spore/mL. The flasks were then incubated for 48 hours at 28 °C at 200 rpm in an orbital shaker. After 48 hr of germination, the broth was transferred to a 2 L baffled flask containing 500 mL defined medium (see table 2.1 for the composition) or complex medium (see table 2.2 for the composition). The flasks were incubated at 28 °C and 200 rpm on an ISF-I-V orbital shaker (Adolf Kuhner, Schmeiz, Switzerland). The duration of the fermentation in this step was 48 h in defined medium or 30 h in complex medium. The sterilisation method for complex medium was the same as shake flask experiments (see section 2.2.6). For inoculum preparation for defined medium, nitrate and phosphate were dissolved in 45 mL of reverse osmosis (RO) water whilst the glucose was dissolved in 400 mL of RO

water, these were autoclaved, 20 min at 121°C , 15 Psig separately. A 100-fold concentrated solution of the trace elements was prepared, 5 mL of this solution was filter sterilised through a Whatman 0.2 μm polysulfone Membrane Syringe Filter and added to the nitrate and phosphate salts. The pH of the trace element solution was adjusted to 1 with adding concentrated hydrochloric acid.

2.2.7.2 Inoculum development for 450-L scale fermenter

7-L fermenter with 5.3 L complex medium was inoculated at 750 rpm, as it will be described in section (2.2.8.1). When the carbon dioxide evolution rate was 30 mmolL^{-1} h^{-1} (dry cell weight = 7.1 gL^{-1}), the content of 7-L fermenter was used as the inoculum for 450-L fermenter.

2.2.8 Fermentations

2.2.8.1 7-L fermentations

The total volume was 5.3 L at the start of the fermentation, and a total sample volume of 500 mL was taken during the 120 hours of fermentation. Glucose solution and antifoam were sterilised *in situ* for 20 min at 121 °C and 15 psig by passing steam at about 20 psig through the heat exchanger rings. In the case of defined medium fermentations, nitrate and phosphate solutions were sterilised in an autoclave, and trace element solution was filter sterilised through a Whatman 0.2 μm polysulfone Membrane Syringe Filter and added to the medium aseptically. In the case of complex medium fermentations, yeast extract, bactopeptone, glycine and magnesium sulphate in one bottle and potassium dihydrogen orthophosphate in another bottle were sterilised in an autoclave and added to the medium aseptically.

The ancillaries, i.e. filters, sampling device and sample bottles, acid and base containers, inoculum flask including their addition lines and needles were sterilised in an autoclave at 121 °C, 15 Psig for 20 min.

The fermentation medium was cooled down to 28°C using cooling water and then other components were added aseptically and inoculated with 500 mL of inoculum.

Temperature was maintained at 28°C. pH was controlled at 7.0 by addition of 4 N NaOH and 5N H_2SO_4.

In order to achieve a precise and reliable control of DOT, the DOT probe was carefully calibrated in sterile medium before inoculation. A DOT of 100% air saturation was determined by allowing the probe to equilibrate with an air saturated medium which was, in turn, obtained by sparging the medium with air. To determine 0% DOT, oxygen -free nitrogen gas was sparged through the medium instead of air.

Gas flow rate was 5 Lmin^{-1} in complex medium and it was 2.5 Lmin^{-1} at 500 rpm in defined medium and 3.75 Lmin^{-1} at 750 rpm in defined medium. Gas mixtures were used to control the level of dissolved oxygen tension for the experiments with DOT control. Total gas flow rate kept constant. DOT was controlled by changing the proportion of nitrogen to air in the case of defined medium or oxygen to air in the case of complex medium.

2.2.8.2 450-L fermentation

The complex medium was used (see table 2.2 for its component) and the working volume was 300 L. Glucose solution and antifoam were sterilised *in situ* for 40 min at 121 °C, by passing steam through the jacket of the vessel. The fermentation medium was cooled down to 28 °C by passing cooling water through the jacket. Yeast extract, bactopeptone, glycine and magnesium sulphate were sterilised in another vessel at 121 °C for 20 min and added to the vessel through a sterile line. Potassium dihydrogen orthophosphate was sterilised in an autoclave at 121 °C for 20 min and added to the vessel under aseptic conditions. Air flow rate was 210 Lmin^{-1}. Two fermentations were carried out one at 300 rpm (P300) and the other at 450 rpm (P450).

Temperature was maintained at 28 °C and pH was controlled at 7.0 by adding 4 M NaOH and 3 M HNO_3. The DOT probes were calibrated with the same procedure as in the 7-L fermenter (see section 2.2.8.1). Inoculum was added from 7-L fermenter through a sterilised line to the fermenter. The pressure was 0.05 bar during the experiments,

71

except during the rapid growth at 300 rpm where the pressure was increased to 0.35 bar to keep the dissolved oxygen tension above 50%.

2.3 Analysis of samples

Samples were taken once or twice a day when using defined medium and 3 or 4 times a day when using complex medium. Generally three universal bottles were filled (each containing 20 mL). The first bottle was discarded since it contained the dead volume from the sampling tube, one bottle used for rheological measurements and one bottle was used for other analysis. A further universal bottle was filled if the sample was to be homogenised.

It was necessary to obtain a clarified solution for the erythromycin, nitrate, and phosphate assays, therefore some of the broth was centrifuged in a lab top centrifuge (Beckman, CS-6R) at 4,200 rpm for 10 minutes. For preparation of samples for erythromycin assay with HPLC method, the broth was centrifuged in a microfuge (Beckman, microfuge 11) at 13,000 rpm for 10 minutes. All supernatants were stored at -20°C until they were used for the assays.

2.3.1 Erythromycin measurement using bioassay

The punched bioassay method as described by Huck *et al.* (1991) was used with some modification. A culture of *Arthrobacter citreus* was grown in a 500 mL shake flask containing 50 mL Nutrient Broth (Oxoid) for 24 hours at 28 °C and 200 rpm.

The glass plates used for the assay were washed with disinfectant (Tego 2000, TH Goldschmidt Ltd., Milton Keynes, UK), sterilised with industrial methylated spirit and allowed to dry in laminar flow cabinet. The assay plates were 450 × 450 mm square and 10 mm deep. 600 mL of nutrient agar (comprising 12 g of Oxoid bacteriological agar and 7.8 g of Oxoid nutrient broth) was autoclaved and cooled down to approximately 40°C before being inoculated by 3-5 mL of the *A.citreus* culture. The culture was well mixed and poured into the plate. The agar was allowed to solidify, then the plate was placed onto a paper template and 49 wells (7 × 7) were punched using a 7.5 mm cork-

borer (Pattersons, Luton, U.K). The upper end of the borer was attached to a tube which led to the conical flask of a vacuum pump set up. In this way all the agar which was sucked up was collected in the vacuum flask.

100 µL of sample, either fermentation supernatant or calibration solution was pipetted into the wells in duplicates. The calibration standard was erythromycin dehydrate (Aldrich Chemical Co. Ltd., Gillingham, Dorset. U.K.), and the solutions were in the range 5-100 µg/mL. The assay plates were incubated at 28 °C for approximately 24 hours before leaving one more day at room temperature in order to obtain clear inhibition zones, which then were measured with a ruler.

The logarithm of antibiotic concentration is proportional to the square of the distance between the reservoir and the inhibition zone border , as described below:

$$\ln m = (d_1 - d_2)^2 / 4 D_c T_0 \qquad (2.1)$$

where: m, antibiotic concentration

$\qquad$ d_2, diameter of resorvoir

$\qquad$ d_1, dimeter of inhibition zone

$\qquad$ D_c, diffusion coefficient

$\qquad$ T_0, absolute temperature

Standard curves were constructed based on this theory on Origin (Microcal Software Inc., Northampton, USA); The value of ln m was plotted against $(d_1 - d_2)^2$ for erythromycin standards and the standard curve was determined by linear regression. This standard curves was used for determination of erythromycin in the samples.

2.3.2 Erythromycin measurement using HPLC

All the solvents used were HPLC grade (BDH, UK) and all other components were Analar grade (BDH, UK). All HPLC assay were performed using a system Gold Chromatographic system (Beckman Instruments). The system composed of a pump (model 126), autosampler (model Beckman 507e), ultraviolet detector (model 166).

Control and data logging facilities were provided by System Gold software run on an IBM computer.

Organic eluents filtered through a PTFE filter paper, 2.5 μm pore (Whatman) and aqueous eluents filtered through a Whatman No. 1. All eluents degassed with helium (BOC, Guilford, Surrey, UK). All the samples were filtered through a disposable 0.2 μm pore PTFE syringe filter (Whatman).

The reverse phase analytical column used was Phenomenex Prodigy ODS (250 × 4.6 mm). This column was protected by a 45 × 4.6 mm guard column containing the same material. The columns were maintained, cleaned and re-equilibrated as necessary and according to the manufacturer's instruction. The column temperature was controlled at 50 °C with a block column heater and the samples injection volume was 50 μL. Acetonitrile-20 mM Potassium dihydrogen phosphate (pH 7) (45:55) at 1.0 mLmin^{-1} was used as the mobile phase.

Erythromycin A (93% pure), erythromycin B (92% pure) and erythromycin C (92% pure) kindly provided by Dr Peter Dusseljee (Gist-Brocades, Italy) and used to obtain the retention times and standard curve of peak areas. Concentration of prepared standards were in the range of 0.25-10 gL^{-1}. Repeated injection of the crude erythromycin standard (Kindly provided by Abbott Laboratories) and fermentation samples showed that the peak areas of erythromycin A were accurate to within less than 1.2% (95% confidence limits expressed as a percentage of the mean).Where desired, the elutate from the HPLC column was collected manually. Antibiotic activity was measured in the collected fraction using bioassay.

Fermentation samples were not appropriate for direct analysis of HPLC due to their high amount of impurities and relatively low concentration of erythromycin. Therefore, solid phase extraction was developed for cleaning and concentrating of erythromycin. The C18 bond elut cartridges (Phenomenex cat. 1211-3001) were used to carry out the extraction. Five steps were used for the purpose of the extraction: The step by step extraction procedure was optimised and is explained in section 3.2.1. Initially crude

erythromycin kindly provided by Abbott Laboratories (Chicago, U.S.A), was used as the sample to optimise the 5 steps. Once the above steps were optimised, fermentation samples were used. The optimised procedure was as follows:

1) conditioning the column : 5 mL methanol consisting of 0.5% diethyl amine was used.

2) rinsing the column: 5 mL 10 mM phosphate buffer pH 7 was used to remove the activation solvent in the conditioning step.

3) applying the sample : 10 mL samples was applied

4) rinsing: after applying the samples the interfering compounds were washed from the cartridge using 5 mL 10 mM phosphate buffer pH 7.0.

5)elution: finally 1 mL methanol was passed through the column to elute erythromycin from the solid sorbents.

Liquid-liquid extraction was also applied to a few samples to compare the results with solid phase extraction. The pH of the sample was adjusted to 10 by adding 5 M sodium hydroxide. Then 100 mL chloroform was added to 100 mL of sample and mixed for 10 minutes at room temperature. The mixture was transferred to a separating funnel and allowed to separate for 30 minutes. The organic layer was removed and washed with equal volume of NaOH. This solution was mixed for 2 minutes by hand and was then transferred to the separating funnel and allowed to separate for a further 30 minutes. The organic layer was removed and dehydrated with anhydrous sodium sulphate. The sodium sulphate was added gradually until the solution became transparent. The known amount of transparent solution was separated and left to dry overnight in the fume cupboard and then redisolved in known amount of acetonitrile to give a 10 times concentration. It should be noted that all the experiments was carried out in a fume cuboard.

2.3.3 Dry cell weight measurement

Dry cell weight was utilised to determine growth of the cultures. 10 mL of the fermentation broth was filtered through a predried and preweighed GF/F Glass microfilters with a pore size of 0.65 μm (Whatman Ind. Ltd., Maidstone, U.K.), washed

with 20 mL of RO water and dried overnight at 100 °C. To maintain a constant weight, the filters were always left in a vacuated desicator for 10 minutes prior to weighing.

2.3.4 Nitrate assay

A nitrate reductase assay kit (Boehringer Mannheim Cat.No.950658) was employed for the nitrate assay. Nitrate is reduced by reduced nicotamide-adenine dinucleotide phosphate (NADPH) to nitrite in the presence of the enzyme nitrate reductase.

$$Nitrate + NADPH + H^+ \rightarrow Nitrite + NADP^+ + H_2O$$
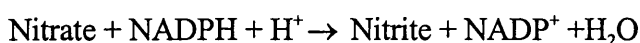
The amount of NADPH oxidised during the reduction is stoichiometric with the amount of nitrate. The decrease in NADPH was measured by means of its absorbance at 340 nm. All the measurements were carried out in duplicates and on average the standard deviation was 10.2% of the mean.

2.3.5 Glucose assay

The test used is based on a glucose oxidase reaction. Glucose HK reagent (Sigma Diagnostics), which is normally designed for monitoring sugar in blood, was used for measurement of glucose consumption during the fermentations. The enzymatic reactions involved in the assay are as follows:

$$Glucose + ATP \Rightarrow G\text{-}6\text{-}P + ADP$$
$$G\text{-}6\text{-}P + NAD \Rightarrow 6\text{-}PG + NADH$$
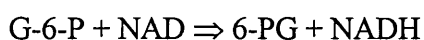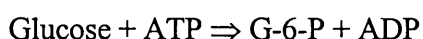
Glucose is first phosphorylated by adenosine triphosphate (ATP), in the reaction catalysed by hexokinase (HK). The glucose-6-phosphate (G-6-P) formed is then oxidized to 6-phosphogluconate (6-PG) in the presence of nicotinamide adenine dinucleotide (NAD). This reaction is catalysed by glucose-6-phosphate dehydrogenase (6-G-PDH). During this oxidation, an equimolar amount of NAD is reduced to NADH. The consequent increase in absorbance at 340 nm is directly proportional to glucose concentration. All the measurements were carried out in duplicate and on average the standard deviation was 5% of the mean.

2.3.6 Phosphate assay

Phosphate concentration in samples was measured colorimetrically (Mirjalili and Linden, 1995). The sample (100 µL) was incubated with 350 mL of an ammonium molybdate reagent for 10 min at 37 °C. Absorbance of the mixture was read at 700 nm after cooling approximately for 10 min. Reagent was prepared with mixing 2 volume RO water, 1 volume 6N H_2SO_4, 1 volume 10% ascorbic acid, 1 volume 2.5% ammonium molybdate. The inorganic phosphate present in the sample reacts with ammonium molybdate to form phosphomolybdate. The phosphomolybdate is then converted by reduction with ascorbic acid to the colloidal molybdenum blue, which is then determined photometrically. The molybdenum blue formed is proportional to the quantity of inorganic phosphate present.

All the measurements were carried out in triplicates and on average the standard deviation was 9.0% of the mean. The reason for high level of error was low concentration of phosphate in the samples. This method was not accurate for phosphate levels less than 0.1 gL^{-1}.

2.3.7 Protein assay

A Bio-Rad protein assay (Bio-Rad laboratories, Hemel Hempstead, Herts., UK) was used for measurement of soluble protein in the homogenate supernatants. This method is based on the shift in the maximum absorbance of a dye, Coomassie Brilliant Blue G-250, when it binds protein under acidic conditions.

Reagent was diluted 5 times with RO water. 50 µL of sample was pipetted into a plastic disposable cuvette and 1 mL of the diluted reagent was added to this. The absorbance was read at 595 nm between 5-10 minutes after adding the samples at room temperature. The spectrophotometer was blanked against 1 mL of dye reagent containing 50 µL of RO water. Samples were diluted with RO water prior the addition of the dye reagent such that the absorbance was kept below 0.7 AU.

The standard curves were prepared by making various dilution of Bovine Serum Albumin (BSA) supplied by Bio-Rad. Concentration of standards was in the range of 25 to 400 mgL^{-1}. The data for BSA concentration was plotted against their absorbance at 595 nm. A curve was fitted to this data by linear regression analysis in Package Origin (Microcal Software Inc., Nothampton, USA). The soluble protein content of the samples was then determined using the standard curves. All the measurements were repeated in triplicates. On average the standard deviation of error was 3.0% of the mean value.

2.3.8 Image analysis

The morphological measurements were made using the automatic Image analysis described by Packer and Thomas (1990). A television camera was mounted on a Polyvar microscope (Reichert-Jung, Vienna, Austria) and the video signal of the field of view was processed by a Magiscan 2A image analyser (Joyce Loebl Ltd, Gateshead, U.K).

Morphological characterisation was completed from dry slides which were prepared immediately after sample removal from the fermenter. By examining the microscope slides prepared at various dilution, a suitable slide was chosen for image analysis . The slide needed a high concentration of micro-organisms, to ensure a reasonable number of measured objects per field. If the concentration is too low the amount of time spent image analysing becomes excessive. If the concentration is too high then the excessive hyphal overlap and analysis will assume the objects to be a single entity and produced errorous data. Culture samples were diluted 200 to 4000 times in 50 mM potassium phosphate buffer (pH = 7.0) depending on concentration of biomass. With the examination of many samples, it was found that 2000 times dilution is appropriate for 10 gL^{-1} biomass. Then 50 µL of the diluted samples were spread over the surface of the slide and allowed to air-dry on a level surface. For staining, 0.3 g of methylene blue was dissolved in 100 mL 30% ethanol solution. Slides were immersed in the staining liquid for 1 min. The slides were rinsed in water for 2 minutes and allowed to air dry in a vertical position for 2 h. Eight slides were prepared for each sample. The slides were examined and the appropriate one was selected for image analysis.

Objects other than the microorganisms are also present in the binary image. These tend to be undissolved solids from medium or small particles present in the liquid or even just particles of dust from atmosphere. These may be distinguished from the microorganisms by their size and shape. One parameter, the circularity proved to be very useful in removing the particulate material as it depends on the sphericity of the object (Packer, 1991):

$$\text{Circularity} = 4 \times \pi \times \text{total area} /(\text{perimeter})^2 \qquad (2.2)$$

Total area is described in Table 2.6. Circularity equals one for a circle and it is close to zero for a long thin fibre. It has been found, that objects with circularity of 0.4 and greater are undesirable objects in the case of *S. clavuligerus* organism (Packer and Thomas, 1990; Packer, 1991). By examination of many samples, it was found that none of the mycelia in this study have circularity above 0.4, therefore, any objects with circularity of greater than 0.4 were excluded. Filamentous organisms have been divided into three types : freely dispersed mycelia, mycelial clumps or aggregates and pellets (Figures 3.18 and 3.19). There were no pellets in these experiments except very few cases at 350 rpm. Therefore, objects were divided to two main parts: freely dispersed mycelia and clumps. If there were any pellets it was considered as a clump. Any object including a hole was regarded to be a clumps. The measured morphological parameters are shown in Table 2.6 (Packer and Thomas, 1990; Tucker *et al.*, 1992).

Magnification was 100× 25 and at least 300 organisms were analysed and processed by statistical analysis in each sample and the mean values of the morphological parameters were obtained and reported for characteristics of morphology.

Table 2.6 : Morphological parameters measured by Image analysis

Measurement	Nomenclatue	Description
Main hyphal length[1]	ML	The longest connected path through the cells
Branch length[1]	BL	Other parts of the mycelia apart from the main length
Total hyphal length[1]	HL	=ML + BL
Number of tips[1]	NT	The number of branches (growing tips)
Major axis[2]	OL	Maximum mycelia diameter, (Figure 2.3).
Minor axis[2]	OB	Longest distance perpendicular to the major axis
Average length[2]	aveL	=(OB + OL)/2
Mycelia area	MA	Projected area of the freely dispersed mycelia
Clump area	CA	Projected area of the clumps mycelia
Projected area[2]	OD	MA or CA
Total area[2]	OA	= OD + internal holes
Circularity[2]	OC	= $(4 \times \pi \times OA)/(Perimeter)^2$
Roughness[2]	R	=1/OC

(1): Applied only for freely dispersed mycelia

(2): Applied to both freely dispersed mycelia and mycelial clump.

80
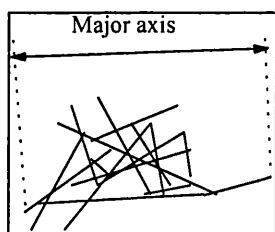
Figure 2.3: Schematic diagram to show the major axis

The level of error was determined for 35 samples repeated in duplicates and the average of the standard deviation was calculated and is summarised in table 2.7 for different morphological parameters.

Table 2.7: Average standard deviation of morphological parameters

Morphological parameter	Average standard deviation /mean ×100
Mean Main length	6.1
Mean branch length	5.6
Mean total hyphal length	5.55
No of tips	3.35
Mean major axis for mycelia (freely dispersed and clumps)	3.55
Mean major axis for mycelial clumps only	6.2
mean Minor axis	7.0
Average length for mycelial clumps only	6.4
Percentage of clump area	7.5
Clump area	7.1
Roughness	7.1

2.3.9 Rheological measurements

The rheological measurements were carried out using a Rheomat 115 rotational viscometer (Contraves AG, Zurich, Switzerland) with a plug in 7/7 module operating

system and a concentric cylinder (MS-0/115) measuring unit with quick release coupling. Measurements were carried out at room temperature, which was 20-24 °C. Metz *et al.* (1979) reported that viscosity for mycelial broths was only slightly dependent on temperature, therefore, it was not necessary to maintain the temperature of the samples constant during rheological measurements. Measurements were carried out immediately after taking the sample from the fermenter. The cup was filled with 20 mL of broth, the cylinder bob put in place and rotated for 10 seconds at the highest speed (step 12, shear rate = 1250 s^{-1}). Torque was recorded as the speed was reduced to (step1, shear rate = 24.3 s^{-1}). Reading were taken in a short time (5 second for each reading) to minimise settling. Speed was translated into shear rate and the torque reading was translated to shear stress using the table supplied by Contraves.

The power law model (equation 2.3) was considered to determine the rheological behaviour of the fermentation broth samples.

$$\tau = K.\gamma^n \tag{2.3}$$

Shear stress (τ) was plotted against shear rate (γ) in a log-log plot and its slope and intercept were considered as values of flow behaviour index (n) and consistency index (K) respectively. Experimental data showed a good agreement with power law model for fermentation broth (Figure 2.4).

Apparent viscosity (μ_a) at any stirrer speed (N) was obtained using Metzner and Otto technique (1957) with a value of 11.4 for the impeller shear rate constant (k_s). thus:

$$\gamma_a = k_s.N \tag{2.4}$$

$$\mu_a = \tau/\gamma_a = K\gamma^n/\gamma = K(k_s.N)^{n-1} \tag{2.5}$$

In order not to change the total volume of each fermentation more than 10%, limited number of samples could be taken in each experiment. Therefore, it was not possible
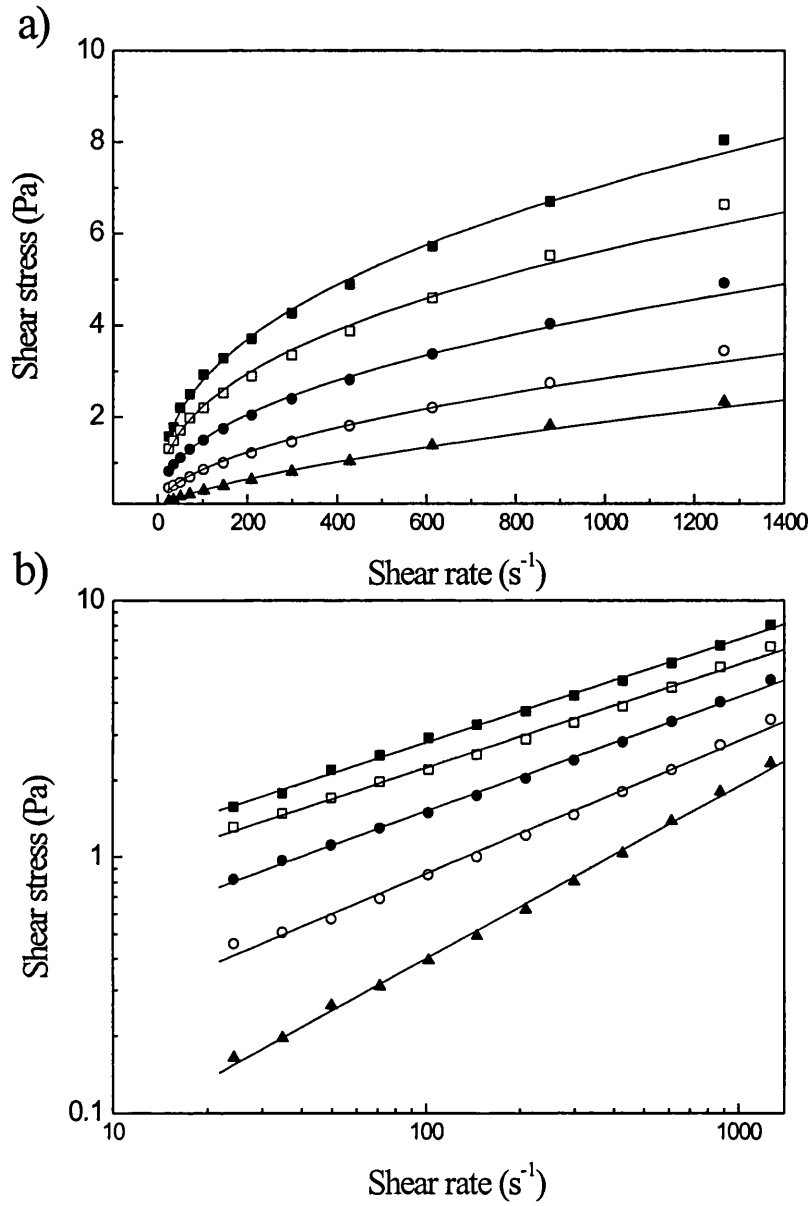
Figure 2.4: Power law model for *S. erythraea* fermentation broth samples a) in normal scale and b) in log-log scale. Samples were taken during fermentation at 7-L scale and 500 rpm. The dry cell weight of the samples was as:

11.7 gL^{-1} (■), 7 gL^{-1} (□), 4.6 gL^{-1} (●), 2.7 gL^{-1} (○), 1.7 gL^{-1} (▲). Fitting model (———).

to repeat the rheological measurements for all samples. However, duplicate measurements for over 20 samples showed that on average the standard deviation was 5.3% of the mean consistency index and it was 1.7% of the mean flow behaviour index.

2.4 Homogenisation of fermentation broth samples

Samples were disrupted using a 'Gaulin Micron Lab40, High-Efficiency Homogeniser' (APV Gaulin GmbH). The homogeniser acted as a hydraulic pump working batchwise at single strokes, with an operating range of 100 - 1600 bar. The homogeniser requires 40 mL samples. All parts contacting the sample liquid consist of high grade stainless steel, stellite, rubber and PTFE and these parts are cooled by passing glycerol through an external coil.

Homogenisation was carried out at 6 different pressures (100, 200, 400, 600, 800 and 1200 bar). Therefore for each assessment, 240 mL samples were required. Fermentation samples were diluted 20 times with 50 mM potassium phosphate buffer, pH 7.0 before disruption. A 0.5 mL volume was removed with pipette into a 1.6 mL Eppendorf standing in an ice bath, this sample was used to determine the background level of constituents in the subsequent assays. Three or four discrete passes were made through the homogeniser, and 0.5 mL of sample was removed after each pass into a 1.6 mL Eppendorf in the ice batch. After each high pressure pass, the homogeniser assembly was wiped clean with a sheet of engineers blue roll paper. After, homogenisation the Eppendorf were centrifuged (Beckman Microfuge 11) at 13000 rpm for two minutes to remove debris and the supernatant was used for protein assay.

3. RESULTS

3.1 Effect of dissolved oxygen concentration and shear using defined medium

3.1.1 Effect of dissolved oxygen concentration

Fermentations were carried out at 500 rpm and 0.5 vvm without dissolved oxygen control (D500a) and with dissolved oxygen control at 10% saturation (D500b) by addition of nitrogen to the inlet gas of the fermenter (see section 2.2.4). This ensured that the gas distribution and mixing conditions were identical in each case. In the experiment without dissolved oxygen control, minimum oxygen concentration was 65% air saturation (Figure 3.1). The data was not enough to calculate the exact growth rate, and maximum growth rate was about 0.07 h^{-1}. This relatively low growth rate could be partly due to using nitrate as the only nitrogen source in the medium (Bushell *et al.*, 1997). The culture entered the stationary phase at 10% DOT earlier than in other experiment (Figure 3.2). The maximum dry cell weight for higher dissolved oxygen tension (65% saturation) was 5.7 gL^{-1}, whereas it was 4.65 gL^{-1} for 10% dissolved oxygen tension, which showed growth was inhibited at low dissolved oxygen tension. This was also observed in the carbon dioxide evolution rates (CER) of the culture (Figures 3.1 & 3.2). The carbon dioxide evolution rate was relatively low, the maximum values for 10% dissolved oxygen tension was 8.5 mmolL^{-1}h^{-1} and for 65% dissolved oxygen tension was 10.1 mmolL^{-1}h^{-1} and they were also biphasic. Its biphasic behaviour could be because of release of some intracellular material with nitrogen source and reuse of them by the organisms. The value of RQ was almost 1 at experiments without dissolved oxygen control. And when nitrogen was mixed with air to keep dissolved oxygen at 10%, OUR measurements were not possible.

The biomass data was not enough to find the exact point for the end of the rapid growth phase, however CER data showed that respiration fell at 80 h, as nitrate was depleted (Figures 3.1 & 3.2). Erythromycin synthesis began with a slow rate, and its production seems to be growth linked. The percentage of erythromycin production
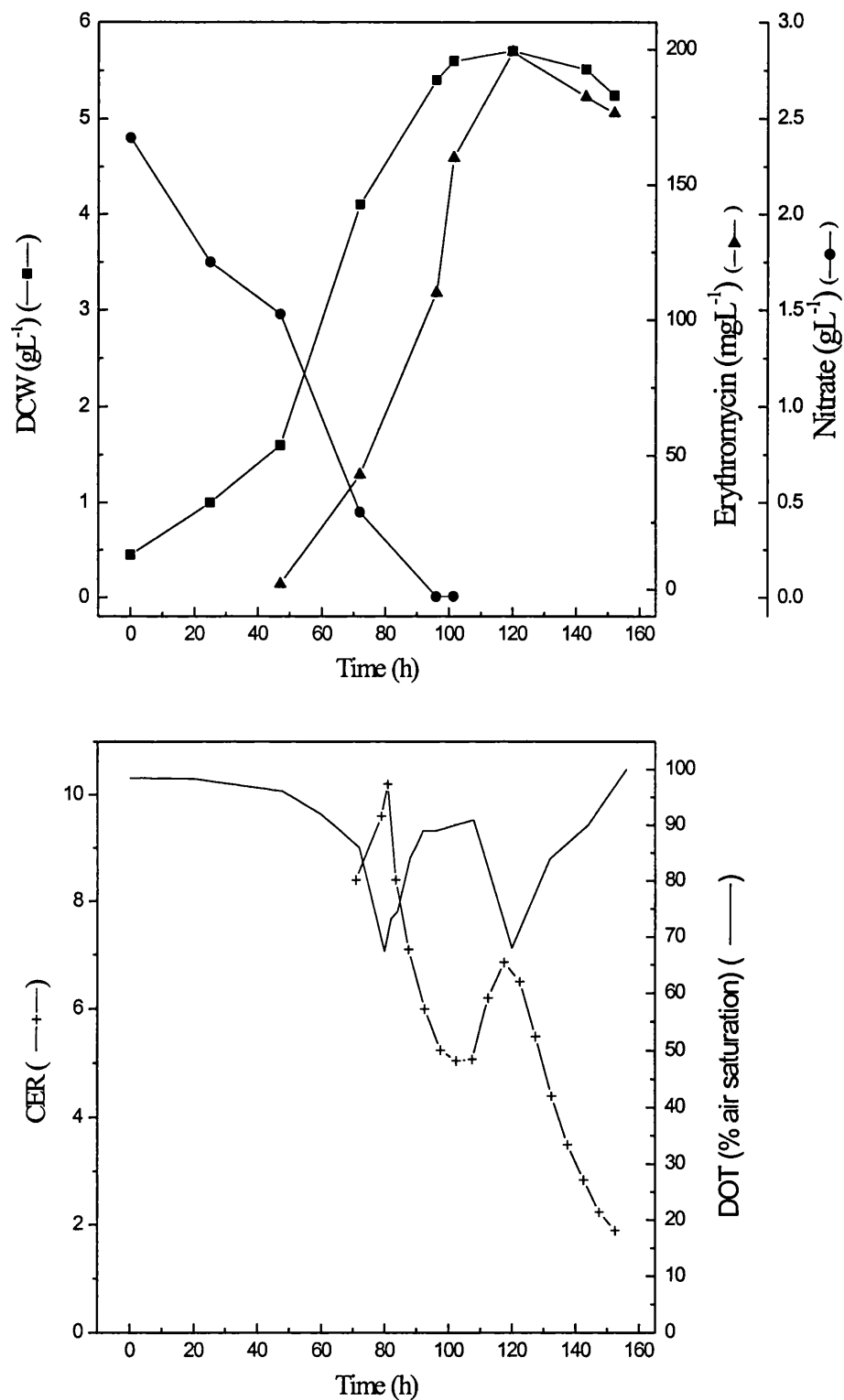
Figure 3.1: Changes of DCW, nitrate, erythromycin production, CER and DOT at 7L fermentation of *S. erythraea* using defined medium (stirrer speed = 500 rpm, gas flow rate = 0.5 vvm & DOT>65%).

86
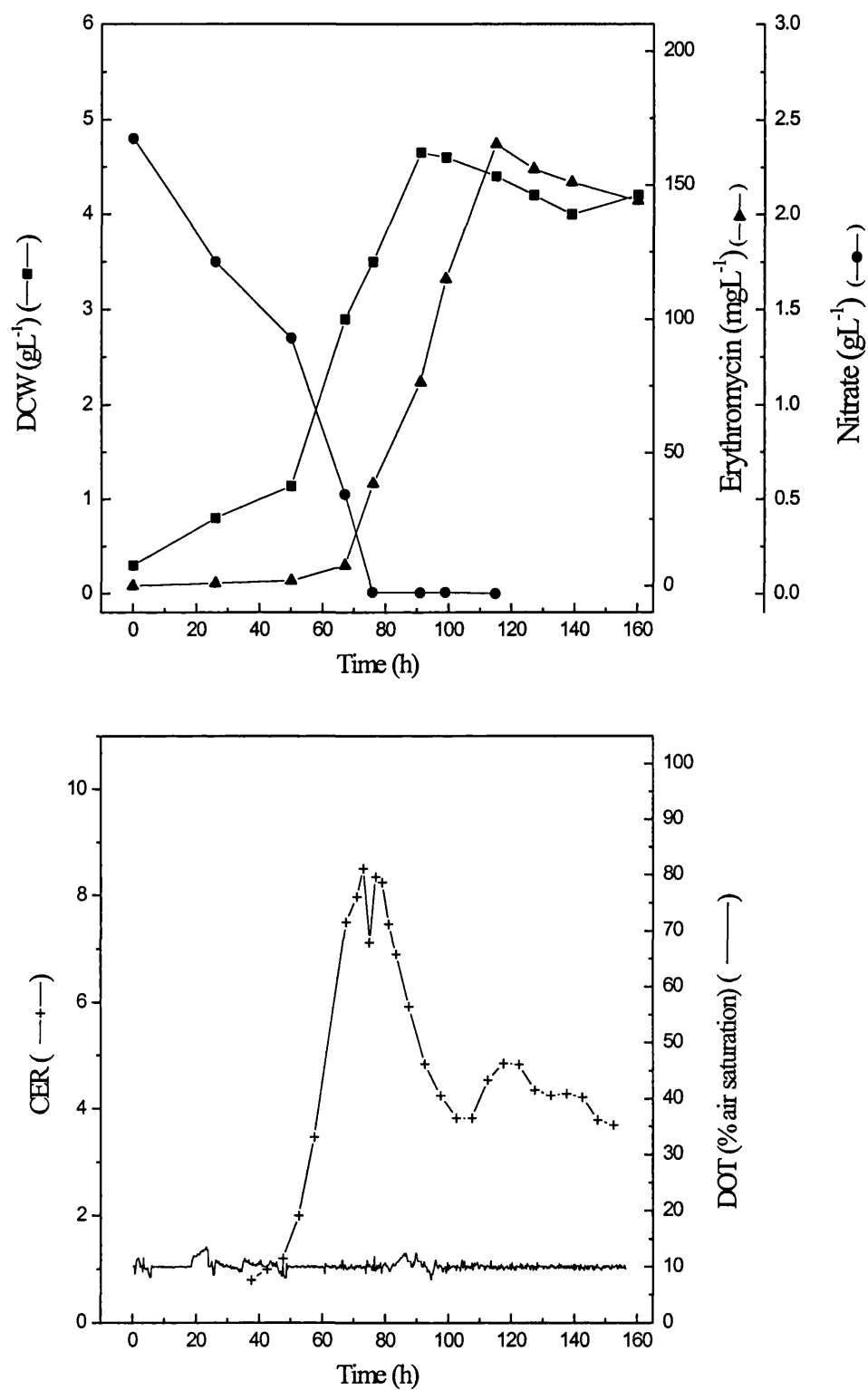
Figure 3.2: Changes of DCW, nitrate, erythromycin production, CER and DOT at 7-L fermentation of *S. erythraea* using defined medium (stirrer speed = 500 rpm, gas flow rate = 0.5 vvm & DOT=10%).

before the end of the rapid growth phase (it coincided with sudden decrease in CER) was about 40% in experiments with DOT>65% (Figure 3.1), and this was about 60% in the experiments with dissolved oxygen concentration of 10% (Figure 3.2). Maximum values of erythromycin were 199 and 165 mgL^{-1} for dissolved oxygen concentrations above 65% and 10% respectively, and it then decreased slightly. Instability of erythromycin in fermentation broth has been reported previously by Wilson et al., (1995) and Gavin et al., (1995). Instability of erythromycin in fermentation broth could be due to its degradation by non-specific enzymes released by old lysing mycelia (Martin et al., 1975).

Specific erythromycin production was calculated by dividing the erythromycin concentration (mgL^{-1}) by DCW (gL^{-1}) at any time, except after the end of the growth phase where erythromycin concentration was divided by maximum DCW. The specific erythromycin was not affected by the DOT and these were virtually identical throughout the culture (Figure 3.3). Consequently, the productivity of erythromycin does not appear to be related to the oxygen level, provided that it is above 10% in this medium.
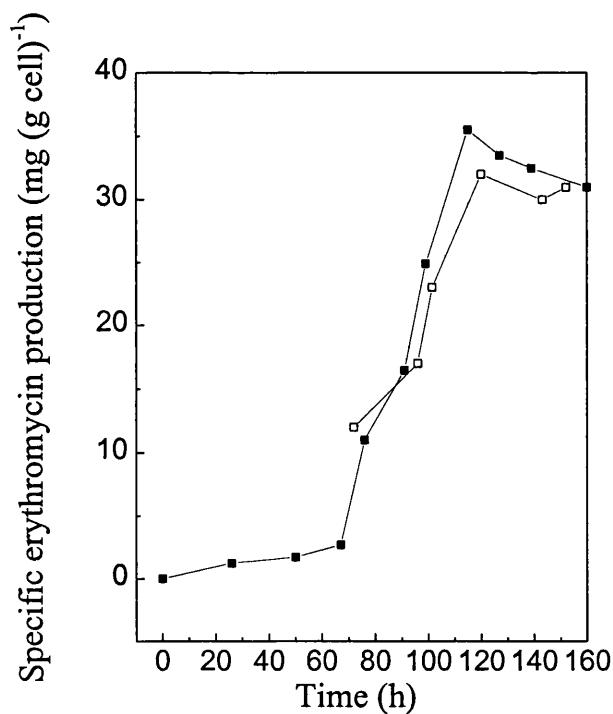
Figure 3.3: Comparison of specific erythromycin production at 500 rpm between DOT 10% (—■—) and DOT>65% (—□—).

3.1.2 Effect of mixing and shear

Two different fermentations were carried out at 500 rpm and 750 rpm using defined medium. Dissolved oxygen was controlled at 10% by mixing nitrogen with air. Figures (3.2 & 3.4) show the development of the dry cell weight for the cultures, the erythromycin production and carbon dioxide evolution rates (CER). Maximum dry cell weight was 3.0 gL^{-1} and 4.65 gL^{-1} for 750 rpm and 500 rpm respectively. Specific carbon dioxide evolution rate (mmol (g cell)$^{-1}$h^{-1}) was higher in the early stage of growth for the higher stirrer speed, nitrogen was consumed more rapidly and the growth rate was also higher at this stage for higher stirrer speed (Figures 3.2 &3.4). A nitrate- reductase based assay kit was used for nitrate assay, this assay was not accurate for less than 0.1 gL^{-1} nitrate levels. In addition, the number of samples taken were not enough to find the exact time of nitrate depletion (the only nitrogen source). Figures (3.2 & 3.4) show that nitrate was finished after 66 h for 750 rpm experiment, whereas it was finished after 78 h for 500 rpm, and the cell production for the same amount of nitrogen consumption was higher at lower stirrer speed. This could be partly due to release of intracellular material at higher stirrer speed (Tanaka and Ueda, 1975). However, earlier exhaustion of nitrogen from the medium at 750 rpm, led to earlier mycelial disintegration.
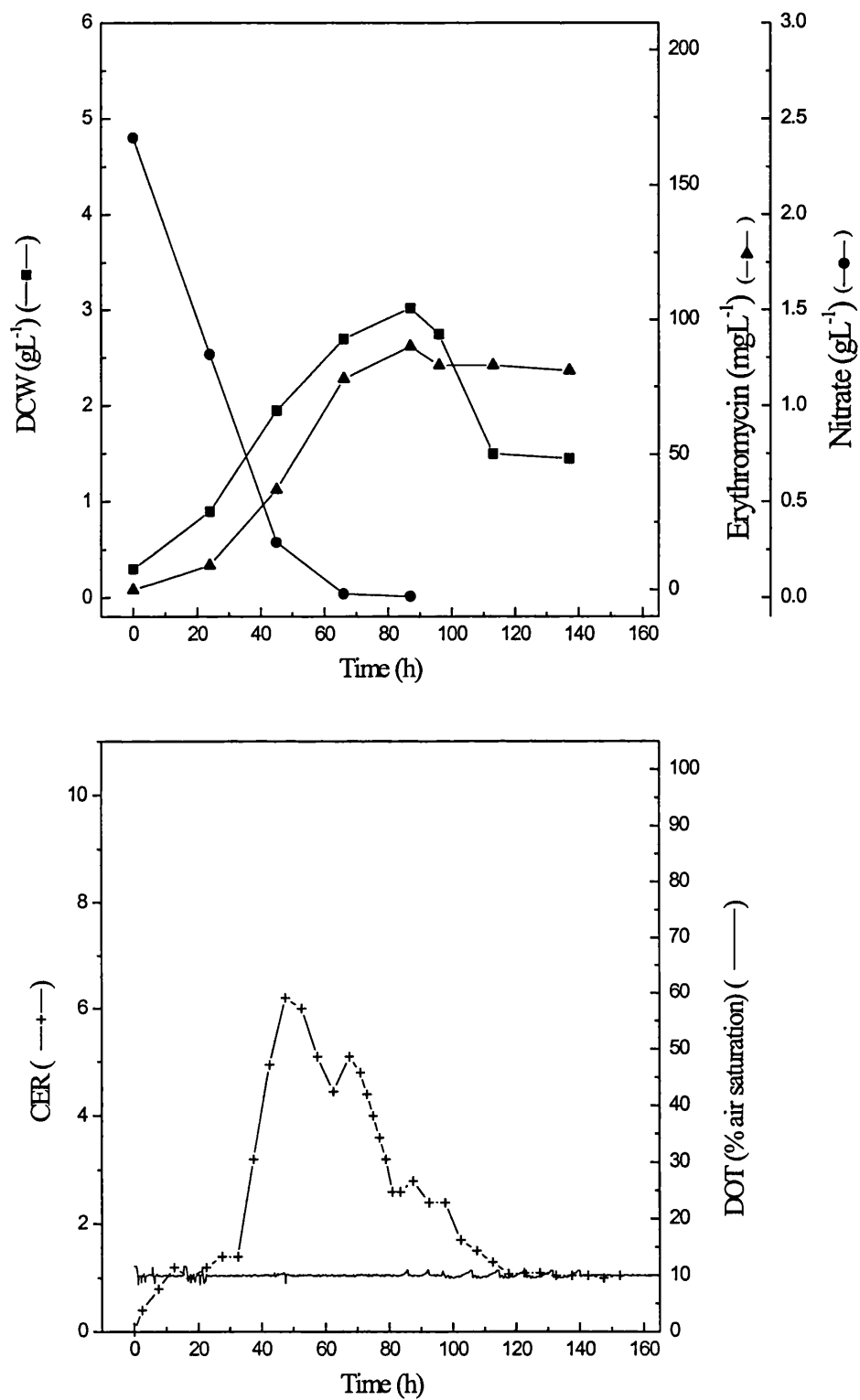
Figure 3.4: Changes of DCW, nitrate, erythromycin production, CER and DOT at 7-L
fermentation of *S. erythraea* using defined medium (stirrer speed = 750 rpm, gas flow rate =
0.75 vvm & DOT=10%).

Antibiotic production was growth linked and maximum production was less at higher stirrer speed due to lower cell production, but maximum specific production was not changed significantly (Figure 3.5). Erythromycin production started earlier at higher stirrer speed (750 rpm) and reached a maximum value (90 mgL^{-1}) at 87 h (see Figure 3.4), whereas a maximum value of erythromycin (165 mgL^{-1}) was obtained at 115 h at 500 rpm (Figure 3.2). The maximum specific production was 30 mg (g cell)$^{-1}$ at 750 rpm and 35 mg (g cell)$^{-1}$ at 500 rpm (Figure 3.5). The earlier commencement of the erythromycin production at higher stirrer speed (750 rpm) could be due to differences in inoculumn or earlier limitation of nitrogen source.
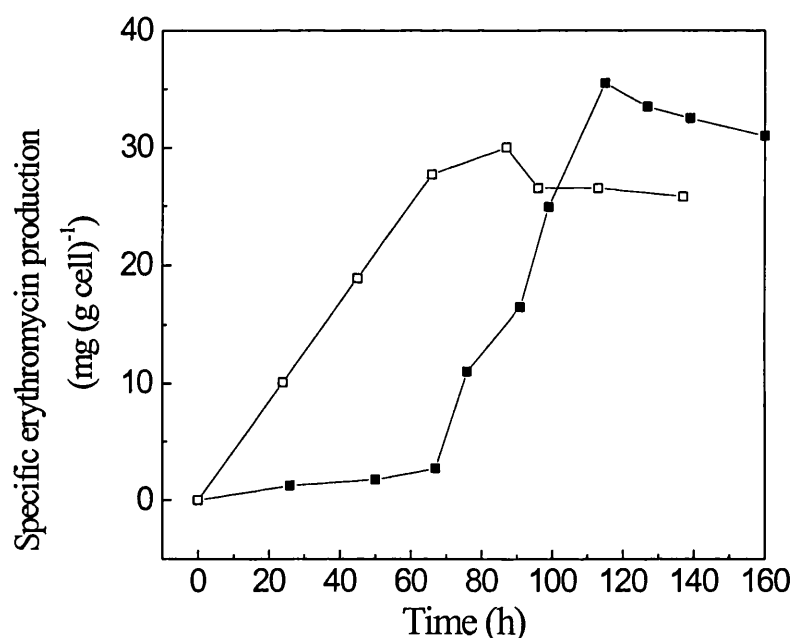
Figure 3.5: Comparison of specific erythromycin production at 500 rpm (—■—) and at 750 rpm (—□—).

Using image analysis, morphological parameters were measured and the major axis of the mycelia (both freely dispersed and clumps) and main length for the freely dispersed mycelia are shown in Figure 3.6. Mean major axis of the mycelia decreased from the beginning for fermentation at 750 rpm. For fermentation at 500 rpm, major axis of the mycelia decreased after 55 hr. Microscopical observation of samples taken
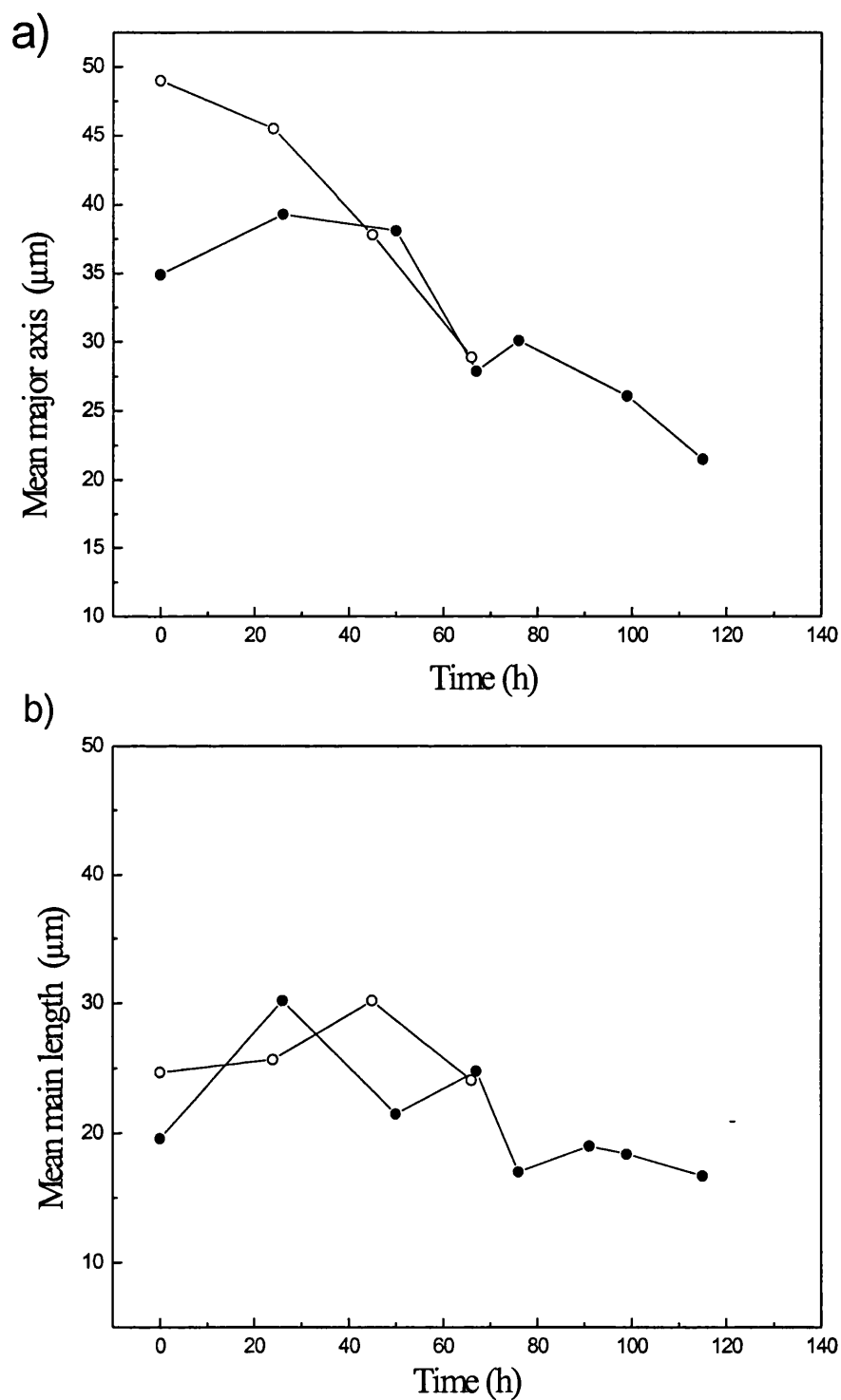
Figure 3.6: Changes of a) mean major axis of the mycelia (both freely dispersed and clumps), b) mean main length of the freely dispersed mycelia during the fermentation at 500 rpm (—●—) and 750 rpm (—○—). Define medium was used.

92

at 96 h and after this time from fermentation agitated at 750 rpm showed that mycelia were broken to small pieces. It was difficult to distinguish between very small pieces which were released by mycelia breakage and debris in the slides and this made morphological measurements impossible. This serious damage was also observed at a very late stage in the fermentation at 500 rpm (samples taken at 125 h and after this time).

3.2 Development of method for erythromycin analysis

Several analytical methods are available for quantification and isolation of erythromycin. These include: thin layer chromatography (TLC) (Khan *et al.*, 1994), gas liquid chromatography (Pellegatta *et al.*, 1983), bioassay (Pellegatta *et al.*, 1983) and high performance liquid chromatography (HPLC) (Tsuji and Geotz, 1978). In the first part of these experiments (experiments with defined medium) bioassay was used. The bioassay was not sufficiently accurate and in addition it was not specific for the different erythromycins. The errors in the determination of the erythromycin concentration may be as great as 20%. These errors can arise from pipetting and the control of the thickness of the agar layer on the bioassay plate (section 2.3.1); the errors increase with clearance diameter due to the logarithmic association (equation 2.1).

HPLC is the most common quantitative method for erythromycin analysis. However, due to the poor absorbance of erythromycin by UV (Grgurinovich and Mathews, 1988) and RI (Grgurinovich and Matthews, 1988), extraction and concentration of erythromycin prior to its analysis by HPLC is required. Liquid-liquid extraction (LLE) has been traditionally used to extract and concentrate erythromycin (Trilli et al., 1987). Several successive extractions and a large sample volume is required (see section 2.3.2). In addition, LLE is a lengthy process involving the use of hazardous solvents (chloroform was used in these experiments). Therefore, solid phase extraction using bond elut C18 cartridge was developed for concentration and cleaning the fermentation samples.

3.2.1 Development of solid phase extraction (SPE)

The characterisation of bond elut column has been explained in section (2.3.2). The typical steps in solid phase extraction are:

1) Conditioning the column: this step is done to activate the solid sorbents by passing an appropriate solvent through.

2) Rinsing: it is necessary to remove the activation solvent in the conditioning step by passing a liquid similar to the sample.

94

3) Applying the sample.

4) Rinsing: after applying the sample, the interfering compounds are washed from the cartridge, leaving the desired analyte on the solid sorbents.

5) Elution: the final step is to elute the desired analyte from the solid sorbents by passing an appropriate solvent through the column.

Initially a crude erythromycin standard (Abbott) was used to optimise the conditions and subsequently fermentation samples were used.

Step 1: Conditioning

Methanol with various concentration of diethylamine (DEA) were used for conditioning the cartridge. The recovery of the erythromycin is summarised in Table 3.1 (10 mM phosphate buffer pH 7.0 was used in steps 2 and 4; 1 mL 80% methanol in water was used in step 5; 10 mL samples used in step 3). Recovery was 80.5% when 100% methanol was used in step 1. This recovery increased as the DEA concentration was increased from 0 to 0.5%. Further increase in the concentration of DEA to 1% and 2% had no change on the recovery of erythromycin. Therefore, methanol consisting of 0.5% DEA was used for further study. DEA has both hydrophilic (amine group) and hydrophobic (ethyl group) groups and may react like ion-pair agent in HPLC column and alter the retention behaviour of erythromycin in the column. The various DEA concentrations did not have an effect on the shape of erythromycin A HPLC peak.

Table (3.1): Effect of DEA concentration on recovery

of erythromycin

% DEA in methanol	% erythromycin recovery
0	80.5 ± 1.5
0.25	90 ± 1.0
0.5	94 ± 0.5
1.0	94 ± 0.6
2.0	93.8 ± 1.1

Step 2 and 4: Rinsing

Step 2 was necessary for removing the activation solvent in the first step. Chromatograms for a sample without applying step 2 (10 mM phosphate buffer pH 7.0 was used in step 4), show tailing of erythromycin A peak and very low recovery (18%). Three different aqueous solutions were tested in step 2 and 4 including RO water, phosphate buffer (10 mM) and tris (20 mM) buffer at pH 7.0 and resulted in similar results for all three cases, except when tris buffer was used, a peak with retention time of 11 minute appears in the chromatogram, compared with two other cases (chromatograms is shown in Figure 3.7). Then phosphate and tris buffers at pH 6.5-8.0 were tested and there was no effect from the pH either on percentage of recovery or in the shape of the chromatogram.

Step 3 and 5: Applying the sample and elution

In order to concentrate the samples 2.5-20 times, 2.5, 5, 10 and 20 mL crude erythromycin standard (Abbott) was passed through the column and diluted with 1 or 2 mL of appropriate solvent. A sample volume of 20 mL resulted in considerably lower recovery of erythromycin (65%) with either 1 or 2 mL eluent volume, whereas the results were the same for other cases. Therefore, 10 mL was determined to be the maximum volume of sample which should be passed through the column. There was no difference in percentage of recovery of erythromycin when 1 or 2 mL of eluent was used with 10 mL of sample. Since erythromycin is both hydrophobic and hydrophilic, various concentrations of methanol in water were tested as eluent. Erythromycin recovery increased with increasing methanol concentration from 60 to 80% (v/v); further increase in methanol concentration did not have a significant effect (Table 3.2). Acetonitrile (100%) was also used to elute the erythromycin from the solid sorbents; again this resulted in lower (81%) recovery. Another solvent tested in elution step was 0.5% (v/v) DEA in methanol resulting in 77% erythromycin recovery. These results, were then applied to fermentation samples and similar results were obtained, except when acetonitrile was used for the elution the collected eluted samples were cloudy. Therefore, 1 mL 100% methanol was used as a eluent for the further studies.

a)

b)
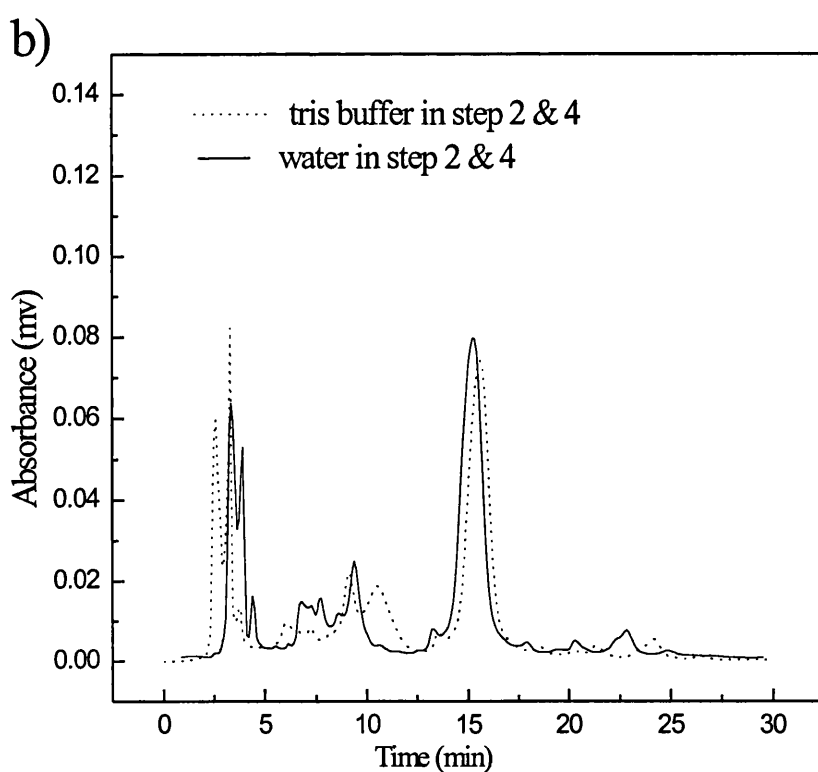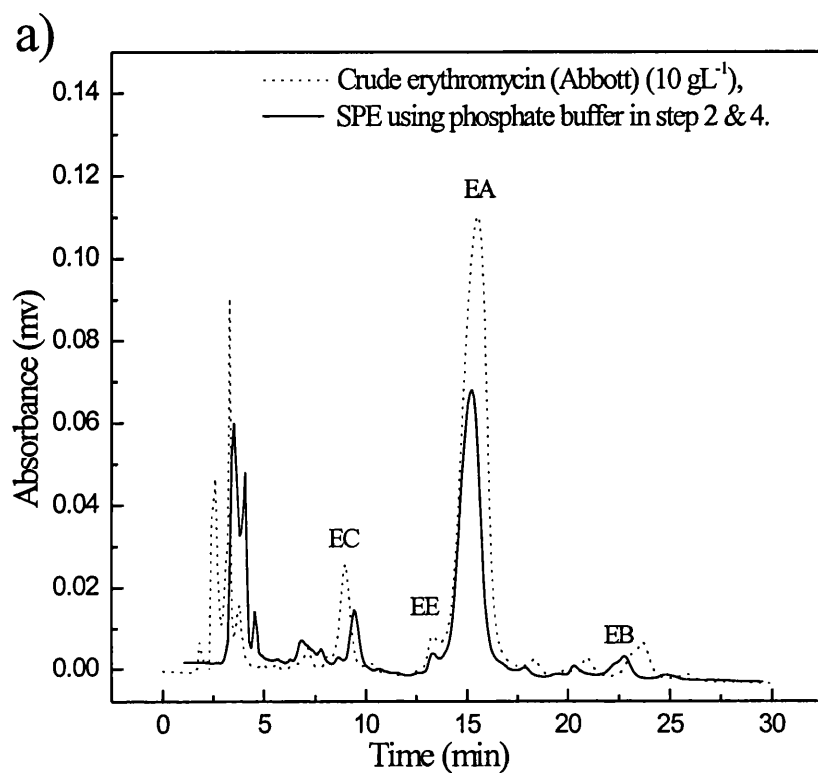
Figure 3.7: HPLC chromatograms of crude erythromycin (Abbott) and eluent obtained from solid phase extraction.

Table 3.2: Erythromycin recovery from a crude standard solution (Abbott) with various concentrations of methanol in the elution step.

% methanol in water (v/v)	% erythromycin recovery
60	32 ± 1.0
70	90 ± 2.2
80	94 ± 2.8
90	94 ± 2.5
100	95 ± 2.2

Using the following 5 steps, a 0.5 gL^{-1} crude erythromycin A solution in water was concentrated with 95% erythromycin recovery.

1) activate the cartridge by passing 5 mL methanol consisting of 0.5% DEA through the column.

2) wash the activation solvent by passing 5 mL 10 mM phosphate buffer pH 7 through the column.

3) apply 10 mL sample

4) rinse the interfering compounds of the samples by passing 5 mL 10 mM phosphate buffer pH 7 through the column.

5) elute erythromycin with 1 mL 100% methanol

The above optimised steps were then followed to extract erythromycin from *S. erythraea* fermentation samples. Fermentation samples were centrifuged on a lab top centrifuge (model CS-6R) at 4200 rpm for 20 minutes. Initially only 70% of the erythromycin could be recovered following the above mentioned steps. Sample volume then reduced in step 3 to 2.5 and 5 mL; this resulted in an increase in the recovery of erythromycin from 70% to 85%. The increase in erythromycin A recovery with smaller volume could be due to 1) 10 mL fermentation sample volume is overloading the cartridge, or 2) fermentation samples used are not free of insoluble particles, hence clogging the solid sorbents. To test the second hypothesis, supernatant obtained from the above mentioned centrifugation was centrifuged again with microfuge (Beckman, microfuge 11) for 10 min at 13,000 rpm, and then applied in

step 3. Ten mL of twice centrifuged fermentation samples resulted in 85% erythromycin recovery; sample volume of 2.5 and 5 mL did not change this recovery if samples had been centrifuged at 13,000 rpm in microfuge. These results indicate that the insoluble particles in fermentation samples had caused the low initial recoveries and the cartridge was not overloaded with 10 mL fermentation sample. The lower erythromycin recovery from fermentation samples compared with the crude erythromycin solution could be attributed to the increased amount of interfering compound present in the fermentation broth.

Solid phase retentates from both standard solutions and fermentation samples were periodically collected and analysed for erythromycin. The collected retentates were run through the cup plate bioassay to measure their antibiotic activity. The results showed that <1% of the erythromycin crude standard (Abbott) solution was passed through the cartridge without binding to the solid sorbents; this retentate concentration was <5% when fermentation samples were used. This shows that the reduced recovery of erythromycin is mainly due to its irreversible binding to the solid sorbents.

Comparing LLE and SPE

Liquid-liquid extraction (see section 2.3.2) of erythromycin from fermentation samples, resulted in 80 ± 5% recovery. The chromatogram of both liquid liquid extract and solid phase extract of a fermentation sample are shown in Figure 3.8. There were no preference for any methods as far as shape of chromatogram or the percentage of recovery is concerned. However, the time involved in performing the extraction is much reduced when solid phase extraction is utilised (30 minutes vs. 12 hours). The exposure to hazardous solvents is also reduced in solid phase extraction. For economic reason the reusability of the column has also been tested (Heydarian *et al.*, 1998). The column can be regenerated by passing 10 mL 80% (v/v) methanol in water through it under light vacuum. Each column can be used twice with 2-3% loss of recovery.

3.2.2 Erythromycin measurement in fermentation samples

The concentrated samples obtained with optimised solid phase extraction method were analysed by HPLC (see section 2.3.2). The elutate from HPLC was collected (see section 2.3.2) and run through cup plate bioassay. It was found that antibiotic activity corresponded only for the peaks with retention time of erythromycin A, B and C. Antibiotic activity of the collected eluate was also measured and compared with the result obtained by the area of HPLC chromatograms (see section 2.3.1). The results showed that the amount of the erythromycin A obtained from chromatograms is in a good agreement with the results obtained from running the eluate through the bioassay cup plate (Table 3.3). The chromatograms had relatively symmetric peaks with a good resolution and base line (Figure 3.8). This leads to reliable results for measuring erythromycin A. A very small peak before erythromycin A (retention time = 13 min) seems to be erythromycin E and its area was <2% of the erythromycin A (EA). The peaks obtained for erythromycin B (EB) and erythromycin C (EC) did not have a good resolution and were asymmetric; in addition the base line of the erythromycin C peak was not good (Figure 3.8). This led to inaccuracy for measurements of erythromycin B and C.
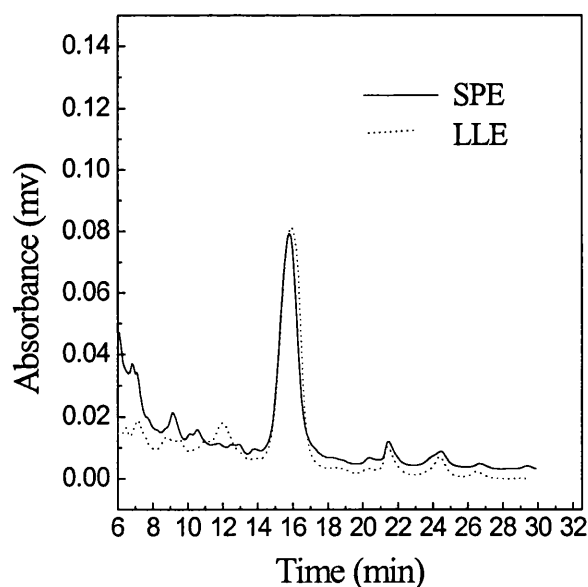
Figure 3.8: HPLC chromatogram of liquid-liquid extraction (LLE) and solid phase extraction (SPE) of fermentation sample.

100

Table 3.3: Comparison of results obtained with area of HPLC
chromatogram and bioassay:

Sample	EA (mgL⁻¹)		EB (mgL⁻¹)		EC (mgL⁻¹)	
	HPLC	Bioassay	HPLC	Bioassay	HPLC	Bioassay
S1	3740	3915 ± 420	426	260 ± 32	199	191 ± 20
S2	4120	4160 ± 320	286	87.6 ± 21	198	248 ± 32
S3	4730	4948± 390	296	90.2± 12	45	154 ± 12

To obtain a better chromatogram for erythromycin B and C addition of an ion pair agent such as tetrabutyl ammonium sulphate (Nasr and Tschappler, 1997) under gradient elution is suggested. Nevertheless, the measurements of erythromycin A in fermentation samples showed that the amount of erythromycin A is between 85-95% of the total erythromycin.

Summary

Extraction and concentration of erythromycin from the fermentation samples is required prior to its analysis by HPLC. Liquid-liquid extraction has been traditionally used to extract and concentrate erythromycin. A rapid and simplified solid phase extraction of erythromycin from fermentation broth was developed. This method results in 85% recovery of erythromycin with a batch to batch variability of less than 3 percent. In comparison with previous method of erythromycin extraction (LLE), solid phase extraction is cleaner, less time consuming and exposure to hazardous solvents is reduced.

3.3 Effect of agitation at 7-L fermenter using complex medium

The defined medium used was very poor in nitrogen resulting in slow growth rates (maximum 0.07 h^{-1}), a low biomass level (maximum 5.6 gL^{-1}) and low erythromycin production (maximum 200 mgL^{-1}) thus its results were dissimilar to the typical industrial fermentation. Therefore for further studies, complex medium was preferred and used to find the effect of shear on morphology and erythromycin production of *S. erythraea*.

3.3.1 Shake flask experiments

Before performing experiments in a stirred tank, some experiments were carried out at shake flasks to understand the growth pattern and erythromycin production of *S. erythraea* in complex medium. Experiments were carried out without adding buffer and with adding buffer (MOPS) to the medium (see section 2.2.6), and the DCW, erythromycin and the glucose concentration of the culture were measured every 24 hr.

S. erythraea was cultured for 7 days. In experiments without buffer the pH was decreased to 5.9 during growth phase, and remained constant for 72-96 h. A rise in pH followed and continued until near the end of the fermentation, and the final value of pH was 9.1. In experiments with adding buffer, minimum pH was 6.5 due to the addition of buffer to the medium. Development of the biomass, erythromycin production and glucose concentration are shown in Figure 3.9 for experiments with addition of buffer and and in Figure 3.10 for experiments without addition of buffer. Using baffled flasks caused high agitation and the sticking of biomass to the wall of flask which led to errors in dry cell weight measurements. Maximum dry cell weight was 6.7 ± 0.2 gL^{-1} for experiments without buffer and it was 7.3 ± 0.2 gL^{-1} for the experiments with pH control. The sample taken was not enough, to find the exact growth curve, the end of the growth phase was approximately 70 h. Maximum erythromycin production was 385 ± 60 mgL^{-1} for the experiments with buffer, whereas it was 153 ± 12 mgL^{-1} for the experiment without buffer. Optimum pH for erythromycin production has been reported around 6.85 (Osman *et al.*, 1968), whereas *S. erythraea* can grow over a wide pH- range (pH 5-9). Instability of erythromycin at
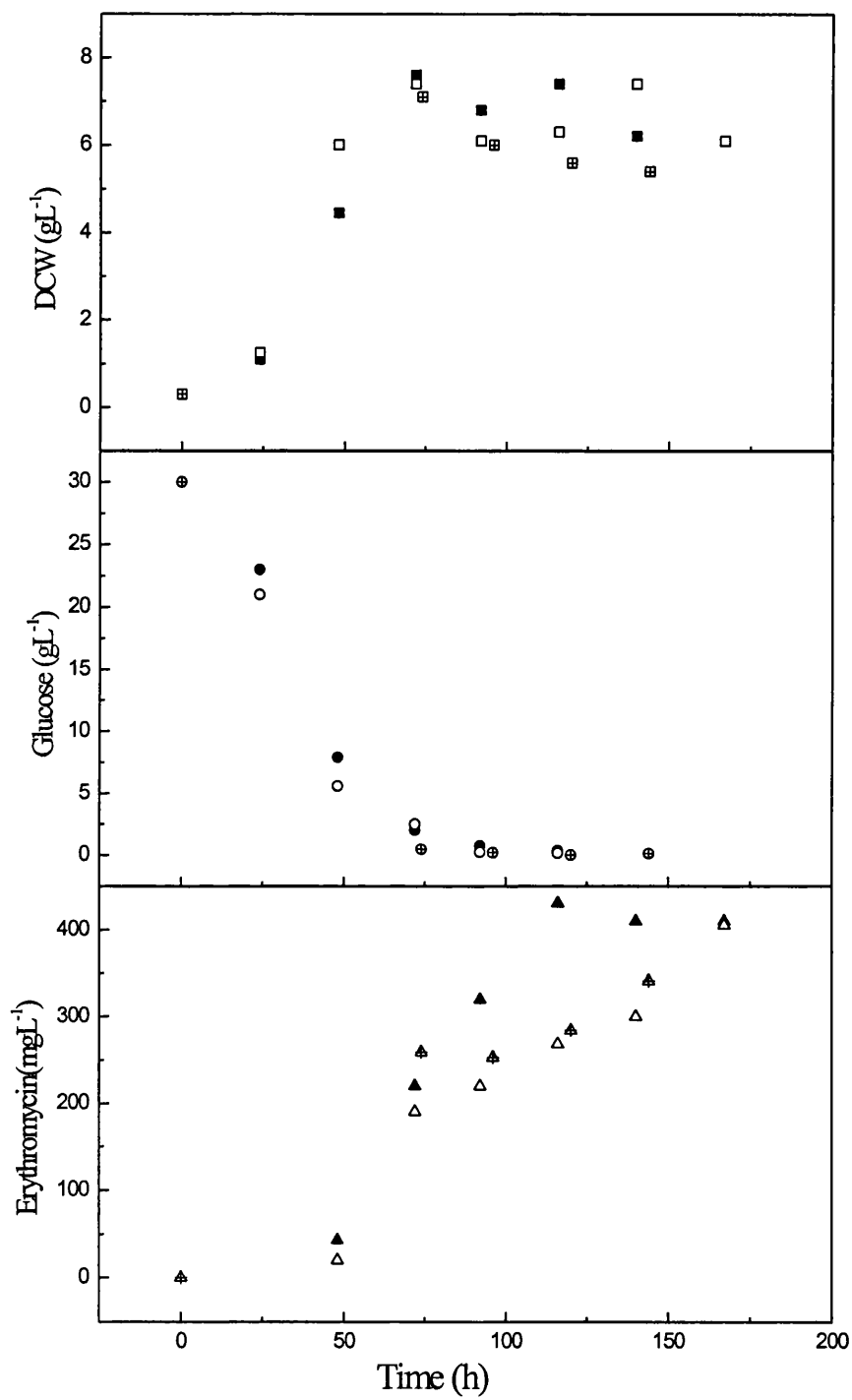
Figure 3.9: Changes of DCW, glucose and erythromycin production during shake flask experiments. Complex medium used with adding buffer. Different symbols belong to different experiments.
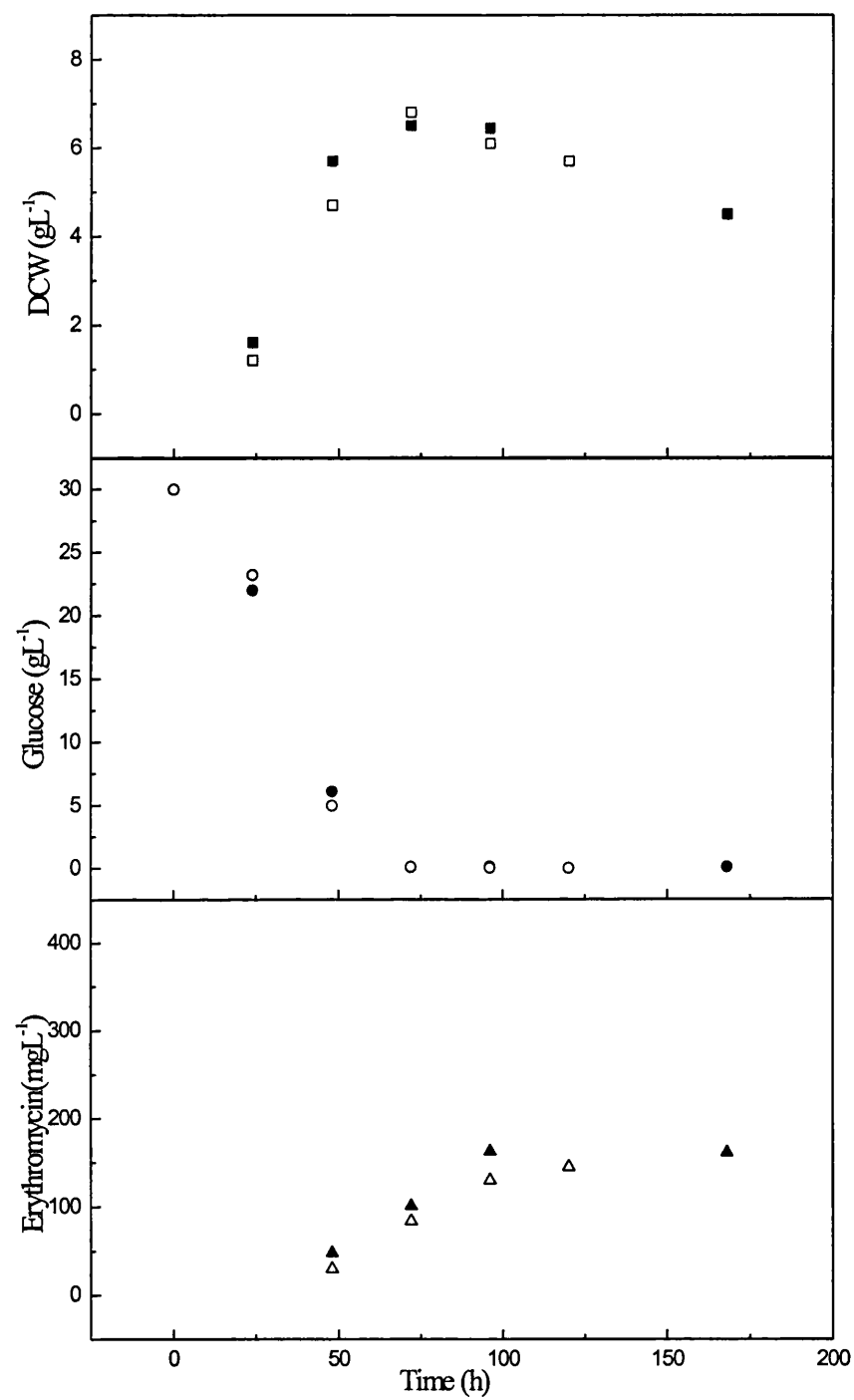
Figure 3.10: Changes of DCW, glucose and erythromycin production during shake flask experiments. Complex medium used without adding buffer. Different symbols belong to different experiments.

acidic pH was reported by Kibwage (1987), which might be another reason for lower erythromycin at lower pH. Specific erythromycin production for experiments with pH control was 53 ± 7 (mg gcell^{-1}), which is 2.3 times higher than experiments without pH control. These experiments showed that pH has a significant effect on erythromycin production, whereas its effect on growth is minor, provided that it is between 5.9 to 9.1.

3.3.2 Effect of agitation on growth and erythromycin production

In order to examine the effect of agitation on the growth and morphology of *S. erythraea* and subsequent effect of these on erythromycin production and also rheology of the culture, a range of fermentations were carried out as reported in section (2.2.3). Five different speeds were used: 300, 500, 750, 1000 and 1250 rpm. Tip speed was between 1.07 and 4.45 (Table 3.4), which covered the entire range of the speeds practical for the scale of fermenter.

Table 3.4 : Tip speed of the fermentation at 7-L scale

Stirrer speed (rpm)	Tip speed (ms^{-1})
350	1.07
500	1.78
750	2.7
1000	3.56
1250	4.45

The DOT was kept above 60% by adding oxygen to the air inlet at 350 and 500 rpm (Figures 3.11 & 3.12). For other stirrer speeds, DOT was not controlled. At 750 rpm, DOT dropped to 45% (Figure 3.13) and at 1000 and 1250 rpm the DOT was above 60% (Figures 3.14 & 3.15) during the entire fermentation. It has been reported that no significant effects on growth, morphology, and productivity are to be expected from drop to such a DOT level (Belmar-Beiny and Thomas, 1991), therefore, differences in culture behaviour may be considered to be mainly due to mechanical forces.

All the experiments were carried out twice except at 1000 rpm. Figures 3.11, 3.12, 3.13, 3.14 and 3.15 show the reproducibility of the system for dry cell weight, glucose consumption and erythromycin production at each stirrer speed.
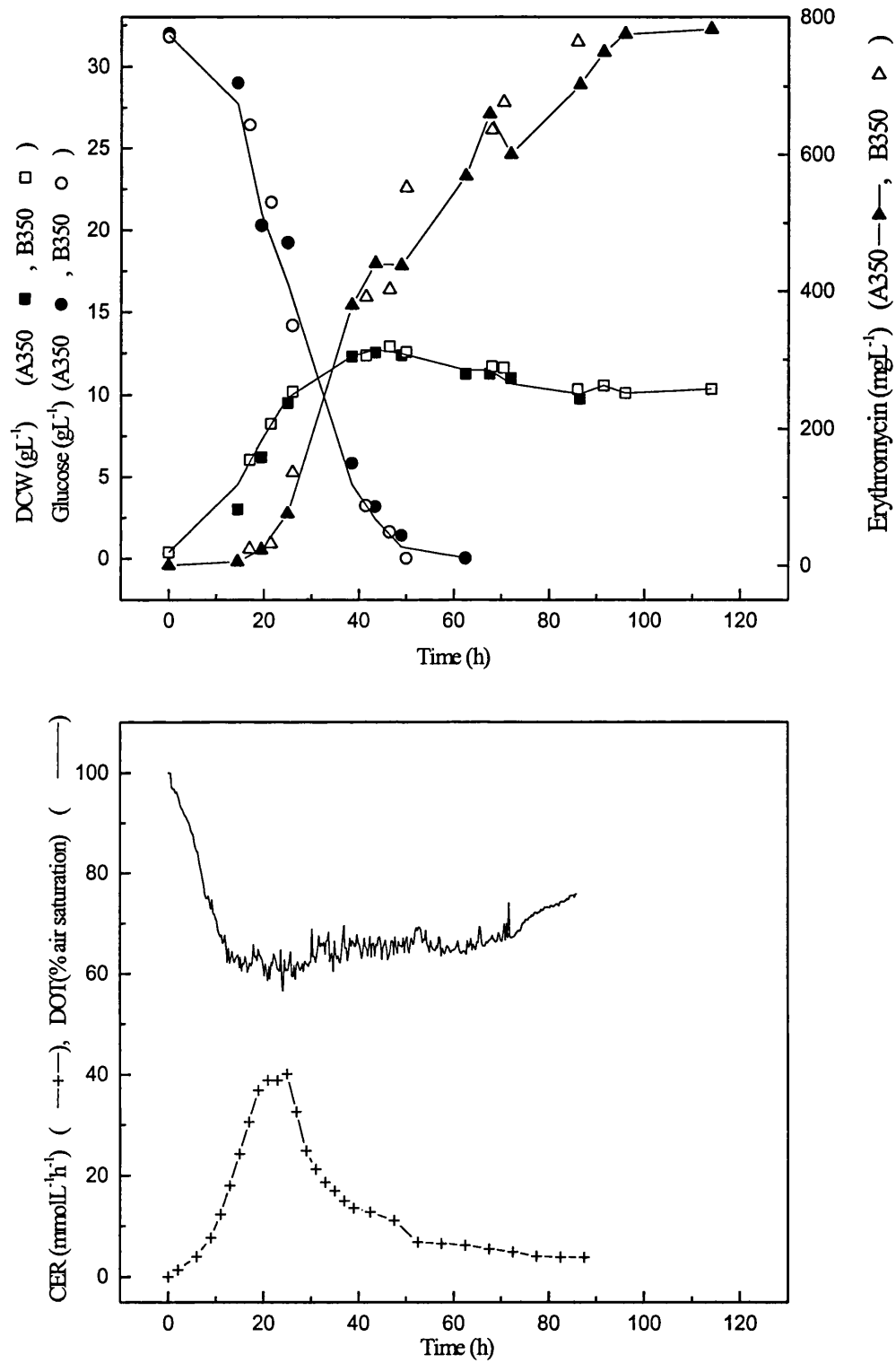
Figure 3.11: Changes of DCW, glucose, erythromycin production, CER and DOT at 7-L fermentation of *S. erythraea* using complex medium (stirrer speed = 350 rpm).
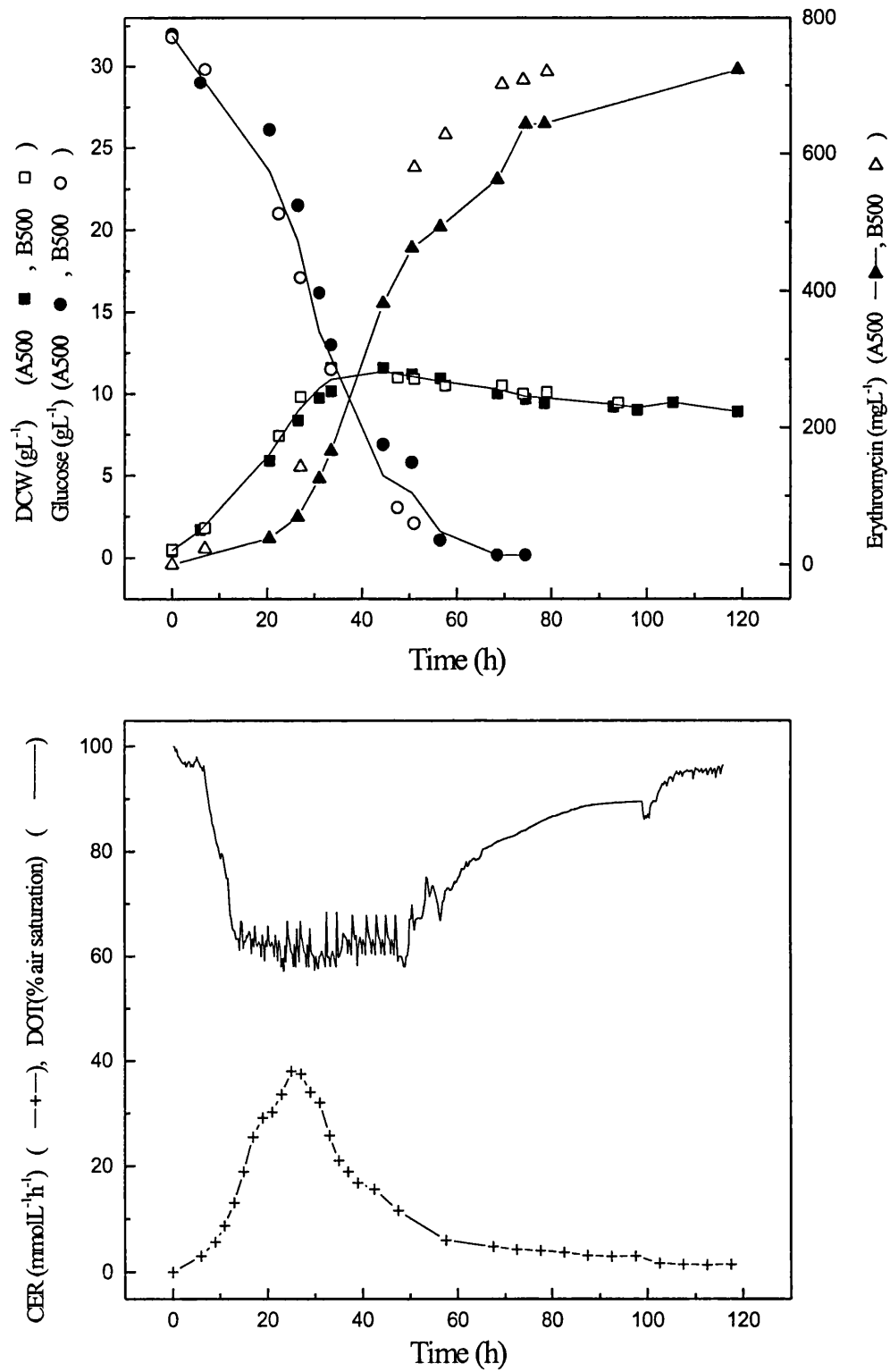
Figure 3.12: Changes of DCW, glucose, erythromycin production, CER and DOT at

7-L fermentation of *S. erythraea* using complex medium (stirrer speed = 500 rpm).
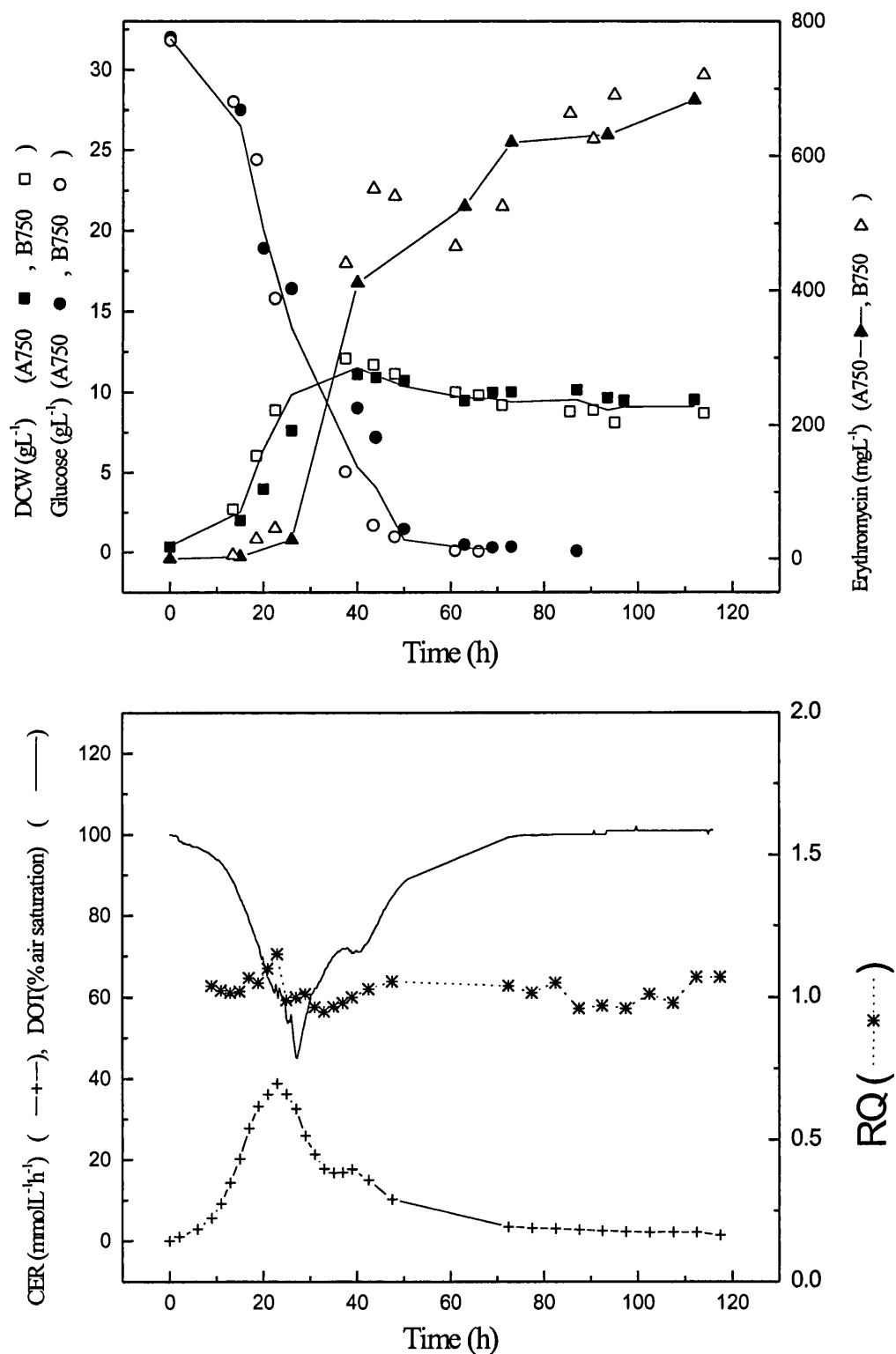
Figure 3.13: Changes of DCW, glucose, erythromycin production, CER, RQ and DOT at 7-L fermentation of *S. erythraea* using complex medium (stirrer speed = 750 rpm).
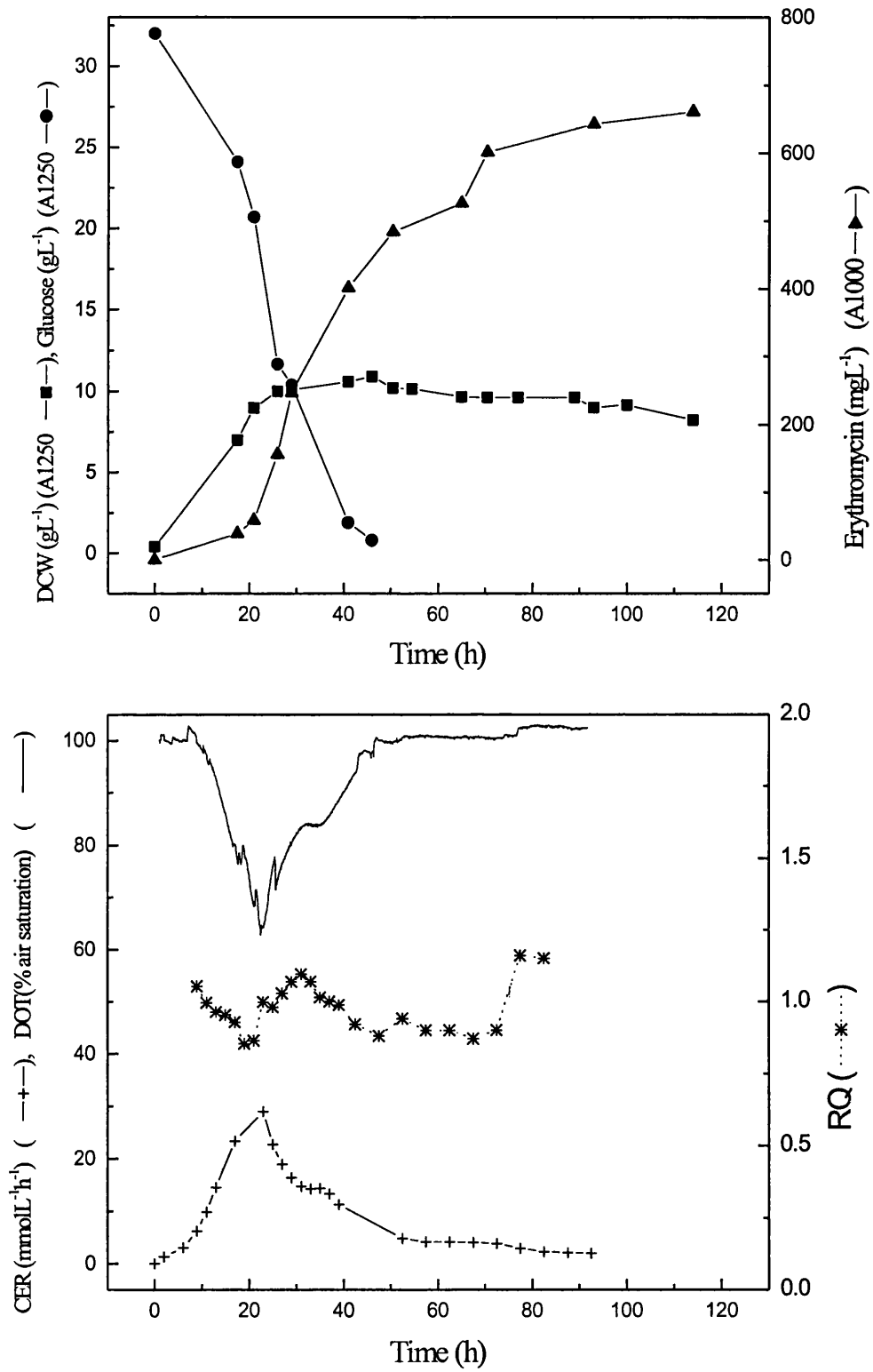
Figure 3.14: Changes of DCW, glucose, erythromycin production, CER, RQ and DOT at 7-L fermentation of *S. erythraea* using complex medium (stirrer speed = 1000 rpm).
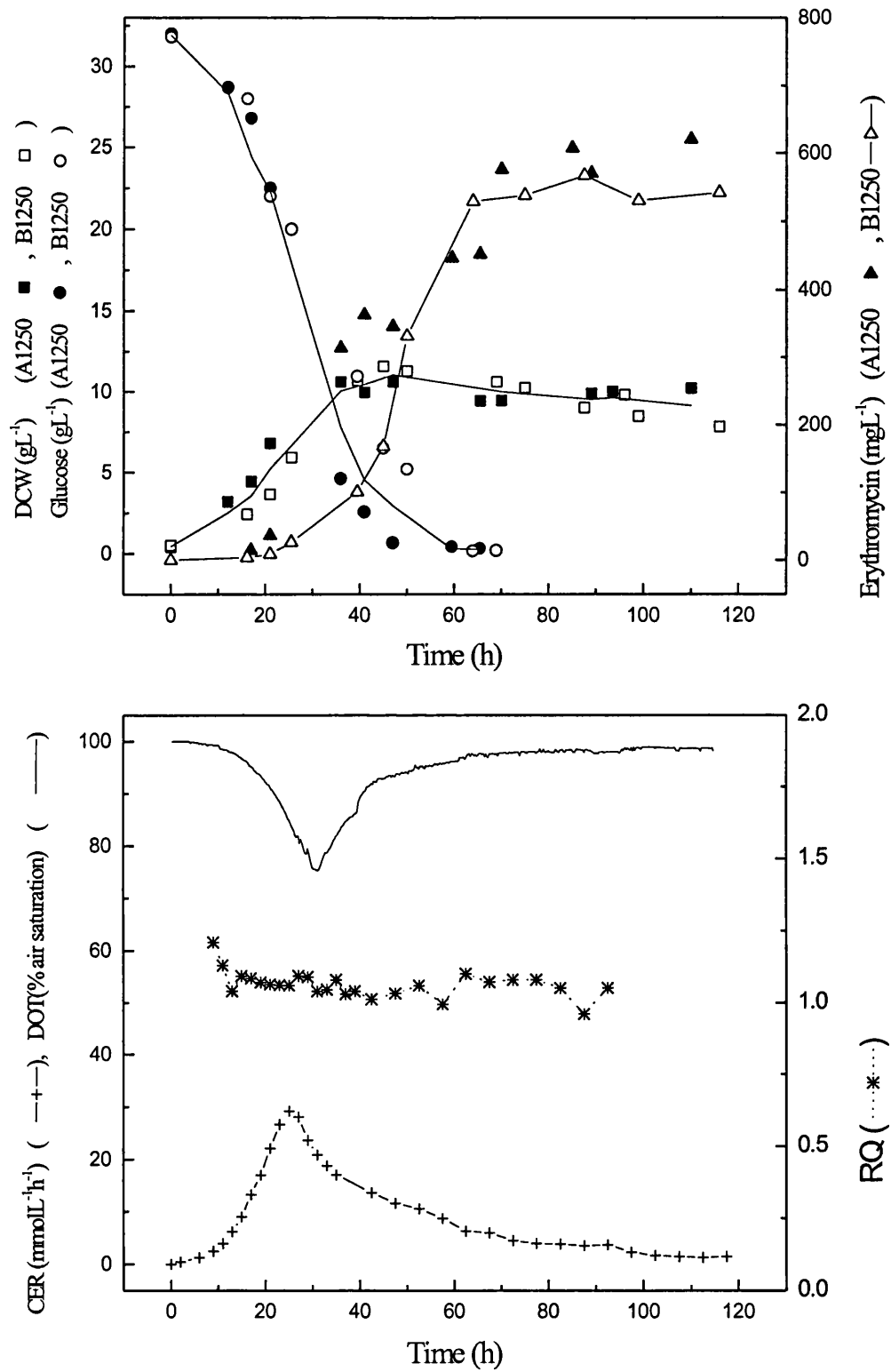
Figure 3.15: Changes of DCW, glucose, erythromycin production, CER, RQ and DOT at 7-L fermentation of *S. erythraea* using complex medium (stirrer speed = 1250 rpm).

The reproducibility of the system was excellent at 350 rpm and 500 rpm and the differences in time course of the fermentation at 750 & 1250 rpm might be caused by variation in the condition of the inoculum. Although great precaution was taken to have the same inoculum for all the experiments. However, still some differences between the quantity of the biomass and its morphology occurred (see Table 3.5).

Table 3.5: DCW and morphology of the inoculum

Fermentation	DCW (gL^{-1})	Mean major axis of the mycelia (μm)	%Clump
A350	2.6	50.1	77
B350	2.5	51.8	68
A500	2.0	55	91
B500	1.9	47.8	65
A750	1.5	-	-
B750	2.1	44.8	76
A1000	2.5	58.7	92
A1250	2.3	43.9	87
B1250	2.6	56.5	91

There was a similar pattern in each experiment of the rapid growth phase from 10 to 25 h, followed by deceleration phase till 40 h. Maximum biomass concentration was lower at higher speeds (Figures 3.11 & 3.15). Maximum biomass was 11.1 ± 0.5 gL^{-1} at 1250 rpm, whereas it was 12.7 ± 0.2 gL^{-1} at 350 rpm. The growth rate was relatively high in all the experiments, the data is not sufficient to calculate the exact growth rate for the cultures, and maximum specific growth rate was about 0.15 - 0.20 h^{-1} , and occurred around 20 h. For comparison of fermentations at different stirrer speeds, the data on each measurement at each speed were pooled and a curve representing the average time course constructed (by hand) through the points, and average time course was shown for all the experiments in Figure 3.16. It appears that the maximum biomass
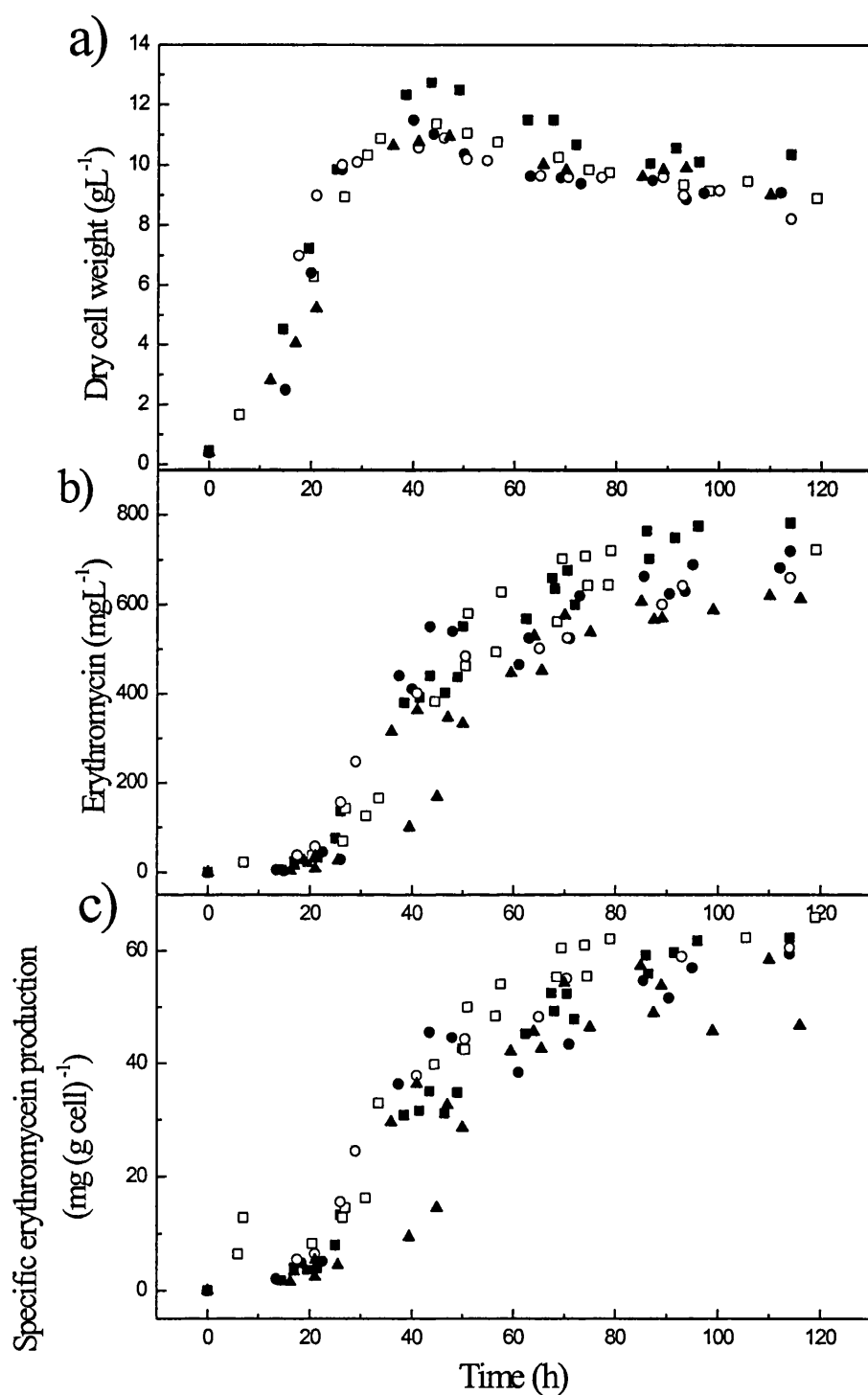
Figure 3.16: Growth and erythromycin production in *S. erythraea* fermentation a) Dry cell weight b) erythromycin c) specific erythromycin production. Experiments at 7-L scale and stirrer speed (rpm): 350 (■), 500 (□), 750 (●), 1000 (○) and 1250 (▲).

concentration was slightly higher at 350 rpm compared with other stirrer speeds. The biomass decreased to 9-9.5 gL^{-1} for 500, 750, 1000 and 1250 rpm toward the end of the fermentation (120 h), and it was slightly higher (10 ± 0.2 gL^{-1}) at 350 rpm.

The pattern of glucose consumption was similar to each other (Figures 3.11, 3.12, 3.13, 3.14 and 3.15). The initial concentration of glucose was 32 gL^{-1} which was 2 gL^{-1} above the considered concentration of the glucose in the medium, due to the addition of unconsumed glucose in the inoculum to the medium. Glucose concentration decreased slowly to 25 gL^{-1} in the early stage of the growth, followed by a rapid decrease in the rapid growth phase, and it was almost depleted by 50 -60 h.

The concentration of KH_2PO_4 was 0.7 gL^{-1} at the start of the fermentation which correspond to 0.5 gL^{-1} of PO_4^{3-} or 0.16 gL^{-1} of phosphorus. The concentration of phosphate in fermentation samples was only measured for B350 and B1250 and is plotted against time in Figure 3.17. The concentration of phosphate decreased from 0.7 gL^{-1} at the start of the fermentation to 0.07-0.11 gL^{-1} at the end of the rapid growth phase (20 - 25 h) in both experiments. The level of phosphate was slightly less at higher stirrer speed (1250 rpm) compared to lower speed (350 rpm). The concentration of phosphate decreased till 40 h and then it was fluctuated toward the end of the fermentation. It should be noted that the method used for phosphate measurement was not accurate for concentrations below 0.1 gL^{-1}.
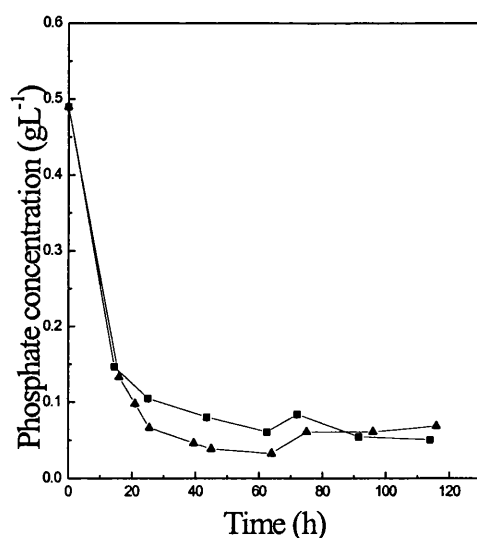
Figure 3.17; Changes of phosphate concentration during fermentations at 350 (—■—) and 1250 rpm (—▲—).

The time course of the carbon dioxide evolution rate (CER) and respiratory quotient (RQ) for fermentation agitated at 750, 1000 and 1250 rpm are shown in Figures 3.13, 3.14 and 3.15. Data for the oxygen uptake rate (OUR) and consequently RQ is not available for 350 rpm and 500 rpm fermentations (see section 2.2.4), and the time course of the CER for these experiments are shown in Figures (3.11 & 3.12). The data suggested that germination began around 5 h. The peak of CER occurred around 20-25 h and it was about 40 mmolL^{-1}h^{-1} at lower speeds (350, 500 and 750 rpm) and 32 mmolL^{-1}h^{-1} at higher speeds (1000 and 1250 rpm). At 1000 rpm, the RQ was almost 1 in the early stage of the growth, it decreased to 0.85 at the end of the rapid growth phase (25h) followed by an increase in slow growth phase (25-35h) to 1 and then decreasing again to 0.85. At 750 and 1250 rpm, RQ is almost 1.0 during the experiments, without any special trends, except it is increasing to 1.1 during the rapid growth phase. The differences between RQ at 1000 rpm and 750 or 1250 rpm was not significant and might be because of experimental errors like calibration errors.

Erythromycin production started from the beginning of the fermentation at a very slow rate and the concentration was 30 - 40 mgL^{-1} at the end of the rapid growth phase

(20 - 25 h) (Figures 3.11, 3.12, 3.13, 3.14 & 3.15). Erythromycin was produced at the highest rate in deceleration phase and the level of erythromycin was about 400 mgL^{-1} at the end of the deceleration phase (40 h). Then erythromycin production continued till 70 h. The level of the erythromycin tended to increase slightly between 70 to 110 h (Figure 3.16). The final level of erythromycin (average value between 90 to 110 h) was higher at lower stirrer speeds (Table 3.3.2.3). The final level of erythromycin was 736 ± 49 mgL^{-1} at lower speeds (350), decreasing to 570 ± 32 mgL^{-1} at higher speeds (1000 and 1250 rpm). Specific erythromycin (mg (g cell)$^{-1}$) was almost the same at stirrer speeds of 350 to 1000 rpm, and it decreased by 10% at 1250 rpm (Table 3.6).

Table 3.6: Final level of erythromycin for fermentation

at 7-L scale

Stirrer speed (rpm)	Concentration of erythromycin (mgL^{-1})	Specific erythromycin (mg (g cell)$^{-1}$)
350	736 ± 49	58 ± 3.8
500	692 ± 26	59.5 ± 2.4
750	665 ± 37	57.1 ± 3
1000	652 ± 13	59.9 ± 1.2
1250	571 ± 32	52 ± 1.8

3.3.3 Effect of agitation on morphology of cell

Microscopical observation showed that there were no pellets in these experiments, except in very few cases in fermentation at 350 rpm (Figures 3.18 and 3.19). The results of the determination of morphological measurements (see Table 2.6 for definition of the morphological parameters) are shown in Figures 3.20 to 3.28 according to Table 3.7. The data at any stirrer speed are for two sets of the experiments (except at 1000 rpm) demonstrating the degree of reproducibility of the results. Dotted lines representing the trend of the data and are fitted (by hand) through the points.

Table 3.7: Figures corresponding to morphological parameters

Figure	Morphological parameters[1]
3.20	mean major axis [2]
3.21	mean major axis for mycelial clumps
3.22	minor axis / major axis for mycelial clumps
3.23	mean clump area
3.24	roughness of the mycelial clumps
3.25	percentage of the clumps area
3.26	mean main length of the freely dispersed mycelia
3.27	mean branch length of the freely dispersed mycelia
3.28	mean number of tips for freely dispersed mycelia

(1) see Table 2.6 for definition of the morphological parameters

(2) data is for both freely dispersed mycelia and mycelial clumps

The mean major axis of the mycelia (both freely dispersed and clump) tended to increase during the rapid growth phase (10 to 20-25 h), and then decreased to an equilibrium size at 60-70 h (Figures 3.20 and 3.21). The equilibrium major axis was lower at higher speeds. It appeared from the data in Figures 3.20 and 3.21 that the mean major axis slightly increased after 60-70 h, but its increase appears to be in the
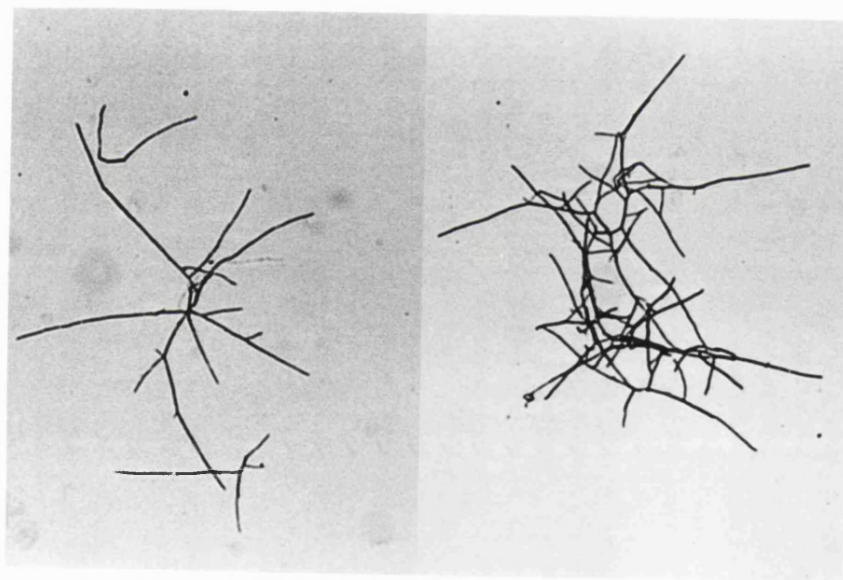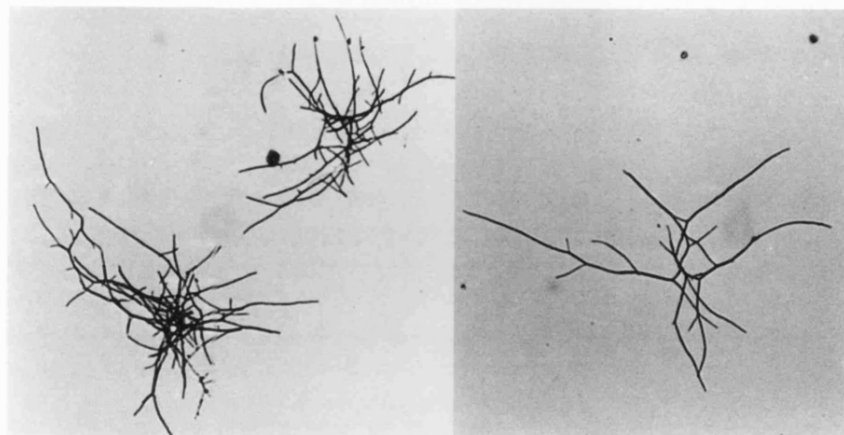
Figure 3.18: Photographs of Mycelial clumps observed in the *S. erythraea* fermentation. Scale, (——) = 20 μm

Figure 3.19a : Photographs of freely dispersed mycelia observed in *S. erythraea* fermentation. Scale, (———) = 20 μm.
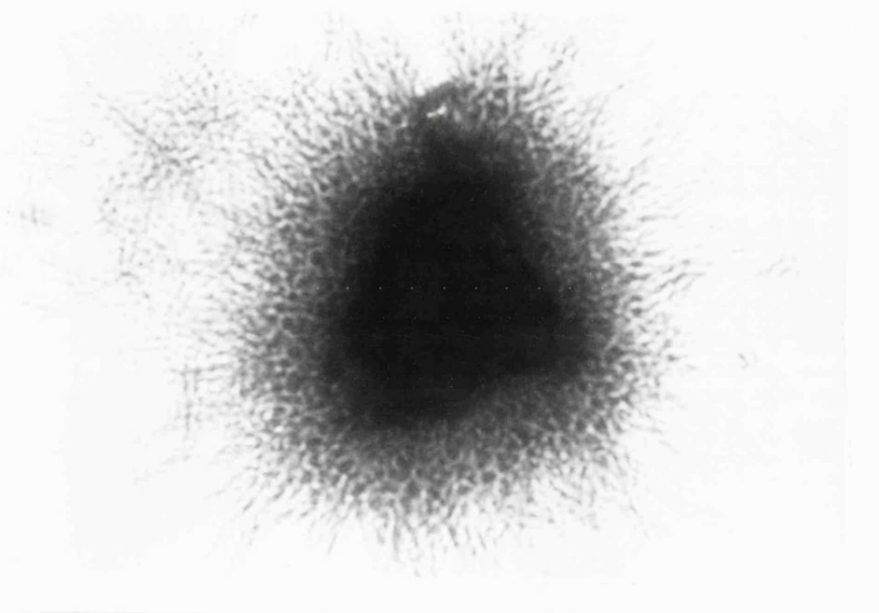
Figure 3.19b: Photographs Hairy pellets obseved in very few cases in *S. erythraea* cultures at 350 rpm. Scale, (———) = 20 μm.
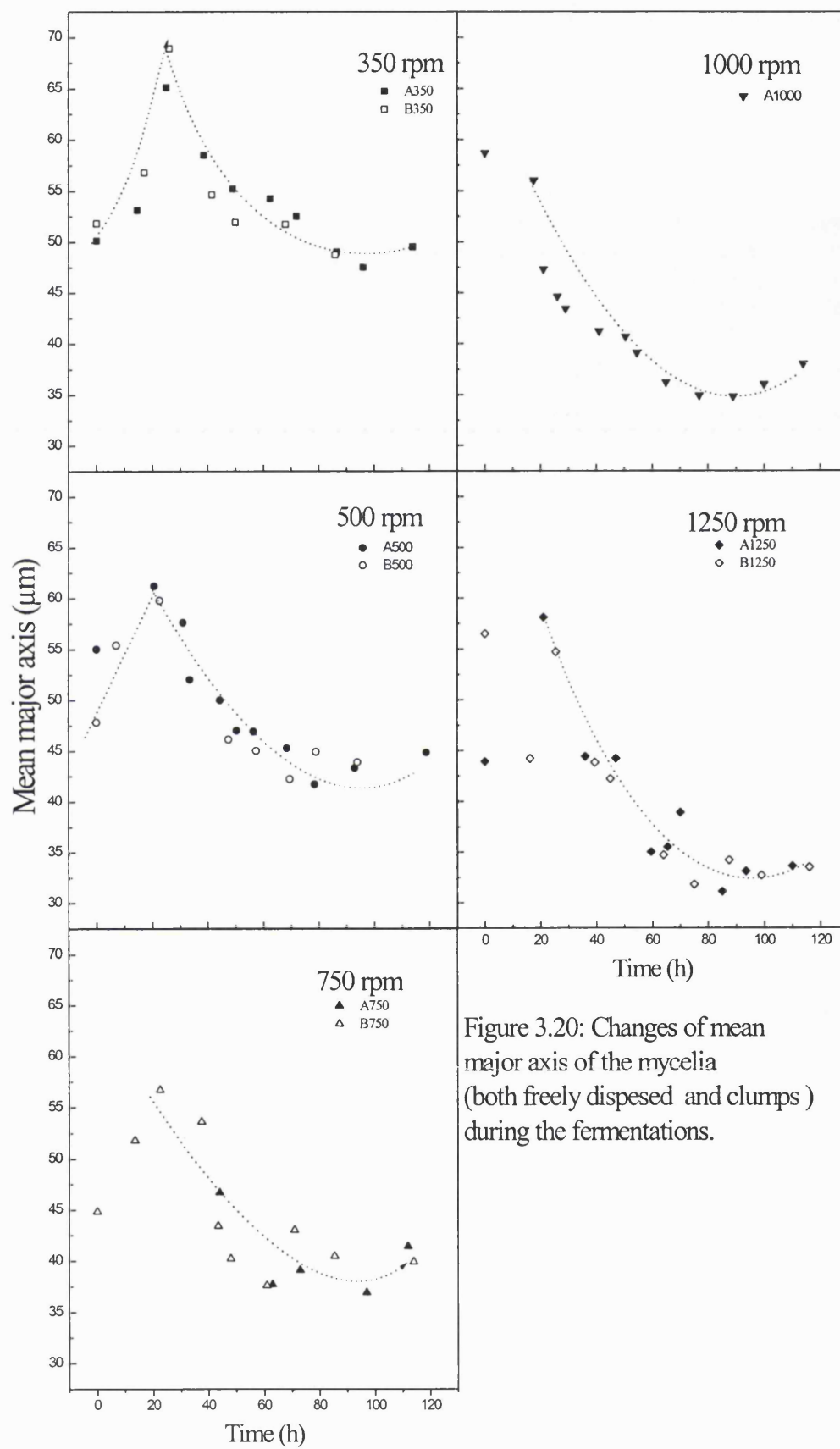
Figure 3.20: Changes of mean major axis of the mycelia (both freely dispesed and clumps) during the fermentations.

120
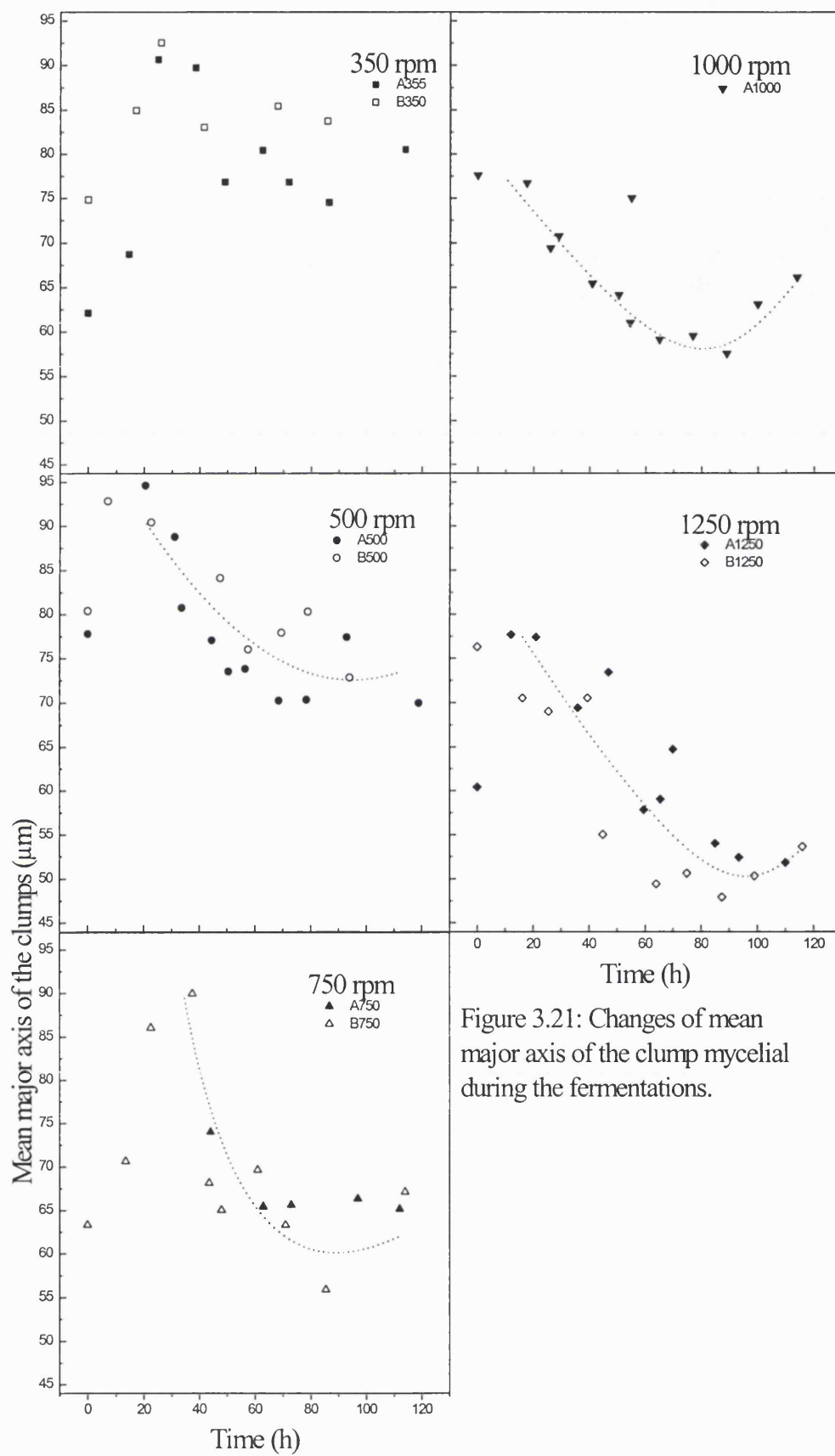
Figure 3.21: Changes of mean major axis of the clump mycelial during the fermentations.
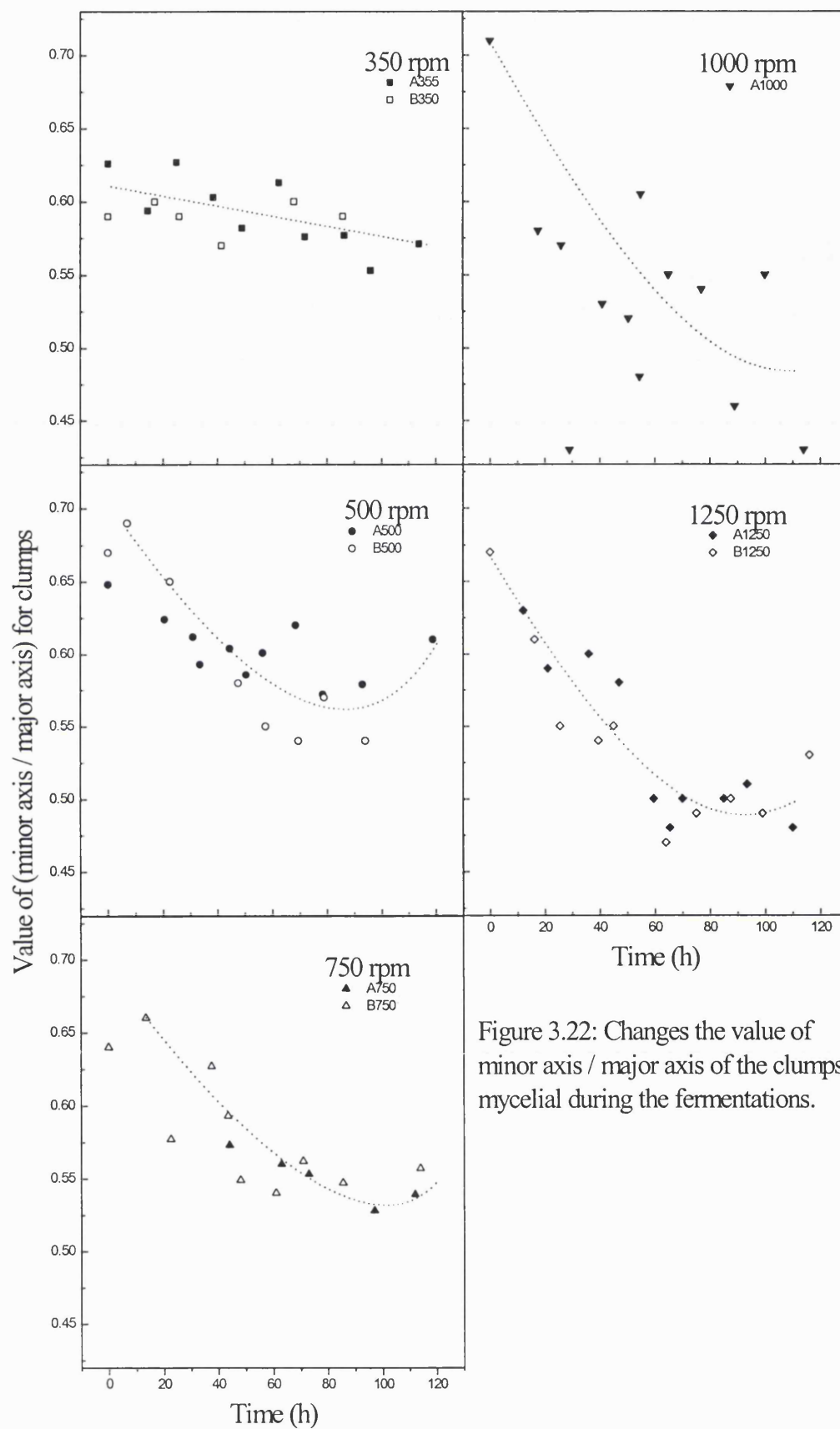
Figure 3.22: Changes the value of minor axis / major axis of the clumps mycelial during the fermentations.
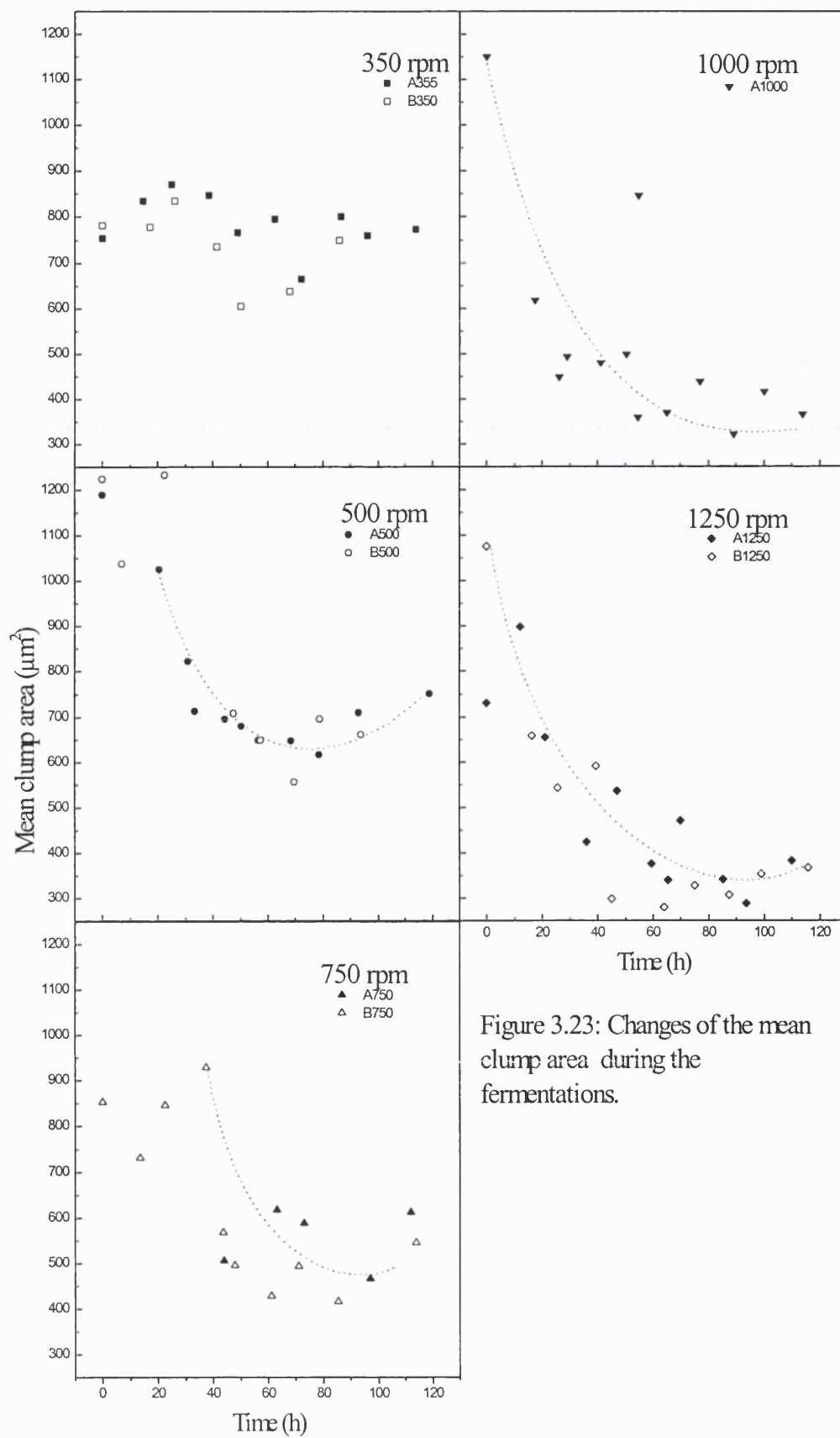
Figure 3.23: Changes of the mean clump area during the fermentations.

123
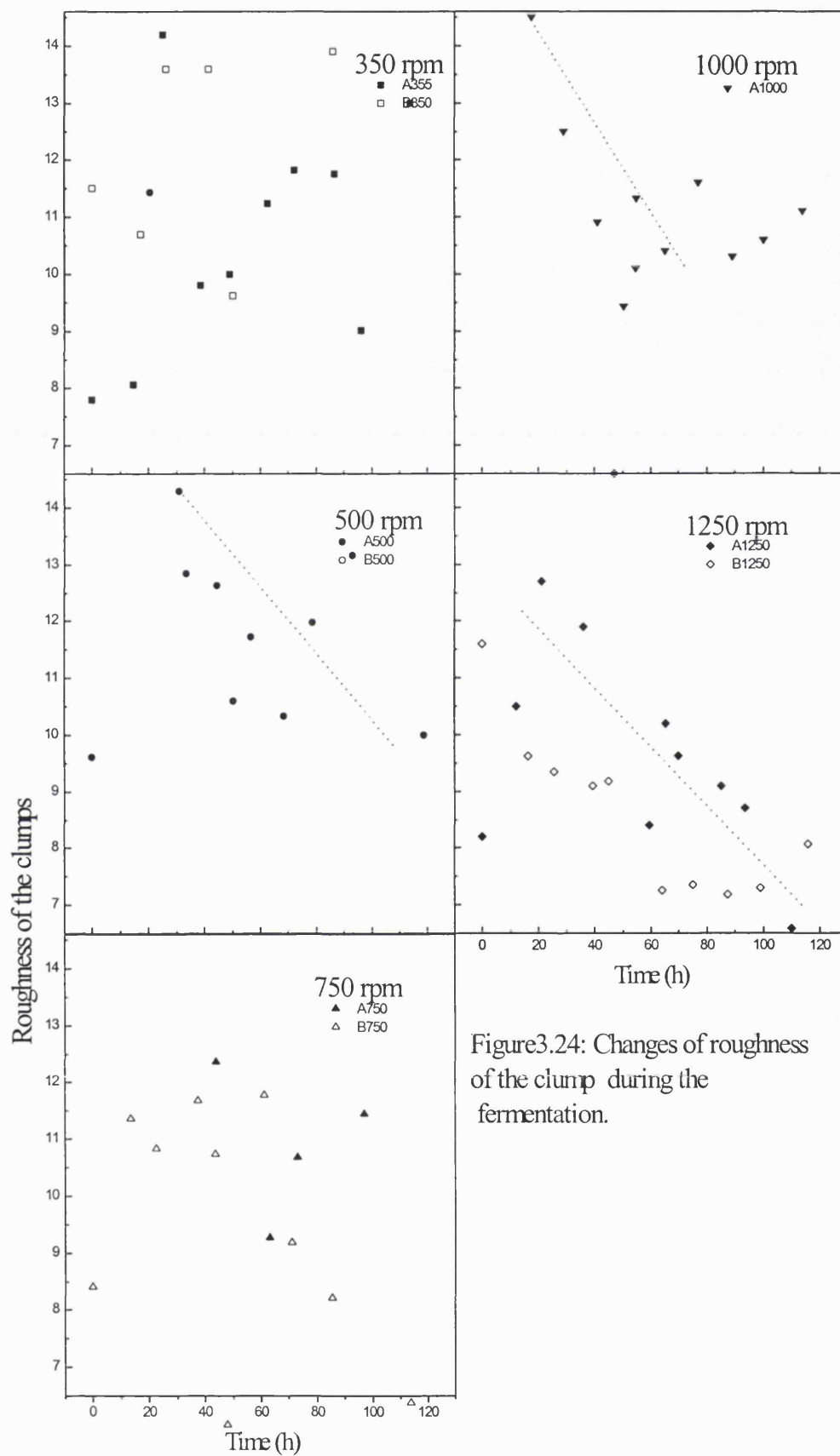
Figure3.24: Changes of roughness of the clump during the fermentation.
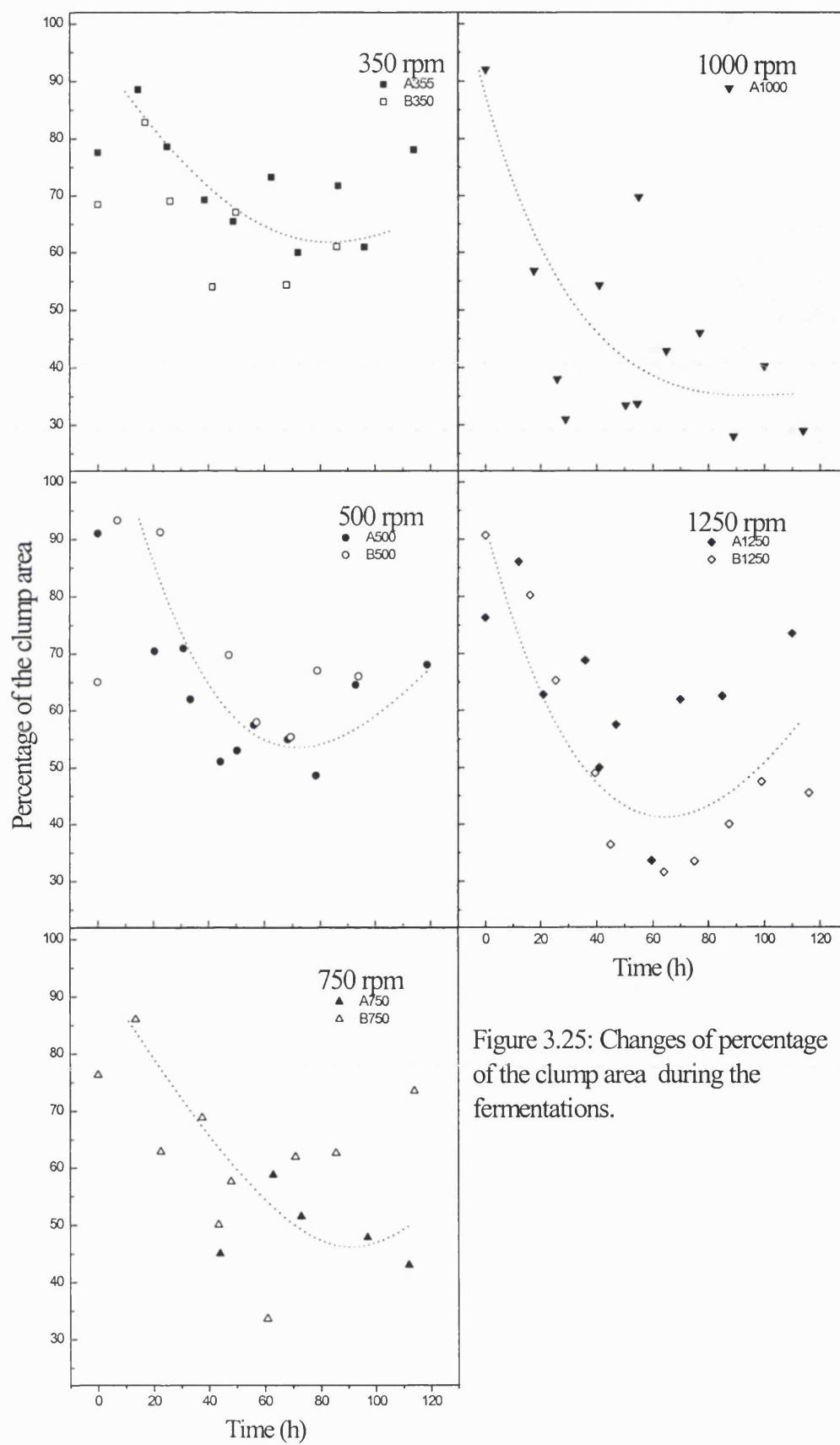
Figure 3.25: Changes of percentage of the clump area during the fermentations.

125
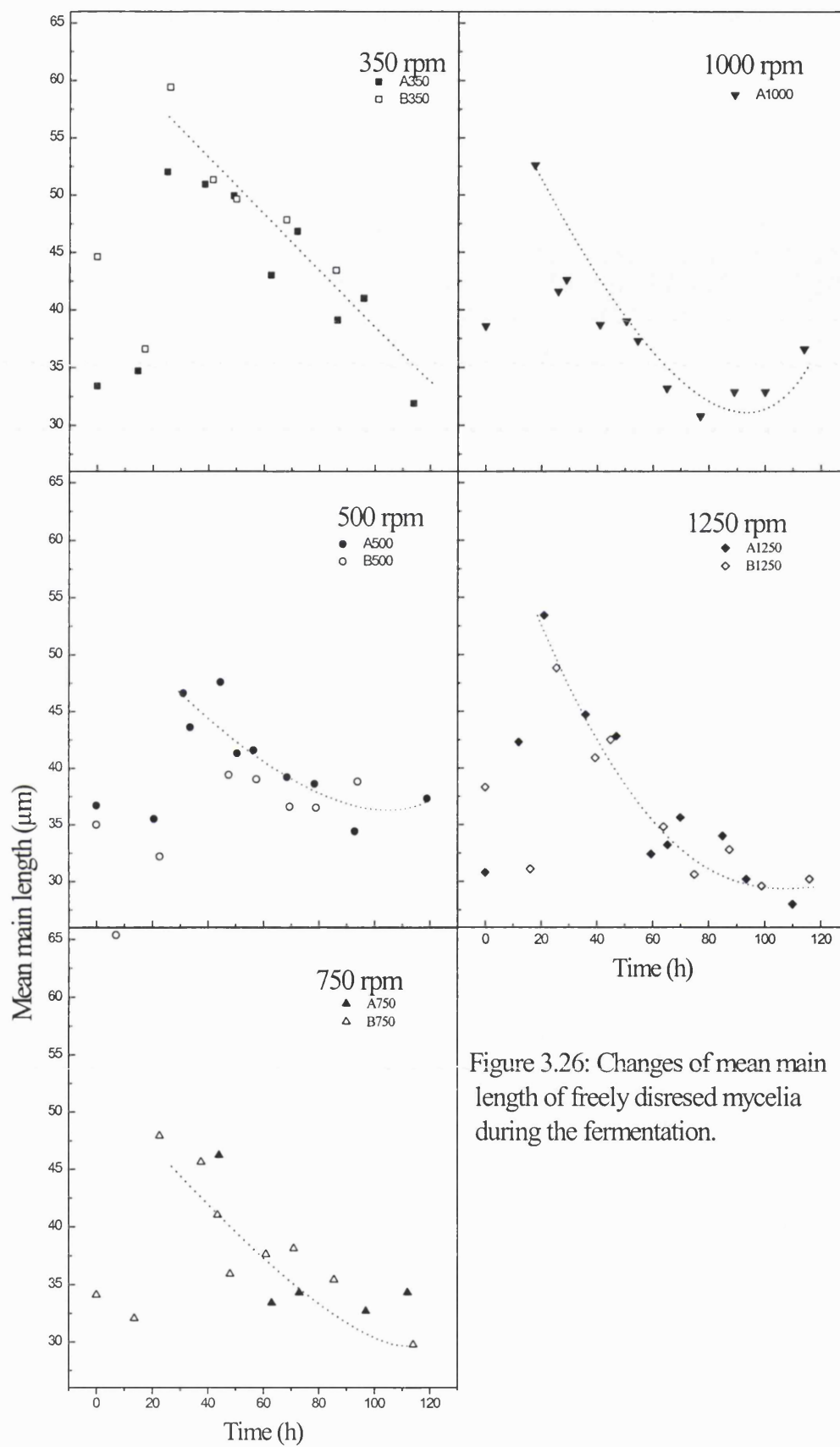
Figure 3.26: Changes of mean main length of freely disresed mycelia during the fermentation.
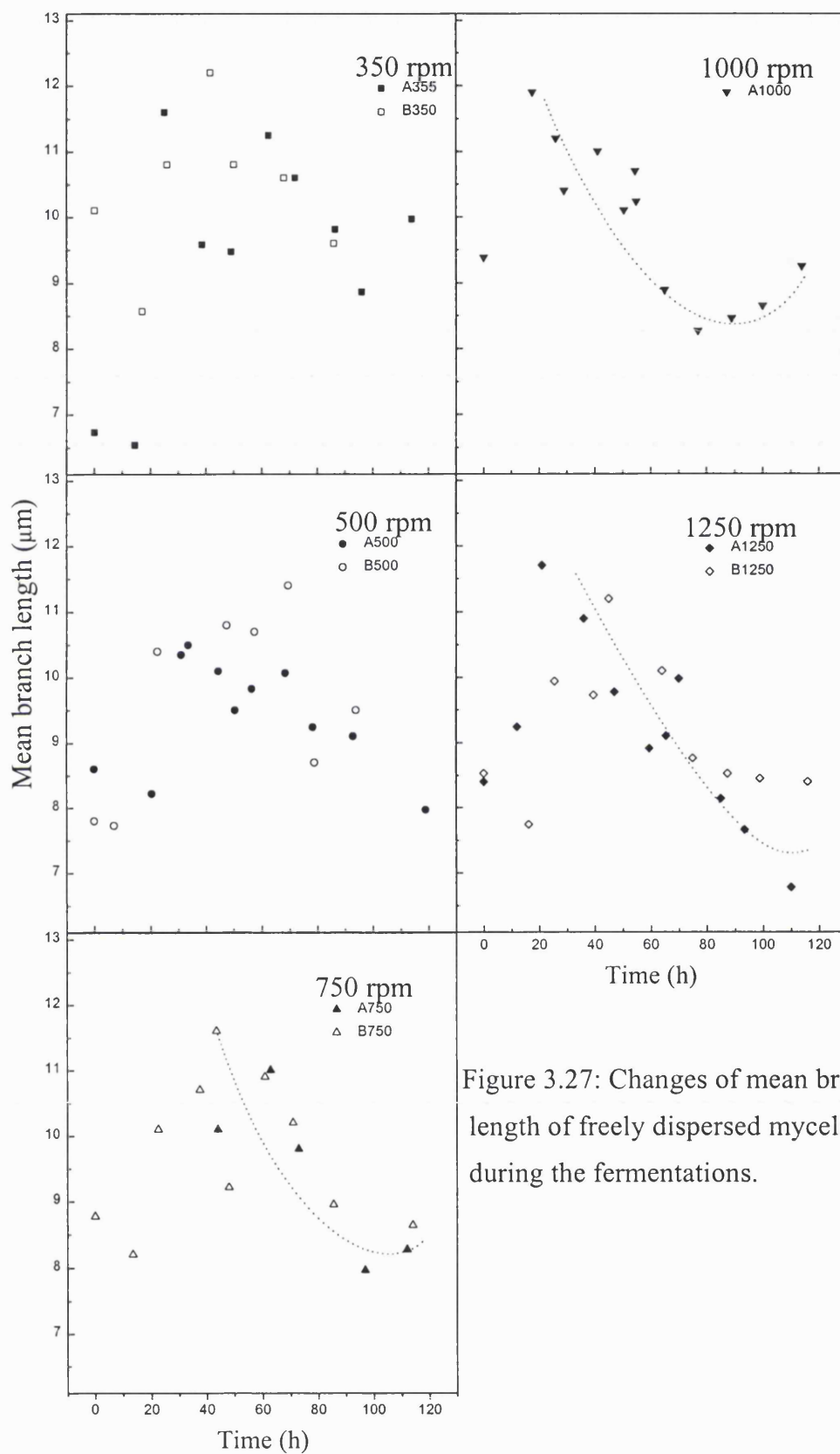
Figure 3.27: Changes of mean branch length of freely dispersed mycelia during the fermentations.

127
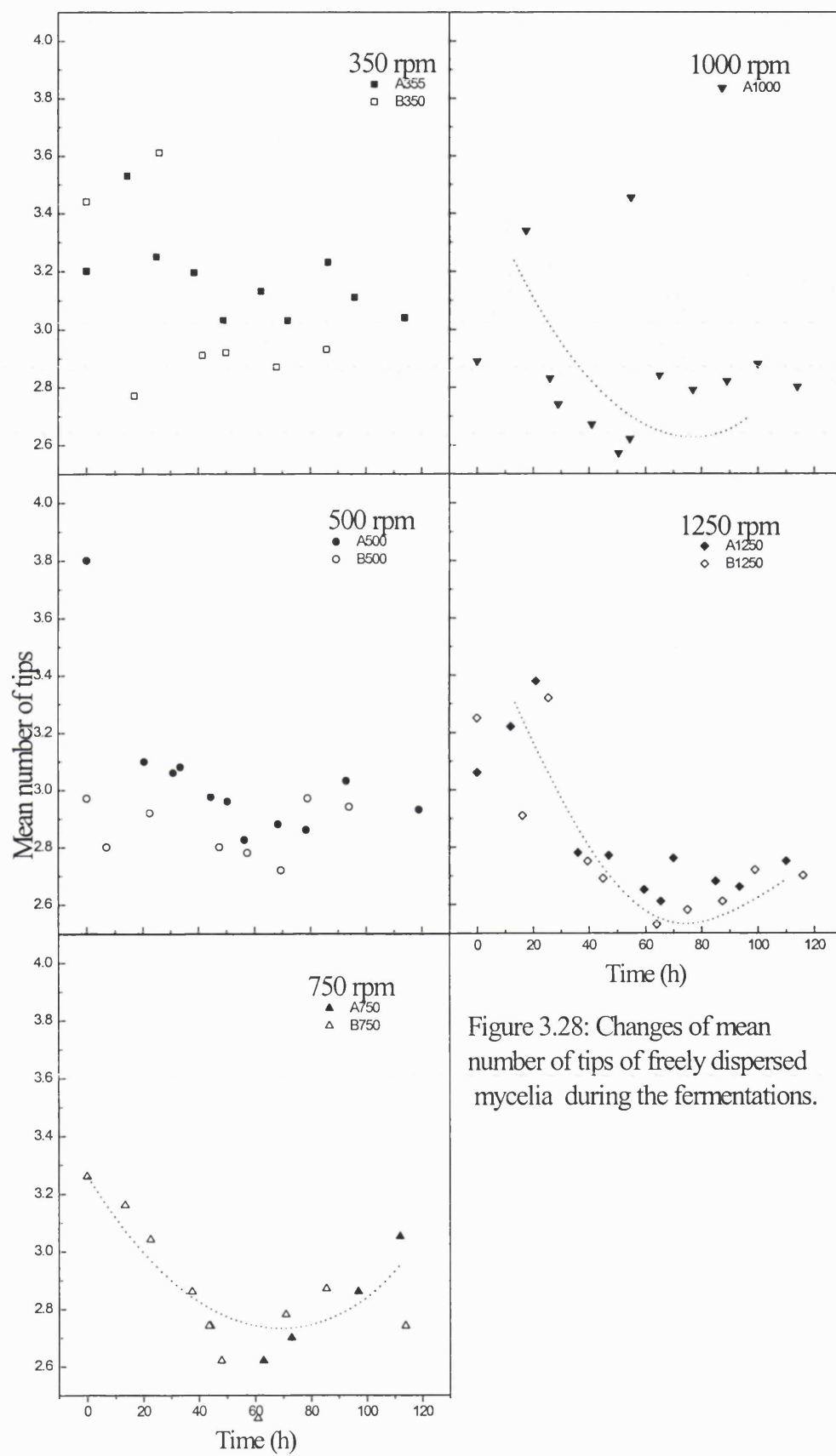
Figure 3.28: Changes of mean number of tips of freely dispersed mycelia during the fermentations.

range of the experimental errors. On average the standard deviation was 3.5% of the mean value for the data in Figure 3.20 and 6.2% for the data in Figure 3.21 (section 2.3.8). The equilibrium major axis for all the experiments (arithmetic mean of the data after 70 h) is shown in Table 3.8. Figures 3.20 and 3.21 also showed that mycelia have a lower breakage rate after the deceleration phase (40 h) compared with deceleration phase (20-25 to 40 h). Reproducibility of the data in Figure 3.20 was good after the end of the rapid growth phase (after 20-25 h).

Table 3.8: Equilibrium mean major axis (μm)

Fermentation	Equilibrium mean major axis of the mycelia (both freely dispersed and clump)	Equilibrium mean major axis of clumps
A350	49.5 ± 2.0	79.1 ± 5.0
B350	50.6 ± 1.3	84.5 ± 1.2
A500	44.0 ± 1.3	76.7 ± 3.1
B500	43.3 ± 1.5	72.6 ± 4.2
A750	39.1 ± 2.2	65.6 ± 1.0
B750	41.1 ± 1.6	65.2 ± 2.0
A1000	35.9 ± 1.5	61.5 ± 3.8
A1250	32.6 ± 1.3	52.7 ± 1.2
B1250	33.0 ± 1.0	50.6 ± 2.3

The mean minor axis had the same trend as major axis. It increased up to 20 - 25 h and then decreased to the equilibrium size at 60-70 h. The ratio of mean minor axis to mean major axis (OB / OL) are shown in Figure 3.22. The value of (OB/OL) was (0.6-0.7) before the end of the rapid growth phase (20-25 h) and it tended to decrease progressively with stirrer speed and over the course of the fermentation till 60-70 h. The value of (OB/OL) after 65 h was 0.53-0.57 for lower stirrer speeds (350 and 500 rpm) and it was 0.45-0.5 for higher stirrer speeds (1000 and 1250 rpm).

Mean clump areas for fermentations agitated at 500, 750, 1000 and 1250 rpm tended to decrease till 50 h progressively with increasing stirrer speed and over the course of

the fermentation (Figure 3.23). Clump area fluctuated around its value at 50 h till end of the fermentations.

The roughness for the clumps are shown in Figure 3.24. The reproducibility of data is poor. Roughness tended to increase till 20-25 h (except for B1250) and it tended to decrease progressively to its minimum value at (40-50 h). Roughness tended to be lower at higher stirrer speeds (1000 and 1250 rpm) comparing with lower stirrer speeds (350, 500 and 750 rpm).

The percentage of the clump area decreased from the beginning at higher stirrer speeds (1000 and 1250 rpm) to 30% at the end of the deceleration phase (40 h) and it was between 30 to 50% after 40 h (Figure 3.25). On the other hand for the lower stirrer speeds (350, 500 and 750 rpm) the percentage of the clump area increased to 85-90 % up to 15-20 h followed by a decrease to a minimum value at 45-50 h (Figure 3.25). Its minimum value was 40 ± 6% at 750 rpm, 52 ± 5% at 500 rpm and 57.5 ± 2.5% at 350 rpm. After 45 h the percentage of the clump area was (55 ± 15%), (60 ± 10%) and (65 ± 10%) at 750, 500 and 350 rpm respectively.

The mean main length of the freely dispersed mycelia tended to increase during the rapid growth phase (10 to 20-25 h) to its maximum value (50 μm to 60 μm), and then decreased towards the end of the fermentation (Figure 3.26). The data for the period of 0-25 h was not enough to compare the results, and the reproducibility was poor in this period (Figure 3.26). The differences in the morphological parameters of the inoculum (Table 3.5) might be a reason for poor reproducibility in this period. After the end of the rapid growth phase, the main length decreased and the rate of its decrease is higher at higher stirrer speeds. The minimum value for the mean main length was 28-33 μm, for all the experiments during 120 h of the fermentation. However this minimum value for mean main length occured at 75 h at higher speeds (1000 rpm and 1250 rpm), whereas it was at 100 h at 500 and 750 rpm and at 120 h for 350 rpm. The reproducibility of the data at different speeds was good after 25 h for all stirrer speeds (Figure 3.26).

The mean branch length tended to increase during the rapid growth phase from 8 ± 1 μm to 11.5 ± 0.5 μm, followed by a decrease after the end of the rapid growth phase to 8 ± 1 μm (Figure 3.27). The number of tips generally increased during the rapid growth phase to 3.3 ± 0.3 followed by a decrease after the end of the rapid growth phase to 2.7 ± 0.2 for higher speeds (750, 1000 and 1250 rpm) and 2.9 ± 0.1 for the lower speeds (350 and 500 rpm) (Figure 3.28). This indicated that the number of tips tended to be lower at higher speeds. These results also showed, the majority of the freely dispersed mycelia were unbranched or had only one branch. Nearly, 50% of the total number of the organisms were without any branches (data not shown). The percentage of non-branched organisms was 50-60% at 1250 rpm and 40-50% at 350 rpm (data not shown). The reproducibility for the number of tips was better at higher stirrer speeds (Figure 3.28).

The size distribution for major axis of the mycelia (both freely dispersed and clumps) for fermentation samples at 1250 rpm are shown in Figures 3.29. The size distribution showed wider range of the size of the organism at the beginning and then it became narrower till 60 - 65 h. The standard deviation for above histograms and also for fermentation at 350 and 1250 rpm are shown in Figure 3.30. The standard deviation tended to decrease progressively with stirrer speed and over the course of the fermentation till 60-65 h and then it increased toward the end of the fermentation (Figure 3.30). These results will be discussed in section 5.3.
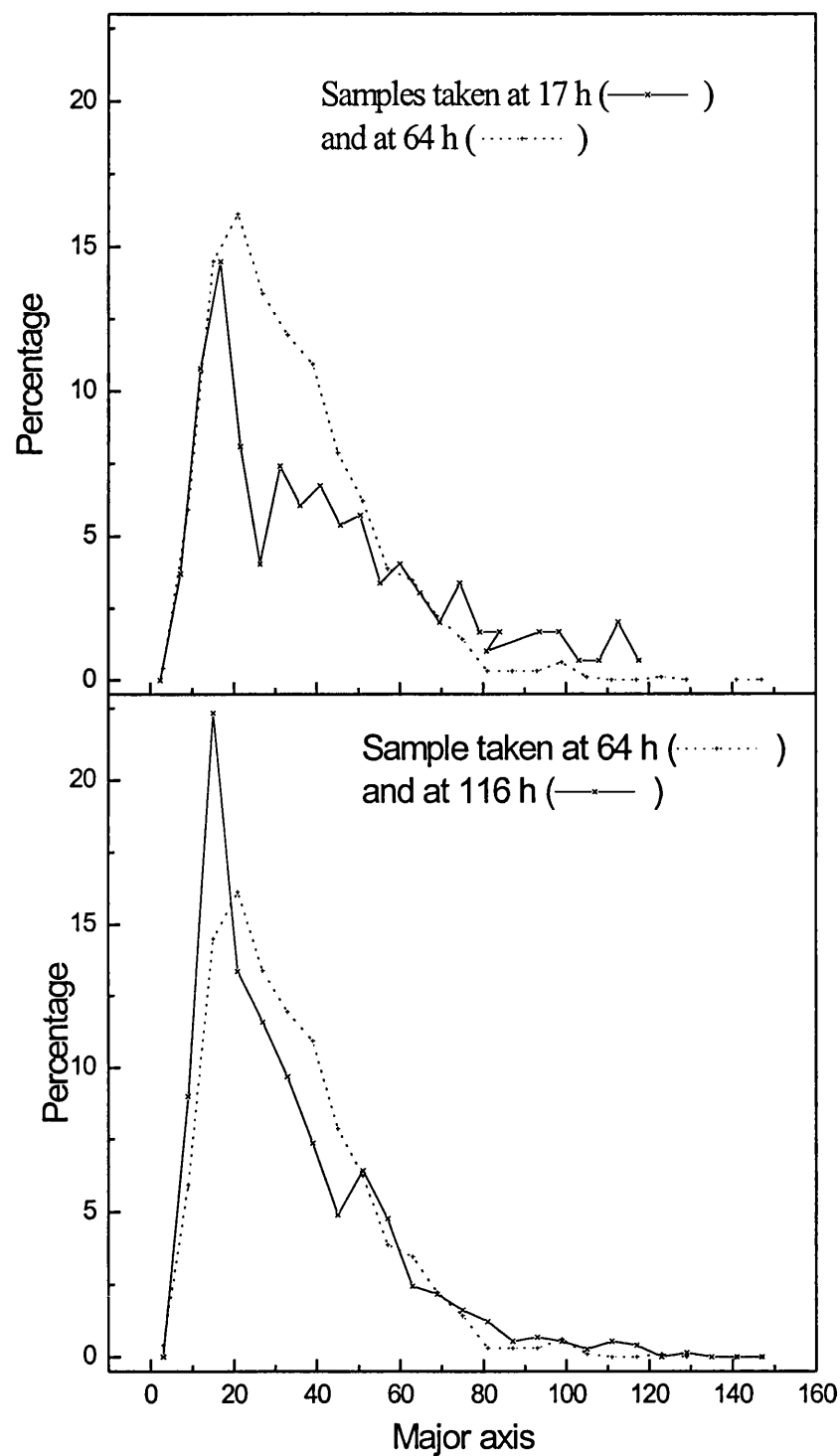
3.29: Size distribution of major axis of the mycelia (both freely dispersed and clumps) for fermentation samples agitated at 1250 rpm.
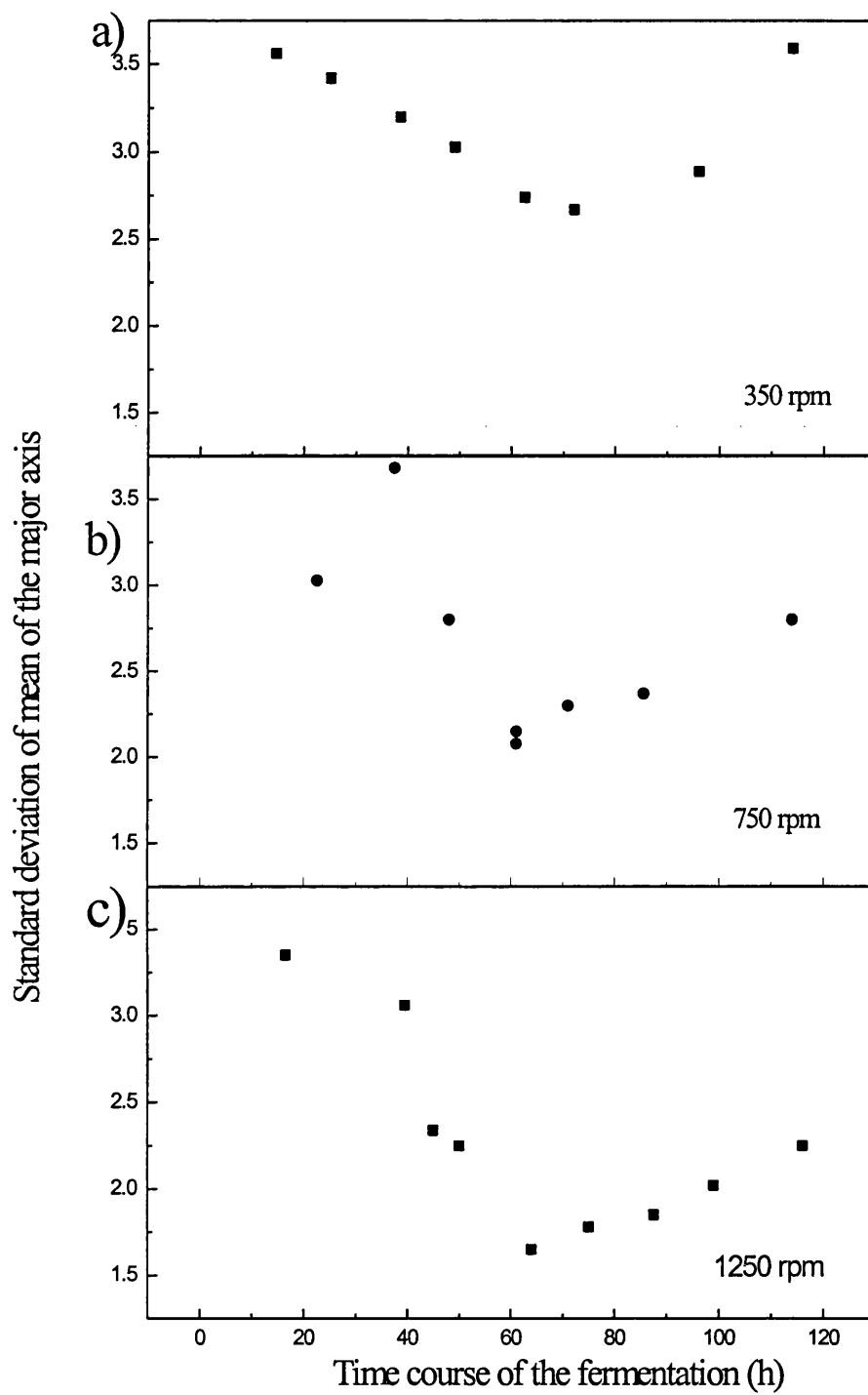
Figure 3.30: Standard deviation of the mean major axis for fermentation samples agitated at 350, 750 and 1250 rpm.

133

3.3.4 Effect of agitation on rheology of the culture

3.3.4.1 Changes of rheology during fermentations

It was shown (section 2.3.9) that power law model fitted well for the experimental data. Therefore, the rheology of the broths described by the consistency index, K, and the flow behaviour index, n, and apparent viscosity (μ_a) was calculated (equation 2.5) by these parameters. The variation of rheological paramters (K, n and μ_a) for the fermentation broths agitated at 350 rpm and 1250 rpm are shown in Figures 3.31 and 3.32. Concentration of biomass (DCW) also shown in Figures 3.31 and 3.32. Experimental data for any speed is for two sets of the data to show the reproducibility of the data.

Consistency index, flow behaviour and apparent viscosity showed relatively good reproducibility. The consistency index and flow behaviour index changed continuously during fermentations (Figures 3.31 and 3.32). The culture initially had water-like Newtonian properties, but developed non-Newtonian shear thinning characteristics during the early stage of growth which lasted to about 10-15 hr. During this period the biomass concentration increased slowly to a value of about 3 gL^{-1} (Figures 3.31 & 3.32), the corresponding flow behaviour index, n was about 0.6 (Figures 3.31 & 3.32). The flow behaviour index fell to about 0.35 during the rapid growth phase lasting for a further 15 hr. Following the rapid growth phase, the flow behaviour index remained practically unchanged for up to approximately 40 hr beyond which it gradually increased to about 0.45 after about 60 hr, changes in flow behaviour index changed slightly between 60 and 120 hours of the fermentation.

For the fermentation samples agitated at 350 rpm, consistency index, K, increased from 0.0013 $Pa.s^n$ at the start of the fermentation to its maximum value 0.92 $\pm$ 0.03 $Pa.s^n$, at the end of the rapid growth phase (25 hr) and it was almost constant during the deceleration phase (25 - 40 h) (Figure 3.31). The maximum value of the consistency index was 0.40 $\pm$ 0.03 $Pa.s^n$ for the fermentation broths samples agitated at 1250 rpm (Figure 3.32). This significant difference in the maximum consistency
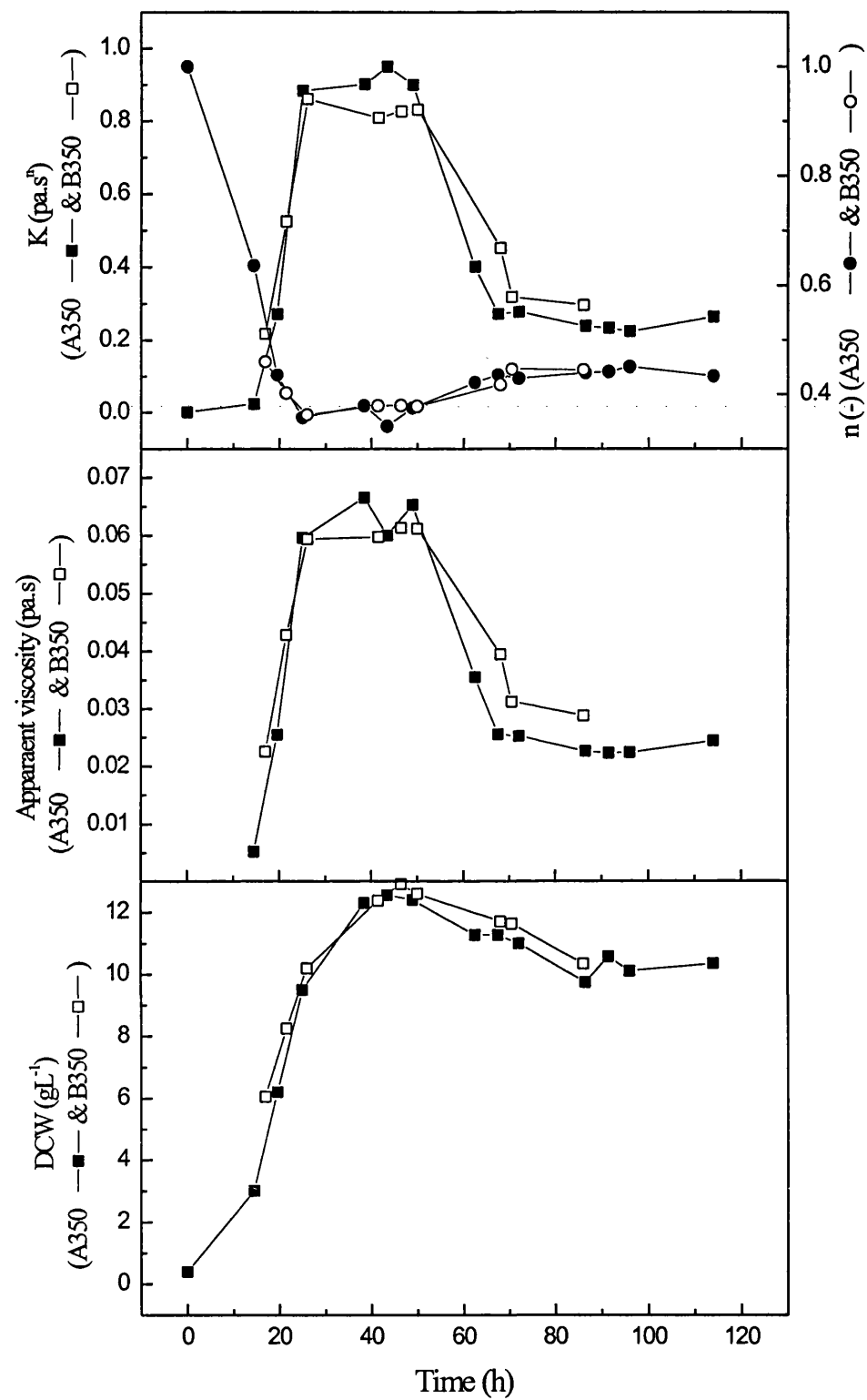
Figure 3.31: Changes of DCW and rheology of the fermentation broths agitated at 350 rpm.
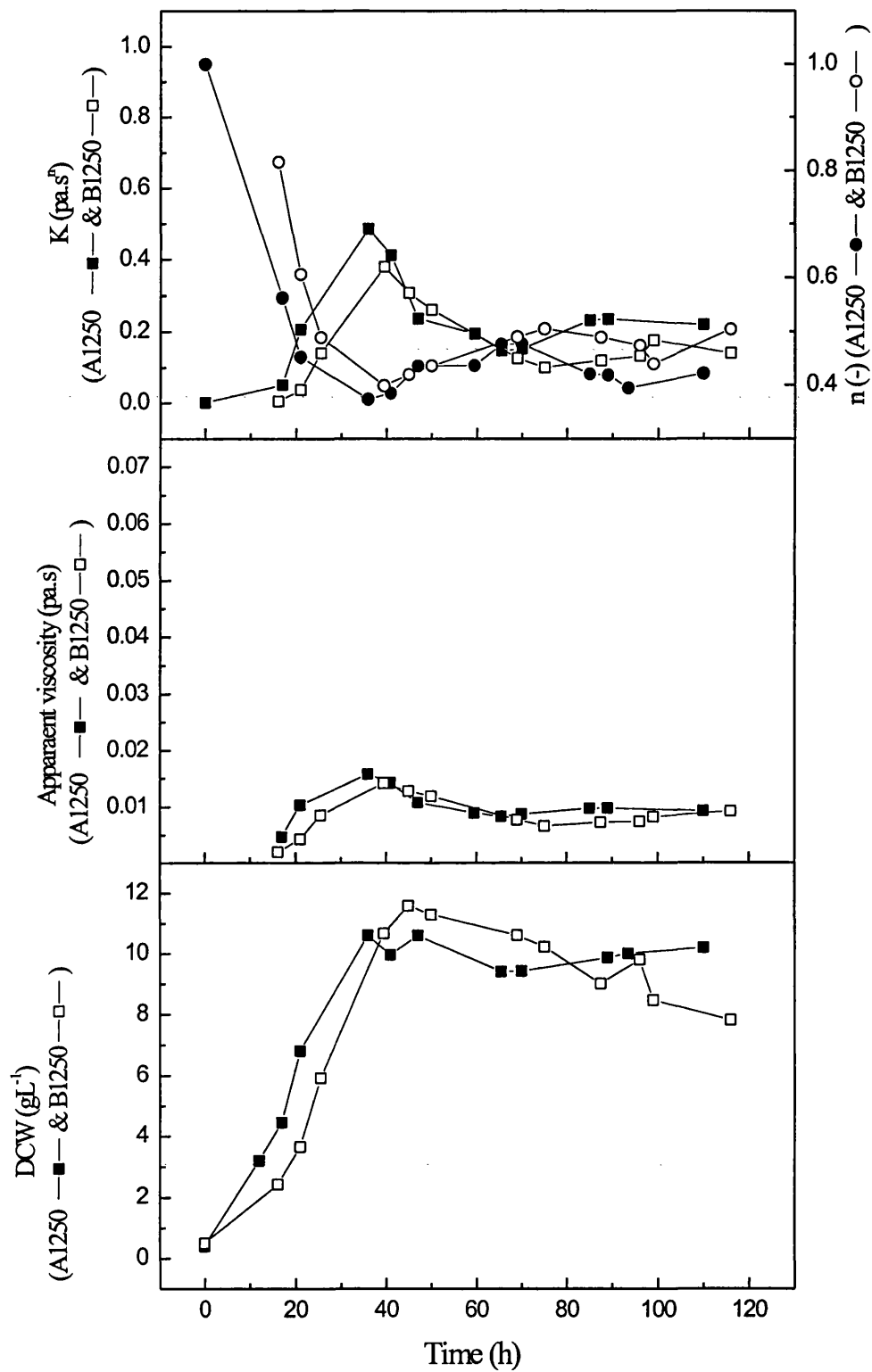
Figure 3.32: Changes of DCW and rheology of the fermentation broths agitated at 1250 rpm.

index of the broths agitated at 350 rpm and 1250 rpm could be partly due to the smaller size of the mycelia (e.g. major axis) at higher stirrer speed and this will be discussed in section 5.4. The value of the consistency index decreased sharply after the end of the growth phase (40 h), to 0.27 ± 0.02 Pa.s^n at 70 h for the fermentation samples agitated at 350 rpm (Figure 3.31), whereas its value decreased to about 0.13 ± 0.02 Pa.s^n for the fermentation samples agitated at 1250 rpm (Figure 3.32). These differences in consistency index will be discussed in section 5.4. Between 70 to 100 h, the consistency index tended to increase slightly for the fermentation broths agitated at 1250 rpm (Figure 3.32). This slight increase of consistency index after about 70 h, also observed for experiments at 500, 750 and 1000 rpm (Figure 3.33) and will be discussed in section 5.3.

Apparent viscosity, μ_a, obtained from $\mu_a = K(k_sN)^{n-1}$ (see section 2.3.9), indicating that agitation speed of fermenter (N) can affect apparent viscosity of the broth directly and indirectly. Stirrer speed affects apparent viscosity directly through the relation N^{n-1} and can affect it indirectly through the variation on value of the consistency index, K. Shear thinning behaviour of the broths (n<1) leads to lower value of apparent viscosity at higher stirrer speed according to relation $\mu_a \, \alpha \, (N)^{n-1}$. In addition, as was mentioned earlier, the value of K was lower at higher stirrer speed at the same period of the fermentation. Both of these effects lead to a lower value of apparent viscosity at higher stirrer speed (Figures 3.31 and 3.32).

Consistency index and flow behaviour index of the fermentation broths agitated at 350, 500, 750, 1000 and 1250 rpm are shown in Figure 3.33 to compare the results at different speeds. Data for the fermentations at 350 and 1250 rpm are from two sets of data and the data for 500, 750 and 1000 rpm are for A500, B750 and A1000 respectively. The consistency index increased during growth phase (till 30-40 h) and the flow behaviour decreased during this period. The fermentation broth showed Newtonian behaviour at the beginning, then the flow behaviour decreased to 0.35-0.4 at 30 - 40 h and the consistency index increased to its maximum value 0.92 ± 0.03 Pa.S^n at 350 rpm and the maximum value for the consistency index was 0.4 ± 0.03 Pa.s^n at 1250 rpm. The consistency index decreased and flow behaviour index
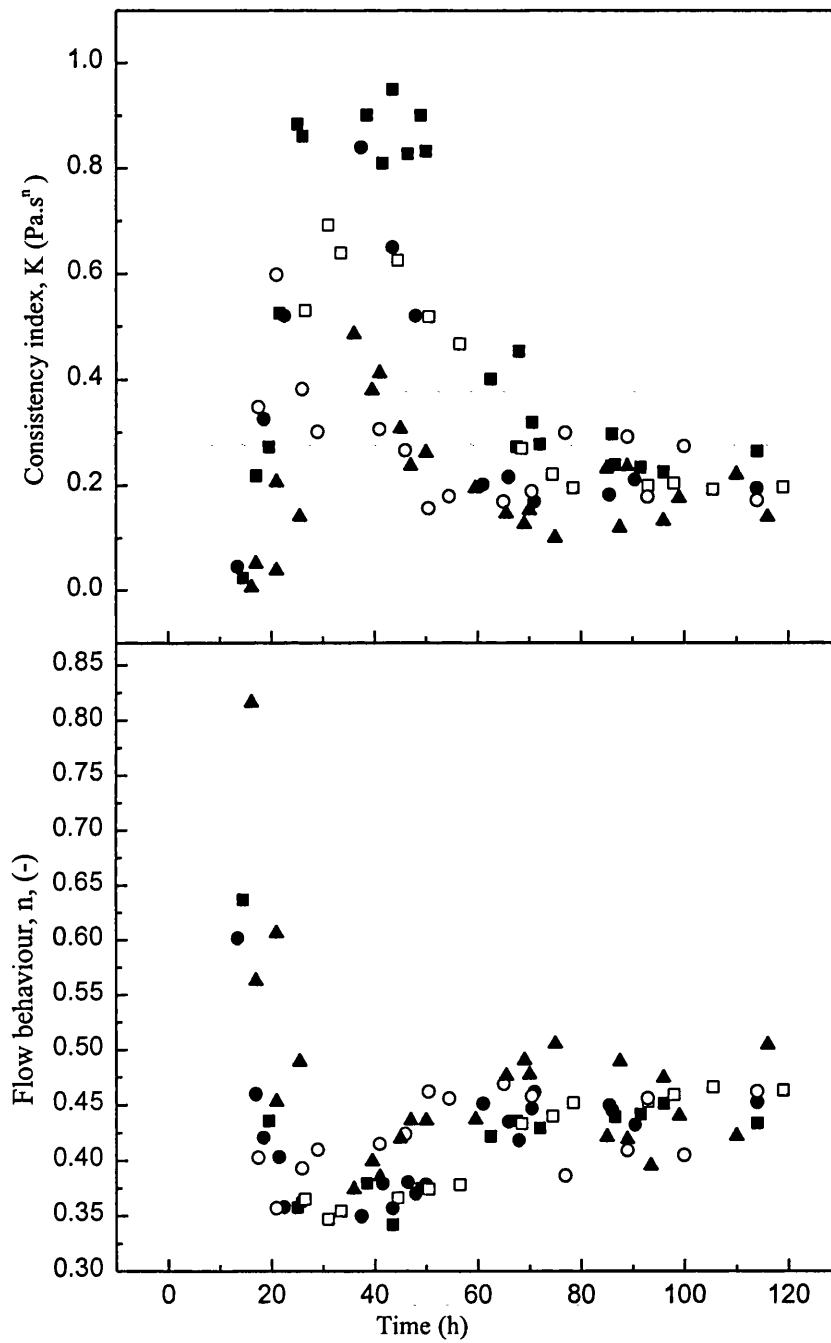
Figure 3.33: Changes of rheological parameters a) consistency index, b) flow behaviour index for fermentation at 7-L scale and agitated at 350 (■), 500 (□), 750 (●), 1000 (○) and 1250 rpm (▲).

increased after end of the growth phase for all the experiments till 60 - 70 h, and the rheological parameters changed little after this time. Between 70-100 h there was a slight trend of increasing consistency index, whereas the flow behaviour decreased slightly in this period. For the same period of the fermentation before 70 h, the consistency index tended to be lower at higher stirrer speeds (Figure 3.33). These results will be discussed in section 5.4.

3.3.4.2 Relation between rheology and biomass concentration

In order to find the influence of biomass concentration in the absence of any morphological changes, samples were removed from the fermenter and diluted with its own supernatant to different biomass concentrations, and used to estimate the dependence of consistency index on the biomass concentration. Samples were selected from fermentations at the lowest speed (350 rpm), highest speed (1250 rpm) and a mid-range speed (750 rpm). The dry cell weight of the samples used for determination of rheology was between 3 to 12 gL^{-1}. Figure 3.34 shows the changes of consistency index with biomass level for different samples on a log-log plot. Figure 3.34 showed a good agreement for equation ($K \propto (DCW)^c$), The regression correlation (R^2) was between 0.95 to 0.99. Figure 3.34 shows, 'c' changes between 1.92 to 2.45 with average value of 2.1 and standard deviation of error was 9% of the mean. Therefore, this data suggested the relation between consistency index and biomass as:

$$K \propto (DCW)^{2.1} \qquad\qquad (3.1)$$

The variation of flow behaviour (n) with biomass was also plotted on a log-log plot (Figure 3.35). The correlation coefficient (R^2) of the lines was between 0.90-0.99. The slope of the fitted lines varies between 0.34 to 0.51 with average value of 0.43 and standard deviation of the error was 14% of the mean. Therefore, this data suggested the relation between flow behaviour and biomass as:

$$n \propto (DCW)^{-0.43} \qquad\qquad (3.2)$$
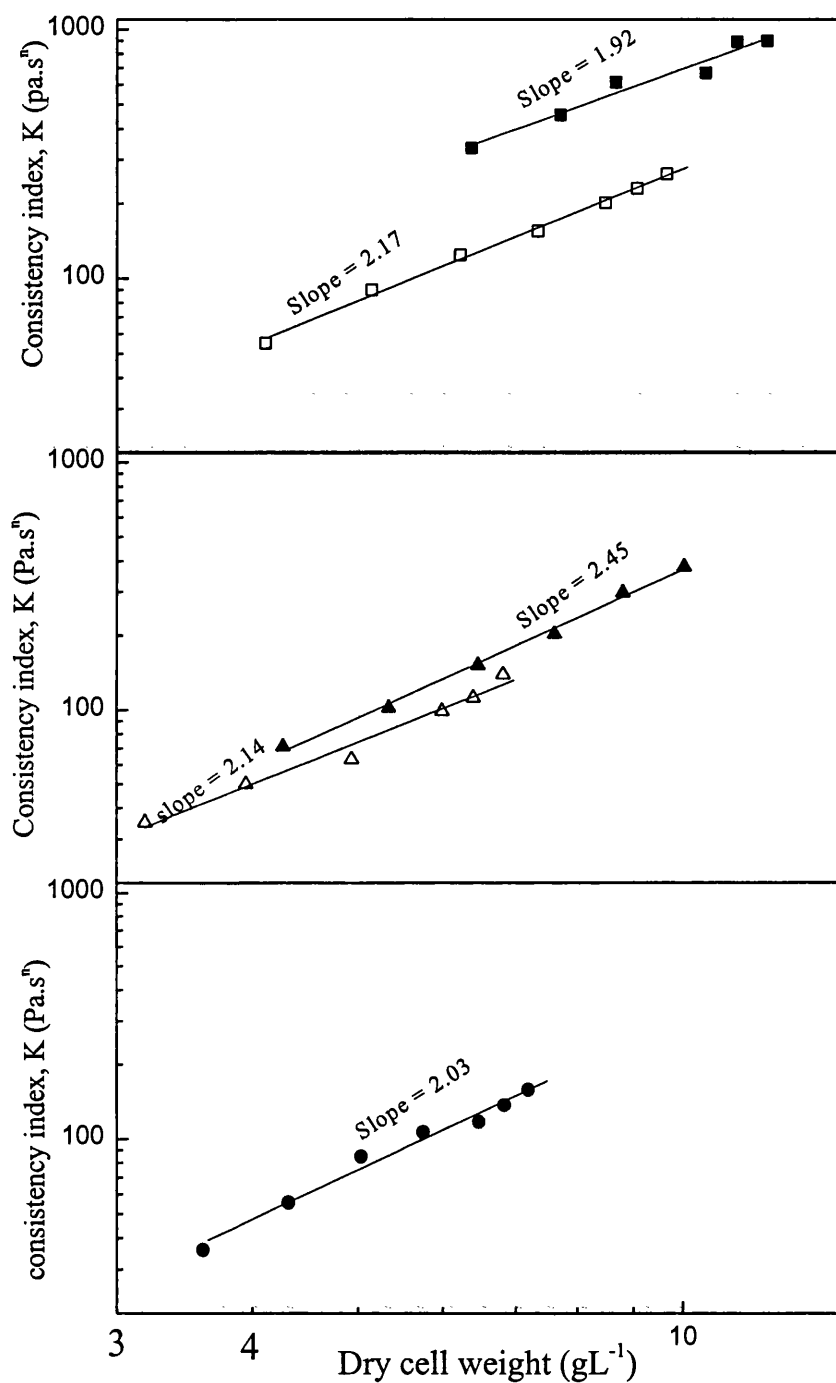
Figure 3.34: Changes of consistency index for diluted samples from *S. erythraea* fermentation at 7-L scale. Samples were taken from fermenter at : B350 (■) at 38.5 h, B 350 at 114 h (□), B1250 (▲) at 39.5 h, B1250 at 116 h (△) and B750 at 140 h (●).
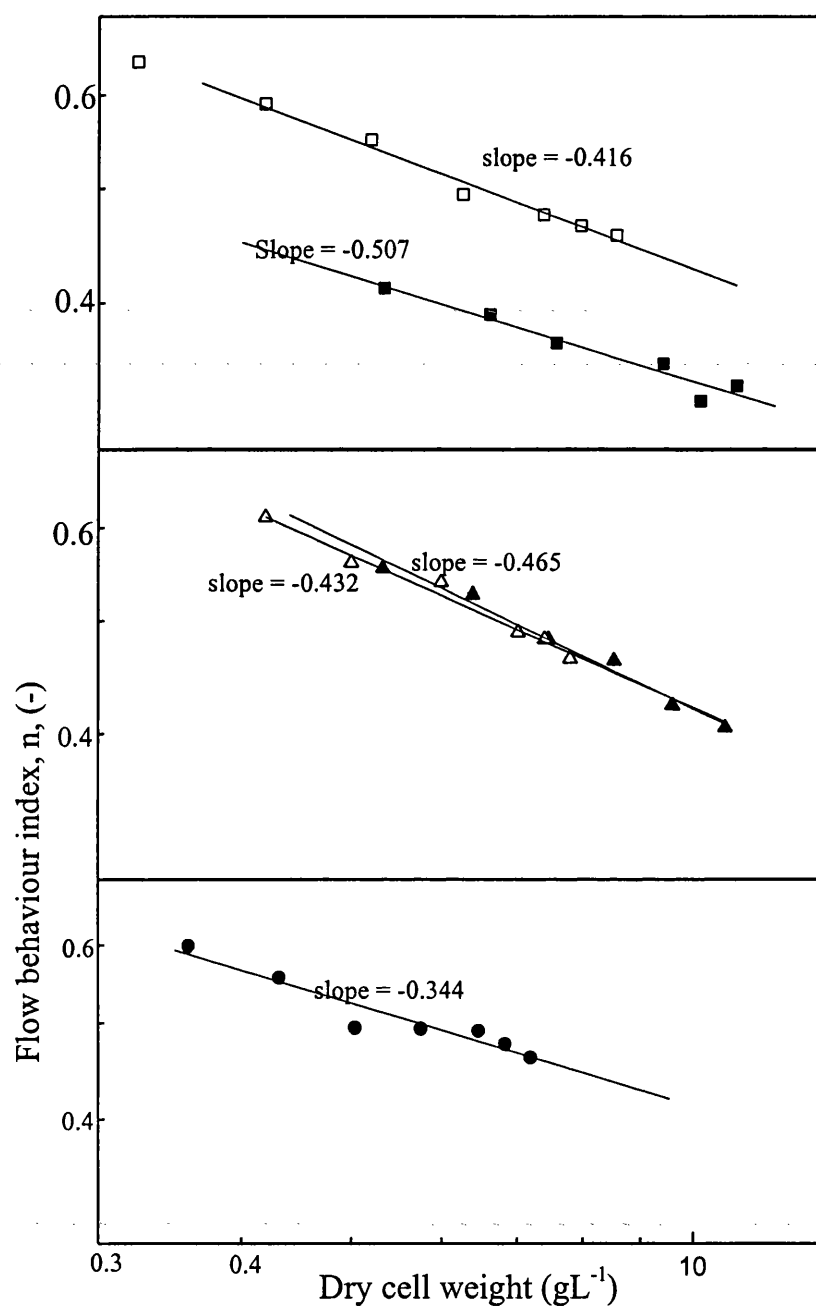
Figure 3.35: Changes of flow behaviour index for diluted samples from *S. erythraea*
fermentation at 7-L scale. Samples were taken from fermenter at : B350 (■) at 38.5 h,
B 350 at 114 h (□), B1250 (▲) at 39.5 h, B1250 at 116 h (△) and B750 at 140 h (●).

3.3.4.3 Relation between rheology and morphology

During the course of a batch filamentous organism fermentation considerable changes in both organism concentration and morphology occur. Both of these effects have a profound influence on the rheological properties of the fermentation broth (see section 1.5.2). Having estimated the effect of biomass on consistency index (section 3.3.4.2), it was possible to seek the relation between the consistency index and the morphological characteristics of samples taken during the fermentation at the different stirrer speed according to equation 3.3 (Olsvik *et al.*, 1993):

$$K \, / \, (DCW)^c = constant \times (MP)^b \ . \ ...$$
(3.3)

where MP is morphological parameter (e.g. major axis). The value of 'c' was estimated to be 2.1 (equation 3.1). Therefore, the relation between consistency index and biomass is considered as $(K \; \alpha \; (DCW)^{2.1})$. Variation of $K \, / \, (DCW)^{2.1}$ during the fermentation at different stirrer speeds is shown in Figure 3.36. Value of $(K \; \alpha \; (DCW)^{2.1})$ decreased sharply between 30-70 h. The size of the mycelia (main length or major axis) or size of the clump (e.g. major axis) also decreased during this period (Figures 3.20 & 3.26), which could be partly attributed for decreasing of $(K/(DCW)^{2.1})$ during this period. Value of $(K/(DCW)^{2.1})$ changed little during the period of 70 to 120 h and the variation in the morphological parameter (e.g. major axis) in this period was also little (Figure 3.36). The value of $(K/(DCW)^{2.1})$ tended to be lower at higher stirrer speed (Figure 3.36), which could be partly due to smaller size of the mycelia (e.g. major axis) at higher stirrer speed. These results suggested that there should be a relation between rheology of the broths and morphology of the cells.

The relation between consistency index and different morphological parameters was examined according to equation 3.3 using linear regression in log-log scale (e.g. Figure 3.37 for major axis) and its results was summerised in Table 3.9. The correlation coefficient (R^2) obtained from this linear regression (Table 3.9) indicated that the interpretation of the
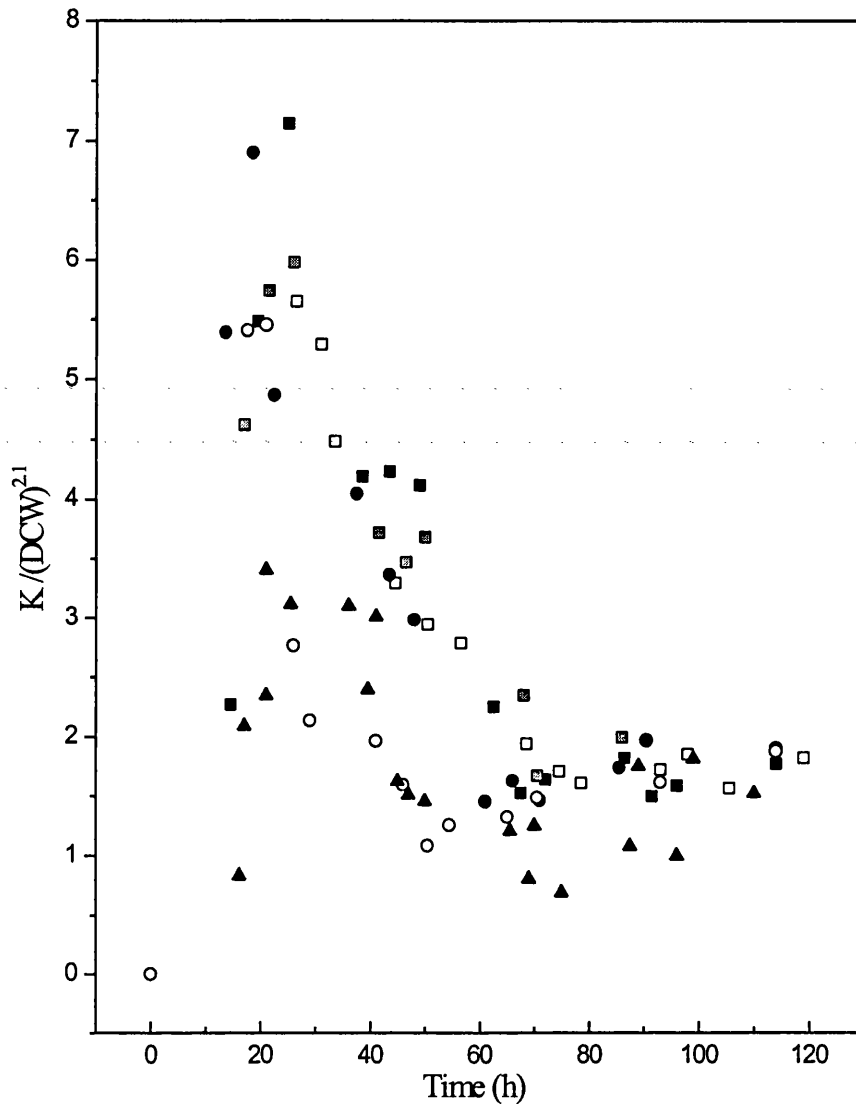
Figure 3.36: Variation of the value of $K/(DCW)^{2.1}$ during the *S. erythraea* fermentation at 7-L scale and agitated at 350 (■), 500 (□), 750 (●), 1000 (O) and 1250 rpm (▲). Units is gL^{-1} for DCW and $Pa.s^n$ for K.

·

consistency index according to equation 3.3 was not good (Table 3.9). These results will be discussed in section 5.4.
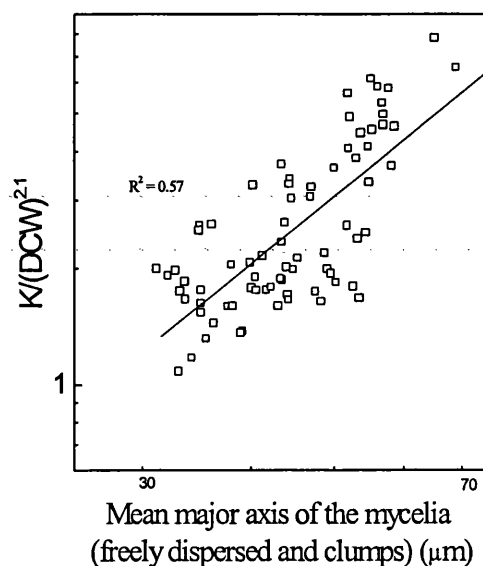
Figure 3.37: Variation of the value of $K/(DCW)^{2.1}$ with major axis of the mycelia.

Table 3.9: correlation between consistency index and morphological parameters

mophological parameter	experession for K	R^2
Mean major axis of the mycelia (both freely dispersed and clumps) (OL)	$K \propto (DCW)^{2.1}(OL)^{1.9}$	0.57
Mean clump area (CA)	$K \propto (DCW)^{2.1}(CA)^{0.6}$	0.26
Average length of the clumps (aveL)	$K \propto (DCW)^{2.1}(aveL)^{1.75}$	0.45
Mean main length (ML)	$K \propto (DCW)^{2.1}(ML)^{1.88}$	0.44
Total hyphal length (HL)	$K \propto (DCW)^{2.1}(HL)^{1.74}$	0.45
Roughness of the clumps (R)	$K \propto (DCW)^{2.1}(R)^{0.82}$	0.18

3.4 Effect of agitation at 450-L scale

Two fermentations were carried out at 450-L scale at 300 rpm and 450 rpm, giving tip speeds of 3.14 and 4.71 ms^{-1} respectively. DOT at 450 rpm never was below 65% and it was kept above 50% for the fermentation at 300 rpm by adjusting pressure of the fermenter manually (See section 2.2.8.2). Pressure was increased manually to 0.35 bar in the rapid growth phase (10 to 25 h) to keep the dissolved oxygen tension above 50%.

3.4.1 Growth and erythromycin production

The trend of growth rate for both fermentations at 300 rpm and 450 rpm was similar to fermentation at 7-L scale. Rapid growth phase was between 10 to 25-28 h, followed by deceleration phase till 40 h. Maximum dry cell weight was obtained at 40 h and it was 12.1 gL^{-1} at 300 rpm and 11 gL^{-1} at 450 rpm (Figures 3.38 & 3.39). The data for carbon dioxide evolution rate and RQ is not available for fermentation at 450 rpm and for fermentation at 300 rpm is shown in Figure 3.38. The peak of CER was at 25 h and it was 33 mmol L^{-1}h^{-1}. RQ was almost 1 during the experiment. There was the same trend for glucose consumption for both fermentation and it was decreased from 32 gL^{-1} to 27 gL^{-1} at the early stage of the growth, followed with a sharper decrease in rapid growth phase and it was almost consumed till 60 h (Figures 3.38 & 3.39). The trend for erythromycin production was also the same as 7-L scale. Erythromycin production rate was slow at rapid growth phase (till 25 h), followed by its highest rate of production in deceleration phase (25 to 40 h). Then erythromycin production continued to the level of 680 mgL^{-1} in experiments at 300 rpm and the maximum level of erythromycin was 650 mgL^{-1} in experiments at 450 rpm (Figures 3.38 & 3.39).

145
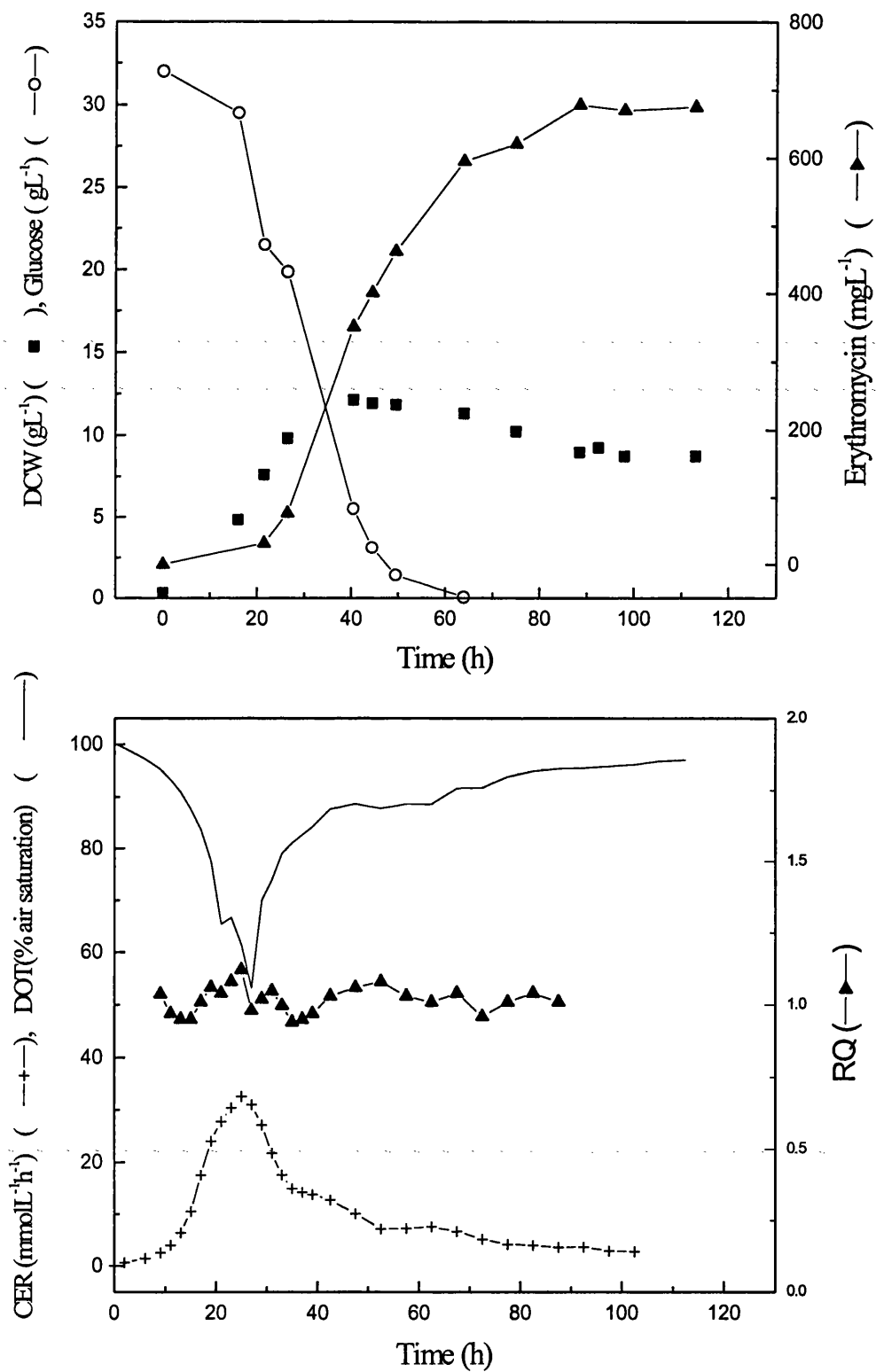
Figure 3.38: Changes of DCW, glucose, erythromycin production, CER , RQ and DOT at 450-L fermentation and 300 rpm of using complex medium.
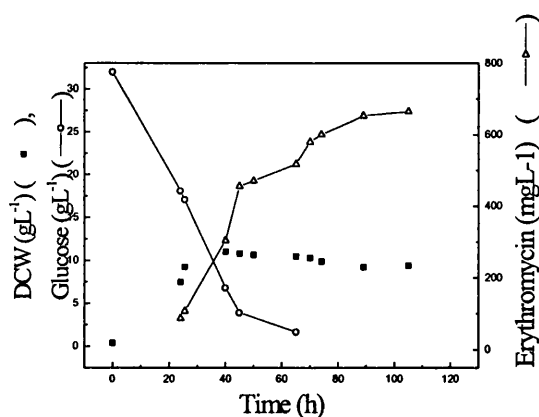
Figure 3.39: Changes of DCW, glucose and erythromycin production at 450-L fermentation of *S. erythraea* using complex medium (stirrer speed = 450 rpm).

3.4.2 Morphology

The variation of morphological parameters including mean major axis, mean main length, clump area and the percentage of the clump area are shown in Figure 3.40. The trend of moropholgical parameters were similar to 7-L scale. The mean major axis tended to increase from the beginning till end of the rapid growth phase (30 h) and then it decreased progressively over the course of the fermentation till 70-80 h (Figure 3.40). The mean major axis of the mycelia (both clumps and freely dispersed) between 80 to 110 h was 43.5 ± 2 μm for fermentation at 300 rpm and it was 37 ± 2 μm at 450 rpm. The percentage of the clump area for fermentation at 450 rpm decreased from the beginning to its minimum value (33%) at 40 h and then it increased. The percentage of clumps area after 40 h for fermentation at 450 rpm was between 33 and 52% (Figure 3.40). Percentage of the clump area for fermentation at 300 rpm, increased till 20 h and then it decreased till 40 h. The percentage of the clumps area after 40 h for fermentation at 300 rpm was 56-68%. Mean main length of the mycelia and clumps area had the same trend as major axis (Figure 3.40). These results will be discussed in section 4.
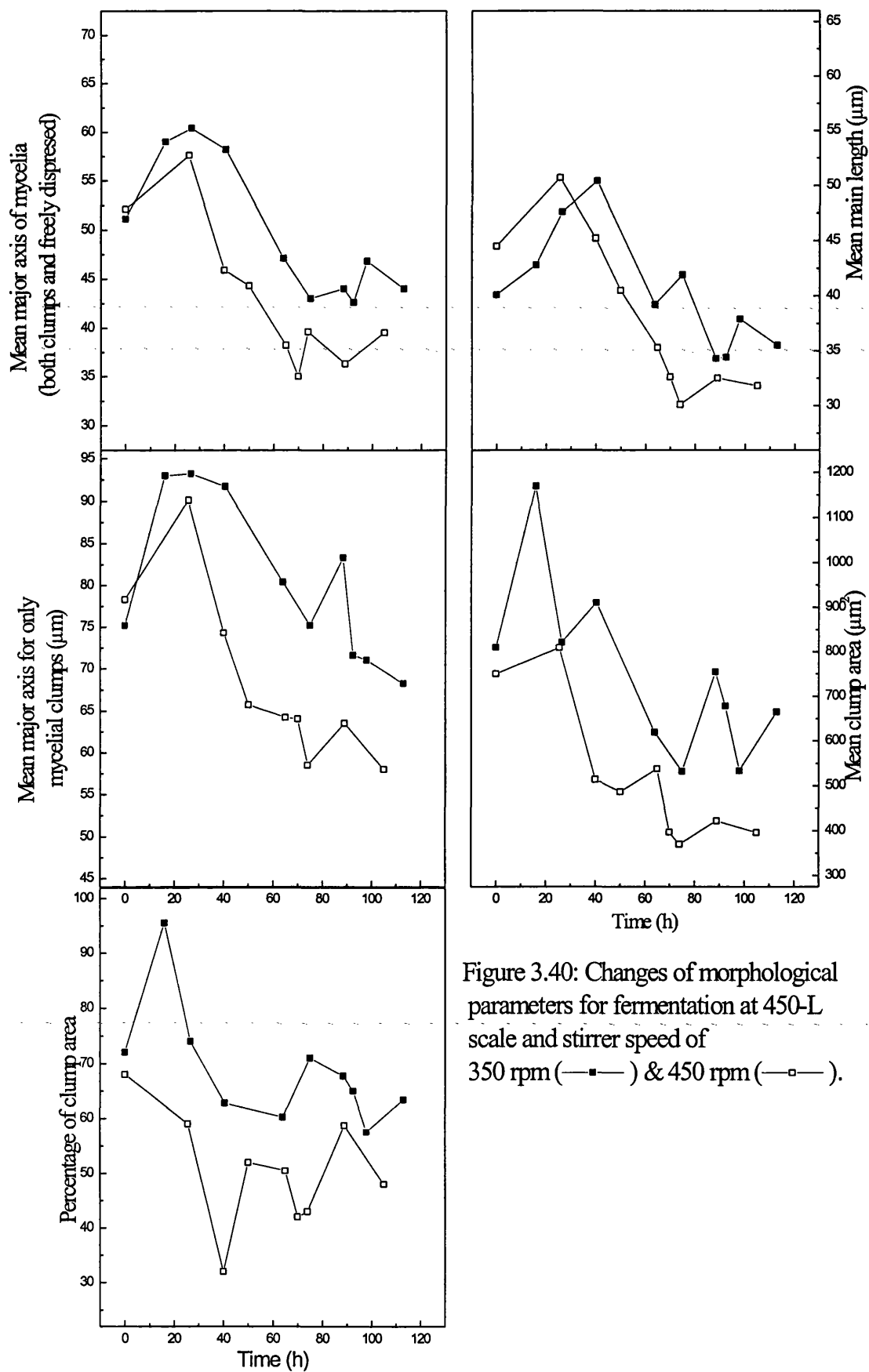
Figure 3.40: Changes of morphological parameters for fermentation at 450-L scale and stirrer speed of 350 rpm (———■———) & 450 rpm (———□———).

3.5 Homogenisation of fermentation broth for assessing cell wall strength

The description of factors involved in fragmentation, are not only limited to disruptive forces, but counterbalanced by stablising forces generated by the hyphal cell wall. Recent advances in the use of micromanipulation techniques have allowed measurements of the cell wall strength with a reasonable degree of accuracy for baker's yeast cells (Zhang *et al.*, 1991; Robert *et al.*, 1994). However, this technique has not yet been successful for measuring the cell wall mechanical properties of filamentous actinomycetes. Another way of approaching this problem is by using indirect measurements. In these experiments, disruption of cells in a homogeniser was selected. The results obtained in this part of the research will be used to explain some aspects of the mycelia breakage in the shear enviroment of the fermenter in section 4.2 and 5.3.

3.5.1 Assessments of protein release results

Fermentation broth samples were disrupted in the Lab-40 homogeniser at different pressures (100 to 1200 bar) and protein release of the disrupted cells measured to assess the parameters influencing the cell wall strength. Samples were taken from fermentations at 3 different stirrer speeds: 350 rpm (B350), 750 rpm (B750) and 1250 rpm (B1250). Samples were selected at different periods of fermentation (Table 3.10).

Table 3.10:Selected samples for the homogenisation experiments

Sample No	Fermentation time (h) for:			Phase of fementation
	B350	B500	B750	
S1	17	14	16	Rapid growth
S2	41	38	40	End of the growth phase
S3	68	61	64	Biomass decline
S4	86	86	87	Biomass decline

It has been reported that cell disruption in homogeniser is first order with respect to passes and can be described by the general derivation (Hetherington et al., 1971).

$$dR_{n,p}/dN = K_p (R_{m,p} - R_{n,p}) \qquad (3.4)$$

$$dR_{n,p} / (R_{m,p} - R_{n,p}) = K_p\, dN \qquad (3.5)$$

$$\log R_{m,p} / (R_{m,p} - R_{n,p}) = K_p.N \qquad (3.6)$$

or

$$R_{n,p} = R_{m,p}.(1 - \exp(-K_p.N)) \qquad (3.7)$$

Where

N = number of passes

$R_{n,p}$ = protein release at disruptive pressure P and N passes

$R_{m,p}$ = maximum protein which could be released when cells were disrupted at pressure P (e.g. $R_{m,100}$ means maximum protein which could be released at 100 bar disruptive pressure).

K_p = dimensionless constant dependent on physico-chemical properties of the cell wall and disruptive pressure.

Equation (3.7) was divided by maximum protein release at 1200 bar ($R_{m,1200}$) to make it dimensionless.

$$R_{n,p} / R_{m,1200} = R_{m,p} / R_{m,1200} (1 - \exp(-K_p.N)) \qquad (3.8)$$

To find the value $R_{m,p}$ and K_p in equation (3.8), the value of $R_{n,p} / R_{m,1200}$ was plotted against number of passes for each sample and curve fitting in the software package Origin was used. The fitting curves are shown in Figures 3.41 for B350, 3.42 for B750 and 3.43 for B1250. The results obtained from this curve fitting were used to evaluate the cell wall strength which will be explained in section 3.5.1.1.& 3.5.1.2 and will be discussed in section 5.5.
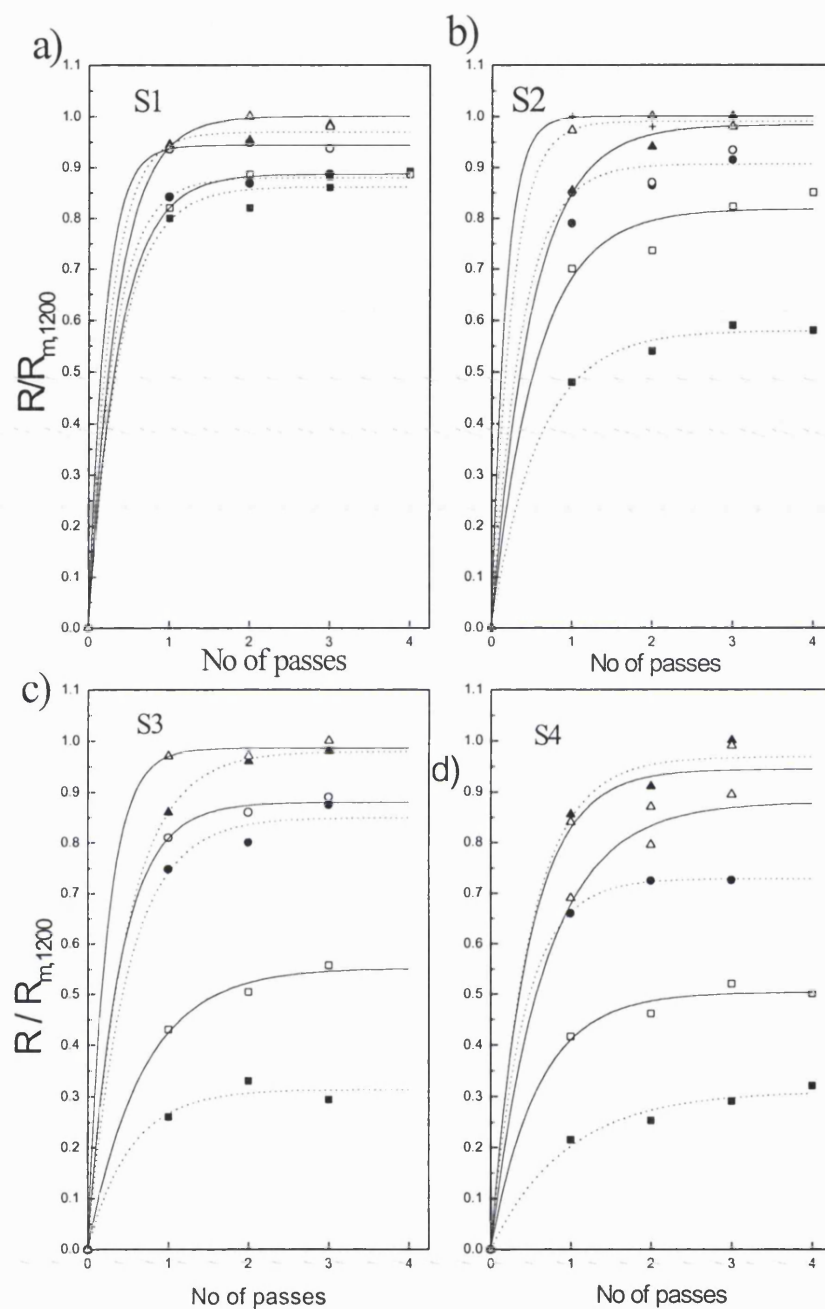
Figure 3.41: Protein release from disruption of fermentation broth samples using Lab-40 homogeniser. Samples was from fermentation at 350 rpm (B350). Disruption at 100 bar (■), 200 bar (□), 400 bar (●), 600 bar (O), 800 bar (▲) and 1200 bar (△).

151
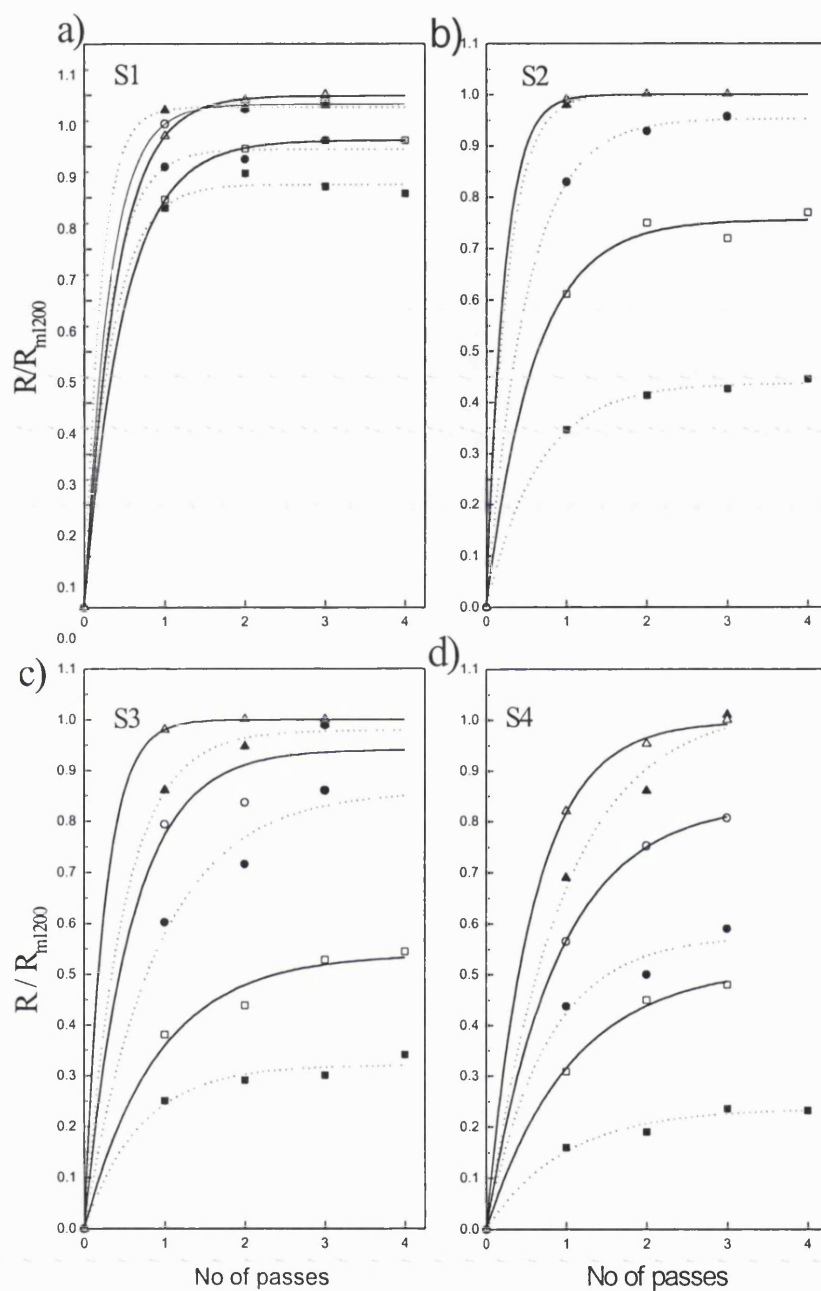
Figure 3.42: Protein release from disruption of fermentation broth samples using Lab-40 homogeniser. Samples was from fermentation at 750 rpm (B750). Disruption at 100 bar (■), 200 bar (□), 400 bar (●), 600 bar (○), 800 bar (▲) and 1200 bar (Δ).

152
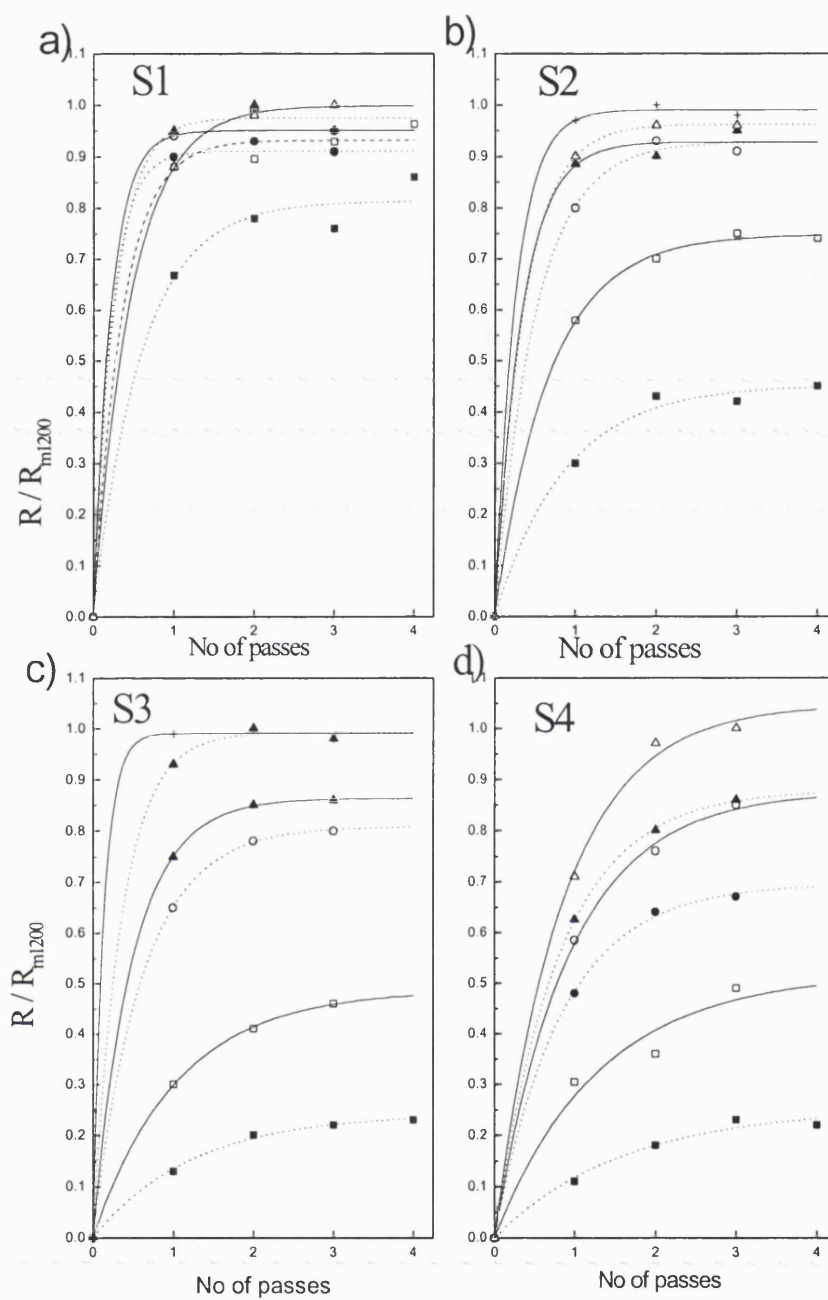
Figure 3.43: Protein release from disruption of fermentation broth samples using Lab-40 homogeniser. Samples was from fermentation at 1250 rpm (B1250). Disruption at 100 bar (■), 200 bar (□), 400 bar (●), 600 bar (○), 800 bar (▲) and 1200 bar (△).

3.5.1.1 Value of K_p from Hetherington equation:

The value of dimensionless K_p obtained from equation 3.8 varied between 0.6 to 5.0 depending on the pressure, age of the samples and agitation condition of the fermentation. The value of K_p at 100 bar disruptive pressure (K_{100}) are plotted against fermentation time in Figure 3.44a. It has been reported that cell wall strength is inversely related to the value of K_p obtained from Hetherington equation (Hetherington *et al.*, 1971). Value of K_{100} for fermentation samples at 1250 rpm was 1.7 in the rapid growth phase (16 h), 1.15 at the end of the growth phase (40 h), 0.81 at 64 h and 0.62 at 87 h (Figure 3.44). This shows that a sample from a later time in the fermentation had lower value of K_p which might be an indication of stronger cell wall. There was the same trend for fermentations at 350 and 750 rpm (Figure 3.44). Values of K_p for fermentation samples agitated at high stirrer speed (same fermentation time) were lower compared with lower stirrer speed (Figure 3.44). This might be an indication for a stronger cell wall at higher stirrer speed and this will be discussed in section 5.5.

The value of K_{200} showed a similar trend as the value of K_{100} (see Figure 3.44). Values of K_{400}, K_{600}, K_{800} and K_{1200} also decreased toward the end of the fermentation (Figure 3.45). However, there was no general trend regarding the agitation speed in the fermenter for the value of k_{400}, k_{600}, k_{800} and k_{1200}. This could be due to the fact that most of the protein was released during the first pass at the high pressures (400, 600, 800 and 1200 bar). The value of K_{100} and K_{200} varied between (0.6 to 3.0) (Figure 3.44), whereas the value of K_{400}, K_{600}, K_{800} and K_{1200} varied between 1.0 and 5.0 (Figure 3.45). This higher value of Kp at higher disruptive pressure means higher rate of protein release at higher disruptive pressure. These results are thoroughly discussed in section (5.5).
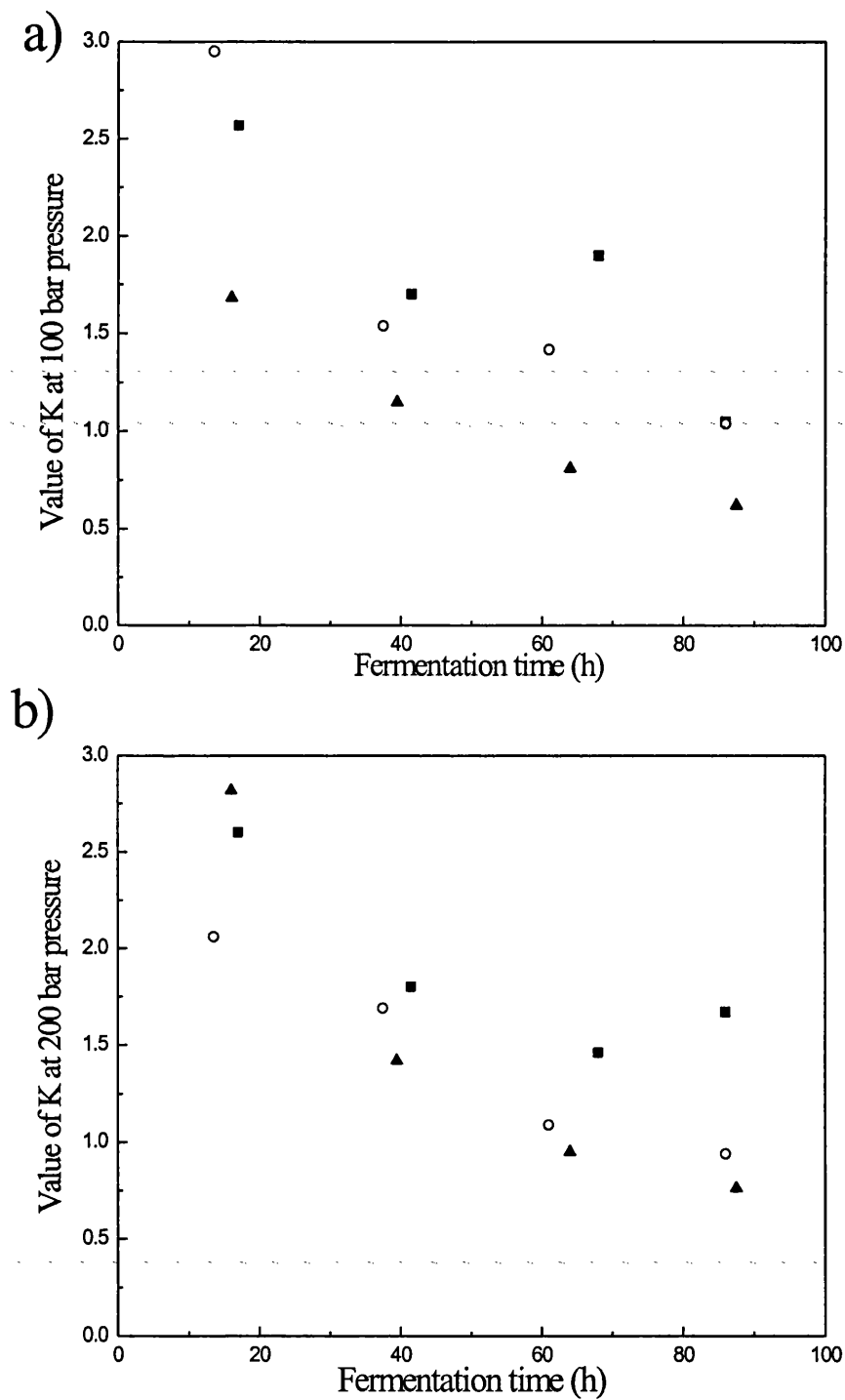
Figure 3.44: Values of K from Hetherington equation at 100 bar and 200 bar disruptive pressure. Samples were from fermentation at 350 rpm (■), 750 rpm (O) and 1250 rpm (▲).
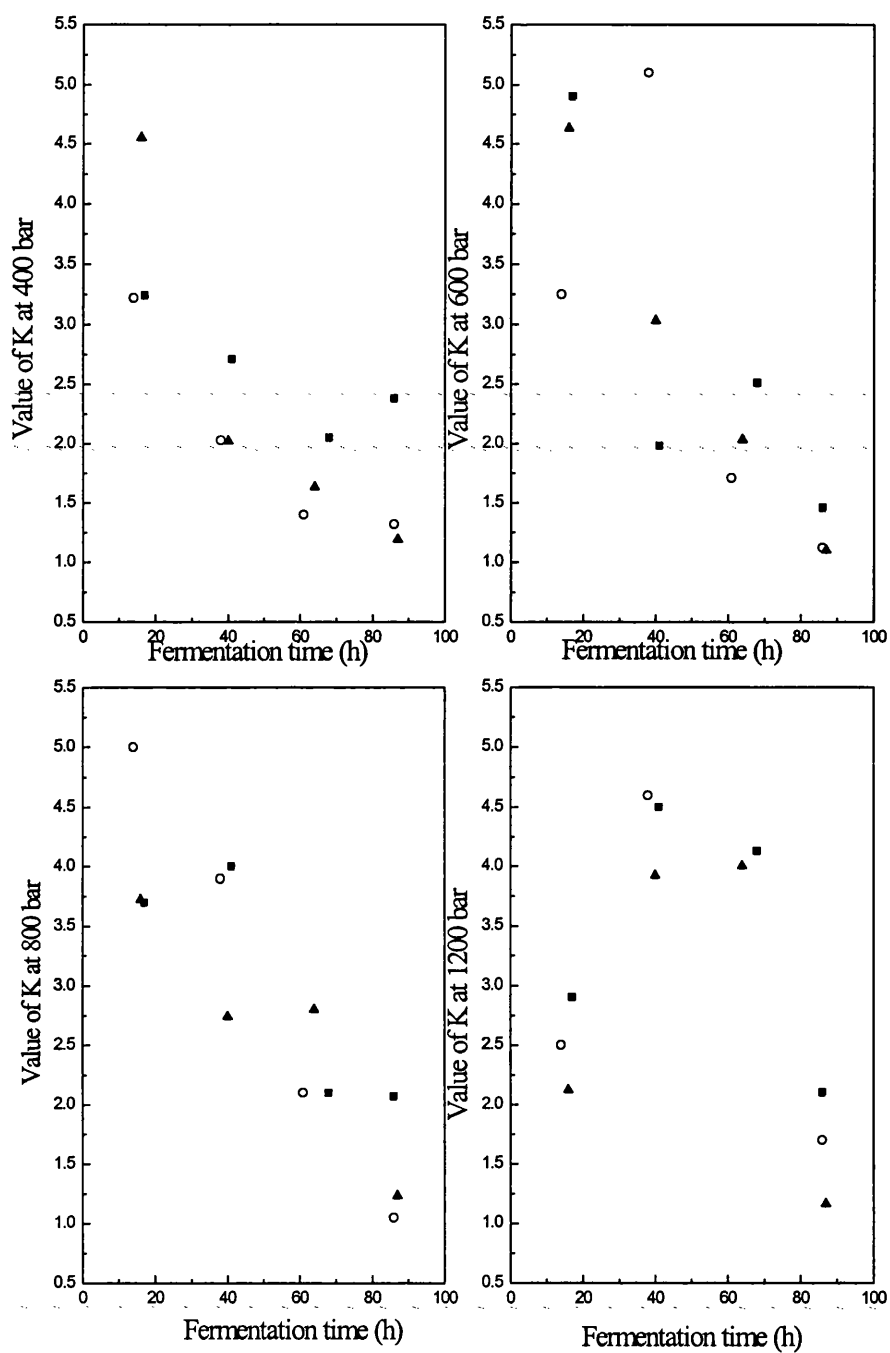
Figure 3.45: Values of K from Hetherington equation at 400, 600, 800 and 1200 bar disruptive pressure . Samples were from fermentation at 350 rpm (■), 750 rpm (O) and 1250 rpm (▲).

3.5.1.2 Maximum protein release ($R_{m,p}$)

The value of maximum protein release at each pressure for different samples was found using curve fitting (Figures 3.41, 3.42 & 3.43). It is evident from these figures that pressure not only affected the rate of release but also the final level of release. This maximum protein release at different pressures ($R_{m,p}$) was divided by the maximum protein release at 1200 bar pressure to make it dimensionless. This dimensionless number for different samples and different disruptive pressure is shown in Table 3.11. It should be noted that increasing the pressure above 1200 bar had no further effect on protein release (data not shown), therefore the value of $R_{m,1200}$ is the maximum protein which can be released with homogenisation and the value of $R_{m,p}$ /$R_{m,1200}$ is the percentage of protein which can be obtained at pressure P (e.g. $R_{m,100}$ /$R_{m,1200}$ = 0.3 means that 30% of the releasable protein can be released at 100 bar disruptive pressure).

Table 3.11: Values of $R_{m,p}$/$Rm,_{1200}$

Stirrer speed (rpm)	Sample*	R_{m100}/R_{m1200}	R_{m200}/R_{m1200}	R_{m400}/Rm_{1200}	R_{m600}/R_{m1200}	R_{m800}/R_{m1200}
350	S1	0.8	0.88	0.87	0.94	0.985
350	S2	0.57	0.82	0.9	0.98	0.98
350	S3	0.31	0.55	0.85	0.87	0.98
350	S4	0.31	0.5	0.73	0.88	0.97
750	S1	0.825	0.91	0.89	0.98	0.98
750	S2	0.437	0.756	0.95	1	1
750	S3	0.32	0.54	0.86	0.94	0.98
750	S4	0.23	0.51	0.57	0.83	1
1250	S1	0.81	0.93	0.91	0.95	0.97
1250	S2	0.45	0.75	0.92	0.92	0.96
1250	S3	0.24	0.48	0.8	0.86	0.99
1250	S4	0.25	0.51	0.69	0.87	0.87

* See Table 3.10 for the time course of the fermentation

The value of $R_{m,p}$ / $R_{m,1200}$ for 100 and 200 bar disruptive pressure is plotted in Figure 3.46. For S1 (early sample during fermentation), more than 80% of releasable protein was obtained at 100 bar disruptive pressure. Whereas, only 45% to 55% of the releasable protein was obtained for S2 at the same pressure (100 bar). This percentage was further reduced to 25% - 30 % for S3 and S4. These results indicate that the value of $R_{m,100}$/$R_{m,1200}$ decreased toward the end of the fermentation. These results are discussed in section 5.5. There was a similar trend for the value of $R_{m,200}$/$R_{m,1200}$ (Figure 3.46).
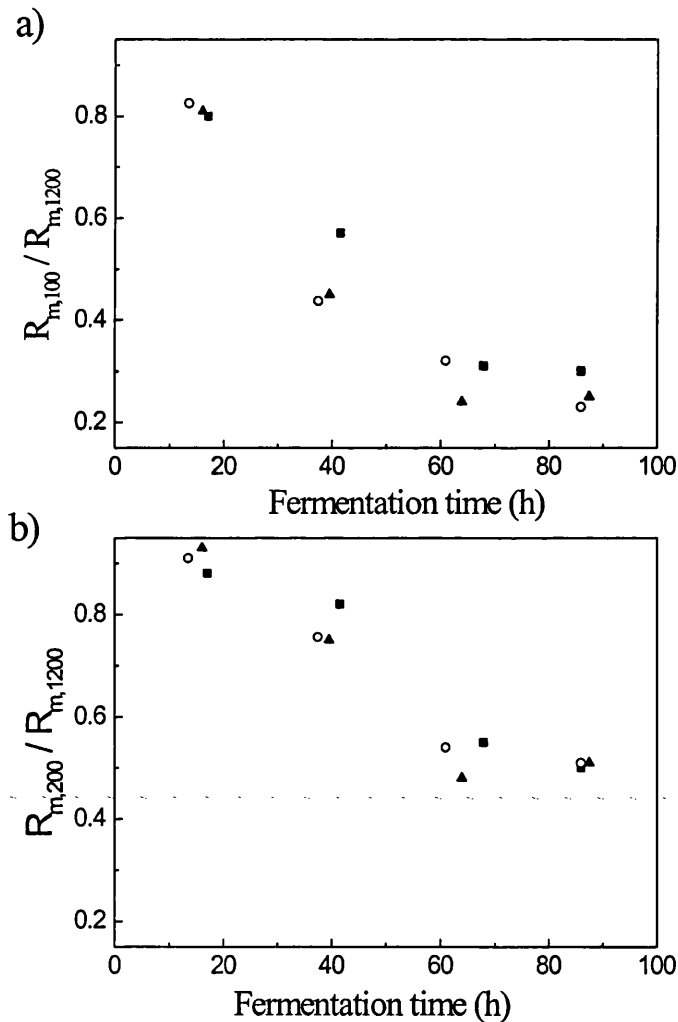
Figure 3.46: Values of $R_{m,100}$ / $R_{m,1200}$ and $R_{m,200}$ / $R_{m,1200}$. Samples were from fermentation at 350 rpm (■), 750 rpm (○) and 1250 rpm (▲).

The specific soluble protein release at 1200 bar disruptive pressure (mg (g cell)$^{-1}$) is shown in Figure 3.47. Fermentation samples agitated at 500 and 1000 rpm were disrupted only at 1200 bar and therefore were not discussed in this section. This Figure shows that the amount of soluble protein released at 1200 bar disruptive pressure decreased from 320 ± 20 (mg (g cell)$^{-1}$) for the fermentation samples taken at the end of the rapid growth phase (20-25 h) to 180 ± 10 (mg (g cell)$^{-1}$) at biomass decline phase (65 h).
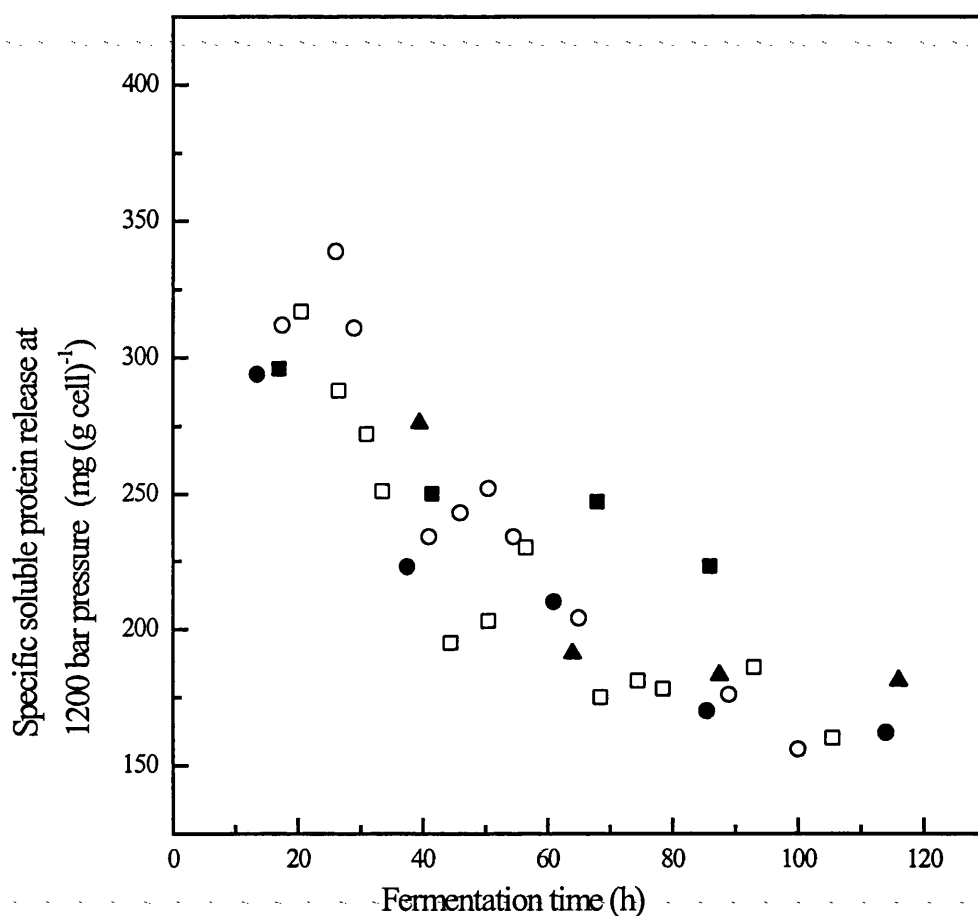
Figure 3.47: Soluble protein release at homogeniser at 1200 bar disruptive pressure from fermentation samples agitaded at Experiments at : 350 (■), 500 (□), 750 (●), 1000 (O) and 1250 rpm(▲).

3.5.1.3 Relation between $R_{m,p}$ / $R_{m,1200}$ and pressure

The maximum protein release ($R_{m,p}$) increased with pressure. Maximum protein release was plotted against disruptive pressure in log-log scale in Figure 3.48. Linear regression used to find the best line through the data for different samlpes and equation 3.9 recommended for the relation between maximum protein release and pressure. In this equation value of 'c' changed with age of the samples (Table 3.12).

$$R_{m,p} \propto P^b \qquad\qquad\qquad (3.9)$$
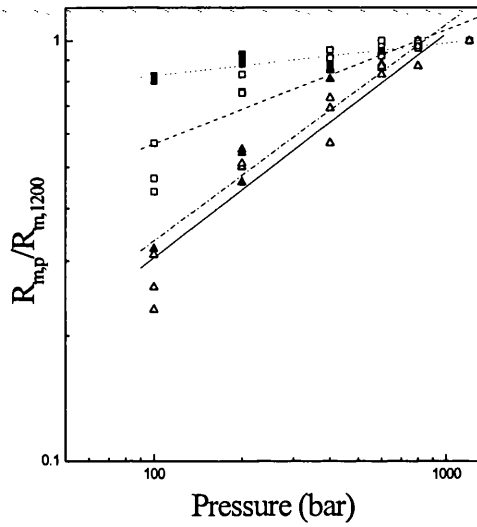
Figure 3.48: Effect of disruptive pressure on final level of protein release. Real data are as S1 (■), S2 (□), S3 (▲), S4 (△) and fitted lines are as S1(·······), S2(- - - -), S3 (- · - · -), S4 (———).

Table 3.12: Values of b for equation $R_{m,p} \propto P^b$

Sample	Value of c
S1	0.075
S2	0.27
S3	0.51
S4	0.53

3.5.2 Microscopic observations and morphological measurements of disrupted cells

Microscopy observations of homogenates disrupted at 100 bar and one pass showed that there were no clumps and most of the disrupted mycelia were without any branches (Figure 3.49). Homogenate disrupted samples from the rapid growth phase (S1) were very fine and it was mostly debris even at moderate pressure (100 bar). It was much smaller compared with other samples (S2, S3 or S4) (Figure 3.49, see also Figures 3.18 & 3.19 for undisrupted cells morphology).

The size of the disrupted cells (e.g. major axis) at 100 bar and one pass was also measured using image analysis and the results are shown in Figure 3.50. The mean major axis of the disrupted cells at the end of the deceleration phase (38-41 h) was significantly bigger compared with samples taken in rapid growth phase (14-17 h). The mean major axis of the disrupted cells was not changed significantly after the end of the deceleration phase (Figure 3.50a). The mean major axis of the disrupted cells also divided by the mean major axis of the original cells is shown in Figure 3.50b. This ratio increased till 60-68 hr, and then it was not changed significantly till 90 h. The mean major axis of the disrupted cells was 30-70% of the original cells (Figure 3.50b). This ratio was always less at higher stirrer speed.

Increasing the disruption pressure makes the length of the disrupted cells smaller and the disrupted cells were mostly debris at pressure higher than 400 bar (Figure 3.51). Microscopical observations showed no significant differences for disrupted cells with increasing number of passes (Figure 3.49c). Morphological measurements using image analysis for three different samples also showed that major axis of the disrupted cells at 100 bar and 4 passes was $15 \pm 1.5\%$ less than the size of the disrupted cells at 100 bar. As it was mentioned earlier, while increasing the disruptive pressure has a significant effect on protein release (up to 400% for 12 fold increase in pressure, see Figure 3.41), increasing the number of passes at 100 bar increased the protein release only 15-20%. These results suggested that in a homogeniser, protein release and breakage of the cells are correlated together.

161
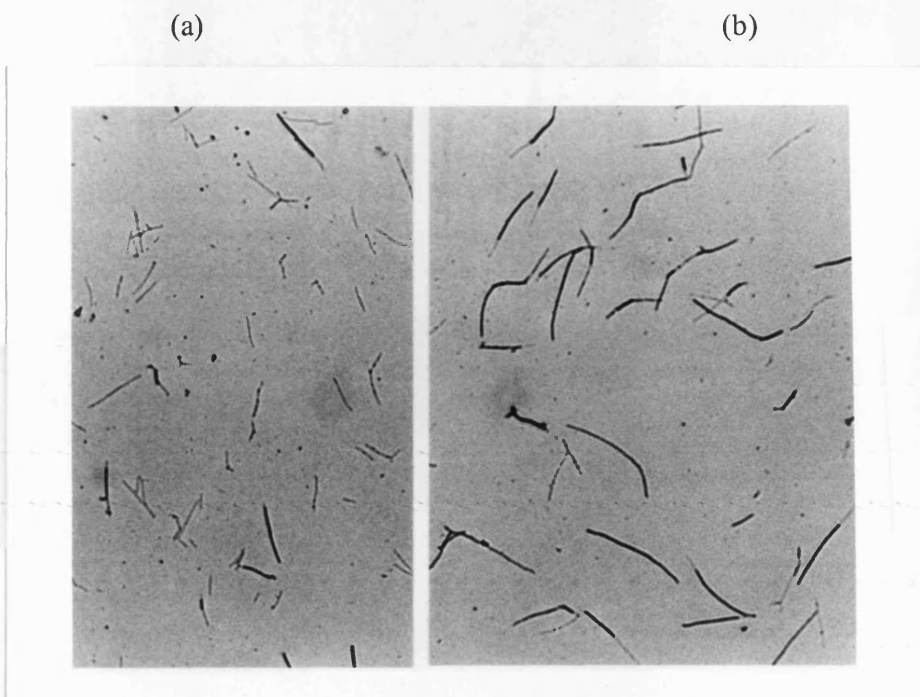
Figure 3.49 (a & b): Photographs 0f disrupted cells at 100 bar and one pass in Lab-40 homogeniser. Samples was from fermentation at 750 rpm. a) S1 (in rapid growth phase) b) S3 (in decline phase). Scale, (———) = 20 μm
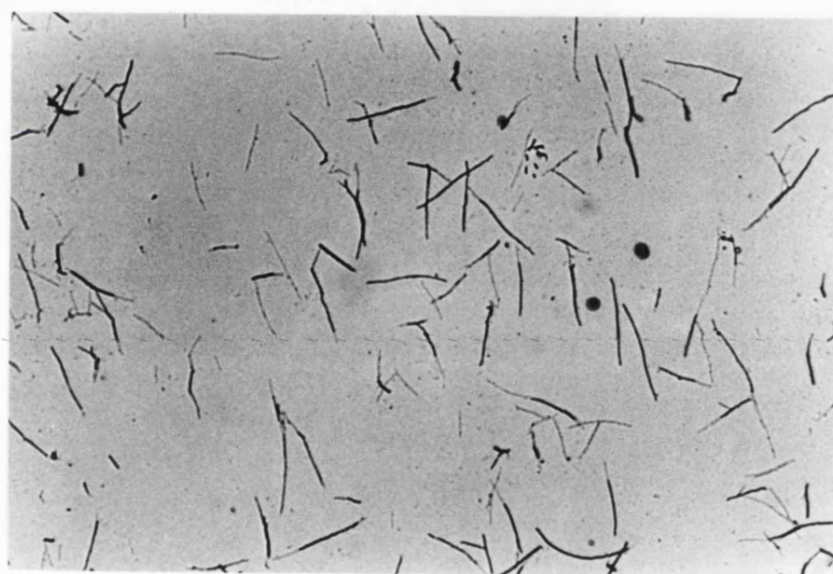
Figure 3.49 (c): Photographs of disrupted cells at 100 bar and 4 passes in Lab40 homogeniser. Sample was from fermentation at 750 rpm in deline phase (S3). Scale, (———) = 20 μm.
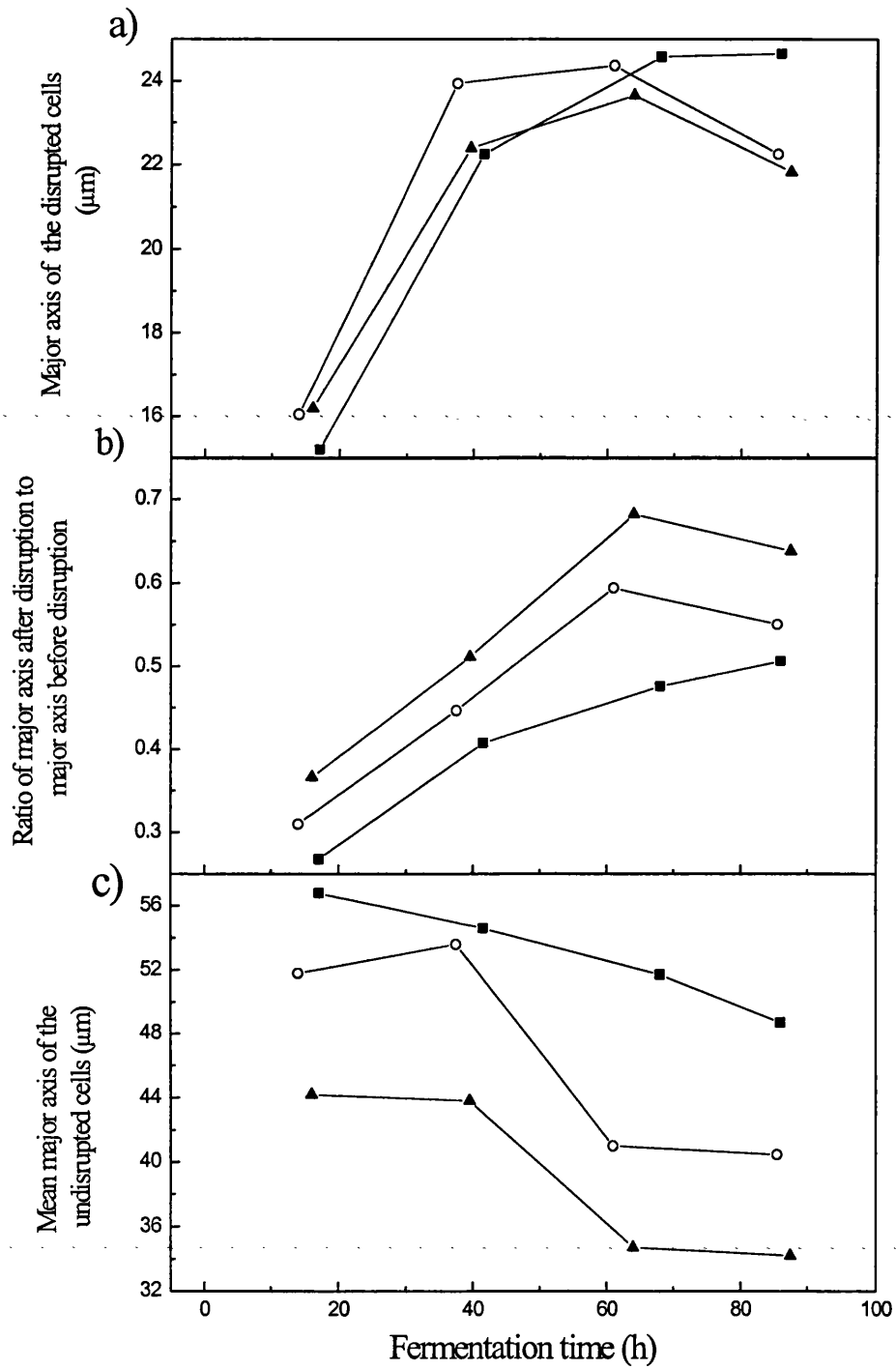
Figure 3.50: Size of the cells before and after the disruption in Lab-40 homogeniser. Agitatation speed of the fermentation was 350 rpm (—■—), 750 rpm (—○—) and 1250 rpm (—▲—).

163

(a) (b)
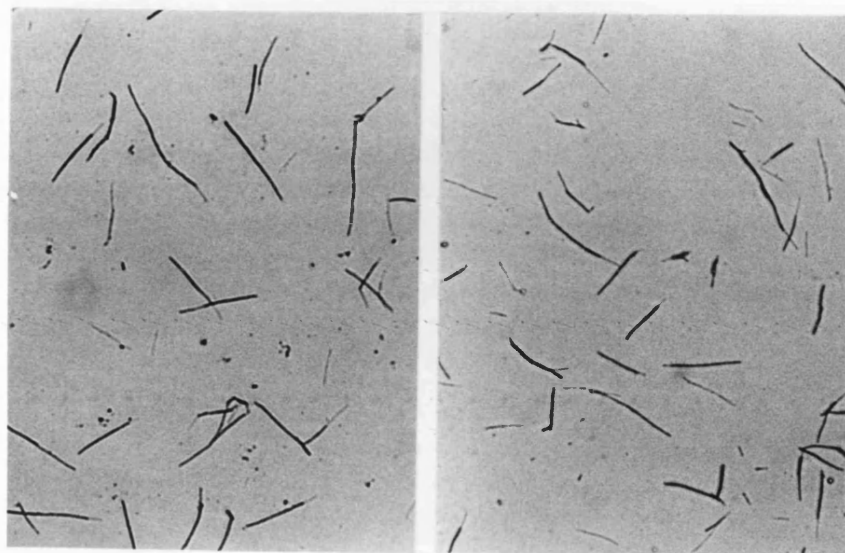
(c) (d)
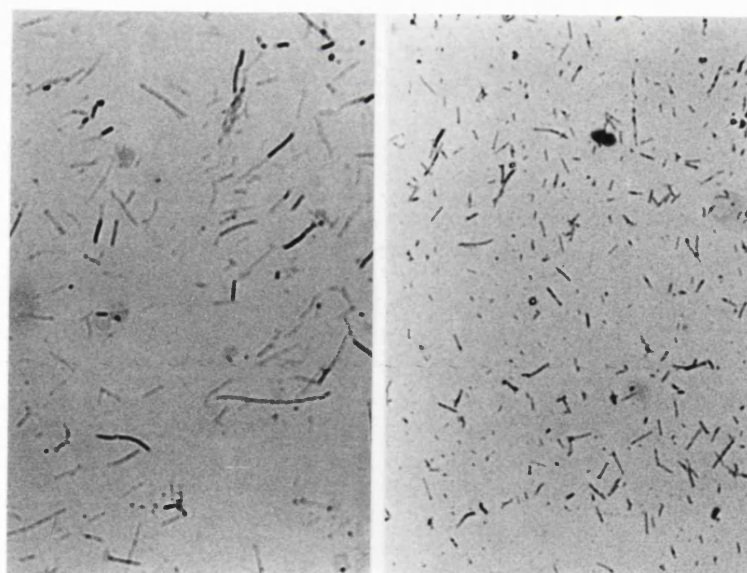
Figure 3.51 (a, b, c &d): Photographs of disrupted cells in Lab40 homogeniser after one pass at a) 100 bar b) 200 bar c) 400 bar d) 600 bar. Scale in decline phase (S3). Scale, (———) = 20 μm.

4 Turbulent breakage of the mycelia in stirred tank

4.1 Theoretical model

According to previous studies in fully turbulent flow in a stirred tank, the most plausible mechanisms of disruption of filamentous organisms are based on the fluid dynamic forces originating from the turbulent velocity fluctuation in the tank (Bhavaraju and Blanch, 1976; van Suijdam and Metz, 1981; Ayazi Shamlou et al., 1994; Cui et al., 1997). The turbulent dynamic forces result either from the instantaneous pressure difference on opposite sides of the mycelium (van Suijdam and Metz, 1981; Ayazi Shamlou et al., 1994) or viscous shear stress result from local velocity gradients (shear stresses) (Tomi and Bagster, 1978). The ratio of mycelial length to turbulent microscale $(\nu^3\varepsilon^{-1})^{0.25}$ is an important factor in establishing the ways in which cell disruption occurs in a turbulent environment (see section 1.4.6). Given the filamentous nature of the mycelia, the major axis was taken to represent an appropriate dimension for consideration (see Figure 3.18 and also section 2.3.8). The mean major axis of the mycelium in this experiment is in order of 30-70 μm (Figure 3.20), comparable to the microscale of turbulence in the bioreactor used in this study (10-200 μm). Therefore, the turbulent rupture of mycelium is assumed to be due to shear stresses in viscous dissipation subrange, which are induced within the structure by velocity fluctuations experiences over the surface of the mycelia.

In developing the model, the cell wall of the mycelium is assumed to behave elastically under the prevailing stress condition. Therefore, from the classical definition of strain energy total strain energy (S) absorbed by the mycelium can be written by equation 4.1:

$$S = \left[\frac{V\sigma_w^2}{2E}\right]P'^{\alpha} \qquad (4.1)$$

where S is the total strain energy absorbed by the mycelium, V is its volume , E is the Young's modulus of elasticity of the hyphal wall and P' is the number of passes through the high shear zone of the impeller.

In equation 4.1, σ_w is the longitudinal stress in the wall matrix and is obtained from a force balance as follows. The fluid shear forces that act at the mycelium wall interface are transferred into the cell wall structure. If a single hypha is considered as an idealised thin wall tubular cylinder with outer diameter, d_h, and inner diameter, d_i, the interfacial shear stress (τ), acting on the small element of width, dx, is equal to $\tau \pi d_h \, dx$. This shearing force causes a longitudinal stress in the wall matrix, $d\sigma_w$. Therefore, the force that balances the imposed shear force is the product of $d\sigma_w$ and the cross sectional area of the thin wall of the hyphae. Thus,

$$\tau \pi d_h dx = d\sigma_w \, \frac{\pi}{4}\left(d^2_{\,h} - d^2_i\right) \qquad (4.2)$$

Rearranging equation 4.2 gives

$$\frac{d\sigma_w}{dx} = \frac{4\tau \, d_h}{d_h^2 - d_i^2} \qquad (4.3)$$

Noting that $\left(d^2_{\,h} - d^2_i\right) = (d_h - d_i)(d_h + d_i) = w(d_h + d_i)$, where w is the hyphal wall thickness, gives

$$\frac{d\sigma_w}{dx} = \frac{4\tau \, d_h}{w(d_h + d_i)} \qquad (4.4)$$

Integrating equation 4.4 gives the variation of the longitudinal stress, σ_w, in the wall matrix as a function of its axial position, x. Thus

$$\int_0^{\sigma_{wx}} d\sigma_X = \int_{\frac{L_h}{2}}^x \frac{4\tau \, d_h}{w(d_h + d_i)} \ dx \qquad (4.5a)$$

$$\sigma_{wx} = \frac{2\tau \; d_h(L_H - 2x)}{w(d_h + d_i)} \qquad\qquad (4.5b)$$

Since the wall of the hyphae is relatively thin, $d_h \approx d_i$, therefore equation 4.5b reduces to:

$$\sigma_{wx} = \frac{\tau}{w}\left(L_h - 2x\right) \qquad\qquad (4.6)$$

Equation 4.6 states that the longitudinal wall stress increases from zero at the tip where $x=(L_h/2)$ to its maximum, $\sigma_{w(max)}$, at $x=0$ (centre) where L_h is the length of the hyphae. Because of the variation in the longitudinal wall stress, σ_w, the determination of the total strain energy via equation 4.1 requires the integration of the stress, σ_w, over the entire volume of the mycelium. The volume of the mycelium however is not an easy parameter to determine (Fig 3.18) and is complicated by its fractal nature. According to models of fractal behaviour, the relationship between the volume of a fractal object, V, and its length scale, x, is determined by the fractal dimensionally, β (section 1.1.2). Therefore the relationship between the volume of the fractal mycelium and its characteristic length scale, x, can be expressed as

$$V \propto x^\beta \qquad\qquad (4.7)$$

Differentiating equation 4.7 gives

$$\frac{dV}{dx} = \beta(x)^{\beta-1} \quad \rightarrow \quad dV = \beta(x)^{\beta-1} \; dx \qquad\qquad (4.8)$$

Using equation 4.1, the strain energy in the elemental volume of the fractal mycelium, dV, can be written as

$$dS \propto \left(p'\right)^{\alpha} \frac{\sigma_{wx}^2}{2E} \, dV \tag{4.9}$$

Substituting into equation 4.9 for dV using equation 4.8 and for σ_{wx} using equation 4.6, assuming mean major axis (OL) is proportional to hyphae length (L_h) and integrating gives

$$\int_0^S dS \propto \frac{\left(p'\right)^{\alpha}}{E} \int_0^{\frac{OL}{2}} \left[\frac{\tau^2}{w^2} \left(L_h - 2x\right)^2 \frac{\beta}{2}(x)^{\beta-1} \right] dx \tag{4.10}$$

Cell wall thickness (w) is a function of the hyphal length, x (see section 5.3), the limited data available (Trinci and Collinge, 1975) suggest an approximately linear inverse relationship between the two. Thus, in equation 4.10 substitution of $w \propto$ (1/x) and integrating gives

$$S \propto \frac{\beta}{2} \left(\frac{p'^{\alpha}}{E} \right) \tau^2 \frac{\left(\dfrac{1}{\beta+2} + \dfrac{4}{\beta+4} - \dfrac{4}{\beta+3} \right)}{2^{\beta+2}} \left(OL\right)^{\beta+4} \tag{4.11}$$

Micrscopical observations of the mycelia structure during this experiments confirmed that the culture had a highly dispersed morphological structure (Figure 3.18). Patankar et al. (1993) have reported the value of fractal dimensionally of 2.0-2.7 with average value of 2.35, for dispersed mycelia of S. tendae and S. griseus. Therefore in the absence of any data of fractal dimensionally for S. erythraea, the fractal dimensionality, β, was assumed to have a value of 2.35. With $\beta=2.35$, equation 4.11 reduces to

$$S \propto \frac{p'^{\alpha}}{E} \left(\tau^2\right) [OL]^{6.7} \tag{4.12}$$

In above equations , P' , is the total number of passes through the high energy density zone of the impeller and is included in the energy balance to account for the fact that in the fermenter the mycelium is subjected to stress cycling. According to classic theories of solid mechanics, stress cycling reduces the critical (failure) strain energy by a phenomenon known as fatigue. In a mechanically stirred bioreactor, the high shearing zone is confined to a small region close to the impeller. The total number of passes, P' , through the impeller zone is determined from the flow path and the circulation rate, t_c, through the impeller zone. Considerable published experimental work (Smith and Lilly, 1989; Makangiansar *et al*, 1993; Justen *et al*., 1996) confirms that, for other similar conditions, hyphal length depends on circulation rate through the impeller zone. The total number of passes, p', through the high shear zone is related to the circulation time, t_c, as $p' \propto {}^1/t_c$. As far as the exponent of p' in equation 4.12 is concerned, experimental data for non-biological materials suggested a value of $\alpha = \frac{1}{2}$ (Tavernelli and Coffin, 1959) . In the absence of any information for biological systems, in the present model the exponent α is assumed to be equal to $\frac{1}{2}$. Thus, $P'^{\alpha} \propto ({}^1/t_c)^{1/2}$ and the relationship given in equation 4.12 can be rewritten as

$$S \propto \frac{1}{E}\left(\tau^2\right) \; [OL]^{6.7} \; \left(\frac{1}{t_c}\right)^{\frac{1}{2}} \qquad (4.13)$$

The interfacial shear stress, τ, is related to power dissipation rate (ε) by equation 4.14 (Tomi and Bagster, 1978)

$$\tau \; \alpha \; \mu(\varepsilon/\nu)^{0.5} \qquad (4.14)$$

Substitution of equation 4.14 in equation 4.13 leads to equation (4.15)

$$S \propto \frac{OL^{6.7}}{E} \; \left(\varepsilon\rho\mu\right)\left(\frac{1}{t_c}\right)^{\frac{1}{2}} \qquad (4.15)$$

Using the minimum strain energy criterion to define the critical value of the total strain energy, S_F, attained by the mycelium at the point of breakage, after some minor rearrangement, gives

$$OL = \left(S_F E\right) \left[\frac{\rho\mu\varepsilon}{\sqrt{t_c}} \right]^{-0.15}$$

(4.16)

Equation 4.16 gives the relationship between the mean major axis of the mycelium and some of the parameters affecting it.

4.2 Results and discussion

The development of equation 4.16 is based on the assumption that the mean major axis of the mycelium is less than or is comparable to the microscale of turbulence $(v^3/\varepsilon)^{1/4}$ in the vessel. The determination of the turbulent microscale however is difficult because of the uncertainty associated with the variation in the distribution of the energy dissipation rate, ε, in the tank. Several methods have been proposed in the past to facilitate the calculation of the maximum, average and the minimum values of the energy dissipation rate (section 1.4.2).

The determination of the microscale of turbulence is more complicated in this study because of the non-Newtonian nature of *Saccharopolyspora erythraea* culture. Rheological measurements showed that broth rheology changed continuously during fermentation (see section 3.3.4). The culture initially had water-like Newtonian properties, but developed non-Newtonian shear thinning characteristics during the early stage of growth which lasted for about 10 hours (Figure 3.33). Hyphal breakage dominated between 20 and 60 hours (Figure 3.21) during which time the broth had a mean flow behaviour index of 0.4.

The microscale of turbulence was calculated based on the average power input per unit mass, ε_a, using the definition of an average apparent viscosity using the Metzner and Otto technique (1959). Thus, the apparent viscosity, μ_a, at any speed was obtained from equation 2.5, the energy dissipation rate was calculated using the method previously used by Makangiansar (1991) (appendix 1). The microscale of turbulence, λ, was obtained (appendix 2) from the definition $[(\mu_a/\rho)^3/\varepsilon_a]$. Figure 4.1a

shows a plot of the microscale of turbulence against fermentation time for different agitation speeds.

It is assumed that breakage dominates in impeller region (Smith *et al.*, 1991). The value of apparent viscosity in impeller region has been calculated based on energy dissipation in this region, assuming $\varepsilon_i/\varepsilon_a = 0.1$, and the value of microscale of the turbulence in the impeller zone was calculated. The detail of the calculation is in appendix 2.

The value of microscale of turbulence in impeller zone varied between 10-200 μm (Figure 4.1b), while the mean major axis of the mycelia was between 30 to 70 μm. It is generally recognised (Tambo and Hozumi, 1979; Muhle and Domasch, 1991; Ayazi Shamlou *et al.*, 1995) that shear forces originating from the fluid-hyphal interaction in the viscous subrange of turbulence energy spectrum can be extended up to 10λ. Against this background, the assumption of breakage of the mycelia of the *S. erythraea* by turbulent shear forces seems to be reasonably justified.
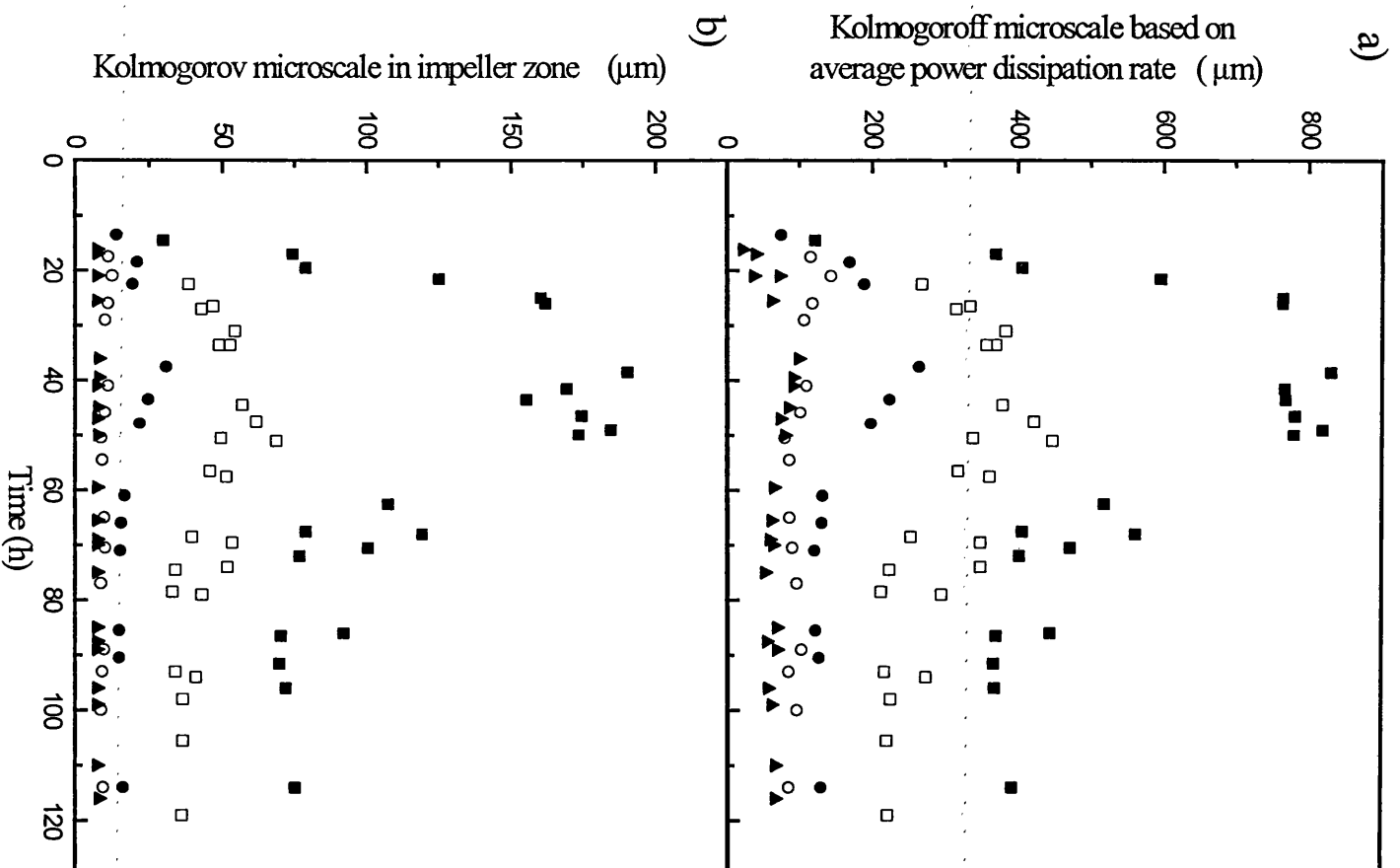
Figure 4.1: Kolmogorov microscale of turbulence for fermentation at 7-L scale and stirrer speed (rpm) of 350 (■), 500 (□), 750 (●), 1000 (○) and 1250 (▲).

In Figure 4.2a the equilibrium mean major axis of the mycelial clumps are plotted as a function of the group in the [ ] in equation 4.16 on log-log scale. The data refer to experiments carried out at the 7-L scale. For the purposes of the plots in Figure 4.2a, the circulation time was obtained from the following expression (Reuss, 1988, Smith *et al*, 1990, Ayazi Shamlou et al, 1994). The detail of calculation is in appendix 3.

$$N\, t_c = 0.76\left(\frac{H}{T}\right)^{0.6}\left(\frac{T}{D}\right)^{2.7} \hspace{3cm} (4.17)$$

The best line of fit through the data points gave a slope of -0.12. Figure 4.2 b also shows the plot of mean major axis for both freely dispersed mycelia and mycelial clumps against the group in the [] in equation 4.16. The best line of fit through the data points also gave a slope of -0.12. There are at least two possible reasons for the difference between the slope of the best lines of fit and model value based on equation 4.16. Firstly, the basic premise behind the derivation of equation 4.16 is that the wall of the hyphae behaves purely elastically. Even though, there is some reports indicating elasticity behaviour of cell wall in the filamentous organisms (Wessels, 1990; Koch, 1994; Kaminskyj and Heath, 1996), assumption of purely elasticity seems to be idealistic. Second, since it is very unlikely that physico-chemical properties of the cell wall is even along the hyphae, assumption of a constant Young's modulus of elasticity, E, seems to be unrealistic. Unfortunately, very little is known about the mechanical properties of biological materials and therefore it is difficult to elucidate further. Against this background the comparison between the slope of the best line of fit of data in Figure 4.2 and the exponent of the group [ ] in equation 4.16 is considered reasonably good.
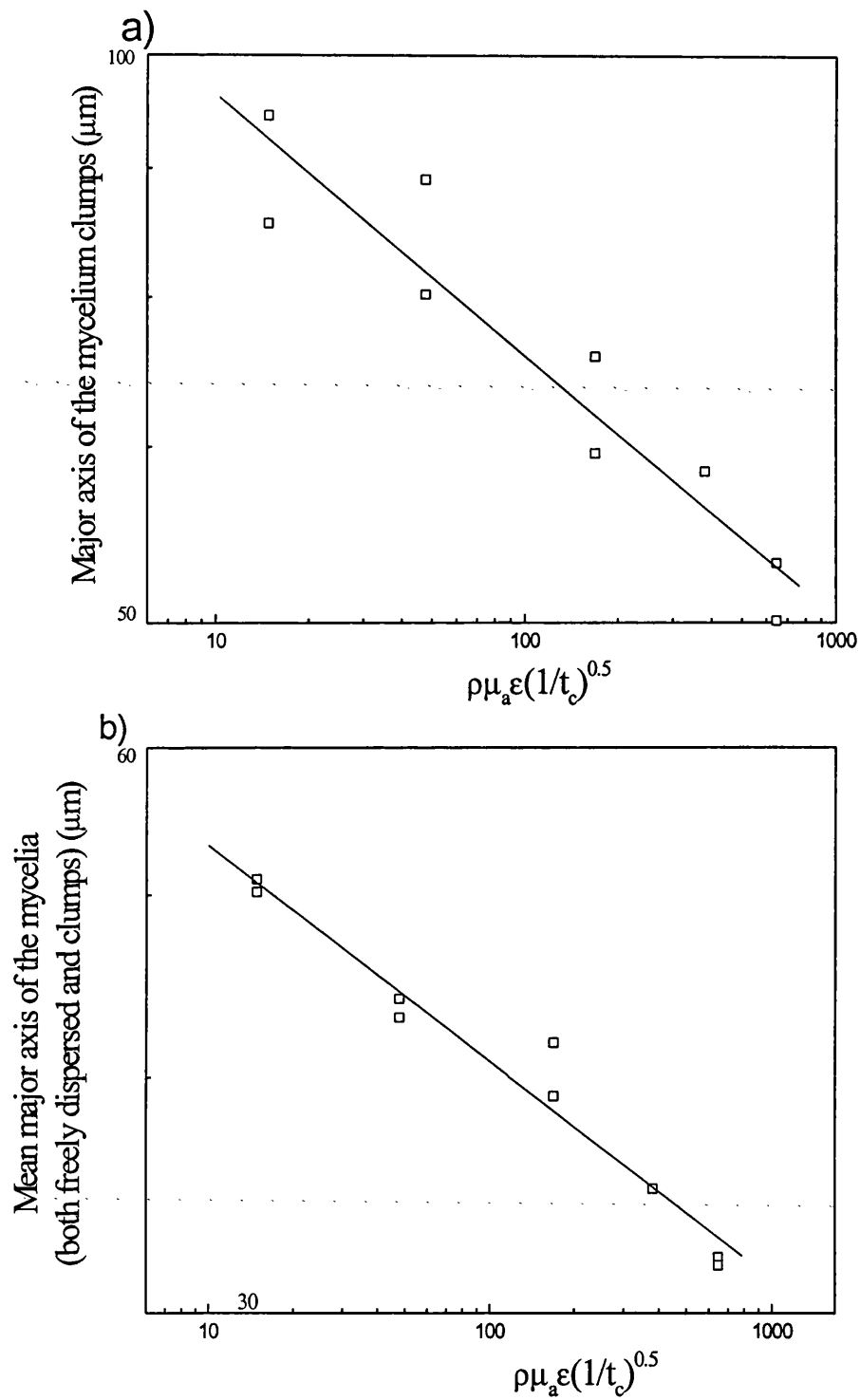
Figure 4.2: Examination of equation 4.16 with experimental data at 7-L scale.

174

Two scale of the fermenters, 7-L and 450-L, used in this study are not geometrically (section 2.2.4) identical and therefore in order to compare the data obtained from the two units, equation 4.16 is rewritten in its more basic form in terms of impeller diameter and power input by noting that in turbulent flow $\varepsilon \propto (P/D^3)$. The results are shown in Figure 4.3 where the solid squares represent data for the 450-L scale and the open symbols refer to the 7-L scale fermentation experiments. The group on the x-axis of the plot in Figure 4.3 has brought the limited data for the two scales together and the slope of the best line of fit remains the same (-0.12).

Equation 4.16 suggests a combination of direct and indirect effects of agitation intensity on the mean major axis, OL. Speed indirectly affects the mean major axis through its effect on the apparent viscosity, μ_a, and impeller power input per unit mass, ε, and directly through the circulation time, since $t_c \propto 1/N$ (equation 4.17). Equation 4.16 can be reduced to relation 4.18 by substituting $t_c \propto 1/N$, $\varepsilon \propto P/D^3 \propto N^3D^2$, assuming constant value for consistency index and value of 0.4 for flow behaviour index.

$$OL \propto N^{-0.42} \qquad\qquad (4.18)$$

The data in Fig 4.4 are plotted to show the overall effect of speed on the mean major axis. The slope for each set of data is shown. Published data for *S. clavuligerus* (Belmar-Beiny and Thomas, 1991) are also shown in Figure 4.4 for comparison. The model prediction of the effect of the speed of rotation on the mean main hyphal length (equation 4.18) is in reasonable agreement with experimental data reported in the present investigation. It is not possible to predict the expected slope of the line through the data for *S. clavuligerus* (Belmar-Beiny and Thomas, 1991) as the slope depends on the value of the flow behaviour index of the culture which is not given in the original paper. Nevertheless a qualitative comparison between the best line of fit through the data for the *S. clavuligerus* culture (slope of -0.3) with our data (-0.35) is not unreasonable.

175
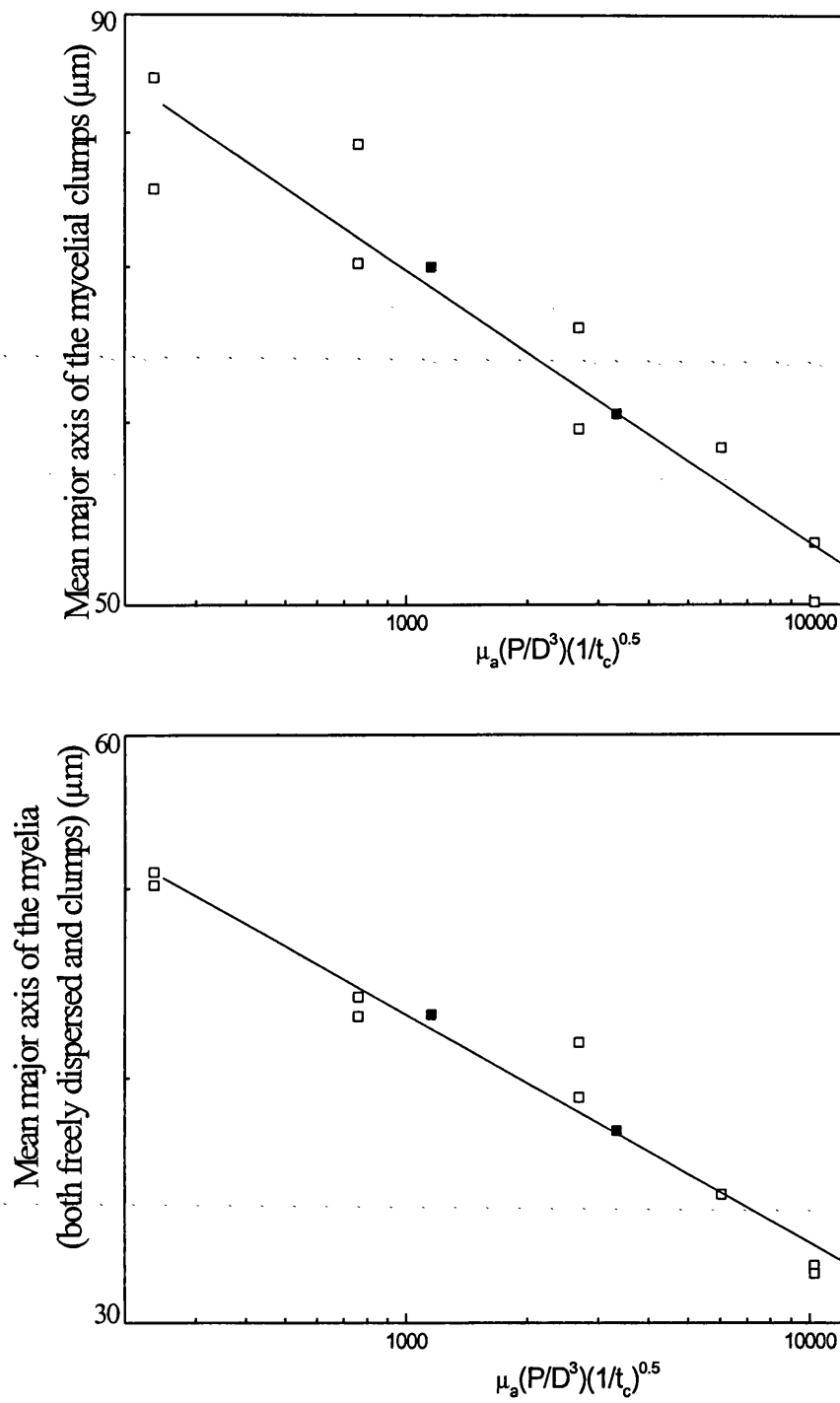
Figure 4.3: Examination of equation 4.16 with experimental data at 7-L (□) and 450-L

(■) scales.
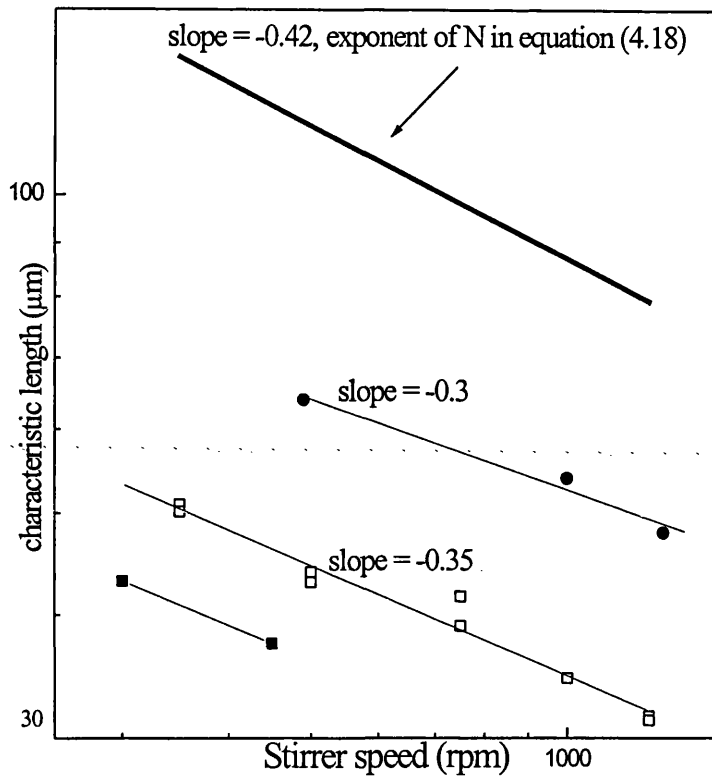
Figure 4.4: Examination of equation 4.18, mean major axis of the mycelia at this experiment at 7-L scale (□), mean major axis of the mycelia at this experiment at 450-L scale (■) and mean main length of the freely dispersed mycelia in *S. clavuligerus* fermentation (Belmar-Beiny and Thomas, 1991) (●).

Breakage in boundary layer around the impeller is another mechanism which has been recommended for other systems including animal cells (Cherry and Papoutsakis, 1986) and oil drops in suspensions (Leng and Quarderer, 1982; Kumar *et al.*, 1991; Boye *et al.*, 1996; section 1.4.5). Relatively high shear rates are expected in the boundary layer around the disk or blades of the rotating Rushton turbine. A particle present in the boundary layer around the disk or blades of a rotating Rushton turbine can experience strong shearing action leading to its breakage provided the particle size is smaller than boundary layer thickness and the residence time of the particle is enough for the breakage (Boye *et al.*, 1996). The boundary thickness in these experiments (200 - 360 µm) seems to be bigger than the size of the mycelia (see appendix 4), therefore it is possible that its shear forces have contributed in breakage of the mycelia.

Schlichting (1979) stated that for a rotating disk, the transition from laminar flow regime to turbulent flow regime occurs at a disk Reynolds number of approximately 3 $\times$ 10^5 indicating that under most conditions of interest including those in the vessel used in the present study, the flow in the boundary layer is laminar (see appendix 4). According to past studies (Schlichting, 1979; Boye *et al.*, 1996) the shear rate in the laminar boundary layer around the blade of the Rushton turbine impeller can be written as equation 4.18 (see section 1.4.5).

$$\gamma_{max} \propto N^{1.5}Dv^{-0.5} \tag{4.19}$$

therefore,

$$\tau_{max} = \mu\gamma_{max} \propto \rho^{0.5} \mu^{0.5}N^{1.5}D \tag{4.20}$$

Substitution of equation 4.20 in equation 4.13 resulted to equation 4.21

$$OL \propto (S_f E)[\rho\mu N^3 D^2 (1/tc)^{0.5}]^{-0.15} \tag{4.21}$$

It should be noted that the equation derived from boundary layer analysis (equation 4.21) is identical to the equation 4.16 by substitution of ($\varepsilon \propto P/D^3 \propto N^3 D^2$). As far as the results obtained in these experiments concern, there is no preference for any of these mechanisms. Therefore any of these two mechanisms or combination of both could be involved in breakage of the mycelia.

Summary

A model of hyphal breakage was set up based on stress cycling (fatigue) resulting from continuous recirculation of the mycelia through the high stress zone of the impeller. The critical strain energy of failure was used, the mycelium assumed to have fractal properties and the individual hypha was assumed to behave elastically with a wall thickness that increases linearly with the distance away from the growing tip. This led to equation 4.16 for prediction of equilibrium major axis of the mycelia. The model was tested with experimental data obtained from two scales of fermentation of *S. erythraea*. Experimental data gave a value of -0.12 for the exponent of the group in [ ]. The discrepancy between the experimental value and theoritical value of -0.15 is perceived to be caused by the complex mechanical properties of the cell wall. There is very little published data on cell wall mechanical properties despite the importance of these in relation to the effect of shear and mechanical damage. Experimental data obtained in high pressure homogeniser as part of this study (see section 3.5 and 5.5) gave some indication of variation of cell wall mechanical properties during the fermentation. Further research is needed of these aspects of cell wall properties before improved models of breakage can be developed.

5 DISCUSSION

5.1 Effect of agitation on growth

Limiting element in complex medium

The end of the rapid growth phase (20-25 h), coincided with the sudden decrease in the CER, which was related to a change in the utilisation of the limiting components (see Figure 3.11). Increasing glucose concentration from 30 to 40 gL^{-1} (other components were the same as this experiment), resulted to extending rapid growth phase till 30-35 h and an increase in the biomass concentration by approximately 30% (Sarra et al., 1996). This suggested that, possibly glucose was the limiting element. However, possibility of limitation in phosphate is not ruled out. The initial concentration of KH_2PO_4 in medium was 0.7 gL^{-1}. Phosphate measurements showed, the amount of the phosphate decreased to almost 0.08 gL^{-1} at the end of the rapid growth phase (Figure 3.17) and then it was fluctuated around this value till end of the fermentation. This concentration of the phosphate was in the range of the phosphate limited medium in other experiments (Martin and Demain, 1980; Trilli et al., 1987).

Effect of agitation for complex medium experiments

A review by Bronnenmeier and Markl (1982) showed that the growth rates of several fungi were stirrer speed dependent. On the other hand some authors have indicated that an increase in agitation speed resulted in low productivity but that does not affect growth of fungi filamentous organisms (Konig et al., 1981; Placek et al., 1981). The matter is often complicated by problem associated with oxygen limitation. The increase in biomass concentration with increasing agitation in the fermentation of filamentous fungi as reported by many authors (Dion & Kaushul, 1959; Konig et al., 1981) is often due to an improved oxygen transfer in the system. Makangiansar et al. (1993) reported a decrease in the specific growth rate with an increase in agitation speed in *Penicillium chrysogenum* fermentation. Cell growth of S. *clavuligerus* fermentation, measured by dry weight was found not to be dependent on agitation speed (Belmar-Beiny and Thomas, 1991). The superimposed effects of biomass

concentration, apparent viscosity, agitation speed and possible formation of small mycelial pellets complicate the relation between mechanical agitation and growth and between the agitation and product yield. In these experiments the minimum dissolved oxygen for experiments at 750 rpm was 45% and for other experiments dissolved oxygen was always kept above 60% by adding oxygen to air inlet. It has been reported, that the critical dissolved oxygen for the growth of *Penicillium chrysogenum* is 35% (Vardar and Lilly, 1982). There is no report for critical dissolved oxygen for *S. erythraea* cultures. In general, streptomycete fermentations are reported to be more tolerant to low dissolved oxygen level than *Penicillium chrysogenum* fermentations, but prolonged low levels will ultimately be harmful (Bader, 1986). Therefore, it seems the level of dissolved oxygen tension was above its critical level for growth and the effects in different cultures was most likely as a result of shear environment.

Agitation speed had minor effect on growth for complex medium experiments. Maximum biomass concentration tended to be lower at higher speeds (Figure 3.16). The maximum biomass concentration was 11.1 ± 0.5 gL^{-1} at higher speeds (1000 and 1250 rpm) compared with 12.7 ± 0.2 gL^{-1} at lower stirrer speed (350 rpm). The experimental data was not enough to find an exact growth rate in different period of the fermentation, however available data suggested slightly lower maximum growth rate at 1250 rpm compared with other experiments (Figure 3.16). Maximum carbon dioxide evolution rate also was lower at 1000 and 1250 rpm comparing with other speeds (Figures 3.11, 3.12, 3.13, 3.14 & 3.15). This may also be as an indication for the lower maximum growth rate at higher speeds.

Effect of agitation for defined medium experiments

The growth rate appeared to be faster in the early stage of the growth at higher stirrer speed (750 rpm) compared to fermentation at 500 rpm (see section 3.1.2). The higher growth rate in early stage of the growth at higher speed could be a result of a lower critical dissolved oxygen for higher stirrer speed as was reported by Wang and Fewkes (1977). Both experiments were at low dissolved oxygen tension (10% of air saturation) such that the oxygen transfer from liquid to cell is considered important. This means that, at constant dissolved oxygen tension and higher stirrer speed resulted

in a high liquid to cell mass transfer rate and better oxygen availability for the mycelia. The cell production for the same amount of nitrogen consumption was lower at higher speed, which could be due to the release of intracellular material (Tanaka *et al.*, 1975). Once the nitrogen was exhausted from the medium at 750 rpm, there was insufficient energy for maintenance, which increases the susceptibility of the cell to mechanical damage and led to lower biomass at the end of the growth phase comparing with 500 rpm. Biomass at the end of the growth phase was reduced from 4.6 gL^{-1} for 500 rpm to 3 gL^{-1} for 750 rpm. Choi *et al.* (1996) also reported oil consumption increased with increasing stirrer speed in *S. fradiae* fermentation, whereas the viscosity was lower at higher stirrer speed. Decreasing the viscosity could be the results of fragmentation of mycelia or reduction of biomass.

Comparing defined medium experiments with complex medium experiments

Defined medium used in these experiments was very low in nitrogen (the ratio of nitrogen to carbon was 2.8/100). Nitrogen was consumed completely at the end of the growth phase, and there was no other nitrogen source to be metabolised by the cell to compensate the damage by the shear environment at higher speed (750 rpm) which led to disintegration of the mycelia (Figure 3.6). On the other hand, limitation in compounds (possibly phosphate) in complex medium decreased the growth rate, however the construction of the biopolymer of cell wall seems to be continued in the deceleration phase and resulted in an increase of the resistance of the mycelia against shear environments. The experiments with the homogeniser also indicated that cell wall mechanical properties of the mycelia improved significantly during the deceleration phase (see section 3.5 and 5.5).

5.2 Effect of agitation on erythromycin production

Association of erythromycin production with growth

Using complex medium, erythromycin synthesis started from the early stage of the growth with a very slow rate till 20-25 h (Figure 3.16 b). Less than 10% of the total erythromycin was produced till 20-25 h. There was a sudden decrease in CER at 20-25 h (Figures 3.11, 3.12, 3.13, 3.14 & 3.15), which coincided with deceleration of the growth and increasing erythromycin production rate (Figure 3.16). This suggested, erythromycin production was associated with depression of the growth as was reported by Bushell et al.(1997). On the other hand, in experiments with defined medium 40-60% of the total erythromycin was produced before the sudden decrease in CER (end of the rapid growth phase) (Figures 3.1, 3.2 & 3.4), which was considerably higher than the percentage of erythromycin production in complex medium before the end of the rapid growth phase (10%). The comparatively early production of erythromycin observed in defined medium experiments was consistent with previous finding (Bushell et al., 1997b) that nitrogen limited batch culture produce this antibiotic according to apparently growth-associated dynamic due to low substrate affinity for nitrate. This was also in agreement with the results obtained for cephalosporin production of S. clavuligerus (Aharonowitz & Demain, 1979).

Effect of shear on production of erythromycin

Results for erythromycin production at different speeds, showed agitation had little effect on specific erythromycin production. Specific erythromycin production was 10% lower at high stirrer speed (1250 rpm), when using complex medium (Table 3.6). Martin et al. (1996) have also shown that while the major axis in S. erythraea fermentation was decreased from 124 μm at 750 rpm to 70 μm at 1500 rpm, antibiotic productivity decreased slightly (5%), which is in agreement with this study.

While, a high shear enviroment is usually undesirable for filamentous fungi secondary metabolite production (Smith et al., 1990; Makangiansar et al., 1993), there are reports indicating no link between secondary metabolite production and shear in the

case of filamentous actinomycetes (Belmar-Beiny and Thomas, 1991; Yang *et al.* 1996). It is possible that decreasing the percentage of very high entangled clumps at high speed (Figure 3.25) is beneficial for erythromycin production (Bushell, 1988) and smaller size of the mycelia at higher speed (Figure 3.22) is detrimental for erythromycin production (Martin *et al.*, 1996), resulting in no or little change in final erythromycin concentration. Changes in growth rate, changes in percentage of viable cells are other consequences of shear which can affect the secondary metabolite production. All of these variables make it difficult to find a relation between mycelia size and secondary metabolite production. To overcome this problem and find the relation between mycelia size and secondary metabolite production, Martin *et al.* (1996) filtered the *Saccharopolyspora erythraea* biomass culture and found that erythromycin yield of retentate (mean average axis 103 μm) was significantly higher than that of the filtrate (mean average axis 88 μm). They hypothesised that there is a critical hyphal particle length (88 μm in their case), below which the particle is incapable of producing antibiotic. However, industrial *S.erythraea* strain with main length of 15-25 μm were capable of producing high levels of erythromycin (Warren *et al.*, 1994). Therefore, if there is any critical length for erythromycin production, it is strain dependent. Changes in chemical composition of cell wall, permeability of the cell membrane are other parameters which might be different between filtrate and retentate and these could also affect the productivity of the organisms. Pickup *et al.* (1993) reported high antibiotic production in Streptomyces fragmentation resistant variant comparing with wild type. It can be concluded that important factors other than morphology may also be the consequence of the shear environment which could affect the productivity of the organism.

5.3 Effect of shear on morphology

The time course of fermentation has been divided for this study into 4 parts, Early stage of the growth, rapid growth phase, deceleration phase, biomass decline phase. Morphological behaviour of the culture is discussed for each part. Early stage of the growth started at the beginning of the fermentation and ended between 7-10 h of fermentation. Rapid growth phase started at 7-10 h and ended at 20-25 h. Deceleration phase started from the end of rapid growth phase 20-25 h and terminated at about 40 h. The growth rate was very slow during deceleration phase and became slower toward the end. Biomass reached its maximum value at 40 h, after which time it gradually declined. This period of fermentation (40 to 120 h) was named as biomass decline phase.

Poor reproducibility at early stage of the growth and rapid growth phases

Few data for morphological parameters are available in the early stage of the growth, therefore it is not possible to draw firm conclusions of morphological behaviour during this period. The general trend will be discussed for the combined phases of early and rapid growth phase, i.e. 0 to 20-25 h. The reproducibility of data was poor in the early stage of the growth and rapid growth. The poor reproducibility between the two fermentations at the same condition could be due to the differences in morphology of the inoculum. Great precaution was taken to inoculate the fermentation medium with seed cultures having reached the same stage of growth. However, the reproducibility of the morphological parameters between different inocula were still not good (Table 3.5). High heterogeneity of the samples in this period (Figure 3.30), also could be partly responsible for large errors in the measurements of the data. Belmar-Beiny and Thomas (1991) also reported that reliable morphological measurements during the early stage of the growth was impossible due to revealed long, highly branched *S. clavuligerus* with a high degree of entanglement.

In general, mean major axis for both freely dispersed mycelia and clumps and the mean main length of the freely dispersed mycelia increased during the combined

phases of early and rapid growth phase (Figures 3.20 and 3.26), i.e. breakage rate was lower than growth rate. At high stirrer speed (1000 and 1250 rpm), the percentage of the clump area decreased during this period (Figure 3.25).

Deceleration phase had the highest breakage rate.

During the deceleration phase, the growth was very slow and the breakage rate was greater than the growth rate which led to a decreasing in the size (e.g. major axis for the clumps in Figure 3.21 or main length for the freely dispersed mycelia in Figure 3.26). The rate of breakage was the highest during this period of the fermentation.

Biomass decline phase led to equilibrium size

Breakage should predominate in biomass decline phase (Makangiansar *et al.*, 1993), and the experimental data substantiate this (e.g. Figures 3.20 & 3.21). However, the rate of the breakage was less in decline phase in comparison with the deceleration phase. A decrease in size of the mycelia (e.g. major axis) could be the reason for decreasing the disruptive forces (see section 1.4.6). The description of factors involved in fragmentation is not only limited to disruptive forces, but counterbalanced by stabilising forces generated by the hyphal cell wall. Experimental data obtained by disruption of cells in a homogeniser revealed that cell wall became stronger toward the end of the deceleration phase (see section 3.5). Experimental observations of cell wall thickness as a function of the distance from the growing tip were described by Trinci and Collinge (1975) for *Neurospora crassa* and *Geotrichum candidum*. This experimental work illustrates that the cell wall thickness increases up to 5 times moving away from the growing tips. The observation reported by Trinci and Collinge (1975) were based on surface growing fungi, but similar effect is reasonable to assume for filamentous actinomycetes in submerged culture. It has been reported that cell wall synthesis in actinomycetes filamentous organisms was not restricted to the hyphal tips (Gray *et al.*, 1990; Miguelez *et al.*, 1993). Therefore it is very likely that cell wall strength is increasing with time in the older part (central zone) by adding new polymer. Newer parts (outer zone) are weaker compared with older parts (central zone) and it is more likely that breakage is happening for the weaker parts; the remainder parts are stronger and more resistant to breakage.

Regrowth in the late biomass decline phase

The change of the standard deviation of the major axis of the mycelia shown in Figure 3.30 provides some additional interesting information on hyphal breakage during fermentation. Based on these plots it appears that following the rapid growth phase, the large hyphae started to break up gradually as a result of the imposed shear forces. Growth was negligible compared with breakage in this period, and thus the net effect was a narrowing of the mycelia size distribution (e.g. major axis) which caused a decrease in the standard deviation of the size distribution. If it is postulated that the mycelia are likely to have a distribution of mechanical strength then it is likely that those that survive the imposed shear forces are physically strong and at the end of the breakage period may begin to grow again (i.e. small mycelia were lysed and a percentage of the rest grew resulting in a widening of size distribution). Therefore, it may be postulated that cell lysis during this period was accompanied by some cell regrowth. Belmar-Beiny and Thomas (1991) have previously suggested regrowth for *Streptomyces clavuligerus* liquid culture in 7-L fermenter at 990 and 1300 rpm (see section 1.3). Even though, the rheological data also showed slight increase in consistency index between 70 to 100 h (Figure 3.33) which could be another indication for regrowth, still physiological evidence is needed to accept it. The interaction between the mycelia in the culture is a complicated process and other factors such as flexibility of the hyphae (Metz *et al.*, 1979) and charges on or close to the surface of the organisms (Warren *et al.*, 1995a) can also affect the rheology of the culture.

Similarity of branching frequency in actinomycetes filamentous organisms

It has been reported, that branching frequency of the filamentous fungi increases at higher shear rate (Van Suijdam and Metz, 1981; Mitard and Riba, 1988; Smith *et al.*, 1990; Makangiansar *et al.*, 1993). In this study the number of tips (as an indication of branching frequency), generally tended to decrease progressively with increasing stirrer speed and over the course of the fermentation after the end of the rapid growth phase untill 70 h. This was not in agreement with the results for filamentous fungi. Experimental results of Belmar-Beiny and Thomas (1991) also showed lower number

of tips at higher stirrer speed for *Streptomyces clavuligerus* batch culture, which is in agreement with this study. This suggested that as far as branching frequency is concerned, the response of the filmentous fungi and filamentous actinomycetes seems to be different in the shear environment.

The mean number of tips at the end of the fermentation (70 - 120 h) was about 2.5- 3 depending on stirrer speed (Figure 3.28). Experimental data for *Streptomyces clavuligerus* also showed that the average number of tips decreased toward 2.5 by the end of the fermentation (Belmar-Beiny and Thomas, 1991). This is another indication for similarity of the morphological development of *Saccharopolyspora erythraea* with *Streptomyces clavuligerus*.

Breakage mechanism

Breakage is more probable for clumps due to their bigger size in comparison with mycelia (see section 1.4.6). The percentage of clump area decreased at high stirrer speeds (1000 and 1250 rpm).

As discussed earlier, the cell wall thickness increases with distance away from the growing tips. Therefore, it is more likely that mycelia is broken in the weaker outer zones. These results also showed that roughness tended to decrease during the breakage period (Figure 3.24). Decreasing the roughness could be an indication of breakage of the outer parts of clumps. It means that breakage of the longest filaments, extensions of the annular zones and smoothing the perimeter of the clumps leads to lower roughness. Durant *et al.* (1994) also reported that the outer part of the *penicillium chrysogenum* clumps are looser compared with more compact zone parts.

The ratio of minor axis to major axis (OB / OL) shown in Figure 3.22 provides some additional interesting information on breakage of the mycelia during the fermentation. Based on this plot it appears that the value of (OB / OL) for mycelial clumps decreased progressively with increasing stirrer speed and over the course of the fermentaion till 60-70 h. If we assume that the major axis is related to main length of the mycelia and the minor axis is related to branch length of the mycelia, a decrease in

the ratio of minor axis to major axis suggests that mycelia (mycelial clumps in this case) are preferentially broken through their weaker parts (branches). Gray *et al.* (1990) has previously shown that cell wall of *Streptomyces coelicolor* becomes thicker preferentially at main hyphal length and this happens to a lesser extend at branches.

Formation of temporary clumps in liquid cultures

It has been reported that in the case of *Streptomyces clavuligerus* percentage of the clump decreased with an increase in the dilution rate, and it was concluded that in the case of streptomyces clumps might be loose enough to disaggregate by dilution (Durant *et al.*, 1994). In this study a high dilution rate was selected (2000 times for 10 gL^{-1} biomass) and it was found that dilution rate above this did not have any effect on percentage of clump area. Great precaution was taken to use the same dilution for the same level of biomass. Therefore, the clumps measured in these experiments were the clumps which were not disaggregated at high dilution rate. However, it is possible that in the case of actinomycetes filamentous organisms, the percentage of the clumps existed in the fermenter culture are higher than the percentage of the clumps measured after dilution with water. The percentage of temporary aggregates or clumps in the cultures is dependent on physico- chemical properties of the filamentous organisms such as charges on outer layer of mycelia or flexibility of the mycelia. Very little known about these parameters rendering it difficult in understanding the relation between morphology and other parameter like rheology in liquid cultures (see section 5.4).

Summary

These experiments revealed that in complex medium (nutritionally rich medium), the rate of the breakage was much higher in the deceleration phase (20-25 to 40 h) compared to biomass decline phase (40 -120 h). It was also shown that cell wall strength improved in during the deceleration phase (see section 3.5). Improvement of the cell wall strength led to an increase in the constructive forces of the mycelia. In addition, decreasing the size of the mycelia during the deceleration phase led to a decrease in the disruptive forces (see section 1.4.5). The consequence of both of these effects was a decrease on the rate of the breakage after the deceleration phase.

Whereas in nitrogen limited defined medium (poor medium), breakage of the mycelia continued after the end of the deceleration phase until the end of the fermentation and finally led to disintegration, as observed under the microscope (section 3.1.2). This revealed the importance of the medium component for improvement of mechanical properties of the mycelium to resist the shear environment.

5.4. Rheology of the cultures

Many types of rheometer have been used to study the rheology of fermentation broths (See table 1.3). For this study a concentric cylinder was chosen against an impeller viscometer due to the difficulty in obtaining laminar flow conditions. Warren *et al.* (1995b) studied the rheology of three Actinomycetes: *A. roseorufa, S. rimosus and S. erythraea* and used both turbine impeller and concentric impeller viscometers and found good agreement between rheological measurements of two systems. Also, Allen and Robinson (1990) found good agreement between the rheological measurements of *S. levoris* broths from pipeline, helical and rotating cylinder rheometers and suggested that slip effects were not significant problems in these viscometers. In selecting a viscometer for a particular application involving a broth of filamentous microorganisms, a rotating cylinder or pipeline viscometer which cover the range of shear rates expected in the process of interest has been recommended, except for some solid substrates such as bran and cellulose (Allen and Robinson 1990). Against this background, a concentric cylinder viscometer was used in our experiments. Disintegration of the mycelium did not occur during the measurements since the annular gap between the cylinders (800 µm) was greater than the size of the largest mycelia aggregates (200 µm).

The fermentation broth became rapidly non-Newtonian and demonstrated pseudoplastic behaviour. It was possible, therefore, to describe the rheology in terms of the consistency index, K, and the flow behaviour index, n. In all fermentations, as soon as substantial growth occurred, n fell to 0.35 - 0.45 (Figure 3.33), which was higher than the value (0.25 - 0.3) reported for industrial strain of *S. erythraea* (Warren *et al.*, 1995a). One of the reasons for the differences could be due to lower biomass concentration in these experiments. The maximum biomass concentration was 12 gL⁻¹, whereas it was 17 gL⁻¹ in Warren *et al.* (1995b) experiments. Differences in morphology (Metz *et al.*, 1981; Olsvik *et al.*, 1993), flexibility of the hyphae (Forgacs *et al.*, 1957; Metz *et al.*, 1979; Olsvik and Kristiansen, 1994), and variation of the charges on or close to the surface of microorganisms (Warren *et al.*, 1995a) could be other reasons for these differences in viscosity.

The relation between consistency index, K, and biomass concentration, DCW, was found in the absence of any morphological changes as $K \propto (DCW)^{2.10}$. Compared with the fungal cultures, the consistency index of *S. erythraea* is less sensitive to changes in biomass concentration (see Table 1.3).

The rheology and morphology of *S. erythraea* grown in submerged batch culture was described, allowing the possible interactions between these parameters to be examined. There was a trend of higher consistency index of the broths for bigger size (e.g. major axis) of the mycelia (Figure 3.37). The relation between rheology and different morphological parameters was also examined and it was found that even though there is a trend for the variation of rheology of the culture with the morphology of the cells (e.g. major axis of the mycelia), the correlation coefficient (R^2 = 0.57) was not good for the recommended expression ($K \propto DCW^{2.1}OL^{1.8}$). These results suggested that the relation between rheology of the culture and morphology of the cells is complicated due to variation on other parameters such as flexibility of the mycelia. Changes in the flexibility of the hyphae may be due to changes in cell wall composition, changing in the branching pattern and diameter of the hyphae, or variations in osmotic pressure (Metz *et al.*, 1979). It has been shown (Olsvik and Kristiansen, 1994) that variation in fermentation conditions like dissolved oxygen tension or growth rate can affect the flexibility of the mycelia and the consequence of this are changes in rheology of the culture. In this study, the dissolved oxygen did not change considerably and it was always above critical level (it was above 60%). However, the experiments were batch fermentation and different stirrer speeds were also used, which might lead to different flexibility of the mycelia due to changes of the cell wall composition or variation in osmotic pressure during the course of the fermentation. In addition, alteration of charges on or close to the surface of the microorganisms is another variable which affects the rheology (Warren *et al.*, 1995a). They have reported for *S. rimosus* fermentation, that variation in pH changed the rheology due to variation of the charge on or close to the surface of the microorganism. In this experiment the pH was constant throughout the course of the fermentation, however it was a batch operation, which might lead to variation of the charges on or close to the surface of the microorganism during the course of the

fermentation. This could affect their entanglement and the formation of temporary clumps in the liquid culture as a result of high cell concentration, which was not observed in microscope slides prepared after dilution. Polymeric componds (e.g. DNA ; protein) in the medium also could affect the interaction between the hyphae (Hobbs *et al.*, 1989).

Even though, there was a general trend for a relation between rheology and morphology of the mycelia (e.g. major axis). The interaction seems to be complicated, because of other variables such as the flexibility of the mycelia. Recent development on the direct measurement of fractal properties of the mycelia may provide a useful basis for further elucidation of these complex interactions. As far as flexibility of the filamentous organisms is concerned much remains for further development of the method for measurements of rheomechanical properties (such as modulus of elasticity) of the filamentous organisms.

5.5 Homogenisation of fermentation broth for assessing cell wall strength

The description of factors involved in fragmentation is not only limited to disruptive forces, but counterbalanced by stabilising forces generated by the hyphal cell wall. Cell wall thickness, elasticity of the cell wall and cell wall strength were the parameters contributing to the equilibrium size of the mycelia as a result of shear in a mechanically stirred tank (see section 4.1). In spite of the importance of these parameters, there is very little known about them on information available in the literature. The construction, regulation and synthesis of the hyphal cell wall is not fully understood, but several aspects in this complicated process for filamentous fungi were described by (Trinci and Collinge, 1975; Miles and Trinci, 1983; Wessels, 1993) and for Streptomyces by (Miguelez et al., 1993), which were reviewed in section 1.1.1. It can be concluded from these reports that the hyphal cell wall becomes more and more thick and rigid as a function of the distance from growing tips.

Recent advances in the use of micromanipulation techniques have allowed measurements of the cell wall strength with a reasonable degree of accuracy for baker's yeast cells (Zhang et al., 1993; Robert et al., 1994). However, this technique has not yet been successful for measuring cell wall strength of the filamentous actinomycete. Another way of measuring mechanical properties is indirect measurements. Khan (1996) used homogeniser to assess mechanical properties of S. erythraea. Khan (1996) measured protein release at 100 bar and different passes and used value of K_p at 100 bar from Hetherington equation for assessment of cell wall strength. Disruption of S. erythraea in homogeniser showed that final level of protein release was dependent on pressure (Figure 3.41). In this study the mechanical properties of cell were not only evaluated by the value of K_p from Hetherington equation but also by comparing final protein release at different pressures. In addition, the morphology of the disrupted cell was also measured in this study. Obviously both of these studies are just the first steps for evaluating mechanical properties of the filamentous actinomycetes and much remains for further study.

A number of researchers have suggested that the fluid mechanical stresses caused by the turbulent fluid field in the core of the homogeniser valve are primarily responsible for the rupturing of microbial cell walls (Doulah and Hammund, 1975; Ayazi Shamlou *et al.*, 1995). The size of the smallest eddies in the Lab-40 homogeniser are less than 0.5 μm (see appendix 5) which is much smaller than the size of the mycelia (20 - 100 μm). Therefore the condition of (L >> λ) is fully satisfied and it is more likely that disruption was happening in the inertial subrange and breakage is thought to occur by shear stress due to fluctuating velocity differences acting on the opposite sides of the cells (see section 1.4.5). The stress acting on the cells has been related to energy dissipation (ε) and size of the mycelia (e.g. major axis = OL) according to equation 5.1 (Thomas, 1963).

$$\tau_i = 2\rho \, (\varepsilon.OL)^{2/3} \qquad\qquad (5.1)$$

Measurements of soluble protein showed that disruption was first order with respect to passes as for *Saccharomyces cerevisiae* (Hetherington *et al.*, 1971). It is noted that protein release was very rapid in our experiments compared with *Saccharomyces cerevisiae*. Even at moderate pressure (100 bar), 80% of the disruption was achieved within one pass. This compares with 20% disruption under similar conditions for *Saccharomyces cerevisiae*. This higher rate of release at a moderate disruptive pressure (100 or 200 bar) could be partly because of longer size of the cells or lower strength of the cell wall in the case of *S. erythraea* compared to *Saccharomyces cerevisiae*. The longer size of the cells of *S.erythraea* compared to *Saccharomyces cerevisiae* increases its susceptibility to disruptive forces (see equation 5.1), possibly lower the strength of the cell wall causing a decrease in the constructive forces. Both of these effects may have resulted in an increase in the disruption rate for *S. erythraea* cells compared to *Saccharomyces cerevisiae*.

The lower the value of K_p from Hetherington equation, means the lower the rate of the release which could be an indication for stronger cell wall. The value of K_p from Hetherington equation decreased toward the end of the fermentation (Figure 3.44),

which could be due to stronger cell wall or a decrease in the size of the cells toward the end of the fermentation. A decrease in the size of the mycelia (e.g major axis) decreases the disruptive forces (see equation 5.1), and an increase in the cell wall strength increases the constructive forces. One or both of these effects could be responsible for the decrease in the value of K_p toward the end of the fermentation. The size of the mycelia (e.g. major axis for both mycelia and clumps) was almost the same for S1 and S2 (Figure 3.50), therefore the differences in value of K_p for samples S1 and S2 should be due to differences in cell wall strength. However, the major axis of the mycelia for S3 is smaller than S2, therefore, the lower the value of K_p for S3 could be due to shorter mycelia size or stronger cell wall of S3 compared to S2, and it is difficult to differentiate between these two effects.

The value of $R_{m,100}/R_{m,1200}$ decreased toward the end of the fermentation (Figure 3.46), this suggested the percentage of mycelia able to resist in shear environment at 100 bar is increasing toward the end of the fermentation. Table 5.1 also shows the minimum pressure needed to obtain >90% of total protein release. A higher pressure is needed to obtain >90% of total protein release for samples taken later in the fermentation. If it is assumed that differences are due to differences in mechanical properties of the cell wall then it is indicated that cell wall was stronger for later samples and therefore higher disruptive forces were needed for breakage of the cell wall to release the protein.

Table 5.1: Disruptive pressure needed to obtain >90%
releasable protein

Sample	Disruptive pressure (bar) needed to obtain more than 90% releasable protein
S1	200
S2	400
S3	600
S4	600

Protein release in this experiment was related to the cell wall mechanical properties while other factors particularly membrane properties may be also involved in this process. However, microscopical observation also showed that major axis of the disrupted cells at 100 bar and one pass was 15 - 16 μm for S1, whereas it was between 22 - 24 μm for S2, even though the major axis of S1 and S2 were almost the same prior to disruption (Figure 3.50). This indicates stronger cell wall of S2 comparing with S1.

It was shown that value of R_m is pressure dependent and increases with pressure. Keshavarz et al. (1990) have reported higher value of R_m at higher disruptive pressure for *Rhizopus nigricans*. They have suggested the apparent variation of R_m with pressure, correlated with micronization of cell debris at higher pressure. In their experiment, a 10 fold increase in pressure led to 25% increase in R_m. However, in this experiment increasing the pressure from 100 bar to 1200 bar increased the R_m value up to 400% in some cases (Table 3.11). While microscopical observation (Figure 3.49) showed the micronisation, it is very unlikely that an increase up to 400% in R_m was only due to micronisation.

Cell wall of the mycelia form gradually by biopolymerisation which starts at the hyphal tip and continues at some distance behind the moving tip (Miguelez et al., 1993; Wessel, 1993). A consequence of the gradual biosynthesis of the cell wall matrix is that the thickness of hyphal wall depends on the extent of the reaction, being thinnest (weakest) near the tip, and becoming thicker (stronger) with distance away from the tip (Trinci and Collinge, 1975, for fungi; Miguelez et al., 1993, for actinomycetes). Increasing the resistance of the mycelia against disruptive forces during the fermentation may have three implications: 1) Construction of the cell wall continues even in biomass decline phase; 2) Mycelia are likely to have a distribution of mechanical strength and the weaker mycelia lysed and the stronger mycelia remained during the fermentation; 3) The weaker part of the mycelia has been broken in shear environment in the fermenter and the remainder part is stronger. Eventhough, there is evidence that cell-wall synthesis is dissociated from total growth (Salton, 1964) in bacteria fermentation (Salton, 1964), more evidence is needed to accept the

197

first point in this case. Nevertheless, while these experiments show that cells become considerably stronger during the deceleration phase (till 40 h), more evidence is needed for comparison of the strength of the cells after the end of the growth phase (after 40 h). Protein release in this experiment was related to cell wall mechanical properties while other factors particularly membrane properties may also be involved in this process.

Summary

1   Protein release was pressure dependent and its dependency to number of passes was less compared with *Saccharomyces cerevisiae*. The rate of release, shown with the value of K_p, was lower for later samples. This may be due to enhanced mechanical properties of the later samples or related to the size of the original cells.

2   A higher pressure is needed to release the protein for later samples. It was assumed that protein release is related on mechanical properties of the cell wall. Therefore, it is believed that mechanical properties of the cells improved toward the end of the fermentation (until 70 h).

3   Morpholological observation and measurement of the disrupted cells in homogeniser showed that cell wall mechanical properties improved in a large extent during the deceleration phase (S2 compared with S1).

5.6 Effect of dissolved oxygen concentration on growth and erythromycin production

Using agitator speed and air flow rate as variable parameters for controlling DOT at a constant level could lead to a wide variety of undesirable consequences especially shear damage and effect of carbon dioxide. Therefore, dissolved oxygen concentration was controlled by the addition of nitrogen to the inlet air of the fermenter and keeping the total gas flow rate constant to ensure that gas distribution and mixing conditions are identical in each case.

The general effects of various dissolved oxygen tensions in the broth on different organisms have been summarised in section (1.3.1). The critical dissolved oxygen concentration, below which the metabolite reaction rate is oxygen concentration controlled, is a variable that is determined by biological as well as by mixing parameters (Wang and Fewkes, 1977; Heydarian et al., 1996). There is no report for critical dissolved oxygen for the S. erythraea fermentation. It was shown that when the defined medium culture is run with a constant dissolved oxygen tension of 10% growth is inhibited in comparison with the other culture (DOT > 65%) (see section 3.1.1). In terms of secondary metabolite production, the optimal values for DOT do not appear to be the same for growth and metabolic production . It was shown that the specific erythromycin production was not affected, when the DOT was decreased to 10% in comparison with the other culture (DOT > 65%). Nikoli et al. (1993) reported an increased percentage of erythromycin D as a result of low DOT, but they did not report effect of dissolved oxygen concentration on total antibiotic production. Clark et al., (1995) have reported, erythromycin was produced in both oxygen-limited and oxygen-sufficient cultures of S. erythraea. In their work dry cell weight decreased from 12 to 3 gL^{-1} in oxygen limited culture, whereas specific erythromycin production was 4.2 times greater in oxygen sufficient culture. It was concluded that oxygen limitation can induce erythromycin production like a limitation in other components (e.g. carbon, nitrogen or phosphate). They used defined medium without any limitation, in this study nitrogen limited medium was used. Therefore, in this research, induction of erythromycin was not performed by oxygen limitation. However,

erythromycin synthesis was not inhibited by oxygen limitation. In experiments with complex medium, comparison of shake flask experiments (section 3.3.1) and stirred tank experiments (section 3.3.2) showed, while DOT had a significant effect on growth of *S. erythraea*, the effect on specific erythromycin production was minor. Specific erythromycin production was 53 ± 7.0 mg (g cell)$^{-1}$ in shake flask, whereas it was 55 - 60 mg (g cell)$^{-1}$ in experiments in the stirred tank bioreactor (section 3.3.2). It should be noted that in shake flask experiments pH was kept between 6.5 to 7.5 by adding buffer to the medium, whereas the pH was controlled at 6.9 ± 0.1 throughout the experiments in stirred tank.

6.0 CONCLUSION AND RECOMMENDATION FOR FUTURE WORK

6.1 Conclusion

1.   In defined medium, the specific erythromycin production (mg (g cell)$^{-1}$) is not affected by DOT levels above 10% air saturation. Consequently, the production of erythromycin does not appear to be significantly related to the oxygen level, provided that this is above 10% air saturation in this medium. However, the growth is affected by this level of dissolved oxygen; maximum dry cell wight decreased by 20% at low dissolved oxygen tension (10% of air saturation) and therefore the volumetric erythromycin (mgL^{-1}) is also decreased.

2.   The mean main length, mean total hyphal length and major axis increased during the rapid growth phase of fermentation and then decreased to a relatively constant value (equilibrium size). An increase in the agitation speeds at 7-L and 450-L scale fermentation leads to a decrease in equilibrium size of major axis. The percentage of the clumps is lower at higher speeds.

3.   The effect of agitation rate on *S. erythraea* fermentation is generally less compared with filamentous fungi shown by the relationship between equilibrium major axis and power dissipation rate per unit volume. The experimental data in the literature shows the relation of (OL α $\varepsilon^{-0.25\pm0.8}$), whereas this study and previous reports for *S. clavuligerus* shows (OL α $\varepsilon^{-0.11\pm0.1}$) in the case of filamentous bacteria fermentation.

4.   A turbulent breakage model of filamentous bacteria has been derived. This leads to $OL = \left(S_F E\right)\left[\dfrac{\rho\mu\varepsilon}{\sqrt{t_c}}\right]^{-0.15}$. The model has been tested with experimental data obtained at 450-L and 7-L scale. Experimental data gave a value of -0.12 for the exponent of the group in [ ]. The discrepancy between the experimental value and theoretical value of -0.15 is perceived to be caused by the complex mechanical

properties of the cell wall. Further research is needed on these aspects of cell wall properties before improved models of cell breakage can be developed.

5.   Cell disruption experiments in Lab-40 homogeniser showed that mechanical properties of the cell wall of *S. erythraea* improved in a large extent in the deceleration phase and resulted in higher resistance of the mycelia in shear environment in the fermenter. To release >90% of the total protein 200 bar disruptive pressure is needed for the sample taken from fermentation during the rapid growth phase, while 400 bar disruptive pressure is needed for the sample at the end of the deceleration phase. Morphological measurements also showed that the size (e.g. major axis) of the disrupted cells was much smaller for the sample taken in the rapid growth phase compared with samples taken after the end of the deceleration phase.

6.   Serious damage occurs in nutritionally weak defined medium. Nutritionally rich medium is more resistant to mechanical damage. It is beleived that cell wall mechanical properties are enhanced during the deceleration phase increasing the resistance of the mycelia in the shear environment. This revealed the importance of the composition of the medium for improvement of mechanical properties of the cell wall.

7.   Maximum dry cell weight appears to be less at higher stirrer speed. Maximum biomass was 11.1 ± 0.5 gL^{-1} at 1250 rpm (tip speed = 4.45 ms^{-1}), whereas it was 12.7 ± 0.2 gL^{-1} at 350 rpm (tip speed = 1.07 ms^{-1}). Specific erythromycin production is not affected by stirrer speed up to 1000 rpm at 7-L scale. The specific erythromycin production decreases by 10% at 1250 rpm. The dissolved oxygen was kept above 60% air saturation by adding oxygen to the air inlet of the fermenter, therefore, differences in culture behaviour may be considered mainly due to mechanical forces. This observation suggests that at least for this fermentation, shear caused by agitation in these experiments does not significantly affect specific erythromycin production. A consequence of this is the ability to rise the agitation rate to increase oxygen transfer and bulk mixing without significant mechanical damage or loss of productivity. This should be applicable at different scale of operation.

8.   The power law model fitted very well with the experimental data to explain the rheology of the culture. The rheology of the culture changed dramatically during the fermentation. The relation between consistency index, K, and biomass concentration, DCW, was found in the absence of any morphological changes as K α $(DCW)^{2.1}$. In general consistency index was less at higher speeds.

6.2 Recommendation for future work

1.   These experiments form the basis of initial studies regarding indirect measurements of cell wall mechanical properties. It is imperative to extend these measurements by taking into account the influence of other variables such as nutrients and cultural condition on mechanical properties of the cell wall. Measurement of the activity of a specific enzyme released by homogenisation would also be important for finding the extent of the contribution of micronisation in the results.

Direct measurement of cell wall mechanical properties is more favourable. This method has not yet been successful for measuring the mechanical properties of the cell wall of filamentous bacteria. Development of such methods is necessary for better understanding of the influence of the shear on organism.

2.   The turbulent breakage model should be tested with other filamentous bacteria systems and the influence of the parameters in the model checked independently.

3.   The results of the experiments in this study showed that dissolved oxygen had a significant effect on growth, not affecting the specific production of erythromycin. Therefore, determination of the critical dissolved oxygen tension for the growth would be important for optimising the volumetric erythromycin production.

7.0 NOMECLATURE

a   interfacial area per unit volume for mass transfer

A   hyphal cross sectional area, m^2

aveL   average length, m, μm

BL   mean branch length, m, μm

c, C, C_1, C_2, C_3 constants

C^* oxygen concentration at gas-liquid interface, kgm^{-3}

Ca   critical capillary number

CA   clump area, m^2, μm^2

CER   carbon dioxide evolution rate, $mmolL^{-1}h^{-1}$

Com   compactness of mycelial aggregate

C_L Concentration of oxygen in the bulk liquid, kgm^{-3}

d   distance between two point, or particle size, m

d_{max} maximum stable particle size

D   impeller diameter, m, mm

DCW   dry cell weight, gL^{-1}

DEA   diethyl amine

DOT   dissolved oxygen tension (% air saturation)

d_i hyphal inner diameter, m

d_h hyphal outer diameter, m

d_p diameter of pellet or mycelial aggregate, m, μm

E   modulus of elasticity of hypha, Nm^{-2}

EA   erythromycin A

EB   erythromycin B

EC   erythromycin C

EE   erythromycin E

E_c Actual pellet volume fraction

F_b breackup forces

F_c constructive forces

FI   the impeller flow number

H   Henry constant

h	width of the homogeniser valve, m
Hi	inter-impeller distance, mm
H_L	liquid height, m, mm
HL	total hyphal length, m, μm
K	consistency index, $Ns^n m^{-2}$
K_b	breakage rate constant
$K_G a$	volumetric oxygen mass transfer rate in gas phase, s^{-1}
$K_L a$	volumetric oxygen mass transfer coefficienti liquid phase, s^{-1}
K_p	dimentionless constant in equation 3.5.1.1
K_s	impeller shear rate constant
L	$= W_i/2$, m
LLE	liquid-liquid extraction
L_i	length of impeller, mm
L_h	Length of individual hyphae, m
L_{hgu}	Length of hyphal growth unit, m
ML	mean main length, m, μm
MOPS	(3-[N-Morpholino]propane-sulfonic acid)
MP	morphological parameter
MA	mycelial area, m^2, μm^2
N	impeller rotational speed, r.p.s
N/	number of passes through the high pressure homogeniser
NT	number of tips
N_p	impeller power number
n	flow behaviour index
OA	total area, m^2, μm^2
OB	minor axis of the mycelia, m, μm
OC	circularity
OD	projected area, m^2, μm^2
OL	major axis of the mycelia, m, μm
OTR	oxygen transfer rate, $kgm^{-3}s^{-1}$
OUR	oxygen uptake rate, $mmolL^{-1}h^{-1}$
P	disruptive pressure in homogeniser, bar

p(d)	pressure fluctuation between two points d apart
P_{G1}	Oxygen partial pressure in gas phase
P_{G2}	Oxygen partial pressure in gas liquid interface
P_g	gassed power, w
P_o	ungassed power, w
P_t	total power dissipation, w
p/	total number of passes through high shear zone of impeller
Q_g	Gas flow rate, m^3s^{-1}, $Lmin^{-1}$
Q_L	flow rate through the homogeniser, m^3s^{-1}, mLs^{-1}
R'	impeller radius, D/2, m, mm
R_1	entry orifice radius in homogeniser, m, mm
R_2	effective radius of the valve rod in homogeniser, m, mm
$R_{m,p}$	maximum releasable protein at disruptive pressure ,P,
$R_{n,p}$	protein release at disruptive pressure, P, and ,n, passes in homogeniser
RO	reversed osmosis
R	Roughness of mycelial aggregate
Re	Reynolds number
Re_d	disk Reynolds number
RQ	respiratory quotient
S	total strain energy, J
S_f	critical total strain energy, J
T_d	derivative time, min
T_i	integral time, min
SPE	solid phase extraction
t	time, s
T	vessel diameter, m
t_c	circulation time, s
$u'_t(d)$	velocity difference between points in a fluid d apart
$u'_r(d)$	velocity difference across a particle of scale d
u_∞	velocity at the tip of the impeller, ms^{-1}
vvm	volume of air per volume of medium per minute
V	volume, m^{-3}

V_L	working volume, m^3
w	thickness of outer layer of the pellet or hyphal wall thickness, m, μm
W_i	impeller blade width, m, mm
W_b	width of baffle, mm
x	length scale, m
X	concentration of biomass, gL^{-1}

Greek letters

ν	kinematic viscosity, m^2s^{-1}
β	fractal dimensionally
δ_w	longitudinal stress in the wall matrix, Nm^{-2}
δ_{wx}	local longitudinal stress in the wall matrix, Nm^{-2}
δ_t	boundary layer thickness, m
ΔP	pressure drop across the valve in homogeniser, Nm^{-2}
ε	energy dissipation rate per unit mass, wkg^{-1}
ε_{ave}	average power input per unit mass, wkg^{-1}
ε_b	energy dissipation in bulk per unit mass, wkg^{-1}
ε_i	energy dissipation rate in impeller zone per unit mass, wkg^{-1}
γ	shear rate, s^{-1}
γ_a	average shear rate, s^{-1}
γ_{max}	maximum shear rate, s^{-1}
λ	Kolmogorov microscale of turbulence, μm, m
μ	viscosity of fluid, $Nm^{-2}s$
μ_a	apparent viscosity of culture, $Nm^{-2}s$
μ_p	plastic viscosity, $Nm^{-2}s$
ρ	density, kgm^{-3}
σ	tensile strength, Nm^{-2}, or interfacial tension, Nm^{-1}
σ_{crit}	limiting strength of the material, Nm^{-2}
τ	shear stress, Nm^{-2}
τ_0	yield stress, Nm^{-2}

8.0 REFERENCES

Agathos, S. N. and Demain, A. L. (1986). Dissolved-oxygen levels and the invivo stability of gramicidin S synthetase. *Appl. Microbiol. Biotechnol.*, **24**: 319-322.

Allen, D. G., Robinson, C. W. (1990). Measurement of rheological properties of filamentous fermentation broths. Chem. Eng. sci. **45**: 37-48.

Ayazi Shamlou, P., Gierczycki, A. T., Tichener-Hooker, N. J. (1996). Breakage of flocs in liquid suspensions agitated by vibrating and rotating mixers. *Chem. Eng. J.* **62**: 23-34.

Ayazi Shamlou, P., Makangiansar, H. Y., Ison, A. P., Lilly, M.D. (1994a). Turbulent breakage of filamentous microorganisms in submerged culture in mechanically stirred bioreactors. *Chem. Eng. Sci.* **43**: 1-11.

Ayazi Shamlou, P., Pollard, A. P., Ison, A. P., Lilly, M. D. (1994b). Gas holdup and liquid circulation rate in concentric-tube airlift bioreactors. *Chem. Eng. Sci.* **49**: 303-312.

Ayazi Shamlou, P., Sidiqi, S. F., Titchener-Hooker, N. J. (1995). A physical model of high-pressure disruption of beakers' yeast cells. *Chem. Eng. Sci.* **50**: 1383-1391.

Ayazi Shamlou, P., Stavrinides, N., Tichener-Hooker, N., Hoare, M. (1995). Turbulent breakage of protein precipitates in mechanically stirred bioreactors. *Bioprocess. Eng.* **502**: 1-7.

Ayazi Shamlou, P., Tichener-Hooker, N. (1993). Turbulent aggregation and breakup of particles in liquids stirred vessels. In Processing of solid-liquid suspensions. First edition. Butterworth Heinemann (pub), 1-26.

Bader, F. G. (1986). Physiology and fermentation development. In: The bacteria: A treatise on structure and function. IX, Antibiotic producing Streptomycetes. Gueener, S. W. and day, L. E. Academic press, New York.

Banes and Holbrook. (1993). High concentration suspensions: preparation and properties. In: In Processing of solid-liquid suspensions. First edition. Butterworth Heinemann (pub), 222-245.

Baverloo, W. A., Tramper, J. (1994). Intensity of microcarrier collisions in turbulent flow. *Bioprocess Eng.* **11**: 177-184.

Belmar-Beiny, M. T., Thomas, C. R. (1991). Morphology and clavulanic acid production of *streptomyces clavuligerus*: effect of stirrer speed in batch fermentations. *Biotechnol. Bioeng.* **37**: 456-462.

Davis, B. D. (1980). Bacterial structure and classification. In: Microbiology. Edited by Davis, B. D., Dulbecco, R. D., Eisen, H. N., Ginsberg, H. S. Harper international edition (pub).

Bhavaraju, S. M., Blanch, H. W. (1976). A model for pellet breakup in fungal fermentation. *J. Ferment. Technol.* **54**: 466-468.

Blakebrough, N., McManamey, W. J., Tart, K. R. (1978). Rheological measurements on *Aspergillus niger* fermentation systems. *J. Appl. Chem. Biotechnol.* **78**: 453-466.

Boye, A. M., Ayazi shamlou, P. (1996). The effect of two-liquid phase rheology on drop breakage in mechanically stirred vessels. *Chem. Eng. Comm.,* **143**:149-167.

Brana, A. F., Manzanal, M., Hardisson, C. (1982). Mode of cell wall growth of *Streptomyces antibioticus. FEMS Microbiol. Lett.,* **13**: 231-235.

Brinberg, S. L. (1959). A study on the effect of the factors stimulating erythromycin production. *Antibiotics (Antibiotiki).* **4:** 13-18.

Bronnenmeir, R., Mark, M. (1982). Hydrodynamic stress capacity of microorganisms. *Biotechnol. Bioeng.* **24:** 553-555.

Buse, R., Qazi, G. N., Onken, U. (1992). Influence of constant and oscillating dissolved oxygen concentrations on keto acid production by *Gluconobacter oxydans* subsps. *melanogenum. J. Biotechnol.* **26:** 231-244.

Bushell, M. E., Dustan, G. L., Wilson, G. C. (1997a). Effect of small scale culture vessel type on hyphal fragment size and erythromycin production in *Saccharopolyspora erythraea. Biotechnol. Lett.* **19:** 849-852.

Bushell, M. E., Growth, Product Formation and Fermentation Technology, pp. 185-217, In: Goodfellow, M., Williams, S. T. and Mondarski, M. (ed.), 'Actinomycetes in biotechnology', Academic Press, London (1988).

Bushell, M. E., Smith, J., Lynch, C. (1997b). A physiological model for control of erythromycin production in batch and cyclic fed batch culture. *Microbiol.* **143:** 475-480.

Camposano, A. Chain, E. B. and Gualandi, G. (1959). *Sel. Sci. Pap. Ist. Super Sanita.*, **2:** 24-30.

Carter, B. L. A., Bull, A. T. (1971). The effect of oxygen tension in the medium on the morphology and growth kinetics of *Aspergillus nidulans. J. Gen. Microbiol.*, **65:** 265-270.

Charles, M. (1978). Technical aspects of rheological properties of microbial cultures. *Adv. Biochem. Eng.*, **8:** 1-62.

Chen, H. C., Wilde, F. (1991). The effect of dissolved oxygen and aeration rate on antibiotic production of *Streptomyces fradiae. Biotechnol. Bioeng.* **73:** 591-595.

Cherry, R. S., Papoutsakis, E. T. (1986). Hydrodynamic effects on cells in agitated culture reactors. *Bioprocess Eng.* **1:** 29-41.

Cherry, R. S., Popoutsakis, E. T. (1989). growth and death rates of bovine embryonic kidney cells in turbulent microcarrier bioreactors. *Bioprocess Eng.*, **4:** 81-89.

Cheruy, A., Durand, A. (1979). Optimization of erythromycin biosynthesis by controlling pH and temperature. *Biotechnol. and Bioeng.* **9:** 303-320.

Chisti, M. Y. (1989). Airlift Bioreactors. Elsevior Applied Science, UK.

Choi, D. B., Tamura, S., Park, Y. S., Okabe, M., Seriu, M., Takeda, S. (1996). Efficient tylosin production from *Streptomyces fradiae* using rapedeed oil. *J. Ferm. Bioeng.* **82:**183-186

Clark, G. J., Langley, D., Bushell, M. E. (1995). Oxygen limitation can induce microbial secondary metabolite formation. *Microbiol.* **141:** 663-669.

Corum, C. J., Stark, W. M., Wild, G. M. Bird, H. L. (1954). Biochemical changes in a chemically defined medium by submerged cultures of *Streptomyces erythraeus. Appl. Microbiol.* **2:** 326-336.

Costes, J., Couderc, J. P. (1988). Study by laser doppler anemometry of the turbulent flow induced by a Rushton turbine in a stirred tank: influence of the size of the units-II. Spectral analysis and scales of turbulence. *Chem. Eng. Sci.* **43:** 2765-2772.

Cui, Y. Q., van der Lans, K. C., Luyben, K. C. A. M. (1997). Effect of agitation intensities on fungal morphology of submerged fermentation. *Biotechnol. Bioeng.* **55:** 715-726.

Cutter, L. A. (1966). Flow and turbulence in a stirred tank. *A. I. Ch. E. J.* **12**: 35-45.

Deindoerfer, F. H. and Gaden, E. L. (1970). Effects of liquid physical properties on oxygen transfer in penicillin fermentation. *Appl. Microbiol.* **3**: 253-257, (1970).

Dion, W. M., Carilli, A., Sermonti, G. and Chain, E. B. (1954). The effect of mechanical agitation on the morphology of some common fungi grown on submerged culture. *Rend. Ist. Super. de Sanita.* **17**: 187-205.

Doulah, M. S., Hammond, T. H. (1975). A hydrodynamic mechanism for disintegration of *Saccharomyces cerevisiae* in an industrial homogeniser. *Biotechnol. Bioeng.* **17**: 845-858.

Durant, G., Cox, P. W, Formisyn, P., Thomas, C. R. (1994). Improved image analysis algorithm for the characterization of mycelial aggregates after staining. *Biotecnol. Tech.* **8**: 759-764.

Edwards, N., Beeton, S., Bull, A. T. and Merchuk. J. C. (1989). A novel device for the assessment of shear effects on suspended microbial cultures. *Appl. Microbiol. Biotechnol.* **30**: 190-195.

Elmayergi, H. (1975). Mechanisms of pellet formation of *Aspergillus niger* with an additive. *J. Ferment. Technol.*, **53**: 722-729.

Escalante, L. Lopez, H., Mateos, R. C., Lara, F., Sanchez, S. (1982). Transient repression of antibiotic formation in *Streptomyces erythraeus. J. Gen. Microbiol.*, **128**: 2011-2015.

Evans, E. A. (1983). Bending elastic modulus of red blood cell membrane derived from buckling instability in micropipet aspiration tests. *Biophys. J.* **43**: 27-30.

Fatile, I. A. (1985). Rheological characteristics of suspensions of *Aspergillus niger*: correlation of rheological parameters with microbial concentration and shape of the mycelial aggregate. *Biotechnol. Bioeng.* **21**: 60-64.

Fisher, L. (1993). Forces between biological surfaces. *J. Chem. Soc. Faraday Trans.* **89**: 2567-2582.

Flores, E., Sanchez, S. (1985). Nitrogen regulation of erythromycin formation in *Stereptomyces erythraeus. FEMS. Microbiol. Lell.* **26**: 191-194.

Flores, M. E., Sanchez, S. (1989). Ammonium-Assimilating enzymes and erythromycin formation in *Saccharopolyspora erythraea. J. Gen. Appl. Microbiol.*, **35**: 203-211.

Forgacs, O. L., Robertson, A. A., Mason, G. C. (1957). *Trans. Symp. Br. Pap. Board Mak. Assoc.* Cambridge. 445-470.

Ganczarczyk, L. D. (1990). Structure of activated sludge flocs. *Biotechnol. Bioeng.* **35**: 57-65.

Ghildyal, N. P., Thakur, M. S., Srikanta, S., Jaleel, A., Prapulla, S. G. (1987). Rheological studies on *Streptomyces fradiae* ScF-5 in submerged fermentation. *J. Chem. Tech. Biotechnol.* **38**: 221-234.

Glazebrook, M. A., Vining, L. C. (1992). Growth morphology of *Streptomyces akiyoshiensis* in submerged culture: influence of pH, inoculum and nutrients. *Can. J. Microbiol.*, **38**: 98-103.

Grace, H. P. (1982). Dispersion phenomena in high viscosity immisibile fluid systems and application of statistic mixer as dispersion devices in such systems. *Chem. eng. Commun.* **14**: 225-277.

Gray, D. I., Gooday, G. W., Prosser, J. I. (1990). Apical hyphal extension in *Streptomyces coelicolor. J. Gen. Microbiol.* **136:** 1077-1084.

Gray, I., Gooday, G. W., Prosser, J. I. (1990). Apical hyphal extension in *Streptomyces coelicolor. Gen. Microb. (1990).,* **136:** 1077-1084.

Grgurinovich, N., Matthews, A. (1988). Analysis of erythromycin and roxithromycin in plasma and serum by high-performance liquid chromatography using electrochemical detection. *J. Chromatogr.* **433:** 298-304.

Heath, I. B. 1995. Integration and regulation of hyphal tip growth. *Can. J. Bot.* **73:** 131-139.

Hetherington, P. J., Follows, M., Dunnill, P., Lilly, M. D. (1971) Release of protein from Baker's Yeast by disruption in an industrial homogeniser. *Trans. Instn. Chem. Engrs.* **49:** 142-148.

Heydarian, S. M., Ison, A. P., Mirjalili, N. (1998). A rapid and simplified extraction method of erythromycin from fermentation broth with bond elut C18 cartridge for analysis by HPLC. *Biotechnolol. Tech.* (Accepted).

Heydarian, S. M., Lilly, M. D., Ison, A. P. (1996). The effect of culture conditions on the production of erythromycin by *Saccharopolyspora erythraea* in batch culture., *Biotechnology Letters* . **18:** 1181-1186.

Higashide, E. (1984). The macrolides: properties, biosynthesis and fermentation. pp. 451-510. In: Vandamme, E. J. (ed.), Biotechnology of industrial antibiotics. Macel Dekker Inc. New York.

Hinze, O. (1955). Fundamentals of hydrodynamic mechanism of splitting in dispersion processes. *AIChE J.* **1:** 289-295.

Hobbs, G., Frazer, C. M., Gardner, D. C. J., Cullum, J. A. and Oliver, S. G. (1989). Dispersed growth of Streptomyces in liquid culture. *Appl. Microbiol. Biotechnol.* **31:** 272-277.

Hodgon, D. (1982). Glucose repression of carbon source uptake and metabolism in *Streptomyces coelicolor. J. Gen. Microbiol.* **128:** 2417-2430.

Holt, J. G., Krieg, N. R., Sneath, P. H. A., Staley, J. T., Williams, S. T. (1994). Bergey's Manual of Determinative Bacteriology. (9th ed), Williams: Baltimore.

Hornby, P. P. (1995). Downstream processing effects on microbial viability. PhD. thesis. UCL, University of Lodon, Lonon-UK.

Huck, T. A., Proter, N., Bushell, M. E. (1991). Positive selection of antibiotic-producing soil isolates. *J. Gen. Microbiol.* **137:** 2321-2329.

Ismail, A. F., Nagase, Y., Imon, J. (1984). Power characteristics and cavity formation in aerated agitation. *A. I. Ch. E. J.* **30:** 487-492.

Jones, C. L., Lonergan, G. T., Mainwaring, D. E. (1993). Mycelial fragment size distribution: and analysis based on fractal geometry. *Appl. microbiol. Biotechnol.* **39:** 242-249.

Jones, C. L., Lonergan, G. T., Mainwaring, D. E. (1993). Mycelial fragment size distribution: an analysis based on fractal geometry. *Appl. Microbiol. Biotechnol.* **39:** 242-249.

Justen, P., Paul, G. C., Nienow, A. W., Thomas, C. R. (1996). Dependence of mycelial morphology on impeller type and agitation intensity. *Biotechnol. Bioeng.* **52:** 672-684.

Kaminskyj, S. G. W., Heath, I. B. (1996). Studies on Saprolegnia ferax suggest the general importance of the cytoplasm in determining hyphal morphology. *Mycologica*. **88:** 20-37.

Karji, F., Moo-Young, M. (1985). In: Comprehensive Biotechnology Vol. 2 (Cooney, C.L. and Humphrey, A.E., ends.), Pergamon Press, Oxford, pp. 5-56.

Keshavarz, E., Bonnerjea, J., Hoare, M. and Dunnill, P. (1990). Disruption of fungal organisms, *Rhizopus, nigricans*, in a high pressure homogeniser. *Enzyme Microb. Technol.* **12:** 494-498.

Khan, K., Paesen, J., Roets, E., Hoomartens, J. (1994). Quantitative TLC of erythromycin-application to commercial bulk samples and biological samples. *J. Planar. Chrom.* **7:** 349-353.

Khan, S. U. (1996). The effect of fermentation scale on the cell qualities of *Saccharomyces cerevisiae* and *Saccharopolyspora erythraea*. PhD. thesis. UCL, University of London, London-UK.

Kibwage, C. I. O., Roets, E., Hoogmartens, R. J., Vanderhaeghe, H. (1987). Optimisation of the separation of erythromycin and related substrates by HPLC. *J. Chromatogr.* **409:** 91-100.

Koch, A. L. (1994). The problem of hyphal growth in streptomyces and fungi. *J. theor. Biol.*, **171:** 137-150.

Kolmogorov, A. W. (1941). Dissipation of energy in the locally isotropic turbulence. *Com. Rend. Acad. Sci.* (U.S.S.R). **32:** 16-19.

Konig, B., Seewald, C. H., Schugerl, K. (1981). Process engineering investigations of penicillin production. *Eur. J. Appl. Microbiol. Biotechnol.* **12:** 205-211.

Konig, B., Seewald, C., Schuger, K. (1981). process engineering investigations of penicillin production. *European J Appl Microbiol Biotechnol.*, **12**: 205-211.

Kresta, S. M. and Wood, P. E. (1991). prediction of the three-dimensional turbulent flow in stirred tanks. *AIChE J.*, **37**: 448-460.

Kretschmer, S. (1982) Dependence of the mycelial growth pattern on individually regulated cell cycled in *Streptomyces granaticolor. Zeit. Allg. Mikribiol.* **22**: 335-345.

Kretschmer, S. (1985). Morphogenetic behaviour of two Streptomyces strains analyzed by the chemostats. *J. Basic Microbiol.*, **25**: 569-279.

Kubicek, C. P., Zehentgruber, O., Housam, K., Rohr, M. (1980). Regulation of citric acid production by oxygen: effect of dissolved oxygen tension on adenylate levels and respiration in *Aspergillus niger. Eur. J. Appl. Microbiol. Biotechnol.* **9**: 101-115.

Kumar, S., Kumar, R., Gandhi, K. S. (1991). Alternative mechanisms of drop breakage in stirred vessels. *Chem. Eng. Sci.*, **46**: 2483-2489.

Kuznetov, L. E. (1985). Temperature effect on erythromycin biosynthesis. *Antibiot. Med. Bioteknol.* **30**: 485-489.

Labeda, D. P. (1987). Transfer of the type strain of *Streptomyces erythraeus* (Waksman and Henrici, 1948) to the genus Saccharopolyspora. *Int. J. of Systematic Bacteriology.* **37**: 19-22.

Larsson, G., Enfors, S. O. (1988). Studies of insufficient mixing in bioreactors- effect of limiting oxygen concentrations and short-term oxygen starvation on *penicillium chrysogenum. Biorocess. Eng.* **3**: 123-127.

Leive, L. L., Davis, B. D. (1980). Cell envelope. In : Microbiology (third eddition). Davis, B. D., Dulbecco, R., Eisen, H., Ginsberg, H. S. , 71-111. Haper International edition.

Leng, D. S., Quarderer, G. J. (1982). Drop dispersion in suspension polymerisation. *Chem. Eng. Commun.* **14:** 177-201.

Logan, B. E., Wilkinson, D. B. (1991). Fractal dimensions and prosities of *Zoogloea ramigera* and *Saccharomyces cerevisiae* aggregates. *Biotechnol. Bioeng.* **38:** 389-396.

Makangiansar, H. Y. (1991). The influence of shear on the fermentation of *Penicillium chrysegenum*. PhD. thesis. UCL, University of Lodon, Lonon-UK.

Makangiansar, H. Y., Ayazi Shamlou, P., Thomas, C. R., Lilly, M. D. (1993). The influence of mechanical forces on the morphology and penicillin production of *Penicillium chrysogenum Bioprocess Eng.* **9:** 83-90.

Mandal. S. K., Bandyopadhyay, A., Das, A .K (1988). Synthesis of erythromycin by resting cells of *Streptomyces erythraeus*. *Indian. J. Exp. Biol.*, **26:** 25-27.

Martin, J. R., Rosenbrook, W. (1967). Studies on the biosynthesis of erythromycins. II. Isolation and structure of a biosynthetic intermediate, 6-Deoxyerythronolide B. *Biochem.* **6:** 435-440.

Martin, S. M., Bushell, M. E. (1996). Effect of hyphal micromorphology on bioreactor performance of antibiotic-producing *Saccharopolyspora erythraea*. *Microbiol.* **142:** 1783-1788.

Matsuo, T., Unno, H. (1981). Forces acting on floc and strength of floc. *J. Env. Eng. Div.* **107:** 527-545.

Meakin, P. (1988). Fractal aggregates. *Adv. Coll. Int. Sci.* **28:** 249-331.

Metz, B., De Bruijn, E. W., Van Suijdam, J. C. (1981). Methods for quantitative representation of the molds. *Biotechnol. Bioeng.*, **23**: 149-162.

Metz, B., Kossen, N. W. F., Van Suijdam, J. C. (1979). The rheology of mould suspension. *Adv. Biochem. Eng.* **11**: 103-156.

Metzner, A. B., taylor, J. S. (1960). Flow patterns in agitated vessels. *A. I. Ch. E. J.*, **6**: 109-114.

Metzner, A. B., Otto, R. E. (1957). Agitation of non-Newtonian fluids. *A. I. Ch. E. J.* **3**: 3-10.

Michel, B. J., Miller, S. A. (1962). Power requirements of gas-liquid agitated systems. *A.I.Ch.E. J.*, **8**: 262-266.

Miguelez, E. M., Hardisson, C., Manzanal, M. B. (1993). Incorporation and fate of N-acetyl-D-glucosamine during hyphal growth in streptomyces. *J. Gen. Microbiol.* **139**: 1915-1920.

Mihail, J. D., Obert, M. Taylor, S. J., Bruhn, J. N. (1994). The fractal dimension of young colonies of *Macrophomina phaseolina* produced from micrsclerotia. *Mycologia.* **86**: 350-356.

Mihail, J. D., Obert, M., Bruhn, J. N., Taylor, S. J. (1995). Fractal geometry of diffuse mycelia and rhizomophs of Armillaria species. *Mycol. Res.* **99**: 81-88.

Mirjalili, N., Linden, J. E. (1995). gas phase composition effects on suspension cultures of Taxus cuspidata. *Biotechnol. Bioeng.* **48**: 123-132.

Mitrad, A., Riba, J. P. (1988). Morphology and Growth of *Aspergillus niger* ATCC 26036 cultivated at several shear rates. *Biotechnol. Bioeng.*, **32**: 835-840.

Mohseni, M., Allen, D. G. (1995). The effect of particle morphology and concentration on the directly measured yield stress in filamentous suspensions. *Biotechnol. Bioeng.* **48:** 257-265.

Mohseni, M., Kautola, H., Allen, D. G. (1997). The viscoelastic nature of filamentous fermentation broths and its influence on the directly measured yield stress. *J. Ferm. Bioeng.* **83:** 281-286.

Mooyman, J. C. (1987). Scaling oxygen mass transfer in agitated fermentors. *Biotechnol. Bioeng.* **24:** 180-186.

Muhle, K., Domasch, K. (1991). Stability of particle aggregates in flocculation with polymers. *Chem. Eng. Process.* **29:** 1-8.

Mukhopadhyay, S. N., Ghose, T. K. (1976). Oxygen microorganism interaction. *Proc. Biochem.* **2:** 19-27.

Musilkova, M., Ujkova, E., Placek, J., Fencl, Z., Seichert, L. (1981). Release of protoplasts from a fungus as a criterion of mechanical interactions in the fermenter. *Biotechnol. Bioeng.* **23:** 441-446.

Muthukumar, M. (1985). Dynamics of polymeric fractals. *J. Chem. Phys.* **83:** 3161-3168.

Muthukumar, M., Winter, H. H. (1986). Fractal dimension of a cross linking polymer at gel point. *Macromolecules.* **19:** 1284-1285.

Nash, C. H. (1974). Effect of carbon dioxide on synthesis of erythromycin. *Antimicrobial Agents Chemotherapy.* **5:** 544-545.

Nasr, M. M.; Tschappler, T. J. (1997). High Performance Chromatographic analysis of erythromycin and related impurities in pharmaceutical formulations. *J. Liq. Chrom. & Rel. Technol.* **20:** 553-565.

Nielsen, J. (1992). Modeling the growth of filamentous fungi. *Adv. Biochem. Eng. Biotechnol.,* **46:** 187-222.

Nienow, A. W. (1983). the effect of rheological complexities on power consumption in an aerated, agitated vessel. *Chem. Eng. Commun.,* **19:** 273-293.

Nienow, A. W., Lilly, M. D. (1979). Power drawn by multiple impellers in sparged agitated vessels. *Biotechnol. Bioeng.* **21:** 2341-2345.

Obert, M. (1994). Microbial growth patterns: fractal and kinetic characteristics of patterns generated by a computer model to simulate fugal growth. *Fractals.* **1:** 354-374.

Obert, M., Pfeifer, P., Sernetz, M. (1990). Microbial growth patterns described by fractal geometry. *J. Bact.* **172:** 1180-185.

Okamoto, Y., Nishikawa, M., Hashimoto, K. (1981). Energy dissipation rate distribution in mixing vessels and its effects on liquid-liquid dispersion and solid-liquid mass transfer., *Int. Chem. Eng.* **21:** 88-94.

Olsvik, E. S., Kristiansen, B. (1992). Influence of the oxygen tension, biomass concentration and the specific growth rate on the rheological properties of a filamentous fermentation broth. *Biotechnol. Bioeng.* **40:** 1293-1299.

Olsvik, E., Kristiansen, B. (1994). Rheology of filamentous fermentations. *Biotech. Adv.* **12:** 1-39.

221

Olsvik, E., Tucker, K. G. Thomas, C. R., Kristiansen, B. (1993). Correlation of *Aspergillus niger* broth rheological properties with biomass concentration and the shape of mycelial aggregates. *Biotechnol. Bioeng.* **42:** 1046-1052.

Onken, U., Liefke, E. (1989). Effect of total and partial pressure (oxygen and carbon dioxide) on aerobic microbial processes. *Advanced in Biochenical Engineering.* **40:** 137-166.

Oosman, H. G., Abou-Zeid, A. A., El-Gamal, A. A. (1968). Factors influencing the biosynthesis of erythromycin by *Streptomyces erythraeus. Zeitschrift F. Allg. Mikrobiologie.* **8:** 421-428.

Oosterhuis, N. M. G., Kossen, N. W. F. (1984). Dissolved oxygen concentration profiles in a production-scale bioreactor. *Biotechnol. Bioeng.* **26:** 546-550.

Packer, H. L. (1991). The use of Image analysis for the characterisation of filamentous microorganisms. PhD. thesis. UCL, University of Lodon, Lonon-UK.

Packer, H. L., Thomas, C. R. (1990). Morphological measurements on filamentous microorganisms by fully automated image analysis. *Biotechnol. Bioeng.* **35:** 870-881.

Packer, H. L., Thomas, C. R. (1990). Morphological measurements on filamentous microorganisms by fully automatic image analysis. *Biotechnol. Bioeng.* **25:** 3049-3078.

Parker, D. S., ASCE, A. M., Kaufman, W. J. ASCE, M., Jenkins, D. (1972). Floc breakage in turbulent flocculation processes. *J. San. Eng. Div.* 79-99.

Patankar, D. B., Liu, T, Oolman, T. (1993). A fractal model for characterization of mycelial morphology. *Biotechnol. Bioeng.* **42:** 571-578.

Pellegatta, G., Carugati, G. P., Coppi, G. (1983). High performance liquid chromatography analysis of erythromycins A and B from fermentation broths. *J. Chromatogr.* **269**: 33-39.

Pickup, K. M., Bushell, M. E. (1995). Non-fragmenting variants of Streptomyces hyphae have enhanced activity of an enzyme (Phospho-N-Acetylmuramyl pentapeptide translocase) in peptidoglycan biosynthesis. *J. Ferm. Bioeng.* **79**: 247-251.

Placek, J.; Tavlarides, L. L. (1985). Turbulent-flow in stirred tank. 1. Turbulent-flow in the turbine impeller region. *AICHE. J.* **31**: 1113-1120.

Placek, J.; Tavlarides, L. L., Smith, G. W., Fort, I. (1986). Turbulent-flow in stirred tank. 2. A 2-scale model of turbulence. *AICHE. J.* **32**: 1771-1786.

Potvin, J., Peringer, P. (1993). Influence of N-propanol on growth and antibiotic production by an industrial strain of *Streptomyces erythraeus*. *Biotechnol. Lett.* **15**: 455-460.

Potvin, J., Peringer, P. (1994). Ammonium regulation in *Saccharopolyspora erythraea*. Part I: Growth and antibiotic production. *Biotechnol. Lett.* **16**: 63-68.

Prasad, P. N. Devi., B. K. Lonsane, *J.* (1987). *Chem. Tech. Biotechnol.* **38**: 221-234.

Precht, V. D. (1973). Theories on physical phenomena of homogenisation. *Kieler Milchwirtschaftliche Forschungs Bericht* (in Germany). **25**: 29-47.

Prosser, J. I., Tough, A. J. (1991). Growth mechanism and growth kinetics of filamentous microorganism. *Crit. Rev. Biotechnol.* **10**: 253-274.

Reuss, M. (1988). Influence of mechanical stress on the growth of *Rhizopus nigricans* in stirred bioreactors. *Chem. Eng. Technol.* **11:** 178-187.

Reuss, M., Popovic, M., Bronn, W. K. Rheology of yeast suspensions. (1979). *J. Appl. Microbiol. Biotechnol.* **8:** 167-175.

Richards, J. W. Studies in aeration and agitation. (1961). *Prog. Ind. Microbiol.* **3:** 253-260.

Ritz, K., Crawford, J. (1990). Quantification of the fractal nature of *Trichoderma viride*. Mycol. Res. **98:** 1138-1152.

Roberts, A. D., Zhang, Z., Young, T. W., Thomas, C. R. (1994). Direct determination of the strength of brewing yeast cells using micromanipulation. *ICHemE Research Event.* 73-75.

Roels, J. A., Van Den Berg, J. (1974). The rheology of mycelial broths. *Biotechnol. Bioeng.* **16:** 181-208.

Rollins, M. J., Jensen, S. E., Westklake, W.S. (1990). Oxygen derepresses deacetoxycephalosporin C synthase and increases the conversion of penicillin N to cephamycin C in *Streptomyces clavuligerus*. *Enzyme Microb. Technol.* **12:** 40-45.

Rollins, M. J., Jensen, S. E., Westlake, W. S. (1988). Effect of aeration on antibiotic production by *Streptomyces clavuligerus*. *J. indust. microbiol.* **3:** 357-367.

Rollins, M. J., Jensen, S. E., Westlake, W. S. (1991). Effect of dissolved oxygen level on ACV synthetase synthesis and activity during growth of *Streptomyces clavuligerus*. *Appl. Microbiol. Biotechnol.* **35:** 83-88.

Rushton, J. H., Costich, E. W., Everett, H. J. (1950). Power characteristics of mixing impellers. Part II. *Chem. Eng. Prog.* **46:** 467-476.

Salton, M. R. J. (1964). The bacterial cell wall. Elsevier Publication company.

Sarra, M., Ison, A. P., Lilly, M. D. (1996). The relation between biomass concentration, determined by a capacitance-based probe, rheology and morphology of *Saccharopolyspora erythraea. J. Biotechnol.* **51:** 157-165.

Schlichting, H. (1979). Boundary layer theory. McGraw-Hill, New York.

Schugerl, K. (1983). Oxygen transfer into highly viscous media. In Advances in Biochemical Engineering., Vol. 19. A. Fiechter (Ed). Springer Verlag, Berlin, pp. 72-174.

Shomura, T., Yoshida, J., Amano, S., Kojima, M., Inouye, S., Nida, T.(1979). Effect of concentration of medium on *S. halstedii* fermentation. *J. antibiotics.* **32:** 427-437.

Smith, J. J., Lilly, M. D., Fox, R. I. (1990). The effect of agitation on the morphology and penicillin production of *Penicillium chrysogenum. Biotechnol. Bioeng.* **35:** 1011-1023.

Smith, T. G., lange, G. D., Marks, W. B. (1996). Fractal methods and results in cellular morphology. *J. Neur. Meth.* **69:** 123-136.

Solmon, G. L. (1980). Fermenter design and fungal growth. In: Fungal biotechnology, Smith, J. E., Berry, D. R., Kristiansen, B. (ed). Academic press, London. 55-80.

Stark, W. M., Smith, R. L.(1961). The erythromycin fermentation. *Progr. Ind. Microbiol.,* 3,211-230.

Suphantharika, A. P., Ison, A. P. Lilly, M. D., Buckland, B. C. (1994). The influence of dissolved oxygen tension on the synthesis of the antibiotic difficidin by *Bacillus subtilis. Biotechnol. Bioeng.* **44:** 1007-1012.

225

Taguchi, H., Yoshida, T., Tomota, Y., Teramoto, S. (1968) The effect of agitation on disruption of the mycelial pellets in stirred fermentors. *J. Ferment. Technol.* **46:** 814-822.

Tambo, N., Hozumi, H. (1979). Physical characteristics of flocs - II. strength of floc. *Water Res.* **13:** 421-427.

Tanaka, H. (1976). Studies on the effect of agitation on mycelia in submerged culture. *J. Ferment. Technol.* **54:** 818-829.

Tanaka, H., Ueda, K. (1975a). Kinetics of mycelial growth accompanied by leakage of intracellular nucleotides caused by agitation. *J. Ferment. Technol.* **53:** 27-34.

Tanaka, H., Mizuguchi, T., Ueda, K. (1975b). An index representing the mycelial strength to maintain physiological activity on mechanical agitation. *J. Ferment. Technol.* **53:** 35-43.

Tarbuck, L. A. Leigh, J. R., Tampion, J. (1985). In modeling and control of biotechnological processes, A. Johnson, Ed. Pergamon Press, Oxford. 171-185.

Thomas, C. R. (1993). Shear effect on cells in bioreactors. In Turbulent aggregation and breakup of particles in liquids stirred vessels. In Processing of solid-liquid suspensions. First edition. Butterworth Heinemann (pub), 158-191.

Thomas, D. (1968). Turbulent disruption of flocs in small particle size suspensions. *A.I. Ch. E. J.* **10:** 517-523.

Tomi, D. T., Bagster, D. G. (1978). The behaviour of aggregates in stirred vessels. Trans *IChemE.* **56:** 1-8.

Trager, M., Qazi G. N., Buse, R., Onken, U. (1992). Influence of constant and oscillating dissolved oxygen concentration on *Aspergillus niger*. *J. Ferment. Bioeng.* **74:** 282-287.

Trilli, A., Crossley, M. V, Kontakou, M. (1987). Relation between growth rate and erythromycin production in *Streptomyces erythraeus*. *Biotechnol. Lett.* **9:** 765-770.

Trinci, A. P. J., Collinge, A. J. (1975). Hyphal wall growth in *Neurospora crassa* and *Geotrichum candidum*. *J. Gen. Microbiol.* **91:** 355-361.

Tsuji, K., Geotz, J. F. (1978). HPLC as a rapid means of monitoring erythromycin and tetracycline fermentation processes. *J. Antibiotics*. **41:** 302-308.

Tucker, K. G., Kelly, T., Delgrazia, P. and Thomas, C. R. (1992). Fully automatic measurement of mycelial morphology by image analysis. *Biotechnol. Prog.* **4:** 353-359.

Ujokova, E., Fencl, Z., Muzilkova, M., Seichert, L. (1980). Dependence of release of nucleotides from fungi on fermenter turbine speed. *Biotechnol. Bioeng.* **22:** 27-241.

Van't Riet, K., Smith, J. M. (1975). The trailing vortex system produced by Rushton turbine agitators. *Chem. Eng. Sci.*. **30:** 1093-1105.

van Suijdam, J. C. (1980). PhD thesis. Delft University of Technology.

van Suijdam, J. C., Metz, B. (1981a). Influence of engineering variables upon the morphology of filamentous molds. *Biotechnol. Bioeng.* **23:** 111-148.

van Suijdam, J. C., Metz, B. (1981b). Fungal pellet break up as a function of shear in a fermenter. *J. Ferment. Technol.* **59:** 329-333.

Vandamme, E. J., Leyman, D., DeVisscher, P., DeBuyser, D., Vansteenkiste. (1981). *J. Chem. Tech. Biotechnol.* **31:** 247.

Vardar, F., Lilly, M. D. (1982). Effect of cycling dissolved oxygen concentrations on product formation in penicillin fermentation. *Eur. Appl. Microbiol. Biotechnol.* **14:** 203-211.

Vecht-Lifshitz, S. E., Magdassi, S. and Braun, S. (1990). Pellet formation and cellular aggregation in *Streptomyces tendae. Biotechnol. Bioeng.* **35:** 890-896.

Vrana, D., Seichert, L. (1988). Cytomorphological comparison of mechanical and chemical deforming of a yeast culture. *Folia Microbiologica.* **33:** 144-147.

Wang, D., Fewkes, R. (1977). Effect of operating and geometric parameters on the behaviour of non-Newtonian, mycelial, antibiotic fermentation. *Develop. Ind. Microbol.* **18:** 39-56.

Warren, S. J. (1994). The relation between the morphology and rheology of mycelial fermentation. PhD. thesis. UCL, University of Lodon, Lonon-UK.

Warren, S. J., Keshavarz-Moore, E., Ayazi Shamlou, P., Lilly, M. D., Thomas, C. R. Dixon, K. (1995 a). Rheological measurements of three actinomycete in submerged cultures. *Bioprocess Eng.* **13:** 45-48.

Warren, S. J., Keshavarz-Moore, E., Ayazi shamlou, P., Lilly, M. D., Thomas, C. R., Dixon, K. (1995 b). Rheologies and morphologies of three actinomycetes in submerged culture. *Biotechnol. Bioeng.* **45:** 80-85.

Wase, D., Patel, Y. R. (1985). Variations in the volumes of microbiol cells with changes in the agitation rates of chemostat cultures. *J. Gen. Microbiol.* **131:** 725-736.

Wessels, J. G. H. (1993). Wall growth, protein excretion and morphogenesis in fungi. *New. Phytol.* **123:** 397-413.

Whitaker, A. (1992). Actinomycetes in submerged culture. *Appl. Biotechnol.* **32:** 23-35.

Wichterle, K., Kadlec, L. Z., Mitschka, P. (1984). Shear rates on turbine impeller blades. *Chem. Eng. Commun.* **26:** 25-32.

Wilson, G. C., Bushell, M. E. (1995). the induction of antibiotic synthesis in *Saccharopolyspora erythraea* and *Streptomyces hygroscopicus* by growth rate decrease is accompanied by a down-regulation of protein synthesis. *FEMS Microbiol. Lett.* **129:** 89-96.

Witter, R., Matthes, R., Schugerl, K. (1983). Rheology of *Penicillium chrysogenum* pellet suspensions. *Appl. Microbiol. Biotechnol.* **18:** 17-23.

Wu, H., Patterson, G. K. (1989). Laser-doppler measurements of turbulent flow parameters in a stirred mixer. *Chem. Eng. Sci.* **44:** 2207-2221.

Yang, H., King, R., Reichl, U., Gilles, E. D. (1992). Mathematical model for apical growth, septation, and branching of mycelial microorganisms. *Biotechnol. Bioeng.* **39:** 49-58.

Yang, Y. K., Morikawa, M., Shimizu, H., Shioya, S., Suga, K., Nihira, T., Yamada, Y. (1996). Image analysis of mycelial morphology in virginiamycin production by batch culture of *Streptomyces virginiae. J. Ferment. Bioeng.* **81:** 7-12.

Yegneswaran, P. K., Gray, M. R., Thompson, B. G. 1991. Effect of dissolved oxygen control on growth and antibiotic production in *Streptomyces clavuligerus* fermentation. *Biotechnol. Prog.* **7:** 246-250.

229

Zetelaki, K., Vas, K. (1968). The role of aeration and agitation on the production of glucose oxidase in submerged culture. *Biotechnol. Bioeng.* **10:** 45-59.

Zhang, Z., Al-Rubaeai, M., Thomas, C. R. (1993). Estimation of disruption of animal cells by turbulent capillary flow. *Biotechnol. Bioeng.* **42:** 987-993.

Zhou, G. and Kresta, S. M. (1996). Impact of tank geometry on the maximum turbulence energy dissipation rate for impellers. *AIChE. J.* **42:** 2476-2490.

Appendix 1: Calculation of power dissipation rate in fermenters

Fermenters in this experiments consisted of 3 Rushton turbine impellers (see section 2.2.4). For the purpose of the calculation of power dissipation, the bottom impeller is assumed to be under aeration and the top two impellers are considered to be ungassed. The gas power was calculated based on the Michel & Miller correlation (Michel & Miller, 1962).

The Reynolds number (Re) was obtained as

$$Re = \frac{\rho N D^2}{\mu_a} \qquad (A.1.1)$$

where

ρ = density of the broth $\cong$ 1000 kgm^{-3}

N = stirrer speed (s^{-1})

D = impeller diameter = 0.068 m at 7 L scale and 0.2 m at 450 L scale

and apparent viscosity was obtained using the Metzner and Otto technique (Metzner and Otto, 1957)

$$\mu_a = K(k_s N)^{n-1} \qquad (A.1.2)$$

where K and n are consistency index and flow behaviour of fermentation broth (Figure 3.33), and for the purpose of this calculation their value at 65-75 h was considered. k_s is the impeller shear rate constant and its value was considered as 11.4 (Metzner and Otto, 1957).

From the Reynolds number correlation for six-blade turbine impeller (Rushton *et al.*, 1950) the value of power number (N_p) obtained and then power dissipation for ungassed impeller (P_o) calculated as,

$$N_p = \frac{P_0}{\rho N^3 D^5}$$
(A.1.3)

For calculation of gassed power Michel and Miller correlation used as

$$P_g = 0.756[\frac{P_0^2 N D^3}{Q_g^{0.56}}]^{0.45}$$
(A.1.4)

Q_g is the gas flow rate and it was 5 Lmin^{-1} or 8.3×10^{-5} m^{3}s^{-1} in 7-L scale and 3.5×10^{-3} m^{3}s^{-1} at 450 L scale. The calculation for power dissipation at 350 rpm are as follows:

K = 0.28 Pa.s^n, n= 0.43 (Figure 3.33)

$\mu_a = 0.28(11.4 \times 350/60)^{0.43-1} = 0.025$ Pa.s

N = 350/60 = 5.83 s^{-1}, D = 0.068 m and ρ = 1000 Kgm^{-3}, therefore Re = 1070. And the power number (N_p) can be obtained for flat six-blade turbine impeller as 4.5. P_0 calculated according to equation (A.1.3) is 1.30 and P_g calculated according to equation A.1.4 is 0.57.

Therefore total power dissipation at 7 L scale and 350 rpm is as:

$$P = P_g + P_0 + P_0$$
(A.1.5)

and the total power at 350 rpm is,

$$P = 3.17 \text{ W}$$

The power dissipation at other stirrer speeds at 7-L scale and also 450-L scale are summarised in table A.1.1.

Table A.1.1: Power dissipation in the fermenter

Scale	N (rpm)	μ_a (Pa.s)	Re	N_p	P_0 (W)	P_g (w)	P_t (W)
7-L	350	0.025	1070	4.5	1.30	0.57	3.17
7-L	500	0.020	1900	5	4.2	1.92	10.32
7-L	750	0.016	3600	5.5	15.6	7.5	38.7
7-L	1000	0.011	7050	5.9	39.6	19.75	98.95
7-L	1250	0.008	12500	6	78.8	40.4	198
450-L	300	0.027	7300	5.9	236	95.6	567
450-L	450	0.017	17750	6	809	347	1965

Appendix 2: Calculation of Kolmogorov microscale of turbulence in fermenter

A.2.1 Average Kolmogorov microscale of turbulence

Kolmogorov microscale of turbulence $(v^3/\varepsilon)^{0.25}$ was calculated based on the average energy dissipation in the vessel (ε_{ave}). The value of ε_{ave} was found by dividing the power, P_t (Table A.1.1) by 5 kg at 7-L scale or 300 kg at 450-L scale. The kinematic viscosity (v) was calculated by dividing apparent viscosity to density of the fluid $(\cong 1000~kgm^{-3})$.

A.2.2 Kolmogorov microscale of turbulence in high shear zone of impeller

The Kolomogorov microscale of turbulence was calculated based on two extreme cases $(\varepsilon_i = 10~\varepsilon_{ave})$. Apparent viscosity of the culture in impeller zone was lower than its average value in the vessel due to pseudoplasticity behaviour of the fluid. For the purpose of the calculation of apparent viscosity in the impeller region equation (A.2.2) was derived as follows:

$$\varepsilon = \tau\gamma/\rho \text{ and } \tau = K\gamma^n \Rightarrow \gamma = (\varepsilon\rho/K)^{1/n+1} \tag{A.2.1}$$

$$\mu_a = \tau/\gamma = K\gamma^n/\gamma = K\gamma^{n-1} = K~(\varepsilon\rho/K)^{n-1/n+1} \tag{A.2.2}$$

therefore:

$$(\mu_a)_i = K~(\varepsilon_i~\rho/K)^{n-1/n+1} \tag{A.2.3}$$

234

Appendix 3: Calculation of circulation time

Circulation time, t_c, was determined from two different methods including the equation recommended by Reuss (1988) and the general method using the pumping capacity of the impeller (Smith et al., 1990).

A3.1 Reuss method for calculation of circulation time:

Circulation time calculated from the geometrical parameter of the fermenter proposed by Reuss (1988) is as follow and the results are shown in Table A.3.1:

$$Nt_c = 0.76 \ (H_L/T)^{0.6}(T/D)^{2.7} \hspace{2cm} (A.3.1)$$

H_L = liquid height in the fermenter = 0.28 m at 7-L scale or 1.06 m at 450-L scale

T = diameter of the fermenter the = 0.15 m at 7-L scale or 0.6 m at 450-L scale

D = impeller diameter = 0.068 m at 7-L scale or 0.2 m at 450-L scale

A3.2 Using pumping capacity of the impeller

Circulation frequency has been estimated by equation A.3.2(Smith et al., 1990)

$$1/t_c = (FI \ ND^3)/V_L \hspace{2cm} (A.3.2)$$

where FI is the impeller flow number, N its speed, D its diameter and V_L the working volume of the fermenter. Equation A.3.3 has been recommended for the calculation of impeller flow number (Justen et al., 1996).

$$FI = (0.91 \ N_p W_i/D)^{0.5} \hspace{2cm} (A.3.3)$$

where Np is the impeller power number (Table A.1.1) and W_i is impeller blade width (Table 2.4). The circulation frequency calculated with this method gave approximately 1.7 times the value of the results obtained with Reuss (1988) method (Table A.3.1). Data obtained from Reuss method has been used in this study. It should

be noted that for the purpose of development of the model in this experiments the ratio between the values are important not the absolute values.

Table A.3.1: Value of circulation frequency

Scale	Working volume	$1/t_c$ (s^{-1})	
		Reuss method	Smith *et al.* method
7-L	5	0.61	0.33
7-L	5	0.87	0.5
7-L	5	1.31	0.8
7-L	5	1.74	1.08
7-L	5	2.17	1.35
450-L	300	0.24	0.14
450-L	300	0.362	0.206

Appendix 4: Calculation of Reynolds number and boundary layer thickness of the impeller

Schlichting (1979) stated that for a rotating disk, the transition from laminar to turbulent flow occurs at a disk Reynolds number number (Lu_∞ / v) of approximately 3 × 10^5, where $u_\infty = \pi ND$ and $L = W_i/2$. Values of impeller blade width, W_i, and impeller diameter, D at 7 L scale is 0.013 and 0.068 m respectively. The value of apparent viscosity in impeller region is calculated (see Appendix 2) and divided by density of the culture (1000 kgm^{-3}) to find the value of, v, and used for calculation of impeller Reynolds number, Re_d and the results are summarised in table A.5.1. The value of boundary layer thickness, δ_t, also calculated by equation $\delta_t = 5L(Re_d)^{-0.5}$ and shown in Table A.4.1.

Table A.4.1: Disk Reynolds number and its boundary layer thickness

Stirrer speed (rpm)	Re_d	δ_t (μm)
350	8100	360
500	11500	305
750	17250	250
1000	23000	220

Appendix 5: Calculation of Kolmogorov microscale of turbulence in homogeniser

The action of the homogeniser can be considered to be similar to pump, and therefore the power dissipation is found by equation A.5.1 (Hornby, 1995).

$$P_t = \Delta P \times Q_L \qquad (A.5.1)$$

where P_t is the power dissipation, ΔP is the pressure drop across the valve and Q_L is the flow rate through the homogeniser. If that the majority of the pressure drop occurs across the "land" of the valve, the volume over which the power is dissipated , V, is given by (Hornby, 1995):

$$V = \pi(R_2^2 - R_1^2) h \qquad (A.5.2)$$

where R_1 and R_2 are the entry orifice radius and effective radius of the valve rod respectively. These are the radii at the entery and exit of the narrowest part of the valve gap, the "land", the region where the gap width is h (Figure A.5.1). An approximation for h is given by equation A.5.3 (Prechet, 1973):

$$\Delta P = b/h^3 \qquad (A.5.3)$$

where
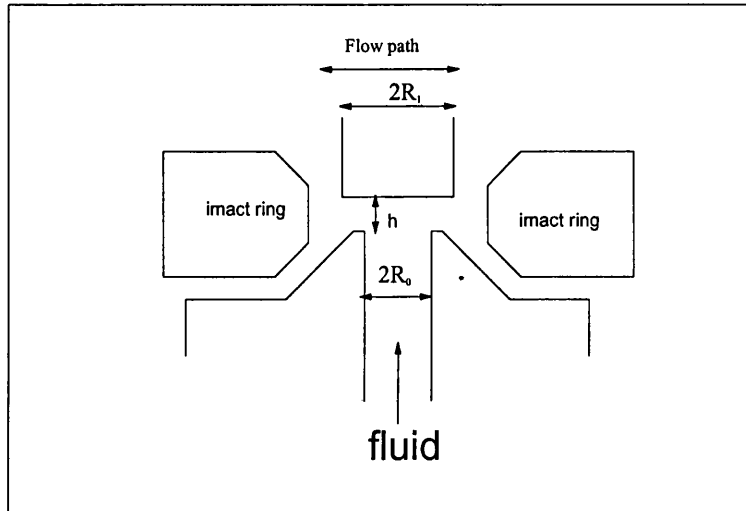
$$b = [6\mu Q_L/\pi]\ln(R_2/R_1) \qquad (A.5.4)$$

Figure A.5.1: Schematic diagram of the Lab-40 homogeniser.

Therefore the power dissipation per unit mass (ε) in the area of high shear zone (land) can be calculated by

$$\varepsilon = P_t/V \times \rho = (\Delta P \times Q_L)/(V \times \rho) = \Delta P^{4/3} Q_L/[\pi \rho (R_2^2 - R_1^2) b^{1/3}] \quad (A.5.5)$$

The value of R_1 for Lab-40 homogeniser is 1.65 mm and the value of R_2 and Q_L has been suggested as 2.05 mm and 7.78 mLs^{-1} (Sidiqi, 1997). The samples were diluted 20 times with phosphate buffer, therefore had a viscosity similar to water ($\mu = 0.001$ Pa.s). The value of power dissipation in the area of high shear zone and Kolmogorov microscale of turbulence (λ) at different disruptive pressure is calculated and shown in Table A.5.1.

Table A.5.1: Kolmogrov microscale of turbulence in homogeniser

ΔP (bar)	ε (w/kg)	λ (μm)
100	2×10^8	0.27
200	5.2×10^8	0.21
400	1.2×10^9	0.17
600	2.1×10^9	0.15
800	3.2×10^9	0.14
1200	5.4×10^9	0.12